Integrated Miocene stratigraphy and correlation of four major oil and gas fields in the Vienna Basin (Austria).

Dissertation
zur Erlangung des Doktorgrades der Naturwissenschaften
an der Karl-Franzens-Universität Graz
Institut für Erdwissenschaften

vorgelegt von
Matthias Kranner, M.Sc., B.Sc.
Graz, April 2021

Contents

Preface

The present thesis is the result of a joint project of the Österreichische Mineralölverwaltungs AG (OMV), the Natural History Museum, Vienna (NHMW) and the Karl-Franzens-University, Graz. This project was initiated by the OMV in 2018 to obtain information on the contact of the pre-Neogene basement with oldest Neogene sediments and about thickness and position of supposed lower Miocene deposits and the stratigraphic content of middle Miocene deposits within the Austrian northern and central Vienna Basin (VB). The aim was to combine resources of industry and academia to create an integrated stratigraphic north-south cross section using micropaleontological, lithological and geophysical (seismic images and wire-logs) data of 52 wells through major hydrocarbon reservoirs resulting in the fundamental understanding of basin evolution in regards of

(A) pinpointing the transition of the pre-Neogene basement to Miocene deposits,
(B) a reevaluation and formalization of Miocene lithostratigraphy,
(C) relative sea level changes taking in account local (tectonics) and global (global climate and eustatic sea level) influences and
(D) accompanying changes of ecological parameters (salinity, sea surface and bottom water temperature, dissolved oxygen, stress factors and trophic levels) compared to surrounding areas and the global record.

The doctoral candidate conducted micropaleontological analyses on benthic and planktonic foraminifers providing biostratigraphical and paleoecological data as backbone for the attempted integrated stratigraphic model and was responsible for coordinating the interests of industry (OMV) and science (NHMW, University of Graz) as well as the integration of the obtained data for publications.

The present thesis summarizes the main results, reconstructions and conclusions of early and middle Miocene wells of the northern and central VB of Austria.

The first chapter provides a brief introduction to the Central Paratethys evolution and its influence on the basin structure of the northern and central VB, the geological setting and the relevance of foraminifers for paleoenvironmental and stratigraphic analysis.

The second, third, fourth and fifth chapter consist of four scientific articles (three with the doctoral candidate as first author and one as co-author) that have been published or are in the final stages of the review process for publishing by international, peer-reviewed journals. Therefore, phrasing and position of figures may differ slightly from this thesis.

Second chapter: Kranner, M., Harzhauser, M., Rögl, F., Ćorić, S., Strauss, P., 2019. Biostratigraphic constraints for a Lutetian age of the Harrersdorf Unit (Rhenodanubian Zone): Implication for basement structure of the northern Vienna Basin (Austria). Geologica Carpathica, 70(5), 405–417.

Third chapter: Harzhauser, M., Kranner, M., Mandic, O., Strauss, P., Siedl, W., Piller, W.E., 2020. Miocene lithostratigraphy of the northern and central Vienna Basin (Austria). Austrian Journal of Earth Sciences, 113, 169-200. https://orcid.org/0000-0002-4471-6655

Fourth chapter: Kranner, M., Harzhauser, M., Mandic, O., Strauss, P, Siedl, W., Piller W.E., 2021. Early and middle Miocene paleobathymetry of the Vienna Basin (Austria). Marine and Petroleum Geology (under review).

Fifth chapter: Kranner, M., Harzhauser, M., Mandic, O., Strauss, P, Siedl, W., Piller W.E., 2021. Miocene ecology of the central and northern Vienna Basin (Austria). Journal of Palaeogeography, Palaeoclimatology, Palaeoecology (under review).

Within **the sixth chapter** the major outcomes and conclusions of the integrated stratigraphic and paleoenvironmental analyses during the early- middle Miocene of the VB are shortly summarized.

To maintain readability, supplementary material of chapters 2–5 is not included in the thesis.

Acknowledgments

At this point I want to express my sincerest thanks to a number of people who contributed to finishing this thesis.

I am grateful to my supervisors Mathias Harzhauser and Werner E. Piller for their advice, critical reviews and countless constructive discussions. Your support did not only enable me to write and finish this thesis but also provided the opportunity to attend international conferences, workshops, summer schools and international fieldtrips. I deeply appreciate your guidance and friendship that contributed not only to my scientific career but also to personal growth.

I want to thank Doris Nagel (University of Vienna) for the opportunity to participate in teaching theoretical and practical courses. Further, I want to thank Diego Antonia Garcia Ramos for the support with the R software, and Erik Wolfgring (University of Milano) for countless discussions on the identification of horribly deformed agglutinated foraminifers.

I am also grateful to my co-authors and co-workers of the project for their precious time and data; in particular, I thank Oleg Mandic (NHMW), Philipp Strauss (OMV), Wolfgang Siedl (OMV), Johannes Loisl (OMV), Fred Rögl (NHMW) and Alexander Lukeneder, as well as all co-workers of the NHMW.

Anton Engelbert, Anton Fürst and specifically Iris Feichtinger, are acknowledged for their help during sampling campaigns, as well as preparing, washing ,sieving and creating thin sections of hundreds of samples.

Many thanks also to Patrick Grunert (University of Cologne) for discussions and support within the early stages of my PhD as well as agreeing to be part of the assessing committee of this work.

Christian, Christoph and Felix thanks for having critical discussions and offering new perspectives, resulting in different scientific expertise. Finally, I want to express my gratitude to my family for the persistent support in so many ways during the last ten years. Kathrin, thank you for all the support and understanding especially in the intense time towards finishing this thesis.

Abstract

The Vienna Basin is an intra alpine pull-apart basin, which originated during the early middle Miocene and contains one of the largest onshore oil and gas fields in Europe. It has been studied since the early 20th century and was penetrated by hundreds of drillings. The focus on single reservoirs by the petroleum scientists resulted in isolated stratigraphic solutions and the complex tectonic setting of the Vienna Basin hampered a straightforward intra basin correlation of Miocene drillings so far. To overcome this unsatisfactory situation a stratigraphic north-south cross-section throughout the Vienna Basin, backed by biostratigraphic correlations of numerous cores from major oilfields (Bernhardsthal, Mühlberg, Rabensburg, Bad Pirawarth, Ringelsdorf, Spannberg Bockfließ, Matzen, Aderklaa, Zwerndorf, Strasshof, Schwechat) has been accomplished within this thesis. One of the main objectives was to determine the contact of Neogene sediments to the pre-Neogene basement, obtaining information about thickness and position of the supposed lower Miocene deposits and the stratigraphic content of middle Miocene deposits, which are varying considerably in thickness from well to well. Often, the tectonic setting impedes with a straightforward correlation of single 3D seismic reflectors but using biostratigraphic data it was possible to resolve the issue and correlations between oilfields were established. The main analyses are based on benthic and planktonic foraminifera to assign the deposits to regional biostratigraphic zones and to allow a correlation with international stages. In addition, paleoecologic data are used to describe the paleoecological settings, tracking changes in sea surface temperature (SST), bottom water temperature (BWT), salinity, trophic levels, stress indicators, mode of life, feeding preferences and diversity as well as changes of depositional environments from bathyal to near shore inner neritic settings. Hence, a reconstruction of relative sea level fluctuations was established. Combined with core-log data, such as spontaneous potential, resistivity as well as modern 3D seismic data, information about paleotopography and paleogeography during deposition were gathered and are discussed. This allowed a correlation to global events during the Miocene (Mi events, Middle Miocene Climate Optimum, Miocene Climate Transition) and explaining the strong influence of local tectonics. Furthermore, misinterpretations concerning the local stratigraphic setting have been resolved and a new intra basin correlation of Ottnangian, Karpatian and Badenian formations is presented. Especially Karpatian, lower and middle Badenian units, unknown from surface outcrops, turned out to be much more complex than previously expected and are re-evaluated. All introduced formations and members were formalized by introducing type sections, providing geographic distribution and thickness, describing typical depositional environments and fossils and discussing age constraints. Therefore, the new biostratigraphic, paleoecologic and paleobathymetric data as well as derived integrated stratigraphy, allowed establishing of a modern lithostratigraphic scheme for most of the seismic units and new insights of the paleoenvironmental evolution, providing a framework for a modern sequence stratigraphy of the Vienna Basin.

Chapter 1

Introduction

1.1. The Paratethys: Paleogeography and stratigraphy

The Paratethys sea was an epicontinental remnant of the ancient Tethys ocean and covered large parts of central Europe from the Eocene-Oligocene boundary to the late Miocene (Fig. 1.1; e.g., Rögl, 1998; Schulz et al., 2005; Allen and Armstrong, 2008). The Paratethys got separated from the Mediterranean in the south by the rise of the Alpine mountains resulting of the collision of the Eurasian plate with the African plate due to the northwards movement of the African plate (Rögl, 1998; Márton et al., 2003, 2006; Márton 2006; Seghedi et al., 2004; Harzhauser and Piller, 2007).

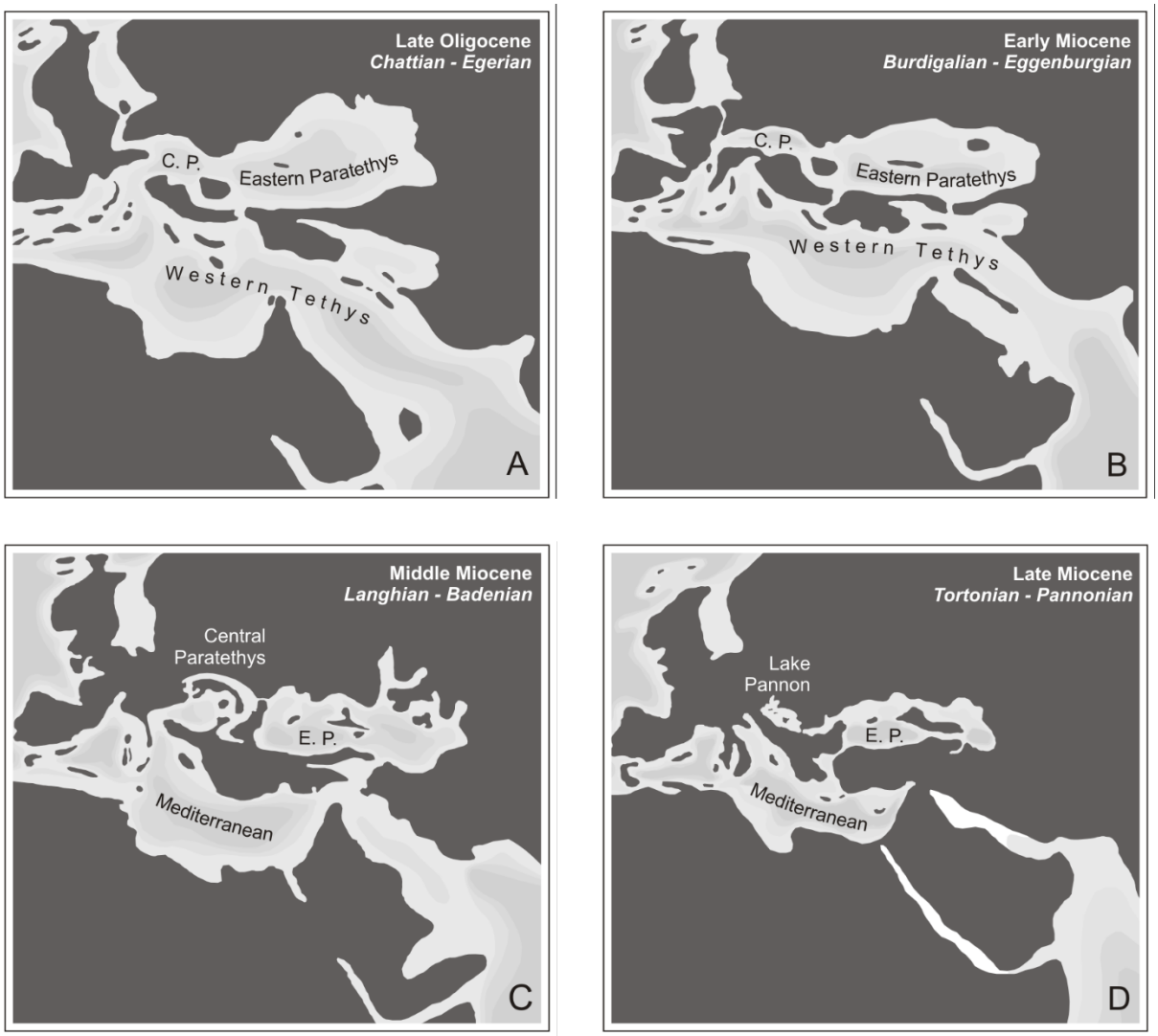

Fig. 1.1 Late Oligocene to late Miocene paleogeographic evolution of the Paratethys and Mediterranean after Harzhauser and Piller (2007).

The Paratethys spread from the Rhône Basin in France towards Inner Asia during its maximum extent and could be subdivided into Western, Central and Eastern Paratethys (Seneš, 1961; Harzhauser and

Piller, 2007). The Western Paratethys covered an area from the Alpine Foreland Basins of France, Switzerland, S Germany to Upper Austria (Seneš, 1961), the Central Paratethys reached from the Eastern Alpine-Carpathian Foreland basins, from Lower Austria to Moldavia, including the Vienna Basin and the Pannonian Basin System and the Eastern Paratethys comprises the Euxinian (Black Sea), Caspian and Aral Sea basins (Nevesskaja et al., 1993). From West to East, the Paratethys dried up since its origination until now and the Eastern Paratethys contains today the last remnants of the former Paratethys sea (Black Sea, Caspian Sea) (e.g., Piller et al., 2007; Abrantes et al., 2012; Zagorchev, 2021). Paleotopography, -ecology and -geography were heavily influences by the changes in the global sea level as well as local tectonics resulting in changing seaways and land bridges (e.g., Harzhauser and Piller, 2007; Piller et al., 2007). Hence, different ecosystems developed in each part of the Paratethys leading to locally influenced biostratigraphic concepts (e.g., Cicha et al., 1967; Papp et al., 1973, 1974, 1978, 1985). The publication series "Chronostratigraphie und Neostratotypen" aimed to correlate and unify these different concepts and several authors contributed to the correlation of the Paratethys stratigraphy with the Mediterranean and the global record since that time and a regional stratigraphy for the Central Paratethys (see Fig. 1.2) was established (Cicha et al., 1967; Steininger and Seneš, 1971; Papp et al., 1973, 1974, 1978, 1985; Baldí and Seneš, 1975; Stevanović et al., 1990; Steininger et al., 1976; Rögl 1996; Popov et al., 2004; Harzhauser and Piller, 2007; Piller et al., 2007). Herein after we focus on the Central Paratethys, which covers the investigated area of this thesis.

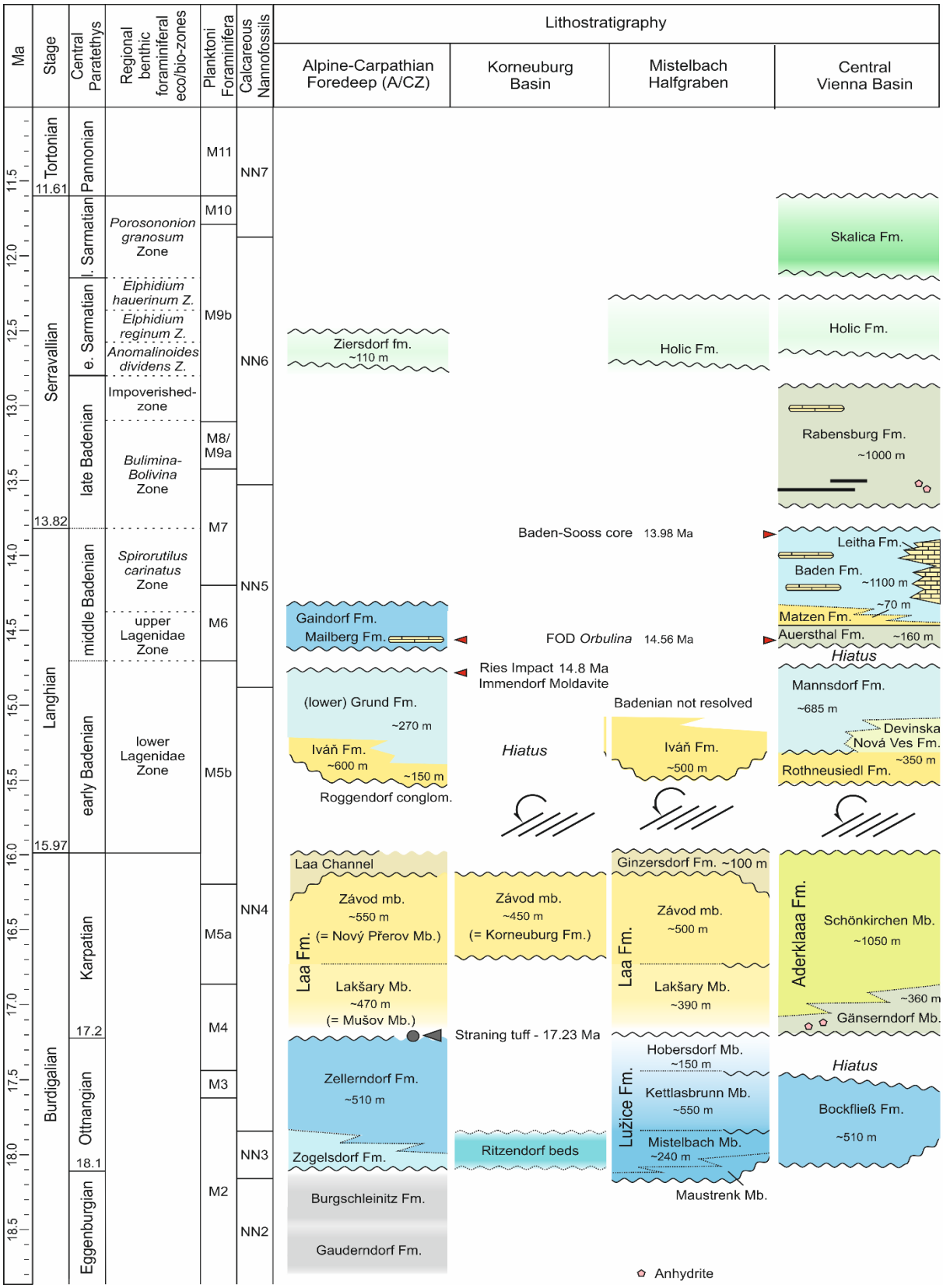

Fig. 1.2. Integrated middle and late Miocene stratigraphy (including regional biozonation, lithostratigraphy and global planktonic foraminifera and calcareous nannoplankton zones of the Central Paratethys, correlating to the regional stages to the Neogene timescale. Modified after Piller et al. (2007), Harzhauser et al. (2017, 2018, 2019).

1.2. The Vienna Basin

During the last decades, several geologists focus on the Vienna Basin (VB) to understand the complex evolution of the Central Paratethys, benefitting of major drilling campaigns aiming for hydrocarbon reservoirs (e.g., Hamilton and Johnson, 1999; Hamilton et al., 2000). The VB is a 200 km long and 55 km wide, rhomboid pull-apart basin (Royden, 1985; Wessely, 1988, 2006), covering large parts of eastern Austria and extends into the Czech Republic in the North and Slovakia in the East (Fig. 1.3.; see Kováč et al., 2004 and Wessely, 2006 for detail description).

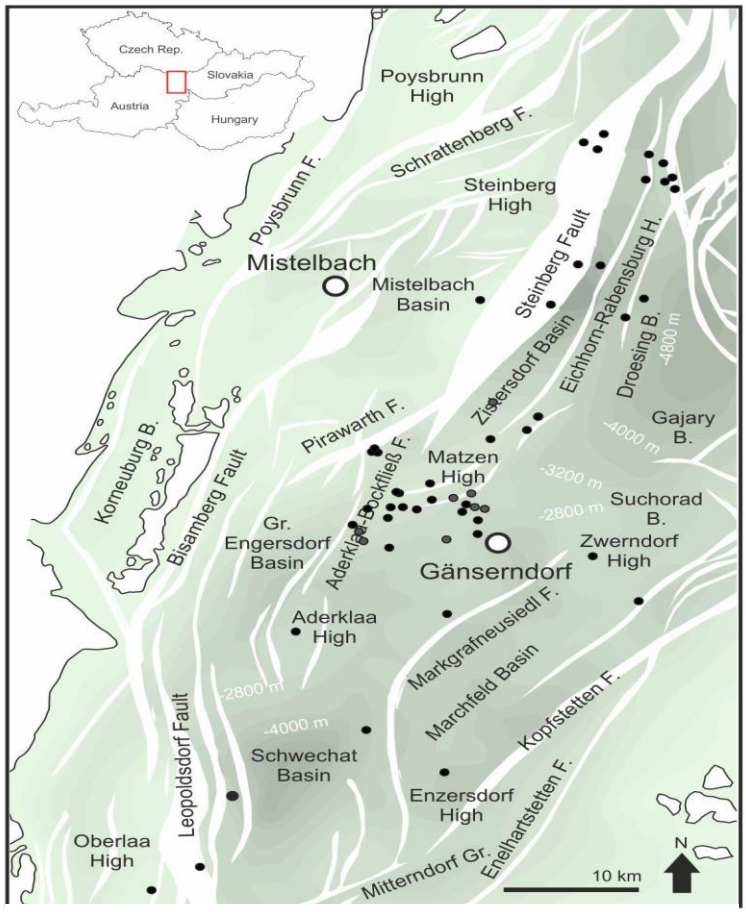

Fig. 1.3. Tectonic setting (modified after Wessely, 2006) of the central and northern Vienna Basin. Black dots correspond to investigated wells of this thesis.

The VB originated in the early Miocene, as a series of small piggy-back sub-basins, herein after referred to as proto-Vienna Basin, on the frontal part of the N- to NW-propagating thrust belt of the Eastern Alps (Jiřiček and Seifert, 1990; Fodor, 1995; Decker, 1996; Lee and Wagreich, 2017). Within these piggy-back basins, marine sedimentation commenced during the middle Burdigalian (= Ottnangian) (Harzhauser et al., 2019). Marine sedimentation remained within the VB from the initiation to the Serravallian/Tortonian boundary (~11.6 Ma; Harzhauser et al., 2019). During the late early Miocene, the Vienna Basin became accentuated by the Styrian tectonic phase and depocenters developed in the northern and central Vienna Basin (Wessely, 2006). Marine sedimentation prevailed in the northern proto-VB during the early Miocene and extended into the S during the middle Miocene (Harzhauser et al., 2019). The tectonic regime of the VB changed from the early to the middle Miocene to predominating extensional tectonics, due to the lateral extrusion of the Eastern Alps (Royden, 1985, 1988; Fodor, 1995; Decker, 1996; Decker et al., 2005; Hölzel et al., 2008, 2010; Lee and Wagreich, 2017, Siedl et al., 2020). Consequently, complex fault systems developed, providing hydrocarbon traps and giving the VB its present shape (Kröll and Wessely, 1993; Hamilton and Johnson, 1999; Hamilton et al., 2000; Wessely, 2006; Hölzel et al., 2010).

Despite the afford of decades, the first initiation of Neogene deposits and their contact to the pre-Neogene basement as well as correlation of single deposits and whole formations remained ambiguous due to the complex tectonic setting of the Vienna Basin (see following chapters). Hence, the results of the project, leading to this thesis, and accompanying publications, improve the knowledge of the paleogeographic, -topographic, -ecologic and -faunistic evolution of the VB.

1.3. Foraminifers - biostratigraphy and paleoecology

Foraminifers are unicellular mostly marine protists with an external shell (test), typically made of organic cements, sedimentary particles or calcium carbonate (Loeblich and Tappan, 1992; Hansen, 2002; Sen Gupta, 2002). Foraminifers are intensely studied protozoans due to their high fossilization potential (e.g., Goldstein, 2002; Murray, 2006; Schiebel and Hemleben, 2007). They inhabit a broad range of ecological habitats from shallow marine lagoons, to the abyssal plain as well as hypersaline lagoons, brackish marshes and estuaries (Armstrong and Brasier, 2005; Murray, 2006). Within the fossil record, foraminifers are documented since the Cambrian and trace markers suggest their origination during the Precambrian (Pawlowski et al., 2003; Todo et al., 2005; Lipps, 2017). Thus, foraminifers are excellent biostratigraphic and paleoenvironmental markers. First, benthic foraminifers (living stationary or agile on the seafloor or within the sediment) were the first to be documented, whereas planktonic foraminifers (freely floating within the water column) were first documented from Jurassic strata (Sen Gupta, 2002; Spezzaferri and Spiegler, 2007). Planktonic species are excellent biostratigraphic markers and allow a reconstruction concerning productivity, surface water temperature and salinity (Bolli et al., 1985; Gradstein et al., 2004; Schiebel and Hemleben, 2017), whereas benthic foraminifers are mostly used to reconstruct paleoecological conditions like salinity, bottom water temperature, nutrient flux, dissolved oxygen and paleobathymetry (e.g., Murray 1991, 2006). Larger benthic foraminifers gained also stratigraphical importance since the Paleozoic, whereas smaller benthics are only of regional stratigraphic importance (Grill, 1941, 1943; Papp and Turnovsky, 1953; Papp et al., 1978; Gradstein et al., 2004). Of the benthic foraminifers about 2500 genus level taxa were identified since the Cambrian, between 3200-4300 extant species, adopted a benthic lifestyle whereas only 40-50 show a planktonic lifestyle. About 1/3 (832) of the extant foraminiferal genera have an agglutinated test whereas the other 2/3 built their test with calcium carbonate (Loeblich and Tappan, 1987; Kaminski, 2014). However, recently modern high-throughput genetic sequencing suggests that agglutinated genera account for even more than 2/3 of all foraminiferal genera throughout the geological record (Pawlowski et al., 2014). These differences in test material further contributes to a broad variety of habitats inhabited by foraminifers, underlining their

importance to reconstruct paleoenvironments (e.g., Murray, 1991; 2006; Armstrong and Brasier, 2005).

1.3.1. Biostratigraphy of the VB

A biostratigraphic concept for the Miocene was introduced by Grill in 1994. Grill defined five different zones for the Badenian based on smaller benthic foraminifers, derived of several drillings of the Austrian Vienna Basin. Several authors afterwards used, extended and adapted these zones (e.g., Papp and Turnovsky, 1953; Papp, 1963; Papp et al., 1978; Bucur and Filipescu, 1994; Báldi, 1997; Cicha et al., 1998; Kováč et al., 1999; Lučić et al., 2001; Gebhardt et al., 2009; Zágor et al., 2009; Filipescu, 2011; Zágoršek et al., 2011; Bojar et al., 2012; Hladilová and Fordinal, 2013; Key et al., 2013; Nehyba, 2014; Schwarzhans et al., 2015; Hyžný et al., 2015; Harzhauser et al., 2017, 2019), leading to the nowadays widely used ecostratigraphic zonation of the Central Paratethys (Fig. 1.2). Normally, foraminifer-biozones are based on planktonic foraminifers (e.g., Filipescu and Silye, 2008; Iaccarino et al., 2011; Wade et al., 2011; Lirer et al., 2019) but due to the mostly restricted location of the Vienna Basin, global (planktonic) marker species could not be found in the area (Cicha et al., 1998; Harzhauser et al., 2019). Hence, this eco-biozones can appear in different settings in different times and their biostratigraphic constrains are only valid for the Vienna Basin, where they originated. Also, in this area they have to be used with caution and we rather suggest using lithostratigraphic and fossil based chronostratigraphic terms to determine and correlate sediments of the Vienna Basin to other Central Paratethys basins and the global record as will be explained in following chapters.

References

Abrantes, F., Voelker, A., Sierro, F.J., Naughton, F., Rodrigues, T., Cacho, I., Ariztegui, D., Brayshaw, D., Sicre, M.A., Batista, L., 2012. Paleoclimate Variability in the Mediterranean Region. In: Lionello P. (Eds.) The Climate of the Mediterranean Region. 1–86. https://doi.org/10.1016/B978-0-12-416042-2.00001-X.

Allen, M.B., Armstrong, H.A., 2008. Arabia–Eurasia collision and the forcing of mid-Cenozoic global cooling. Palaeogeography, Palaeoclimatology, Palaeoecology, 265, 52–58.

Armstrong, H.A., Brasier, M.D., 2005. Foraminifera. Microfossils. Blackwell Publishing, Cornwall, Second Edition, 304 pp.

Báldi, K., 1997. Assumed circulation pattern of the Central Paratethys through Badenian (Middle Miocene) times: quantitative paleoeceological analysis of foraminifera from borehole Tengelic 2 (SW Hungary). Acta Geologica Hungarica 40, p. 57–71.

Baldí, T., Seneš, J., 1975. OM – Egerien. Die Egerer, Pouzdraner, Puchkirchener Schichtengruppe und die Bretkaer Formation. Chronostratigraphie und Neostratotypen, Miozän der Zentralen Paratethys, 5. Verlag der Slowakischen Akademie der Wissenschaften, Bratislava, 577 p.

Bojar, A.V., Barbu, V., Bojar, H. P., 2012. Middle Miocene zeolite-bearing turbidites, Abrămuţ Basin (Pannonian Basin), NW Romania. Geological Quarterly, 56, 2, p. 261–268.

Bolli, H.M., Saunders, J.B., Perch-Nielsen, K., 1985. Plankton Stratigraphy Volume 1: Planktic foraminifera, calcareous nannoplankton and calpionellids. Cambridge University Press, Cambridge.

Bucur, I.I., Filipescu, S., 1994. Middle Miocene Red Algae from the Transylvanian Basin (Romania). Beiträge zur Paläontologie, 19, p. 39–47.

Cicha, I., Seneš, J., Tejkal, J., 1967. M3 (Karpatien). Die Karpatische Serie und ihr Stratotypus. Chronostratigraphie und Neostratotypen, Miozän der Zentralen Paratethys, 1. Verlag der Slowakischen Akademie der Wissenschaften, Bratislava.

Cicha, I., Rögl, F., Rupp, C., Čtyroký, J., 1998. Oligocene-Miocene foraminifera of the Central Paratethys. Abhandlungen der Senckenbergischen Naturforschenden Gesellschaft, 549, 325 p.

Decker, K., 1996. Miocene tectonics at the Alpine-Carpathian junction and the evolution of the Vienna Basin. Mitteilungen der Gesellschaft der Geologie und Bergbaustududenten in Österreich, 41, 33–44.

Decker, K., Peresson, H., Hinsch, R., 2005. Active tectonics and Quaternary basin formation along the Vienna Basin Transform fault. Quaternary Science Reviews, 24(3–4), 305–320.

Filipescu S., 2011. Cenozoic Lithostratigraphic units in Transylvania. In: Bucur I., Săsăran E. (Eds.) Calcareous Algae from Romanian Carpathians. Field Trip Guidebook. Presa Universitară Clujeană, p. 37–48.

Filipescu, S., Silye, L., 2008. New Paratethyan biozones of planktonic foraminifera described from the Middle Miocene of the Transylvanian Basin (Romania). Geologica Carpathica, 59(6), 537–544.

Fodor, L., 1995. From transpression to transtension: Oligocene-Miocene structural evolution of the Vienna basin and the East Alpine-Western Carpathian junction. Tectonophysics, 242(1–2), 151–182.

Gebhardt, H., Zorn, I., Roetzel, R., 2009. The initial phase of the early Sarmatian (Middle Miocene) transgression. Foraminiferal and ostracod assemblages from an incised valley fill in the Molasse Basin of Lower Austria. Austrian Journal of Earth Sciences, 102(2), 100–119.

Goldstein, S.T., 2002. Foraminifera: A Biological Overview. In: Sen Gupta, B.K. (Ed.), Modern Foraminifera, pp. 37–56. Kluwer Academic Publishers, Dordrecht-Boston-London.

Gradstein, F., Ogg, J., Smith, A., 2004. A Geologic Time Scale 2004. Cambridge University Press, Cambridge.

Grill, R., 1941. Stratigraphische Untersuchungen mit Hilfe von Mikrofaunen im Wiener Becken und den benachbarten Molasse-Anteilen. Oel und Kohle, 37, p. 595–602.

Grill, R., 1943. Über mikropaläontologische Gliederungsmöglichkeiten im Miozän des Wiener Beckens. Mitteilungen der Reichsanstalt für Bodenforschung, 6, p. 33–44.

Hamilton, W., Johnson, N ., 1999. The Matzen Project; rejuvenation of mature field. Petroleum Geoscience, 5, 119–125, https://doi.org/10.1144/petgeo.5.2.1190.

Hamilton, W., Wagner, L., Wessely, G., 2000. Oil and Gas in Austria. Mitteilungen der Österreichischen Geologischen Gesellschaft, 92, 235–262.

Hansen, H.J., 2002. Shell Construction in Modern Calcareous Foraminifera. In: Sen Gupta, B.K. (Ed.), Modern Foraminifera, pp. 57–70. Kluwer Academic Publishers, Dordrecht-Boston-London.

Harzhauser, M., Piller, W.E., 2007. Benchmark data of a changing sea. – Palaeogeography, Palaeobiogeography and Events in the Central Paratethys during the Miocene. Palaeogeography, Palaeoclimatology, Palaeoecology 253, 8–31.

Harzhauser, M., Theobalt, D., Strauss, P., Mandic, O., Carnevale, G., Piller, W.E., 2017. Miocene biostratigraphy and paleoecology of the Mistelbach Halfgraben in the northwestern Vienna Basin Lower Austria. Jahrbuch der Geologischen Bundesanstalt, 157, 57–108.

Harzhauser, M., Mandic, O., Kranner, M., Lukeneder, P., Kern, A. K., Gross, M., Carnevale, G. Jawecki, C., 2018. The Sarmatian/Pannonian boundary at the western margin of the Vienna Basin (City of Vienna, Austria). Austrian Journal of Earth Sciences, 111, 26–47.

Harzhauser, M., Theobalt, D., Strauss, P., Mandic, O., Piller, W.E., 2019. Seismic-based lower and middle Miocene stratigraphy in the northwestern Vienna Basin (Austria). Newsletters on Stratigraphy, 221–247.

Hladilová, Š., Fordinál, K., 2013. Upper Badenian Molluscs (Gastropoda, Bivalvia, Scaphopoda) from the Modra-Kráľová locality (Danube Basin, Slovakia). Mineralia Slovaca, 45, p. 35–44.

Hölzel, M., Wagreich, M., Faber, R., Strauss, P., 2008. Regional subsidence analysis in the Vienna Basin (Austria). Austrian Journal of Earth Science, 101, 88–98.

Hölzel, M., Decker, K., Zámolyi, A., Strauss, P., Wagreich, M., 2010. Lower Miocene structural evolution of the central Vienna Basin (Austria). Marine and Petroleum Geology, 27(3), 666–681.

Hyžný, M., Hudáčková, N., Szalma, Š., 2015. Taphonomy and diversity of Middle Miocene decapod crustaceans from the Novohrad-Nógrad Basin, Slovakia, with remarks on palaeobiography. Acta Geologica Slovaca: Ageos, 7, 2, p. 139–154.

Iaccarino, S.M., Di Stefano, A., Foresi, L.M., Turco, E., Baldassini, N., Cascella, A., Da Prato, S., Ferraro, L., Gennari, R., Hilgen, F.J., Lirer, F., Maniscalco, R., Mazzei, R., Riforgiato, F., Russo, B., Sagnotti,

L., Salvatorini, G., Speranza, F., Verducci, M., 2011. High-resolution integrated stratigraphy of the upper Burdigalian-lower Langhian in the Mediterranean: the Langhian historical stratotype and new candidate sections for defining its GSSP. Stratigraphy, 8, 199–215.

Jiříček, R., Seifert, P., 1990. Palaeogeography of the Neogene in the Vienna Basin and the adjacent part of the foredeep. In: Minaříková, D. and, Lobitzer, H., (Eds.), Thirty Years of Geological Cooperation between Austria and Czechoslovakia. Cesky Geologicky Ustav, Praha, pp. 89–105.

Kaminski, M.A., 2014. The year 2010 classification of the agglutinated foraminifera. Micropaleontology 60, 89–108.

Key, M.M., Zágoršek, K., Patterson, W.P., 2013. Paleoenvironmental reconstruction of the Early to Middle Miocene Central Paratethys using stable isotopes from bryozoan skeletons. International Journal of Earth Sciences, 102, p. 305–318.

Kováč M., Holcová K., Nagymarosy A., 1999: Paleogeography, paleobathymetry and relative sea-level changes in the Danube Basin and adjacent areas. Geologica Carpathica, 50, 4, p. 325–338.

Kováč, M., Baráth, I., Harzhauser, M., Hlavatý, I., Hudáčková, N., 2004. Miocene depositional systems and sequence stratigraphy of the Vienna Basin. Courier des Forschungs-Instituts Senckenberg, 246, 187–212.

Kröll A., Wessely G., 1993. Strukturkarte - Basis der tertiären Beckenfüllung 1:200.000. Erläuterung zu den Karten über den Untergrund des Wiener Beckens und der angrenzenden Gebiete. Geologische Bundesanstalt, Wien.

Lee, E.J., Wagreich, M., 2017. Polyphase tectonic subsidence evolution of the Vienna Basin inferred from quantitative subsidence analysis of the northern and central parts. International Journal of Earth Sciences, 106, 687–705.

Lirer, F., Foresi, L.M., Iaccarino, S.M., Salvatorini, G., Turco, E., Cosentino, C., Sierro, F.J., Caruso, A., 2019. Mediterranean Neogene planktonic foraminifer biozonation and biochronology. Earth-Science Reviews, 196, 102869.

Lipps, J.H., 2017. Precambrian Skeletonized Microbial Eukaryotes. In EGU General Assembly Conference Abstracts , 18395.

Loeblich, A.R., Tappan, H., 1987. Foraminiferal genera and their classification. Von Nostrand Reinhold Co., New York, 869p.

Loeblich, A.R., Tappan, H ., 1992. Present status of Foraminiferal Classification. In: Takayanagi, Y., Saito, T (Eds.), Studies in Benthic Foraminifera. Tokai University Press, 93–102.

Lučić, D., Saftić, B., Krizmanić, K., Prelogović, E., Britvić, V., Mesić, I., Tadej, J., 2001. The Neogene evolution and hydrocarbon potential of the Pannonian Basin in Croatia. Marine and petroleum Geology, 18, p. 133–147.

Márton, E., 2006. Paleomagnetic constraints for the reconstruction of the geodynamic evolution of the Middle Miocene-Pleistocene. In: Pinter, N., Grenerczy, G., Weber, J., Stein, S. and Medak, D., (Eds.), The Adria Microplate: GPS geodesy, tectonics and hazards, 55–64. Amsterdam: Kluwer Academic publisher.

Márton, E., Drobne, K., Cosovic, V., Moro, A., 2003. Palaeomagnetic evidence for Tertiary counterclockwise rotation of Adria. Tectonophysics, 377, 143–156.

Márton, E., Jelen, B., Tomljenovic, B., Pavelic, D., Poljak, M., Márton, P., Avanic, R., Pamic, J., 2006. Late Neogene counterclockwise rotation in the SW part of the Pannonian Basin. Geologica Carpathica, 57, 41–46.

Murray J.W., 1991. Ecology and Palaeoecology of Benthic Foraminifera. Longman Scientific and Technical, Harlow, Essex, 397 p.

Murray J.W., 2006. Ecology and Applications of Benthic Foraminifera. Cambridge University Press, Cambridge, 426 p.

Nehyba, S., 2014. Soft-sediment deformation structures in Lower Badenian (Middle Miocene) foreshore sands and their trigger mechanism (Carpathian Foredeep Basin, Czech Republic). Austrian Journal of Earth Sciences, 107, 2 p. 23–36.

Nevesskaja, L.A., Gontsharova, I.A., Paramonova, N.P., Popov, S.V., Babak, E.V., Bagdasarjan, K.G., Voronina, A.A., 1993. Identification book of Miocene bivalve molluscs of south-western Eurasia. Transactions of the Paleontological Institute, Russian Academy of Sciences, 247, 1–412.

Papp, A., 1963. Die biostratigraphische Gliederung des Neogens im Wiener Becken. Mitteilungen der Geologischen Gesellschaft Wien, 56, 1, p. 225–317.

Papp, A., Turnovsky, K., 1953. Die Entwicklung der Uvigerinen im Vindobon (Helvet und Torton) des Wiener Beckens. – Jahrbuch der Geologischen Bundesanstalt, 96, p. 117–142.

Papp, A., Rögl, F., Seneš, J., (Eds.), 1973. Miozän M2 – Ottnangien. Die Innviertler, Salgotarjaner, Bantapusztaer Schichtengruppe und die Rzehakia Formation. Chronostratigraphie und Neostratotypen, Miozän der Zentralen Paratethys 3. Verlag der Slowakischen Akademie der Wissenschaften, Bratislava, 841 p.

Papp, A., Marinescu, F., Seneš, J., (Eds.), 1974. M5 – Sarmatien (sensu E. Suess, 1866). Die Sarmatische Schichtengruppe und ihr Stratotypus. Chronostratigraphie und Neostratotypen, Miozän der Zentralen Paratethys 4. 707 p.

Papp, A., Cicha, I., Seneš, J., Steininger, F., (Eds.), 1978. Chronostratigraphie und Neostratotypen. Miozän der Zentralen Paratethys. Band VI: M4 Badenien Moravien, Wielicien, Kosovien. Verlag der Slowakischen Akademie der Wissenschaften VEDA, Bratislava, 279–284.

Papp, A., Jámbor, Á., Steininger, F.F., (Eds.), 1985. M6 – Pannonien (Slavonien und Serbien). Chronostratigraphie und Neostratotypen, Miozän der Zentralen Paratethys 7. 636 p.

Pawlowski, J., Holzmann, M., Berney, C., Fahrni, J., Gooday, A.J., Cedhagen, T., Habura, A., Bowser, S.S., 2003. The evolution of early Foraminifera. Proceedings of the National Academy of Sciences, 100(20), 11494–11498.

Pawlowski, J., Lejzerowicz, F., Esling, P., 2014. Next-generation environmental diversity surveys of foraminifera: preparing the future. The Biological Bulletin 227(2), 93–106.

Piller, W. E., Harzhauser, M., Mandic, O., 2007. Miocene Central Paratethys stratigraphy–current status and future directions. Stratigraphy, 4, 151–168.

Popov, S. V., Rögl, F., Rozanov, A. Y., Steininger, F. F., Shcherba, I. G., Kovac, M., 2004. Lithological-paleogeographic maps of Paratethys-10 maps late Eocene to Pliocene.

Rögl, F., 1996. Stratigraphic correlation of the Paratethys Oligocene and Miocene: Mitteilungen der Gesellschaft der Geologie-und Bergbaustudenten in Österreich, 41.

Rögl, F., 1998. Palaeogeographic Considerations for Mediterranean and Paratethys Seaways (Oligocene to Miocene). Annalen des Naturhistorischen Museums in Wien 99A, 279–310.

Royden, L.H., 1985. The Vienna basin: a thin skinned pull apart basin. In: Biddle K.T., Christie-Blick N., (Eds.), Strike-slip deformation, basin formation and sedimentation. SEPM Special Publication, 37, 319–339.

Royden, L.H., 1988. Late cenozoic tectonics of the Pannonian Basin System. In: Royden, L.H., Horváth, F., (Eds.). The Pannonian Basin. A Study in Basin Evolution. AAPG Mem., 45, 27–48.

Schiebel, R., Hemleben, C., 2007. Modern planktic foraminifera. Paläontologische Zeitschrift 79, 135–148.

Schiebel, R., Hemleben, C., 2017. Planktic foraminifers in the modern ocean. Berlin: Springer, 358 p.

Schulz, H.M., Bechtel, A., Sachsenhofer, R.F., 2005. The birth of the Paratethys during the Early Oligocene: From Tethys to an ancient Black Sea analogue?. Global and Planetary Change, 49(3–4), 163–176.

Schwarzhans, W., Bradić, K., Rundić, L., 2015. Fish-otoliths from the marine-brackish water transition from the Middle Miocene of the Belgrade area, Serbia. Paläontologische Zeitschrift, 89, 4, 815–837.

Seghedi, I., Downes, H., Szakács, A., Mason, P.R.D., Thirlwall, M.F., Rosu, E., Pécskay, Z., Márton, E., Panaiotu, C., 2004. Neogene-Quaternary magmatism and geodynamics in the Carpathian-Pannonian region: a synthesis. Lithos, 72, 117–146.

Sen Gupta, B.K. (Ed.), Modern Foraminifera, pp. 3–6. Kluwer Academic Publishers, Dordrecht-Boston-London.

Seneš, J., 1961. Paläogeographie des westkarpatischen Raumes in Beziehung zur übrigen Paratethys im Miozän. Geologické práce, 60, 1–56.

Siedl, W., Strauss, P., Sachsenhofer, R. F., Harzhauser, M., Kuffner, T., Kranner, M., 2020. Revised Badenian (middle Miocene) depositional systems of the Austrian Vienna Basin based on a new sequence stratigraphic framework. Austrian Journal of Earth Sciences, 113, 87–110.

Spezzaferri, S., Spiegler, D., 2007. Fossil planktic foraminifera (an overview). Paläontologische Zeitschrift 79, 149–167.

Steininger, F., Seneš, J., 1971. M1 – Eggenburgien. Die Eggenburger Schichtengruppe und ihr Stratotypus. Chronostratigraphie und Neostratotypen, Miozän der Zentralen Paratethys, 2. Verlag der Slowakischen Akademie der Wissenschaften, Bratislava.

Steininger, F., Rögl, F., Martini, E., 1976. Current Oligocene/Miocene biostratigraphic concept of the central Paratethys (middle Europe). Newsletters on Stratigraphy, 174–202.

Stevanović, P., Nevesskaja, L.A., Marinescu, F., Sokac, A., Jámbor, A., 1990. Pl1 – Pontien (sensu F. Le Play, N.P. Barbot, N. I. Andrusov). Chronostratigraphie und Neostratotypen, Neogen der Westlichen (—Zentralen‖) Paratethys 8. Verlag der Slowakischen Akademie der Wissenschaften, Bratislava, 952 p.

Todo, Y., Kitazato, H., Hashimoto, J., Gooday, A. J., 2005. Simple foraminifera flourish at the ocean's deepest point. Science, 307(5710), 689–689.

Wade, B. S., Pearson, P. N., Berggren, W. A., Pälike, H., 2011. Review and revision of Cenozoic tropical planktonic foraminiferal biostratigraphy and calibration to the geomagnetic polarity and astronomical time scale. Earth-Science Reviews, 104, p. 111–142.

Wessely, G., 1998. Geologie des Korneuburger Beckens. Beiträge Paläontologie, 23, 9–23.

Wessely, G., 2006. Niederösterreich. Geologie der Österreichischen Bundesländer. Geologische Bundesanstalt Wien, 416 pp

Zágor, K., Holcová, K., Nehyba, S., Kroh, A., 2009. The invertebrate fauna of the Middle Miocene (Lower Badenian) sediments of Kralice nad Oslavou (Central Paratethys, Moravian part of the Carpathian Foredeep). Bulletin of Geosciences, 84, 3.

Zagorchev, I.S., 2021. Geology of the Balkan Peninsula. Encyclopedia of Geology, 2, 382–407

Chapter 2

Biostratigraphic constraints for a Lutetian age of the subsurface Harrersdorf Unit in the northern Vienna Basin (Austria)

Matthias Kranner[1], Mathias Harzhauser[1], Fred Rögl[1], Stjepan Ćorić[2], Philipp Strauss[3]

[1] Geological-Paleontological Department, Natural History Museum Vienna, Burgring 7, 1010 Vienna, Austria; matthias.kranner@nhm-wien.ac.at, mathias.harzhauser@nhm-wien.ac.at, roegl.fred@aon.at

[2] Geological Survey of Austria, Neulinggasse 38, 1030 Vienna, Austria; stjepan.coric@geologie.ac.at

[3] OMV Exploration and Production GmbH, Trabrennstraße 6-8, 1020 Vienna, Austria; philipp.strauss@omv.com

Abstract

The formations underlying the Neogene filling of the Vienna Basin are still poorly documented. Only few hydrocarbon exploration drillings reached these units, but biostratigraphic data, stored in internal oil company reports, have never been published. Therefore, the correlation of subsurface lithostratigraphic units with those of the Rhenodanubian nappe system and the Magura nappe system, outcropping at the basin margins, is based so far on extrapolations. A recent drilling campaign in the Bernhardsthal oil field in the northern Vienna Basin in Austria reached the pre-Neogene basement and provided cuttings for biostratigraphic and paleoecological analyses. Based on these data, a Lutetian age (middle Eocene) and a bathyal depositional environment for the Flysch of the Harrersdorf Unit was documented.

The lithological similarity of the drilling with the Steinberg Flysch Formation of the Greifenstein Nappe and its Lutetian age suggests, that the middle Eocene part of the Harrersdorf Unit represents a continuation of the Greifenstein Nappe of the Rhenodanubian Flysch, rather than a frontal part of the Rača Nappe of the Magura Flysch as previously thought.

2.1. Introduction

During recent hydrocarbon prospection in the northern Vienna Basin, the Austrian oil company OMV drilled explorative boreholes in the Bernhardsthal oilfield in NW Austria close to the Czech border (Fig.

2.1) (see Harzhauser et al., 2018 for a geological overview and description of the Neogene deposits). Wessely et al. (1993) interpreted the pre-Neogene basement of the Bernhardsthal oilfield as Cretaceous to Eocene flysch. This interpretation was based solely on unpublished internal reports of the OMV and by extrapolation of drilling data from the Steinberg area. Within the current drilling campaign, borehole Bernhardsthal 11 (Be 11) reached these pre-Neogene units, which have not been described so far in terms of biostratigraphy.

Neogene deposits are documented in the borehole Bernhardsthal 11 down to ~2745 m (own data). Deep-water deposits of the lower Miocene Lužice Formation (Kováč et al., 2004) represent these basal Neogene units. Below this level, down to 3140 m, the pelitic facies of the Lužice Formation is replaced by an about 400-m-thick succession of flysch-type deposits of grey to dark grey marly shales alternating with glauconitic sandstone. First thin sections were produced already during the drilling campaign and pointed to the presence of pre-Neogene foraminifera, but a more precise assignment was impossible at the time. Therefore, OMV initiated detailed paleontological analyses of the microfauna and the calcareous nannoplankton to clarify the age and depositional setting of this enigmatic interval.

2.2. Geographic and geological setting

Borehole Bernhardsthal 11 (N 48°41'18.45'', E 16°50'53.25'') is situated in the northern Vienna Basin, which is an about 200 km long and 55 km wide**,** rhomboid pull-apart basin (Royden, 1985; Wessely, 1988, 2006), covering large parts of eastern Austria and extends into the Czech Republic in the North and Slovakia in the East (see Kováč et al., 2004 and Wessely, 2006 for detail description). Due to complex fault systems, the basin was internally subdivided into a series of horst and graben systems (Kröll and Wessely, 1993). Due to these structural elements, its Neogene basin-fill is an important target for hydrocarbon exploration (Hamilton et al., 1999). One of the major oil and gas fields in the Vienna Basin is the Bernhardsthal oil field in NE Austria close to the Czech Republic border (Harzhauser et al., 2018).

Within the Bernhardsthal oil field, the Miocene basin fill is in direct vicinity and sphere of influence of the Steinberg fault (Fig. 2.1), roughly striking in SSW–NNE direction with field Bernhardsthal in the

NNW. Due to their economic importance, numerous boreholes have penetrated the Neogene deposits (Kröll and Wessely, 1993; Harzhauser et al., 2018).

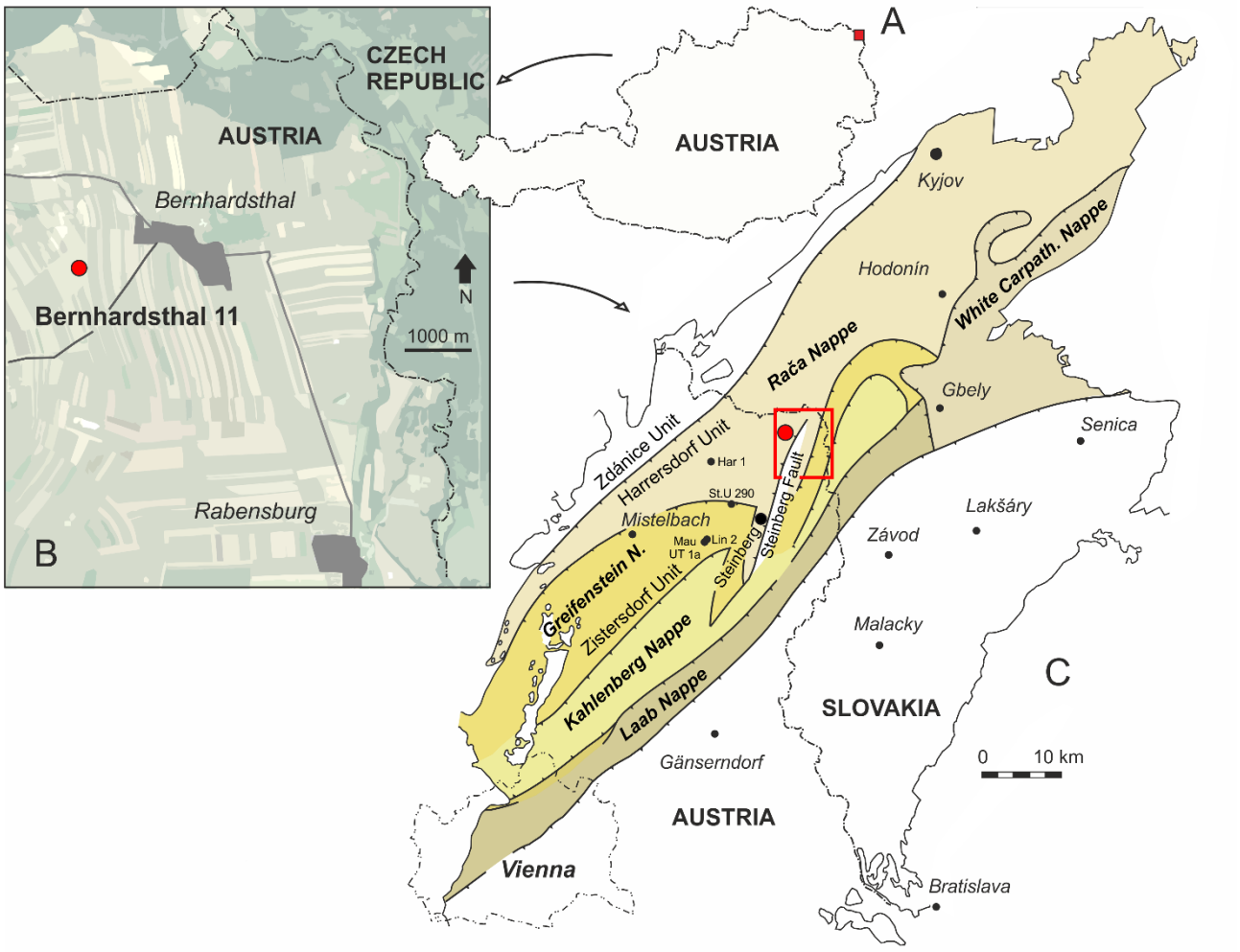

Fig. 2.1: A: Geographic and geological setting of the study area at the Austrian-Czech boundary and **B:** position of the borehole Be 11. **C:** Subsurface distribution of the Rhenodanubian and Magura flysch units in the northern Vienna Basin, compiled from Rammel (1989) and Wessely et al. (1993). The location of Be 11 is shown in the red insert. Note that the boundary between the Greifenstein und Rača nappes as proposed by Wessely et al. (1993) is hypothetical and the Harrersdorf Unit might rather represent a continuation of the Greifenstein Nappe.

2.3. Material and methods

Sixteen cutting samples from the Bernhardsthal Be 11 core interval from 2745 to 3140 m were analyzed (see Fig. 2.2 for sample position). The sedimentological analysis within this project is based on onsite logging, visual analysis of core samples and cuttings. Core samples and cuttings from the core interval above 2745 m contained early Miocene microfaunas (Harzhauser et al., 2018a) and are not discussed herein. Cuttings were taken and cleaned onsite. To widen the sampling interval of the cuttings, four consecutive cutting samples with a standard sample distance of 2.5 m were washed and sieved

together (e.g., 2747.5, 2750, 2752.5, 2755 m). Each sample was treated with diluted H_2O_2 (12%) for several hours and washed afterwards with tab water and sieved through a set of standard sieves. The samples were dried at 40 °C and then split with a microsplitter (as described in Rupp, 1986). The specimens were picked and counted for size fractions 500–250 µm, 250–125 µm and 125–63 µm. For identification of foraminifers several different publications were used (e.g.: Bindiu–Haitonic et al.,2017; Bubík and Kaminski, 2004; Cicha et al., 1998; Loeblich and Tappan, 1987; Papp et al., 1973; Rögl and Spezzaferii, 2003).

In addition, cutting samples from 2855 m, 2930 m, 2945 m, 3040 m, 3070 m and 3100 m were analyzed for calcareous nannoplankton, following standard preparation methods as described in Perch-Nielsen (1985). The standard nannoplankton zonation of Martini (1971) was used for biostratigraphic attribution of investigated material. All samples are barren of macrofossils. SEM (scanning electron microscope) micrographs were taken at the Natural History Museum Vienna. All illustrated foraminifers are stored in the micropaleontological collection of the Natural History Museum Vienna; nannoplankton samples are stored in the Geological Survey, Vienna. Lists of all recorded calcareous nannoplankton and foraminiferal taxa are given in tables 2.1 and 2.2, including authors and years of description. To warrant readability, authors and years of descriptions are not repeated in the following text.

Sedimentological data were logged onsite during drilling by OMV. In addition, wire-log data were provided by OMV for analysis (GR = natural gamma radiation, RES = resistivity).

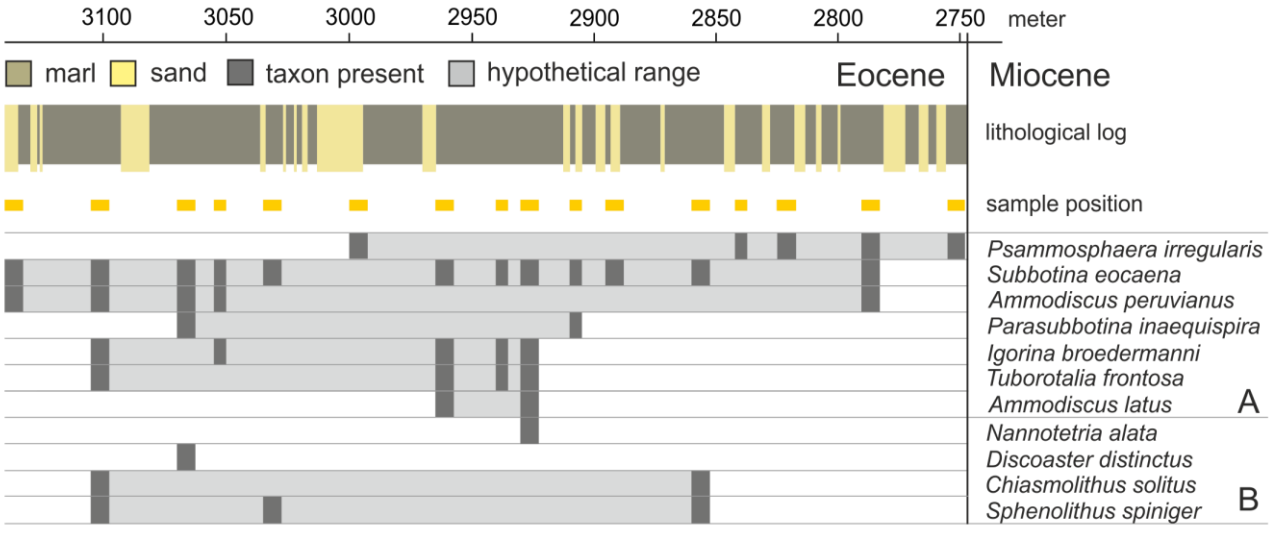

Fig. 2.2: The Eocene part of the Be 11 borehole with sample positions. The occurrences of important taxa of foraminifers (A) and calcareous nannoplankton (B) correlated with the lithological log.

2.4. Results

2.4.1. Lithology and wire-log pattern

Grey to dark grey marly shales, intercalated by thin glauconitic sandstone layers characterize the studied part of the Be 11 core (2745–3140 m) (Fig. 2.2). This lithological alternation is expressed in wire-logs by serrated shale-line intervals alternating with cylinder-shaped or funnel shaped sand bodies (e.g., 2990–3120 m, 3000–3025 m). No trends or cyclicities can be seen and a spectral analysis failed to detect any significant periods. The wire-log patterns differ considerably from those of the overlying Miocene deposits, which display a strikingly cyclic succession of bell-shaped intervals (Fig. 2.3).

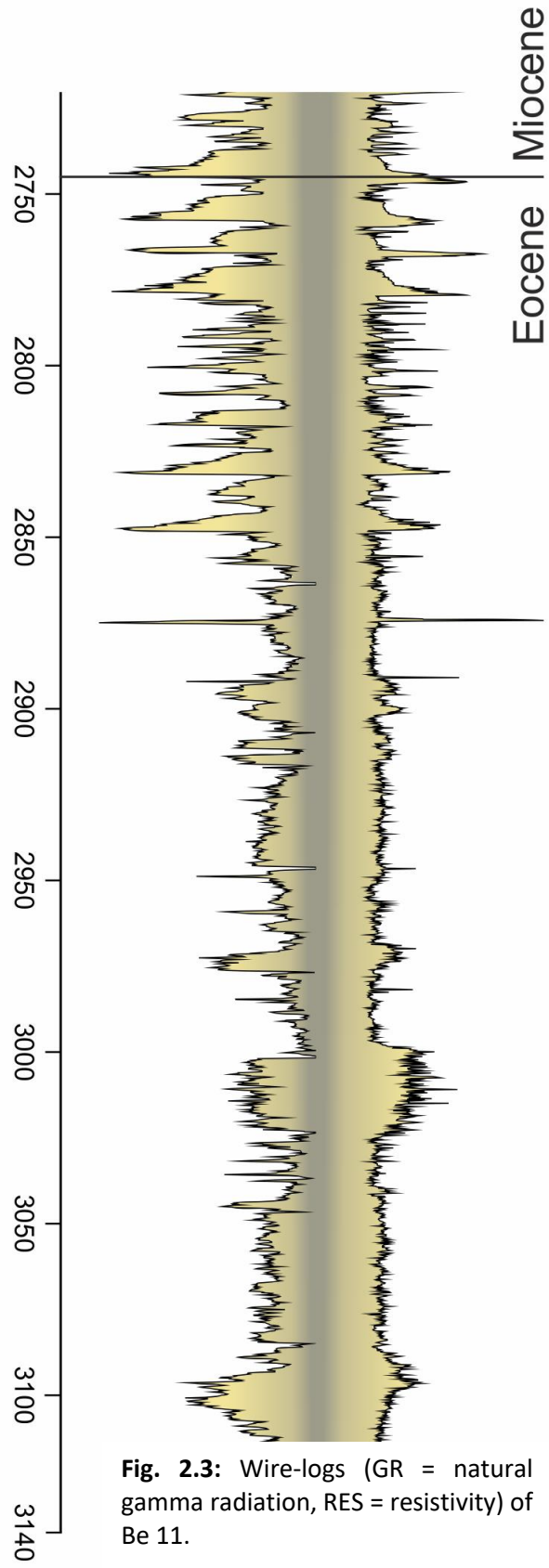

Fig. 2.3: Wire-logs (GR = natural gamma radiation, RES = resistivity) of Be 11.

2.4.2. Micropaleontological data

2.4.2.1. Calcareous nannoplankton**:** The samples yield a moderately diverse assemblage of 51 taxa; individual samples contained 11 to 23 taxa (Table 2.1; Fig. 2.4 A–O). *Coccolithus formosus* (Fig. 2.4 D), *Coccolithus pelagicus* (Fig. 2.4 E), *Reticulofenestra dictyoda* and *Cyclicargolithus floridanus* (Fig. 2.F–G) occur in all samples. *Nannotetrina alata, Discoaster distinctus, Chiasmolithus solitus, Reticulofenestra umbilicus, Lophodolithus nascens* and *Sphenolithus spiniger* are frequent taxa as well. Other species, documented from the lowermost sample (3100 m) to the top sample (2885 m) are *Sphenolithus moriformis* (Fig. 2.4M), *Chiasmolithus grandis*, *Zygrhablithus bijugatus*, *Chiasmolithus oamaruensis* and *Discoaster kuepperi*.

Table 2.1: Calcareous Nannoplankton taxa from the Be 11 borehole (1/0 = presence/absence).

Species	2855	2930	2945	3040	3070	3100
Arkhangelskiella cymbiformis Vekshina, 1959	1	0	0	0	0	0
Blackites sp.	0	0	0	0	0	1
Braarudosphaera bigelowii (Gran and Braarud 1935) Deflandre, 1947	1	0	0	0	0	0
Campylosphaera dela (Bramlette and Sullivan, 1961) Hay and Mohler, 1967	0	0	0	0	0	1
Chiasmolithus grandis (Bramlette and Riedel, 1954) Radomski, 1968	0	1	0	1	1	1
Chiasmolithus oamaruensis (Deflandre, 1954) Hay *et al.*, 1966	1	0	0	1	0	1
Chiasmolithus solitus (Bramlette and Sullivan, 1961) Locker, 1968	1	0	0	0	0	1
Chiasmolithus sp.	0	0	1	0	0	0
Coccolithus formosus (Kamptner, 1963) Wise, 1973	1	1	1	1	1	1
Coccolithus pelagicus (Wallich 1877) Schiller, 1930	1	1	1	1	1	1
Cribrocentrum erbae Fornaciari, Agnini, Catanzariti and Rio in Fornaciari et al. 2010	0	0	0	1	0	0
Cribrosphaerella ehrenbergii (Arkhangelsky, 1912) Deflandre in Piveteau, 1952	1	0	0	0	0	0
Cyclagelosphaera margerelii Noël, 1965	0	1	0	0	0	0
Cyclicargolithus floridanus (Roth and Hay, *in* Hay *et al.*, 1967) Bukry, 1971	1	1	1	1	1	1
Dictyococcites hesslandii Haq 1971 1	0	0	0	1	1	0
Discoaster barbadiensis Tan, 1927	0	0	0	0	0	1
Discoaster deflandrei Bramlette and Riedel, 1954	0	0	0	1	0	0
Discoaster distinctus Martini, 1958	0	0	0	0	1	0
Discoaster kuepperi Stradner, 1959	1	0	1	0	0	1
Discoaster lodoensis Bramlette and Riedel, 1954	1	0	1	0	0	1
Helicosphaera ampliaperta Bramlette and Wilcoxon, 1967	1	0	0	0	0	0
Helicosphaera bramlettei (Müller, 1970) Jafar and Martini, 1975	0	0	0	0	1	1

Helicosphaera euphratis Haq, 1966	1	0	0	1	0	0
Helicosphaera seminulum Bramlette and Sullivan, 1961	0	0	0	0	0	1
Isthmolithus recurvus Deflandre *in* Deflandre and Fert, 1954	0	0	0	1	0	0
Lophodolithus mochlophorus Deflandre *in* Deflandre and Fert, 1954	0	0	0	1	0	1
Lophodolithus nascens Bramlette and Sullivan, 1961	0	1	0	0	0	0
Micrantholithus sp.	0	0	0	1	0	1
Micula staurophora (Gardet, 1955) Stradner, 1963	1	0	0	0	0	0
Nannotetrina alata (Martini, in Martini and Stradner 1960) Haq and Lohmann, 1976	0	0	1	0	0	0
Neochiastozygus sp.	1	0	0	0	0	0
Pontosphaera exilis (Bramlette and Sullivan, 1961) Romein, 1979	0	1	0	1	0	0
Pontosphaera sp.	1	0	0	0	0	0
Reticulofenestra dictyoda (Deflandre *in* Deflandre and Fert, 1954) Stradner *in* Stradner and Edwards, 1968	1	1	1	1	1	1
Reticulofenestra hillae Bukry and Percival, 1971	0	1	0	1	0	0
Reticulofenestra minuta Roth, 1970	0	0	0	1	0	0
Reticulofenestra sp.	0	0	0	0	0	1
Reticulofenestra umbilicus (Levin, 1965) Martini and Ritzkowski, 1968	0	0	1	1	1	0
Sphenolithus dissimilis Bukry and Percival, 1971	0	1	0	0	0	0
Sphenolithus editus Perch-Nielsen *in* Perch-Nielsen *et al.*, 1978	0	0	1	1	0	0
Sphenolithus moriformis (Brönnimann and Stradner, 1960) Bramlette and Wilcoxon, 1967	1	1	0	1	1	1
Sphenolithus radians Deflandre *in* Grassé, 1952	1	1	1	0	0	0
Sphenolithus spiniger Bukry, 1971	1	0	0	1	0	1
Thoracosphaera saxea Stradner, 1961	0	0	0	0	1	0
Toweius callosus Perch-Nielsen, 1971	0	0	1	0	0	0
Toweius rotundus Perch-Nielsen *in* Perch-Nielsen *et al.*, 1978	0	0	0	1	0	0
Toweius sp.	1	0	0	0	0	0
Tribrachiatus orthostylus Shamrai, 1963	0	0	0	0	0	1
Watznaueria barnesiae (Black *in* Black and Barnes, 1959) Perch-Nielsen, 1968	1	0	0	1	0	0
Watznaueria fossacincta (Black, 1971) Bown *in* Bown and Cooper, 1989	0	0	1	0	0	0
Zygrhablithus bijugatus (Deflandre in Deflandre and Fert, 1954) Deflandre, 1959	1	0	1	1	1	0

2.4.2.1. Foraminifera: The core interval 2745–3140 m provided only moderately to poorly preserved foraminifers. In total, 42 foraminiferal taxa have been identified (Table 2.2, Figs 5 A–L, 6 A–L, 7 A–L). The maximum diversity ranges around 21–15 taxa in samples 2922.5–2930 m, 2935–2940 m and 2957.5–2965 m; all other samples display a very low diversity ranging from 3 to 10 taxa. Planktic

foraminifera are more frequent and represented by small sized specimens of *Subbotina eocaena* (Fig. 2.5 D–G), *Igorina salisburgensis* (Fig. 2.5 C), *Igorina broedermanni* (Fig. 2.5 B), *Acarinina bullbrooki* (Fig. 2.5 A), *Turborotalia frontosa* (Fig. 2.5 L), *Pseudohastigerina wilcoxensis* (Fig. 2.5 H), *Globorotaloides eovariabilis* (Fig. 2.5 J), *Parasubbotina inaequispira* (Fig. 2.5 K) and *Pseudohastigerina* sp. (Fig. 2.5 I). The most abundant benthic taxa are *Glomospira charoides* (Fig. 2.6 D–E), *Glomospira gordialis* (Fig. 2.6 F), *Ammodiscus peruvianus* (Fig. 2.6 B), *Ammodiscus tenuissimus*, *Ammodiscus cretaceous* (Fig. 2.6 C), *Lituotuba lituiformis* (Fig. 2.6 A), *Psammosphaera irregularis* (Fig. 2.6 G–H), *Karrerulina conversa* (Fig. 2.6 J), *Bathysiphon saidi*, *Bathysiphon* sp. and *Ammobaculites* sp. (Fig. 2.7 L) and are accompanied by *Melonis pompilioides* (Fig. 2.7 B–C), *Cibicides westi* (Fig. 2.7 F), *Cibicidoides* sp. (Fig. 2.7 E), *Pullenia* sp. (Fig. 2.7 I), *Hyperammina* sp. (Fig. 2.7 G), *Anomalinoides* sp. (Fig. 2.7 H), *Rhabdammina* sp. (Fig. 2.7 J), *Psammosiphonella* sp. (Fig. 2.7 K) and *Caucasina coprolithoides* (Fig. 2.7 K).

Table 2.2: Foraminifera taxa from the Be 11 borehole (1/0 = presence/absence).

Species	2747,5 - 2755	2782,5 - 2790	2817	2845 - 2850	2852,5 - 2860	2887,5 - 2895	2905 - 2910	2922,5 - 2930	2935 - 2940	2957,5 - 2965	2992,5 - 3000	3075,5 - 3035	3050 - 3055	3062,5 - 3070	3097,5 - 3105	3132,5 - 3140
Acarinina bullbrooki (Bolli, 1957)	0	0	0	0	0	0	0	1	1	1	0	0	1	0	1	0
Ammobaculites sp.	0	0	0	0	0	0	0	0	0	1	0	0	0	1	0	0
Ammodiscus cretaceus (Reuss, 1845)	0	0	1	0	0	0	1	0	0	0	0	0	0	1	0	0
Ammodiscus peruvianus (Berry, 1928)	0	1	0	0	0	0	0	0	0	0	0	0	1	1	1	1
Ammodiscus tenuissimus Grzybowski, 1898	0	0	0	1	1	0	1	0	0	0	0	0	0	1	1	0
Anomalinoides sp.	0	0	0	0	0	0	0	1	0	0	0	0	0	0	0	0
Bathysiphon saidi (Anan, 1994)	0	0	1	0	0	1	1	1	1	1	0	0	0	1	1	1
Bathysiphon sp. 1	0	0	0	1	0	0	0	0	1	0	1	1	0	1	1	1
Bathysiphon sp. 2	0	0	0	0	0	0	0	1	0	0	0	0	0	0	0	0
Caucasina coprolithoides (Andreae, 1884)	0	1	1	0	0	0	0	1	1	0	0	0	0	0	0	0
Cibicides westi (Howe, 1939)	0	0	0	0	0	0	0	0	0	0	0	0	0	1	0	1
Cibicidoides pseudoungerianus (d'Orgigny, 1846)	0	0	0	0	0	0	0	0	0	1	0	0	0	0	0	1
Cibicidoides sp.	0	0	0	0	0	0	0	0	0	1	0	0	0	1	0	0
Cibicidoides ungerianus (d'Orgigny, 1846)	1	0	0	0	1	0	0	0	1	0	0	0	0	0	0	0
Dentalina sp.	1	0	0	0	1	0	0	1	1	1	0	0	0	0	0	0
Globocassidulina oblonga (Reuss, 1850)	0	0	0	0	0	0	0	1	0	0	0	0	0	0	0	0
Globorotaloides eovariabilis Huber and Pearson, 2006	0	0	0	0	0	0	0	1	0	0	0	0	0	0	0	0
Glomospira charoides (Jones and Parker, 1860)	0	0	0	0	0	0	0	0	1	1	1	0	1	1	1	1

Glomospira gordialis (Jones and Parker, 1860)	0	0	0	0	0	0	0	1	0	1	1	0	1	0	1	1
Gonatosphaera inflata Bermúdez, 1949	0	0	0	0	0	0	0	1	0	0	0	0	0	0	0	0
Gyroidinoides sp.	0	0	0	0	0	0	0	0	0	0	0	0	0	1	1	0
Haplophragmoides walteri (Grzybowski, 1898)	0	0	0	0	0	0	0	1	0	0	0	0	0	0	0	0
Heterolepa dutemplei (d'Orbigny, 1846)	0	1	0	0	0	0	0	0	0	1	0	0	0	0	0	0
Hormosina veloscoensis (Cushman, 1926)	0	0	0	0	0	0	1	0	0	0	0	0	0	0	0	0
Igorina broedermanni (Cushman and Bermúdez, 1949)	0	0	0	0	0	0	0	1	1	1	0	0	1	0	1	0
Igorina salisburgensis (Gohrbandt, 1967)	0	0	0	0	0	0	0	0	1	1	0	0	1	0	1	0
Karrerulina conversa (Grzybowski, 1901)	0	0	0	0	1	0	1	0	1	1	0	1	0	0	1	1
Lenticulina cf. *inornata* (d'Orbigny, 1846)	0	0	0	0	0	0	0	1	0	0	0	0	0	1	1	0
Lituotuba lituiformis (Brady, 1879)	0	0	0	0	0	0	0	1	0	1	0	0	0	0	0	0
Melonis pompilioides (Fichtel and Moll, 1798)	0	0	0	0	1	0	0	0	1	1	0	0	1	0	0	0
Parasubbotina inaequispira (Subbotina, 1953)	0	0	0	0	0	0	1	0	0	0	0	0	0	1	0	0
Pleurostomella alazanensis Cushman, 1925	0	0	0	0	0	0	0	1	0	0	0	0	0	0	0	0
Psammosiphonella sp.	0	0	0	0	0	0	0	1	0	0	0	0	0	0	0	0
Psammosphaera irregularis (Grzybowski, 1896)	1	1	1	1	0	0	0	0	0	0	1	0	0	0	0	0
Pseudohastigerina sp.	0	0	0	0	0	0	0	0	1	0	0	0	0	0	1	0
Pseudohastigerina wilcoxensis (Cushman and Ponton, 1932)	0	0	0	0	0	1	0	1	1	0	0	0	0	1	1	0
Pullenia bulloides (d'Orbigny, 1826)	0	0	0	0	0	0	0	1	0	0	0	0	1	0	0	1
Pullenia sp.	0	0	0	0	0	0	0	0	0	1	0	0	0	0	0	0
Rhabdammina sp.	0	0	0	0	0	0	0	1	0	0	0	0	0	0	0	0
Subbotina eocaena (Guembel, 1868)	0	1	0	0	1	1	1	1	1	1	0	1	1	1	1	1
Tuborotalia frontosa (Subbotina, 1953)	0	0	0	0	0	0	0	1	1	1	0	0	0	0	1	0
Uvigerina eocaena Gümbel, 1868	0	0	0	0	0	0	0	0	0	0	0	0	0	1	0	0

2.5. Discussion

2.5.1. Biostratigraphy and Paleoecology

2.5.1.1. Calcareous nannoplankton: Assemblages are characterized by the high number of species which display a stratigraphic overlap during the middle Eocene, characterizes the calcareous nannoplankton assemblages. *Nannotetrina alata* and *Discoaster distinctus* are restricted to the Lutetian and are typical for the standard Calcareous Nannoplankton Zone NP15 (Martini, 1971). *Lophodolithus nascens* appears already during the Selandian Zone NP6 and has its last occurrence during the Lutetian Zone NP15 (Perch-Nielsen, 1985) and *Sphenolithus spiniger* ranges from the latest

Ypresian NP14 zone to the Bartonian Zone NP17 (Perch-Nielsen, 1985; Fornaciari et al., 2010). Similarly, the occurrence of *Chiasmolithus solitus*, ranging from the Thanetian Zone NP9 to the Lutetian Zone NP16 (Perch-Nielsen, 1985; Vandenberghe et al., 2012), does not contradict a Lutetian age (Bramlette and Sullivan, 1961).

At first sight, a Priabonian age might be assumed based on the occurrences of *Chiasmolithus oamaruensis* (2855, 3040, 3100 m depth), *Isthmolithus recurvus* (3040 m depth), *R. umbilicus (2945, 3040, 3070 m depth) and C. erbae* (3040 m depth) (Perch-Nielsen, 1985; Vandenberghe et al., 2012). These Priabonian taxa, however, are scarce and are contrasted by a large number of nannoplankton specimens of Lutetian age. Moreover, a Priabonian age would be in conflict with the foraminiferal data (see below). Therefore, several cuttings from the overlaying Miocene deposits have been checked for Priabonian species, which indeed were frequently found (Harzhauser et al., 2018a). This suggests major reworking of upper Eocene nannoplankton during the Miocene. Consequently, the scarce Priabonian taxa are interpreted as borehole contamination due to downfall during the drilling process.

Aside from Priabonian contamination, the assemblages also yields Cretaceous and lower Eocene nannoplankton. Reworking of Mesozoic nannoplankton (especially from Upper Cretaceous units) is documented throughout the core interval by the occurrence of species, such as *Arkhangelskiella cymbiformis*, *Cribrosphaerella ehrenbergii*, *Cyclagelosphaera margerelii*, *Micula staurophora*, *Watznaueria barnesiae* and *Watznaueria fossacincta* (e.g., Bown and Cooper, 1998; Lees and Bown, 2005). Similarly, lower Eocene strata became eroded, indicated by the occurrence of *Coccolithus formosus, Discoaster kuepperi*, *Discoaster lodoensis*, *Toweius rotundus* and *Sphenolithus editus* (Perch-Nielsen, 1985; Vandenberghe et al., 2012). The uppermost samples from depth of 2855 and 2930 m contain scarce *Helicosphaera ampliaperta* and *Sphenolithus dissimilis, which are* lower Miocene taxa (Young, 1998; Raffi et al., 2006; Bergen et al. 2017), indicating further downhole contamination from lower Miocene sediments (Harzhauser et al., 2018a).

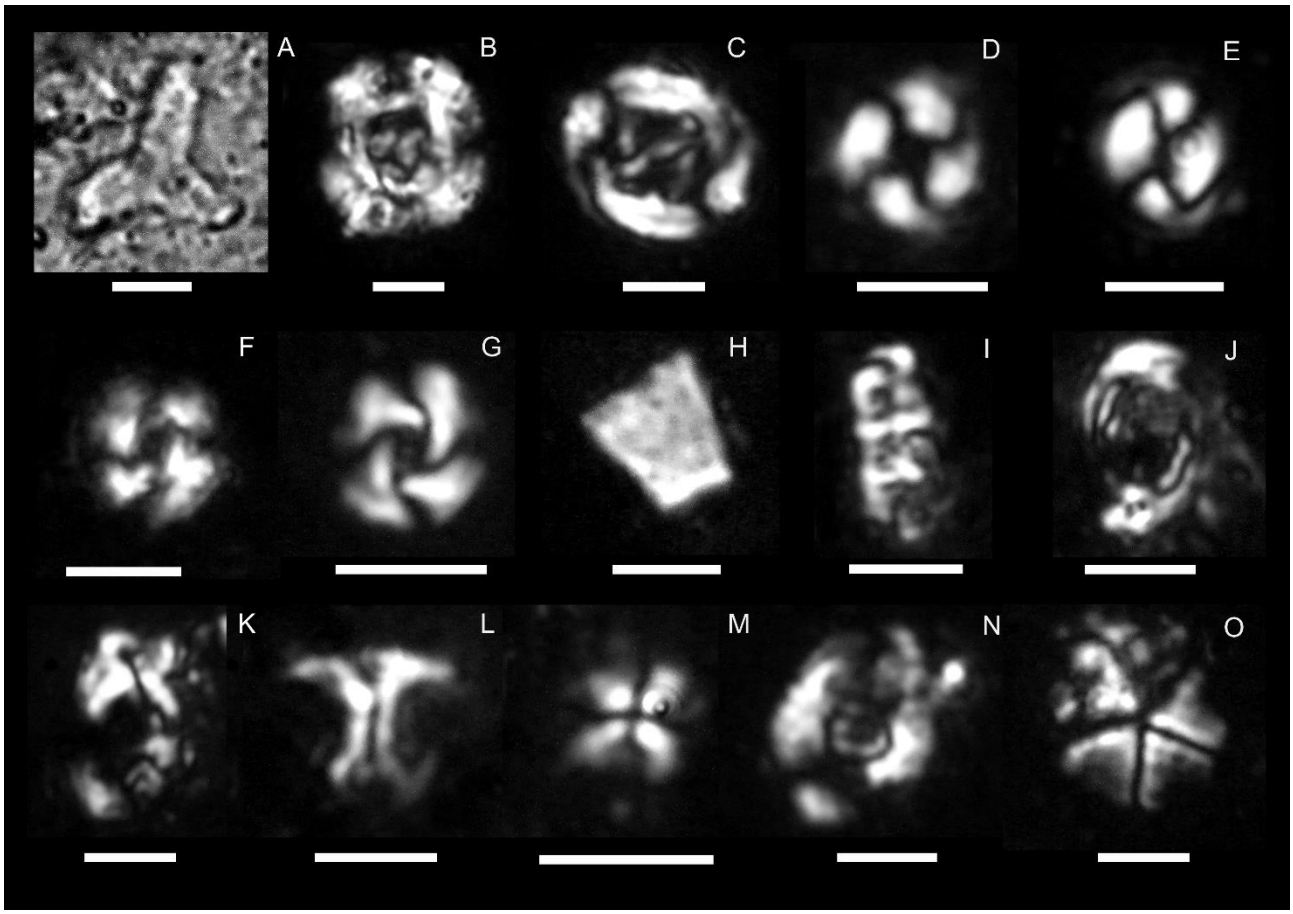

Fig. 2.4: Calcareous Nannoplankton from Be 11. **A:** *Tribrachiatus orthostylus* Shamrai, 1963 (3100 m), **B:** *Reticulofenestra umbilicus* (Levin, 1965) Martini and Ritzkowski, 1968 (3040 m), **C:** *Chiasmolithus solitus* (Bramlette and Sullivan, 1961) Locker, 1968 (3100 m), **D:** *Coccolithus formosus* (Kamptner, 1963) Wise, 1973 (3100 m), **E:** *Coccolithus pelagicus* (Wallich 1877) Schiller, 1930 (3040 m), **F–G:** *Cyclicargolithus floridanus* (Roth and Hay, *in* Hay *et al.*, 1967) Bukry, 1971 (3040 m), **H:** *Braarudosphaera bigelowii* (Gran and Braarud, 1935) Deflandre, 1947 (2855 m), **I:** *Isthmolithus recurvus* Deflandre *in* Deflandre and Fert, 1954 (3040 m), **J:** *Campylosphaera dela* (Bramlette and Sullivan, 1961) Hay and Mohler, 1967 (3100 m), **K:** *Helicosphaera ampliaperta* Bramlette and Wilcoxon, 1967 (2855 m), **L:** *Discoaster kuepperi* Stradner, 1959 (2945 m), **M:** *Sphenolithus moriformis* (Brönnimann and Stradner, 1960) Bramlette and Wilcoxon, 1967 (3100 m), **N:** *Helicosphaera seminulum* Bramlette and Sullivan, 1961 (3100 m), **O:** *Micrantholithus flos* Deflandre *in* Deflandre and Fert, 1954 (3040 m); scale bar = 5 µm.

2.5.1.2. Foraminifera: The foraminiferal assemblages from core interval 2745–3140 m contains mainly taxa, which are restricted to the Ypresian and Lutetian. Species, such as *Igorina salisburgensis*, *Igorina broedermanni*, *Acarinina bullbrooki*, *Glomospira gordialis, Turborotalia frontosa*, *Pseudohastigerina wilcoxensis* and *Parasubbotina inaequispira*, characterize the plankton biozones E7–E8 (Berggren and Pearson, 2005; Kaminski and Gradstein, 2005; Berggren et al. 2006; Olsson and Hemleben 2006; Pearson et al., 2006). Stratigraphically wider ranges are covered by the planktic *Subbotina eocaena* (highest occurrence 2782.5–2790 m), which ranges from the Ypresian to the Chattian (Wade et al.

2018), the agglutinated foraminifer *Psammosphaera irregularis* (highest occurrence: cuttings 2747.5–2755 m), which ranges from the Cretaceous to the Priabonian (Kaminski and Gradstein, 2005; Kaminski and Ortiz, 2014; Benedetti, 2017) and by the planktic *Globorotaloides eovariabilis,* which ranges from the Ypresian to the Chattian (Pearson and Wade, 2009) or even to the Aquitanian (Coxall and Spezzaferri, 2018). Therefore, the stratigraphic ranges of the foraminifera species display a distinct overlap during the Lutetian.

In terms of ecological requirements, the assemblage is typical for deep-water sedimentary successions as described by Golonka and Waśkowska (2012). Especially the high abundance of planktic and agglutinated foraminifera is a clear indicator for bathyal to lower bathyal water conditions (Armstrong and Brasier, 2005). Additionally, the abundance of *Psammosphaera irregularis, Ammodiscus* and *Glomospira* indicate upper to lower bathyal environments with reduced oxygen levels (Kaminski and Gradstein, 2005; Murray, 1991, 2006; Cimerman et al., 2006; Kaminski and Ortiz, 2014; Benedetti, 2017).

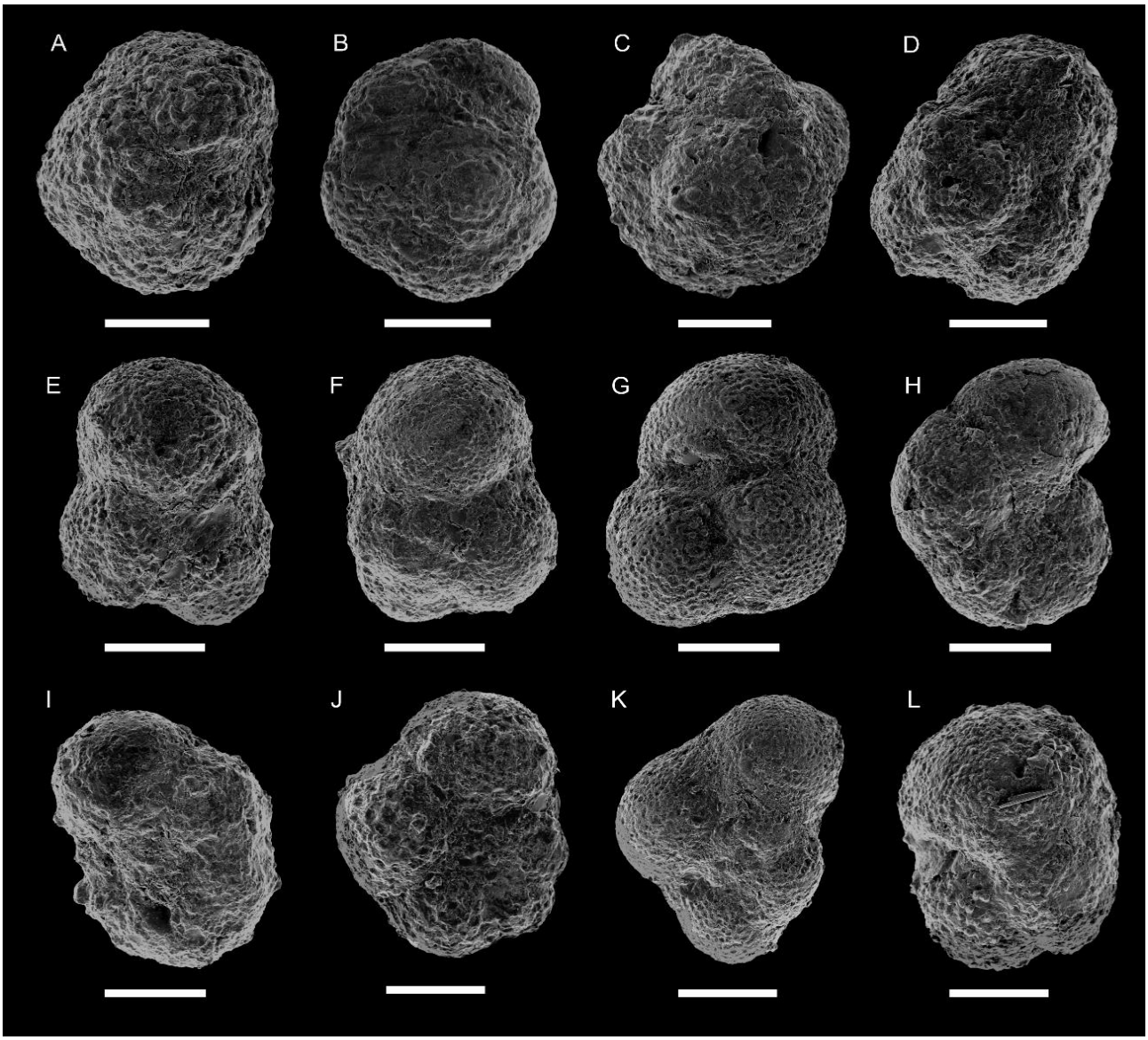

Fig. 2.5: Planktic Eocene foraminifera from Be 11. **A:** *Acarinina bullbrooki* (Bolli, 1957) (2935–2940 m), **B:** *Igorina broedermanni* (Cushman and Bermúdez, 1949) (2935–2940 m), **C:** *Igorina salisburgensis* (Gohrbandt, 1967) (2935–2940 m), **D–G:** *Subbotina eocaena* (Guembel, 1868) (2935–2940 m) (3062.5–3070), **H:** *Pseudohastigerina wilcoxensis* (Cushman and Ponton, 1932) (2935–2940 m), **I:** *Pseudohastigerina* sp. (2935–2940 m), **J:** *Globorotaloides eovariabilis* Huber and Pearson, 2006 (2922.5–2930 m), **K:** *Parasubbotina inaequispira* (Subbotina, 1953) (3062.5–3070 m), **L:** *Turborotalia frontosa* (Subbotina, 1953) (2935–2940 m)**;** scale bar = 100 µm.

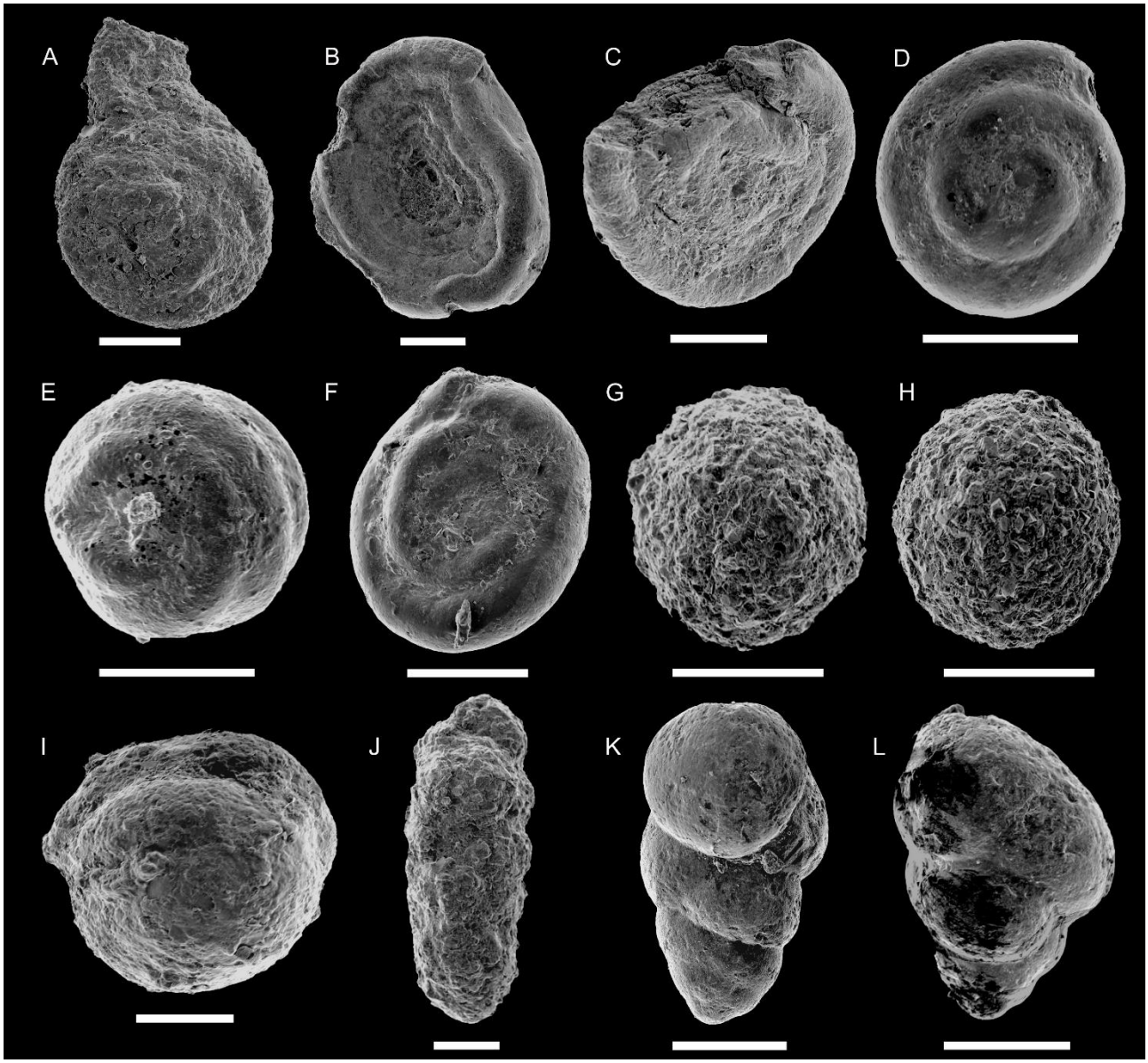

Fig. 2.6: Benthic Eocene foraminifera from Be 11. **A:** *Lituotuba lituiformis* (Brady, 1879) (2957.5–2965 m), **B:** *Ammodiscus peruvianus* (Berry, 1928) (3062.5–3070 m), **C:** *Ammodiscus cretaceus* (Reuss, 1845) (2817 m), **D–E:** *Glomospira charoides* (Jones and Parker, 1860) (2957.5–2965 m), **F:** *Glomospira gordialis* (Jones and Parker, 1860) (2957.5–2965 m), **G:** *Psammosphaera irregularis* (Grzybowski, 1896) (2782.5–2790 m), **H:** *Psammosphaera irregularis* (Grzybowski, 1896) (2817 m), **I:** *Pullenia bulloides* (d'Orbigny, 1826) (2922.5–2930 m), **J:** *Karrerulina conversa* (Grzybowski, 1901) (2922.5–2930 m), **K:** *Caucasina coprolithoides* (Andreae, 1884) (2817 m), **L:** *Bulimina* sp. (2782.5–2790 m); scale bar = 100 µm.

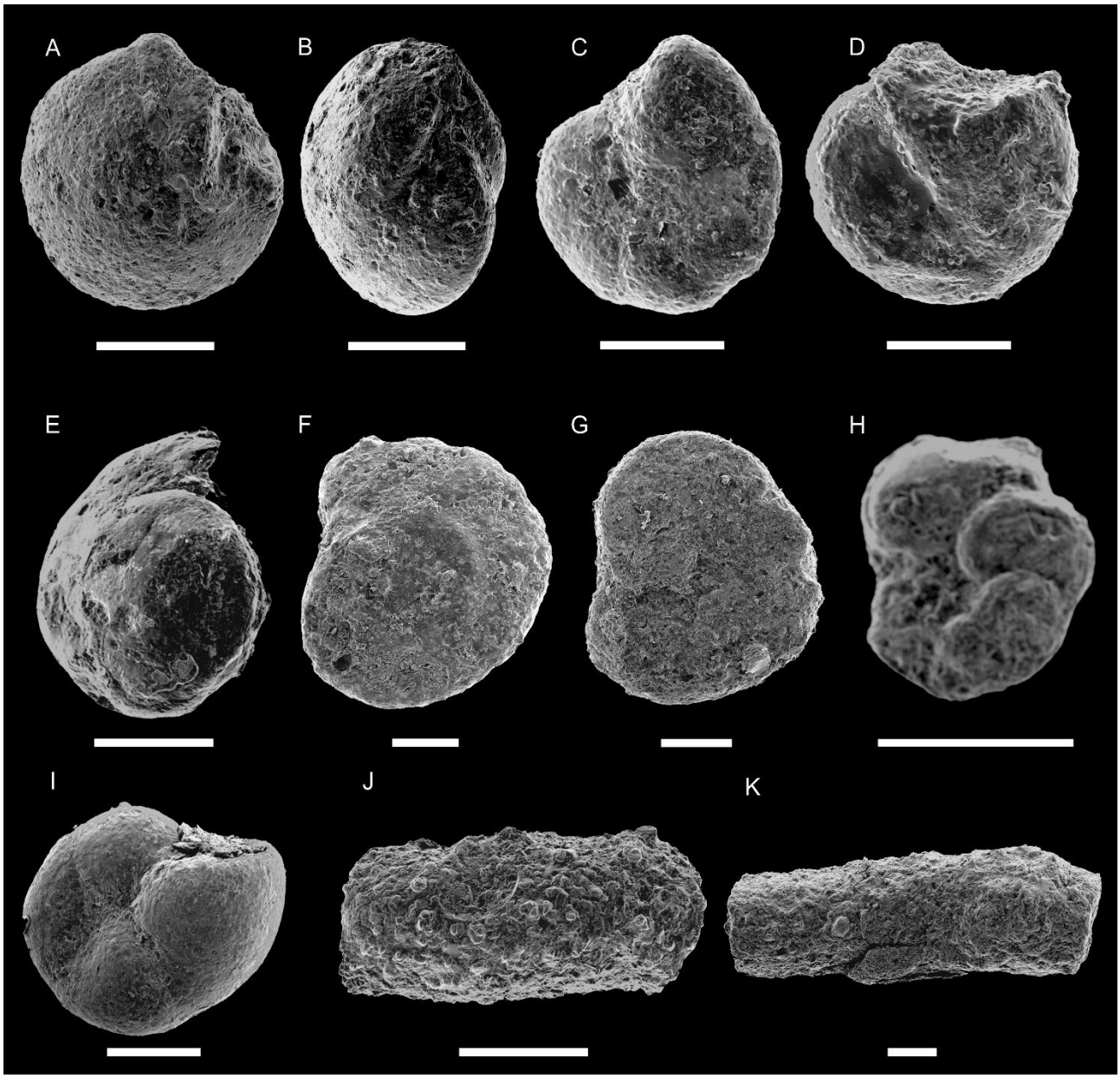

Fig. 2.7: Benthic Eocene foraminifera from Be 11. **A–B:** *Lenticulina* cf. *inornata* (2922.5–2930 m), **C–D:** *Melonis pompilioides* Römer, 1838 (3032–3140 m), (2957.5–2965 m), **E:** *Heterolepa dutemplei* (d'Orbigny, 1846) (2782.5–2790 m), **F:** *Cibicidoides* sp. (3062.5–3070 m), **G:** *Cibicides westi* (Howe, 1939) (3032–3140 m), **H:** *Anomalinoides* sp. (2922.5–2930 m), **I:** *Pullenia* sp. (2957.5–2965 m), **J:** *Rhabdammina* sp. (2922.5–2930 m), **K:** *Psammosiphonella* sp. (2922.5–2930 m); scale bar = 100 µm.

2.5.2. Correlation with Eocene subsurface units in the northern Vienna Basin

Based on data from internal OMV reports, Rammel (1989), Wessely et al. (1993) and Wessely (1993, 2006) extrapolated the distribution of subsurface units of the Rhenodanubian nappe system in the northern Vienna Basin. According to these maps, borehole Be11 is situated on the Harrersdorf unit, which is correlated by the above-mentioned authors to the Rača nappe of the Magura nappe system (Fig. 2.1). Of these, especially the Greifenstein Nappe stretches from the area of the Vienna Basin and

the Korneuburg Basin in NE direction up to the Steinberg region. Numerous drillings around the Steinberg and along the Steinberg Fault reached this nappe and allowed a lithostratigraphic subdivision. The subsurface extension of the Greifenstein Nappe is unknown. Nevertheless, Hamilton et al. (1990) and Picha et al. (2006) assumed a separation from the Rača Nappe, which is part of the Magura Nappe System, by a thrust in the area of the northern Vienna Basin. On their subsurface map of the Vienna Basin, Wessely et al. (1993) placed the boundary between these nappes along a line running from north of the Steinberg in the east to the Mistelbach area in the west (Fig. 2.1). No seismic data or surveys on the structural geology, however, have been published so far to support this hypothesis.

2.5.2.1. Greifenstein Nappe (Rhenodanubian nappe system): The Rhenodanubian nappe system consists of the Greifenstein and Laab nappes. The sedimentary succession of these tectonic units has been lithostratigraphically formalized as Greifenstein (surface outcrops terminate within the standard nannoplankton Zone NP13) and Laab Groups (Egger, 2013; Egger and Wessely, 2014; Ćorić and Egger, 2016; Egger and Ćorić, 2017). The units of the Greifenstein Nappe in the Steinberg area are united in the Zistersdorf Group, which comprises the Upper Cretaceous Altlengbach Formation and the Paleogene Glauconitic Sandstone and the Steinberg-Flysch formations (Rammel, 1989). The up to 750-m-thick Glauconitic Sandstone formation (GSf) comprises several thick units of light grey to greenish grey glauconite-bearing sandstone, partly with nummulitids and polymict pebbles, subdivided by thinner intercalations of variegated shales and marly shales (Hekel, 1968; Grill, 1968). Rammel (1989) subdivided the GSf into three main sandstone-dominated subunits separated by two pelite-dominated intercalations. The correlation of these units with biostratigraphic data of Hekel (1968) revealed a Thanetian to Ypresian age for the GSf. Similarly, the analysis of the foraminiferal assemblages by Küpper (1961) pointed to a late Paleocene to early Eocene age. The depositional environment was interpreted by Rammel (1989) as deep sea fans system with numerous channels. A correlation of the GSf with the unit drilled in Be 11 (2745 – 3140 m depth) can be excluded based on the biostratigraphic data and also by the wire-log pattern of the GFS, which is characterized by up to 200-m-thick, cylinder-shaped units (representing the sandstone packages).

The GSf is overlain by the Steinberg-Flysch formation (SFf), which comprises an up to 1500-m-thick succession of dark grey and greenish grey shales and marly shales with subordinate intercalations of thin layers of glauconitic sandstones (Grill, 1968; Wessely, 2006). According to the few available data, the basal parts of the SFf contain Ypresian foraminifera (Grill, 1968), whereas the upper part seems to range into the Lutetian (Hekel, 1968; Rammel, 1989). The depositional environment is interpreted as

distal deep-sea fan system (Wessely, 2006). Consequently, the Be 11 record (2745 – 3140 m depth) is a time-equivalent of the SFf and shows a similar lithology.

North of the Steinberg, the up to 2500-m-thick Harrersdorf Unit (Wessely, 2006) is either interpreted as frontal part of the Rača Nappe in Austria (Hamilton et al., 1990) or as a continuation of the Greifenstein Nappe (Rammel, 1989). Drillings, which reached the Harrersdorf Unit are Harrersdorf 1 (5136 m), Maustrenk Uet1a (6563 m), Linenberg 2 (4711 m) and St. Ulrich 290 (3000 m) (Wessely et al., 1993), but no sedimentological and paleontological data have been published so far. Rammel (1989) documented a continuation of the GSf into the Harrersdorf Unit based on well-log correlations of Harrersdorf 1 with drillings from the Steinberg area. This suggests a close relation of the Harrersdorf Unit with the Zistersdorf Group of the Greifenstein Nappe.

2.5.2.2. Rača Nappe (Magura nappe system): For north to south the Magura nappe system consists of the Rača, Bystrica and Bile Carpaty nappes. Although the tectonic affiliation of the Harrersdorf Unit remains ambiguous, the lithostratigraphic correlation between Greifenstein and Rača nappes is roughly established. Eliáš et al., 1990, Adamová and Schnabel (1999) and Picha et al. (2006) provided detailed summaries of the geology and lithostratigraphy of the Rača Nappe in the Western Carpathian Flysch belt (see Picha et al. 2006, Fig. 2.17 for a scheme of the Rača Nappe). The mostly Paleocene Soláň Formation yields the oldest post Cretaceous deposits. This nearly 3000-m-thick formation comprises shales and sandstones with general coarsening upward trend (Picha et al., 2006). According to Rammel (1989), the Soláň Formation can be correlated with the Altlengbach Formation and Thanetian parts of the GSf of the Greifenstein Nappe.

The Soláň Formation is overlain by the 300-m-thick Eocene Beloveža Formation, which comprises greenish grey to reddish shales with sandstone intercalations. Its stratigraphic interval is assumed to range from the Paleocene to middle Eocene (Picha et al., 2006), but seems to be mainly of Lutetian age (see Golonka and Waśkowska, 2012 for its equivalent in the Polish Flysch Carpathians). Rammel (1989) correlated this formation with the upper part of the GSf and assumed an Ypresian age. The uppermost unit of the Rača Nappe is the 2500-m-thick Zlin Formation (including the underlying sandy Luhačovice Member) of the middle to late Eocene with an overlap into the Oligocene. The formation is dominated by sandstones and conglomerates, which formed as proximal parts of turbiditic fans and by calcareous shales (Picha et al., 2006).

2.5.2.3. Tectonic affiliation: Rammel (1989) correlated the Steinberg-Flysch formation of the Greifenstein Nappe with the Zlin formation. The age of the Be 11 record (2745 – 3140 m depth) would allow a comparison of both formations. The pelitic lithology of Be 11, however, makes a direct correlation with the Zlin formation rather unlikely. Thus, leads to the assumption that the Lutetian units of Be 11 represent a continuation of the Steinberg Flysch formation in the Harrersdorf Unit. In consequence, this unit must be considered as continuation of the Greifenstein Nappe of the Rhenodanubian nappe system rather than as part of the Rača Nappe of the Magura nappe system. Some paleontological similarities of the Be 11 record can be stated with the middle Eocene Beloveža Formation from the Polish and Slovak part of the Rača Nappe as described by Golonka and Waśkowska (2012). Most of the genera and five species (*Ammodiscus tenuisimus, A. peruvianus, Glomospira charoides, H Haplophragmoides walteri, Karrerulina conversa*) described by Golonka and Waśkowska (2012) appear also in Be 11. Both assemblages indicate identical bathyal depositional environments (Murray 1991, 2006; Kaminski and Gradstein, 2005). These biotic similarities, however, are rather an expression of similar age and near identical paleoecological conditions and are no strong support to affiliate the Harrersdorf Unit with the Rača Nappe.

A relation with the Waschberg-Ždánice Unit is unlikely due to the geographic distance of the surface distribution of the Waschberg-Ždánice Unit outcrops (see maps in Grill, 1968; Schnabel, 2002). Subsurface data revealed the presence of isolated the Waschberg-Ždánice Unit below the Flysch nappes as seen along the escarpment Steinberg fault (Wessely et al., 1993). Within the Waschberg-Ždánice Unit Paleocene and Eocene formations, such as the Paleocene glauconitic and marly sands of the Bruderndorf beds, the lower Eocene Waschberg-Limestone, the ferruginous middle Eocene sandstones of the Haidhof beds and the glauconitic and calcareous sand of the upper Eocene Reingrub Formation have been documented (Krhovsky et al., 2001). Larger foraminifera from Eocene units, studied by Torres-Silva and Gebhardt (2015), confirmed the occurrence of Ypresian to basal Lutetian, Bartonian and Priabonian assemblages, which point to a depositional environment in the inner to middle shelf between 70 to 200 m water depth (Torres-Silva and Gebhardt, 2015). Deeper marine offshore facies, comparable to Be11, is confined to small occurrences of Lutetian marls (Egger et al., 2007) and Priabonian *Globigerina* marls (Grill, 1968; Wessely, 2006). None of these lithological units can be directly correlated with the shales of Be 11, either because of their completely different litho-facies and/or because of their different age. The Lutetian marls of Niederhollabrunn, described by Egger et al. (2007), would be the most similar unit in the surface Waschberg-Ždánice Unit, but they do not represent a turbiditic depositional system. Finally, a flysch cover of subsurface Waschberg-Ždánice Unit units must be expected in the study area.

2.6. Conclusions

The borehole Be 11 in the northern part of the Vienna Basin reached the pre-Neogene units at a depth of about 2745 m, indicated by a strong change in wire log patterns from highly cyclic bell-shaped Neogene GR and RES logs to a succession of cylinder- and funnel-shaped wire-log patterns, lacking any cyclicity. In addition, the predominant lithology changes from silty-sandy clays to marly shales. The drilled virtual thickness of the pre-Neogene unit attains nearly 400 m.

The shales and glauconitic sandstones lack any macrofauna and the microfauna is moderately to poorly preserved and of low diversity. Both foraminifers and calcareous nannoplankton are clearly indicative for an Eocene age. The nannoplankton assemblage yields two distinct species (*N. alata and D. distinctus*) which have not been found in the Miocene samples of the borehole and therefore represent autochthonous species which allow a correlation with the Lutetian standard nannoplankton Zone NP15 spanning over an interval from 43.6 to 47.4 Ma. Nannoplankton assemblages representing reworked taxa were found throughout the Lutetian succession that indicates reworking of older strata during the middle Eocene and downfall during drilling resulting in borehole contamination. Similarly, a large part of the foraminifera indicates a Lutetian age and are representative for the plankton biozones E7–E8 as defined by Berggren and Pearson (2005), spanning an interval from 45.8–50.4 Ma. Therefore, the stratigraphic overlap of these biozones allows a restriction of the depositional time of the turbidites of the Harrersdorf Unit to an interval ranging from 45.8–47.4 Ma.

The Flysch of the Harrersdorf Unit was variously interpreted as front of the Rača Nappe of the Magura Flysch (Hamilton et al., 1999; Wessely et al., 1993) or as continuation of the Greifenstein Nappe (Rammel, 1989). Our results support the latter interpretation as the lower Eocene Glauconitic Sandstone Formation can be traced from the Greifenstein Nappe in the Steinberg area up to the Harrersdorf Unit (Rammel, 1989) and due to the lithological similarities of the Be 11 record with that of the coeval Steinberg Flysch Formation.

Acknowledgements: We thank Godfrid Wessely (Vienna) for support and discussions on subsurface geology of the northern Vienna Basin. We also thank Patrick Grunert (University of Cologne, Germany) for taxonomic discussions and comments on an early draft of this paper. Iris Feichtinger (NHMW) greatly helped during sample preparation. Many thanks to the OMV Exploration and Production working group and especially to Wolfgang Hujer for their cooperation and open-minded policy. This project was financed by the OMV. Terminally we want to thank an anonymous reviewer and Lilian Švábenická (Czech Geological Survey) for professional and helpful remarks to improve this work.

Special thanks also to reviewer Hans Egger (Geological Survey, Austria) for tremendous insights and recommendation of literature concerning the geological setting.

References

Adamová, M., Schnabel, G.W., 1999. Comparison of the East Alpine and West Carpathian Flysch Zone - A Geochemical Approach. Abhandlungen der Geologischen Bundesanstalt, 56, 567–584.

Armstrong, H.A., Brasier, M.D., 2005: Foraminifera. Microfossils, Second Edition, Blackwell Publishing, Cornwall, 1–304.

Benedetti, A., 2017. Eocene/Oligocene deep-water agglutinated foraminifers (DWAF) assemblages from the Madonie Mountains (Sicily, Southern Italy). Palaeontologia Electronica, 20.1.4A, 1–66.

Berggren, W.A., Olsson ,R.K., Premoli Silva I., 2006: Taxonomy, biostratigraphy and phylogenetic affinities of Eocene Astrorotalia, Igorina, Planorotalites, and Problematica (Praemurica? lozanoi). In: Pearson, P.N., Olsson, K.O., Huber, B.T, Hemleben, C., Berggren, W.E., (Eds.), Atlas of Eocene Planktonic Foraminifera. Cushman Foundation Special Publication, 41, 377–400.

Bergen, J.A., de Kaenel, E., Blair, S.A., Boesiger, T.M., Browning, E., 2017: Oligocene-Pliocene taxonomy and stratigraphy of the genus Sphenolithus in the circum North Atlantic Basin: Gulf of Mexico and ODP Leg 154. Journal of Nannoplankton Research, 37, 77–112.

Bindiu–Haitonic, R., Niculici, S., Filipescu, S., Bălc, R., Aroldi, C., 2017: Biostratigraphy and palaeoenvironments of the Eocene deep-water deposits of the Tarcău Nappe (Eastern Carpathians, Romania) based on agglutinated foraminifera and calcareous nannofossil assemblages. In: Kaminski, M.A., Alegret, L., (Eds.), Proceedings of the Ninth International Workshop on Agglutinated Foraminifera Grzybowski Foundation Special Publication, 22, 17–37.

Bown, P.R., Cooper, M.K.E., 1998: Jurassic. In: Bown P.R. (Ed.): Calcareous nannofossil biostratigraphy. British Micropalaeontological Society Publication Series. Chapman and Hall, 34–85.

Bramlette, M.N., Sullivan, F.R., 1961: Coccolithophorids and related nannoplankton of the Early Tertiary in California. Micropaleontology, 7, 129–188.

Bubík, M., Kaminski, M.A. (Eds.)., 2004: Proceedings of the Sixth International Workshop on Agglutinated Foraminifera Grzybowski Foundation Special Publication, 8, 1–486.

Buday, T., Cicha, I., 1956: Nové názory na stratigrafii spodního a středního miocenu dolnomoravského úvalu a pováží. Neue Ansichten über die Stratigraphie des unteren und mittleren Miozäns des inneralpinen Wiener Beckens und des Waagtals. Geologické práce, 43, 3–56.

Cicha, I., Rögl, F., Rupp, C., Čtyroký, J., 1998: Oligocene–Miocene foraminifera of the Central Paratethys. Abhandlungen der senckenbergischen naturforschenden Gesellschaft, 549, 1–325.

Cimerman, F., Jelen, B., Skaberne, D., 2006: Late Eocene benthic foraminiferal fauna from clastic sequence of the Socka - Dobrna area and its chronostratigraphic importance (Slovenia). Geologij,. 49, 7–44.

Coxall, H.K., Spezzaferri, S., 2018: Taxonomy, biostratigraphy, and phylogeny of Oligocene Catapsydrax, Globorotaloides, and Protentelloides. In: Wade, B.S., Olsson, R.K., Pearson, P.N., Huber, B.T., Berggren, W.A., (Eds.), Atlas of Oligocene Planktonic Foraminifera. Cushman Foundation for Foraminiferal Research Special Publication, 46, 79–125.

Egger, H., Rögl, F., Stradner, H., 2007: Kalkiges Nannoplankton und Foraminiferen aus der Chiasmolithus gigas-Subzone (Mitteleozän) von Niederhollabrunn (Waschbergzone, Niederösterreich). Jahrbuch der Geologischen Bundesanstalt, 147, 379–386.

Egger, H., 2013: Zur Lithostratigrafie der Laab-Decke im Rhenodanubischen Deckensystem des Wienerwaldes. Arbeitstagung der Geologischen Bundesanstalt, 1–20.

Egger, H., Wessely, G., 2014: Wienerwald. Sammlung geologischer Führer, 59, 3, 1–202.

Egger, H., Ćorić, S. (Red.) 2017: Erläuterungen zur Geologischen Karte der Republik Österreich 1:50000 Blatt 56 St.Pölten. – Geologische Bundesanstalt Wien, 1 – 168.

Eliáš ,M., Schnabel, W., Stránik, Z., 1990: Comparison of the Flysch Zone of the Eastern Alps and the Western Carpathians based on recent observations. In: Minaříková, D., Lobitzer, H., (Eds.), Thirty years of geological cooperation between Austria and Czechoslovakia. Federal Geological Survey, Vienna and Geological Survey, Prague, 37–45.

Fornaciari, E., Agnini, C., Catanzariti, R., Rio, D., Bolla, E.M., Valvasoni, E., 2010: Mid- Latitude calcareous nannofossil biostratigraphy and biochronology across the middle to late Eocene transition. Stratigraphy, 7, 229–264.

Golonka, J., Waśkowska, A., 2012: The Beloveža Formation of the Rača Unit in the Beskid Niski Mts. (Magura Nappe, Polish Flysch Carpathians) and adjacent parts of Slovakia and their equivalents

in the west ern part of the Magura Nappe; remarks on the Beloveža Formation–Hieroglyphic Beds controversy. Geological Quarterly, 1, 56, 821–832.

Grill, R., 1968: Erläuterungen zur geologischen Karte des nordöstlichen Weinviertels und zu Blatt Gänserndorf. Flyschausläufer, Waschbergzone mit angrenzenden Teilen der flachlagernden Molasse, Korneuburger Becken, Inneralpines Wiener Becken nördlich der Donau. Geologische Bundesanstalt Wien, 1–155.

Grunert, P., Hinsch, R., Sachsenhofer, R.F., Bechtel, A., Ćorić, S., Harzhauser, M., Piller, W.E., Sperl, H., 2013: Early Burdigalian infill of the Puchkirchen Trough (North Alpine Foreland Basin, Central Paratethys): Facies development and sequence stratigraphy. Marine and Petroleum Geology, 39, 164–186.

Hamilton, W., Jiřiček, R., Wessely, G., 1990: The Alpine-Carpathian floor of the Vienna Basin in Austria and ČSSR. In: Minaříková, D., Lobitzer, H., (Eds.), Thirty years of geological cooperation between Austria and Czechoslovakia. Federal Geological Survey, Vienna and Geological Survey, Prague, 46–56.

Hamilton, W., Wagner, L., Wessely G., 1999: Oil and Gas in Austria. Mitt. Österr. Geol. Ges., 82, 235–262.

Harzhauser, M., Grunert, P., Mandic, O., Lukeneder, P., García Gallardo, Á., Neubauer, T.A., Carnevale, G., Landau, B.M., Sauer, R., Strauss, P., 2018: Middle and Late Badenian palaeoenvironments in the northern Vienna Basin and their potential link to the Badenian Salinity Crisis. Geologica Carpathica, 69, 129–168.

Harzhauser, M., Kranner, M., Mandic, O., Rögl, F., Ćorić, S., Grunert, P., Strauss, P., 2018a (unpublished): Miocene stratigraphy of the borehole Bernhardsthal 11 (northern Vienna Basin). Internal OMV report, 1–16.

Hekel, H., 1968: Nannoplanktonhorizonte und tektonische Strukturen in der Flyschzone nördlich von Wien (Bisambergzug). Jahrbuch der Geologischen Bundesanstalt, 111, 293–338.

Kaminski, M.A., Gradstein, F.M., 2005: Atlas of Paleogene cosmopolitan deep-water agglutinated foraminifera. Grzybowski Foundation Special Publication, 10, 1–547.

Kaminski, M.A., Ortiz, S., 2014: The Eocene-Oligocene turnover of Deep-Water Agglutinated Foraminifera at ODP Site 647, Southern Labrador Sea (North Atlantic). Micropaleontology, 60, 53–66.

Kováč, M., Baráth, I., Harzhauser, M., Hlavatý, I., Hudáčková, N., 2004: Miocene depositional systems and sequence stratigraphy of the Vienna Basin. Courier des Forschungs-Instituts Senckenberg 246, 187–212.

Krhovsky, J., Rögl, F., Hamrsmid, B., 2001: Stratigraphic correlation of the Late Eocene to Early Miocene of the Waschberg Unit (Lower Austria) with the Zdanice and Pouzdrany Units (South Moravia). In: Piller, W.E., Rasser, M.W., (Eds.), Paleogene of the Eastern Alps. Österreichische Akademie der Wissenschaften, Vienna, 225–254.

Kröll, A., Wessely, G., 1993: Strukturkarte - Basis der tertiären Beckenfüllung 1:200.000. Erläuterung zu den Karten über den Untergrund des Wiener Beckens und der angrenzenden Gebiete. Geologische Bundesanstalt, Wien.

Küpper, I., 1961: Alttertiäre Foraminiferenfaunen in Flyschgesteinen aus dem Untergrund des nördlichen Inneralpinen Wiener Beckens (Österreich). Jahrbuch der Geologischen Bundesanstalt, 104, 239–271.

Lees, J.A., Bown, P.R., 2005: Upper Cretaceous calcareous nannofossil biostratigraphy, ODP Leg 198 (Shatsky Rise, Northwest Pacific Ocean). Proceedings of the Ocean Drilling Program. Scientific Results, 198, 1–60.

Loeblich, A.R., Tappan, L., 1987: Foraminiferal genera and their classification. Van Nostrand Reinhold Company Inc., New York, 2 vols, 847 plates, 1–970.

Martini, E., 1971: Standard Tertiary and Quaternary calcareous nannoplankton zonation. Proceedings of the II Planktonic Conference. Ed. Tecnoscienza, Roma, 739–785.

Murray, J.W., 1991: Ecology and Palaeoecology of Benthic Foraminifera. Longman Scientific and Technical, Harlow, Essex, 1–397.

Murray, J.W., 2006: Ecology and Applications of Benthic Foraminifera. Cambridge University Press, Cambridge, 1–426.

Olsson, R.K., Hemleben, C., 2006: Taxonomy, biostratigraphy, and phylogeny of Eocene Globanomalina, Planoglobanomalina n. gen and Pseudohastigerina. In: Pearson P.N., Olsson K.O., Huber B.T, Hemleben C., Berggren W.E., (Eds.), Atlas of Eocene Planktonic Foraminifera. Cushman Foundation Special Publication 41, 413–432.

Papp, A., Rögl, F., Seneš, J., 1973: Chronostratigraphie und Neostratotypen: Miozän der zentralen Paratethys. M2 Ottnangien: Die Innviertler, Salgótarjáner, Bántapusztaer Schichtengruppe und die Rzehakia Formation. Verlag der Slowakischen Akademie der Wissenschaften, 1–841.

Pearson, P.N., Wade, B.S., 2009: Taxonomy and stable isotope paleoecology of well-preserved planktonic foraminifera from the uppermost Oligocene of Trinidad. Journal of Foraminiferal Research, 39, 191–217.

Pearson, P.N., Olsson, R.K., Huber, B.T., Hemleben, C., Berggren, W.A., 2006: Atlas of Eocene Planktonic Foraminifera. Cushman Foundation Special Publication, 41, 1–513.

Perch-Nielsen, K., 1985: Cenozoic calcareous nannofossils. In: Bolli, H.M., Saunders, J.B., Perch-Nielsen, K., (Eds.), Plankton stratigraphy. Cambridge University Press, Cambridge, 427–555.

Picha, F.J., Stráník, Z., Krejčí, O., 2006: Geology and hydrocarbon resources of the Outer Western Carpathians and their foreland, Czech Republic. In: Golonka, J., Picha, F.J., (Eds.), The Carpathians and their foreland: Geology and hydrocarbon resources. AAPG Memoir, 84, 49–175.

Raffi, I., Backman, J., Fornaciari, E., Palike, H., Rio, D., Lourens, L.J., Hilgen, F.J., 2006: A review of calcareous nannofossil astrobiochronology encompassing the past 25 million years. Quaternary Science Reviews, 25, 3113–3137.

Rammel, M., 1989: Zur Kenntnis der Flyschzone im Untergrund des Wiener Beckens. Die Glaukonitsandsteinseries. Unpublished PhD University Vienna, II; available via University of Vienna and Geological Service Austria, 1–149.

Royden, L.H., 1985: The Vienna basin: a thin skinned pull apart basin. In: Biddle, K. T., Christie-Blick, N. (Eds.), Strike-slip deformation, basin formation and sedimentation. SEPM Special Publication 37, 319–339.

Rögl, F., Spezzaferri, S., 2003: Foraminiferal paleoecology and biostratigraphy of the Mühlbach section (Gaindorf Formation, Lower Badenian), Lower Austria. Ann. Naturhist. Mus. Wien, 104A, 23–75.

Rupp, C., 1986: Paläoökologie der Foraminiferen in der Sandschalerzone (Badenien, Miozän) des Wiener Beckens. Beiträge zur Paläontologie von Österreich, 12, 1–180.

Schnabel, W., 2002 (Ed.): Geologische Karte von Niederösterreich 1:200.000. Legende und kurze Erläuterung. Geologische Bundesanstalt Wien.

Torres-Silva, A.I., Gebhardt, H., 2015: Eocene Larger Benthic Foraminifera (Nummulitids, Orthophragminids) Waschberg-Ždánice Unit, Lower Austria. Jahrbuch der Geologischen Bundesanstalt, 155, 109–120.

Vandenberghe, N., Hilgen, F.J., Speijer, R.P., 2012: The Paleogene Period. In: Gradstein, F.M., Ogg, J.G., Schmitz, M.D., Ogg, G.M., (Eds.), The Geologic Time Scale 2012, 2, 855–921, Elsevier, Amsterdam, Boston, Heidelberg, London etc.

Vass, D., 2002: Litostratigrafia Západných Karpát: neogén a budínsky paleogén. Lithostratigraphy of Western Carpathians: Neogene and Buda Paleogene. Štátny geologický ústav Dionýza Štúra, Bratislava, 1–204.

Wade, B.S., Olsson, R.K., Pearson, P.N., Huber, B.T., Berggren, W.A., 2018: Atlas of Oligocene Planktonic Foraminifera. Cushman Foundation for Foraminiferal Research Special Publication, 46, 1–524.

Wessely, G., 1988: Structure and Development of the Vienna Basin in Austria. In: Royden, L.H., Horvath, F. (Eds.), The Pannonian System. A study in basin evolution. American Association of Petroleum Geologists Memoir, 45, 333–346.

Wessely, G., 1993: Der Untergrund des Wiener Beckens. In: Brix F., Schultz O., (Eds.), Erdöl und Erdgas in Österreich. Naturhistorisches Museum Wien, 249–280.

Wessely, G., 2006: Niederösterreich. Geologie der Österreichischen Bundesländer. Geologische Bundesanstalt Wien, Wien, 1–416.

Wessely, G., Kröll, A., Jiřiček, R., Němec, F., 1993: Wiener Becken und angrenzende Gebiete. Geologische Einheiten des präneogenen Beckenuntergrundes. Geologische Bundesanstalt Wien, Wien, 1 map.

Young, J.R., 1998: Neogene. In: Bown, P.R., (Ed.), Calcareous Nannofossil Biostratigraphy. British Micropalaeontological Society Publications Series. Chapman and Hall, London, 225–265.

Chapter 3

Miocene lithostratigraphy of the northern and central Vienna Basin (Austria)

Mathias Harzhauser[1*], Matthias Kranner[1,2], Oleg Mandic[1], Philipp Strauss[3], Wolfgang Siedl[3], Werner E. Piller[2]

[1)] Geological-Palaeontological Department, Natural History Museum Vienna, Burgring 7, 1010 Vienna, Austria; mathias.harzhauser@nhm-wien.ac.at; matthias.kranner@nhm-wien.ac.at; oleg.mandic@nhm-wien.ac.at

[2)] Institute of Earth Sciences (Geology and Palaeontology), NAWI Graz Geocenter, University of Graz, Heinrichstr. 26, 8010 Graz, Austria; werner.piller@uni-graz.at

[3)] OMV Exploration and Production GmbH, Trabrennstraße 6-8, 1020 Vienna, Austria; philipp.strauss@omv.com; wolfgang.siedl@omv.com

[*)] Corresponding author: mathias.harzhauser@nhm-wien.ac.at; phone +43 1 52177 250; ORCID ID https://orcid.org/0000-0002-4471-6655

Abstract

For the first time, a clear lithostratigraphic scheme for the lower and middle Miocene (Ottnangian – Badenian) of the northern and central Vienna Basin is proposed, which is based on the integration of core-material, well-log data and seismic information from OMV. For all formations and members type sections are proposed, geographic distribution and thickness are provided, typical depositional environments and fossils are described and age constraints are discussed. This rigid time frame allows for a more reliable calculation of sedimentation rates. This in turn might be important for the reconstruction of the tectonic history of the Vienna Basin as we do not see fundamental differences between the piggy-back stage and the subsequent pull-apart regime.

Following lithostratigraphic units are formalized herein and/or are newly introduced: Bockfließ Fm. (Ottnangian), Aderklaa Fm., Gänserndorf Mb. and Schönkirchen Mb. (Karpatian), Baden Group, Aderklaa Conglomerate Fm. and Mannsdorf Fm. (lower Badenian), Auersthal Fm., Matzen Fm., Baden Fm., Leitha Fm. (middle Badenian) and Rabensburg Fm. (upper Badenian).

3.1 Introduction

Since the early 19th century, the Vienna Basin was one of the most intensively investigated Neogene Basins of the world. Especially during the pioneer phase of geology and paleontology the deposits and their fossil content served as base for international stratigraphic correlations. A renaissance of

geological research was sparked during the 20th century when the Vienna Basin was recognized as the largest oil and gas field of onshore Europe (Hamilton et al., 2000). Geological information from hundreds of drillings and more and more information from 2D and 3D seismics increased our knowledge on the stratigraphic and tectonic situation of the Neogene basin fill of the Vienna Basin (e.g., Kreutzer, 1971, 1974, 1978; Weissenbäck, 1995, 1996). Numerous papers dealt with tectonics, structural geology and depositional environments of the Vienna Basin (e.g., Jiříček and Tomek, 1981; Royden, 1985; Lankreijer et al., 1995; Kováč et al. 2004; Hinsch et al., 2005; Wessely, 2006; Hölzel et al., 2008, 2010; Lee and Wagreich, 2017 and references therein). Very little focus, however, was laid on bringing order into the confused lithostratigraphy of the basin. A major stumbling stone for this task was the historically grown mixture of biostratigraphic, lithostratigraphic and chronostratigraphic terminology in the stratigraphic charts. For example, lower Miocene strata of the northern Vienna Basin were defined by foraminiferal content (e.g., *Cyclammina-Bathysiphon*-Schlier), whereas coeval strata in the central Vienna Basin were named after their geographic occurrence (Bockfließ beds). Similarly, middle Miocene (Badenian) strata were defined according to their foraminiferal assemblages ("eco-biozones" of Grill, 1941, 1943) into which local lithostratigraphic units were squeezed in (e.g., Matzen Sand). Especially, the strongly deviating understanding of authors concerning the content and definition of the various eco-biozones increased confusion enormously (e.g., Lower versus Upper Lagenidae Zone) (e.g., Kapounek et al., 1965; Cicha et al., 1998; Hohenegger et al., 2014).

Stratigraphic tables for the Vienna Basin using information from oil industry have been proposed and compiled early by Austrian geologists, such as Janoschek (1942, 1943, 1951), Grill (1943, 1960, 1968), Kapounek et al. (1965), Papp et al. (1973), Kreutzer (1986, 1992, 1993) and many others. The last synthesis of these data was presented by Piller et al. (2004) in the "Stratigraphic Chart of Austria 2004". Simultaneously, Slovak geologists, such as Buday (1946), Buday and Cicha (1956) and Špička (1966) developed the foundation of lithostratigraphic schemes for the Slovak part of the Vienna Basin, which was refined later by Vass (2002), Kováč et al. (2004) and Fordinál et al. (2012) (see Fordinál et al. 2012 for much more references). All these papers discussed numerous lithostratigraphic units but none of these formations and members were established properly to fulfill the criteria for a formalization following Hedberg (1976), Salvador (1994) and Steininger and Piller (1999). Therefore, nearly all lithostratigraphic units listed by Piller et al. (2004), Kováč et al. (2004) and Fordinál et al. (2012) for the Vienna Basin are only informal terms. Exceptions are Sarmatian and Pannonian formations, which have been formalized by Bartek (1989), Čtyroký (2000), Elečko and Vass (2001) and Harzhauser and Piller (2004). More recently, formations and members were established by Harzhauser et al. (2019) for the lower Miocene deposits of the Mistelbach Halfgraben in the NW Vienna Basin, west of the Steinberg Fault.

Tectonically, the Vienna Basin passed through four distinct phases starting from an early Miocene piggy-back basin stage, a middle to late Miocene pull-apart basin stage, a late Miocene to Pliocene compressional phase with basin inversion, followed by Quaternary basin formation (see Lee and Wagreich, 2017 for references). The changes in tectonic regime are expected to be reflected in changes of regional subsidence and in variations of sedimentation rates (Hölzel et al., 2008; Lee and Wagreich, 2017).

3.2. Geographic and stratigraphic frame

Geographically we focus on the northern Vienna Basin ranging from the Steinberg Fault in the west to the Czech/Austrian border in the north and east down to the Matzen/Spannberg Ridge in the south and the central Vienna Basin spanning from the Bisamberg Fault in the west to the Slovak/Austrian border in the east, and from the Matzen/Spannberg Ridge in the north to the Schwechat Basin in the south (Figure 3.1A). In addition, we discuss lateral equivalents in neighboring areas of the North Alpine-Carpathian Foreland Basin (NACFB), the Mistelbach Basin, the southern Vienna Basin and the Eisenstadt-Sopron Basin. The Mistelbach Basin is a halfgraben, separated from the northern Vienna Basin by the Steinberg Fault (Harzhauser et al., 2019) and it is debatable if this halfgraben is part of the Vienna Basin *sensu stricto*. Its Miocene lithostratigraphy was described in detail by Harzhauser et al. (2019) and is not repeated herein.

Stratigraphically, we describe all formations resting on the pre-Neogene basement of the Vienna Basin from the Ottnangian to the upper Badenian. Eggenburgian deposits, which have been frequently reported from the Vienna Basin (e.g., Kováč et al., 2004 and references therein), have been based on outdated stratigraphic concepts and represent basal Ottnangian strata (Harzhauser et al., 2017, 2019). We do not discuss the Sarmatian and Pannonian strata of the Vienna Basin, because their lithostratigraphy has already been formalized and their biostratigraphy is largely solved (see Harzhauser et al., 2004 and Harzhauser and Piller, 2004).

Since the use of stratigraphic terminology and the mixture of different stratigraphic classification schemes produced glaring confusion we try to summarize and explain the most widely used terms. The historical development of Neogene stratigraphy of the Vienna Basin and Central Paratethys was depicted by Papp (1986) and summarized: Burdigalian = Eggenburgian, Lower Helvetian (Helvetian s. str.) = Ottnangian, Upper Helevtian = Karpatian (Carpathian), Tortonian = Badenian, Sarmatian, Pannonian. In addition to this stage concept a “Series” concept was introduced where the “Luschitzer Serie” represents the Upper Eggenburgian and Ottnangian, the “Laaer Serie” the Karpatian, the

"Badener Serie" the Badenian, the "Sarmatische Serie" the Sarmatian, and the "Pannonische Serie" the Pannonian. The "Series" concept is a lithostratigraphic concept and a series includes several lithostragraphic units which represent beds (= formations). The series are, however, intimately linked with chronostratigraphy. In terms of biostratigraphy a correlation with the Mediterranean region was attempted by using planktic microfossils and also molluscs. This correlation works well in the lower Miocene Eggenburgian to Karpatian but due to a high degree of endemism problems arise in the Badenian, Sarmatian and Pannonian and required a local-regional biozonation. The resulting biozones are ecologically defined zones which are only of limited geographical use. Here we will focus only on the Badenian: the pioneer for establishing a Badenian biostratigraphy was Grill, who distinguished 1941 five zones in the Badenian (Tortonian) based on the foraminiferal fauna (from base to top):

1) "Reiche marine Fauna mit sehr starker Betonung der Lageniden u. mit *Planulina wuellerstorfi* (Lanzendorfer Fauna)" (rich marine fauna with high share of lagenids and with *Planulina wuellerstorfi* (Lanzendof Fauna)) (Grill, 1941).
2) "Reiche marine Fauna mit starker Betonung der Lageniden, *Robulus cultratus*" (marine fauna with high share of lagenids, *Robulus cultratus*) (Grill, 1941).
3) "Reiche marine Fauna mit *Spiroplectammina carinata*, wenig Lageniden" (rich marine fauna with *Spiroplectammina carinata*, few lagenids) (Grill, 1941).
4) "Marine Fauna mit *Bolivina dilatata*" (marine fauna with *Bolivina dilatata*) (Grill, 1941).
5) "Oberstes artenarmes Torton mit *Rotalia beccarii* und *Nerita picta*" (uppermost species-poor Tortonian with *Rotalia beccarii* and *Nerita picta*) (Grill, 1941).

In 1943 Grill introduced the term Lageniden-Zone (p. 37), Lagenidenzone (p. 38) (Lagenidae zone).

Papp and Küpper (1952) defined the Unter-Torton as "Lagenidenzone", the Mittel-Torton as "Zone der Sandschaler" and the "Bolivinenzone = Buliminenzone" and the Ober-Torton as "Rotalienzone". Papp and Turnovsky (1953) splitted the Lagenidenzone into an "Untere Lagenidenzone = Lanzendorfer Fauna" (sensu Grill, 1941) (p. 124) but also mentioned it as the "Niveau der *U. macrocarinata* (= untere Lagenidenzone)" (p. 37) and an "obere Lagenidenzone = Niveau des „Badener Tegels s. str."" Overall, they differentiated 5 biostratigraphic zones based on the foraminiferal genus *Uvigerina*: untere Lagenidenzone, obere Lagenidenzone, untere Sandschalerzone, obere Sandschalerzone, Buliminen-Bolivinen-Zone.

Similarly, Kapounek et al. (1965) subdivided the "Badener Serie" into the "Untere Lagenidenzone mit *Uvigerina macrocarinata*", the "Obere Lagenidenzone mit *Uvigerina acuminata*", the "Sandschalerzone (einschließlich Matzener Sand)" and the "Rotalien- und Buliminenzone".

This subdivision is partly used herein where the Lower Lagenidae Zone represents the lower Badenian, the Upper Lagenidae Zone and the *Spirorutilus* Zone the middle Badenian and the *Bulimina-Bolivina* Zone the upper Badenian. The *Rotalia* Zone, representing the uppermost Badenian, is preserved only

in restricted occurrences. The *Spirorutilus* Zone is also known as *Spiroplectammina* Zone (*Spiroplectammina carinata* Zone) (after an older generic affiliation for *Spirorutilus*) or "Sandschaler Zone" or Zone of agglutinated foraminifera. The *Rotalia* Zone (*Rotalia* is used as an older synonym for *Ammonia*) is often fused with the *Bulimina-Bolivina* Zone to *Bulimina-Rotalia* Zone, but it is also termed "Verarmungszone" (Zone of pauperization, Impoverished Zone).

In addition to these various stratigraphy systems oil industry (OMV) uses a specific terminology for sand and sandstone horizons because they represent the most important oil reservoirs there (Kreutzer, 1971). For the Badenian the "1.-16. Tortonhorizont" (TH, Tortonian Horizon), for the Sarmatian the "1.-10. Sarmathorizont" (SH, Sarmatian Horizon) and for the Lower Pannonian the "1.-5. Unterpannonhorizont" (UP, lower Pannonian Horizon) are defined. Lower numbers represent higher stratigraphic positions; the lowest horizon is the 16. TH. The middle Badenian contains the 11. TH and the 13.-16. TH, the upper Badenian the 1.-10. TH and the 12. TH. All these horizons are used as important correlation markers. In addition to these sand horizons, in the Badenian of the Matzen Field also horizons with enriched coralline red algae occurrences are identified and termed "Nullipora Horizonte" (NPH, Lithothamnia horizons; *Nullipora* is the name used by Reuss (1847) for the first description of a coralline red alga which later was renamed to *Lithothamnion* (Piller, 1994)). The NPHs widely coincide with the TH horizons and occur usually on top of the TH horizons. The most pronounced NPHs occur in the upper Badenian (Kreutzer, 1978).

3.3. Material and Methods

All proposed formations are based on core material and well-log data from several OMV wells (Figure 3.1B). 46 boreholes in the Austrian part of the Vienna Basin have been sampled by us and 595 sediment samples have been analyzed for microfossils (mainly foraminifers, ostracods, otoliths) and macrofossils, such as mollusks, balanids, echinoderms and bryozoans. The full inventory will be published elsewhere. Herein, we refer only to the biostratigraphically and/or paleoecologically relevant taxa.

The well-log data set provided complete spontaneous potential (SP) and resistivity (RES) logs. In addition, 3D seismic data have been made available to us by the OMV during analysis. For all wells, material is stored in the core-shed of the OMV in Gänserndorf (Austria). In addition, well-logs, lithological and paleontological data have been integrated from Hladecek (1965), Papp (1967), Kreutzer (1971, 1974, 1978, 1986, 1992, 1993), Fuchs (1990), Fuchs et al. (2001), Weissenbäck (1995, 1996), Harzhauser et al. (2017, 2018, 2019) and internal OMV reports.

3.4. Results

3.4.1. Ottnangian

3.4.1.1. Bockfließ Formation (Figures 3.2–3.3)

Derivation of name: After the village Bockfließ in the central Vienna Basin (N 48°21’40.53’’, E 16°36’5.57’’). Papp et al. (1973, p. 195) introduced the term “Bockfließer Schichten” (Bockfließ Beds).

Synonyms: “brachyhaline Serie” or “brachyhaline facies with *Rzehakia*” (Hladecek, 1965; Kapounek et al., 1965). Brachyhaline Schichten mit Rzehakia = „Oncophora-Schichten" (Papp et al., 1973), Bockfließer Schichten.

Type section: Designated herein: Well Matzen 269 (2245–2754 m; cores: 17/6 2270.00–2279.00 m, 18/2 2279.00–2281.70 m, 19/6 2281.70–2290.00 m, 20/4 2315.00–2321.50 m, 21/7 2321.50–2325.30 m, 22/1 2325.30–2333.30 m, 23/6 2354.00–2363.00 m, 24/6 2480.00–2489.00 m, 25/6 2650.00–2659.00 m, 26/7 2659.00–2668.00 m, 27/7 2668.00–2677.00 m, 28/7 2677.00–2686.00 m, 29/7 2686.00–2695.00 m, 30/6 2715.00–2724.00 m, 31/7 2724.00–2733.00 m) (N 48°22’59.37’’, E 16°42’22.09’’) (Figures 3.1–3.2).

Remarks: Papp et al. (1973) discussed well Bockfließ 78 (N 48°21’48”, E 16°36’34”) as being characteristic for the Bockfließ Fm. but referred only to a very short interval of 5 m (1948–1953 m) of the total thickness of 323 m (1935–2258 m). Therefore, the short note of Papp et al. (1973) does not meet the requirements for the designation of a type section.

Thickness: The Bockfließ Fm. fills a paleo-relief and is truncated by erosion. Thus, its thickness varies considerably. The maximum thickness of about 500 m is documented from well Matzen 269 (2245–2754 m).

Lithology: The base of the Bockfließ Fm. comprises few meters of Flysch clasts, representing a basal transgressional conglomerate (e.g., Spannberg 11: 2441–2447 m). Lignite is documented from the basal units in wells Spannberg 8 (2546 m) and Matzen 260 (2750 m). Upsection follows light and dark grey, mica-rich marly clay with intercalations of marly silt and sand. Some of these pelitic intervals and sand intercalations are continuous and have been used by Hladecek (1965) for cross-correlations between the various wells.

Well-log characteristics: The well-logs of the Bockfließ Fm. display a rather uniform pattern with high amplitudes in the base followed by a shale line interval, which is overlain by a rapid succession of high amplitude logs consisting of partly amalgamated funnel-shaped units, indicating a general coarsening upward trend.

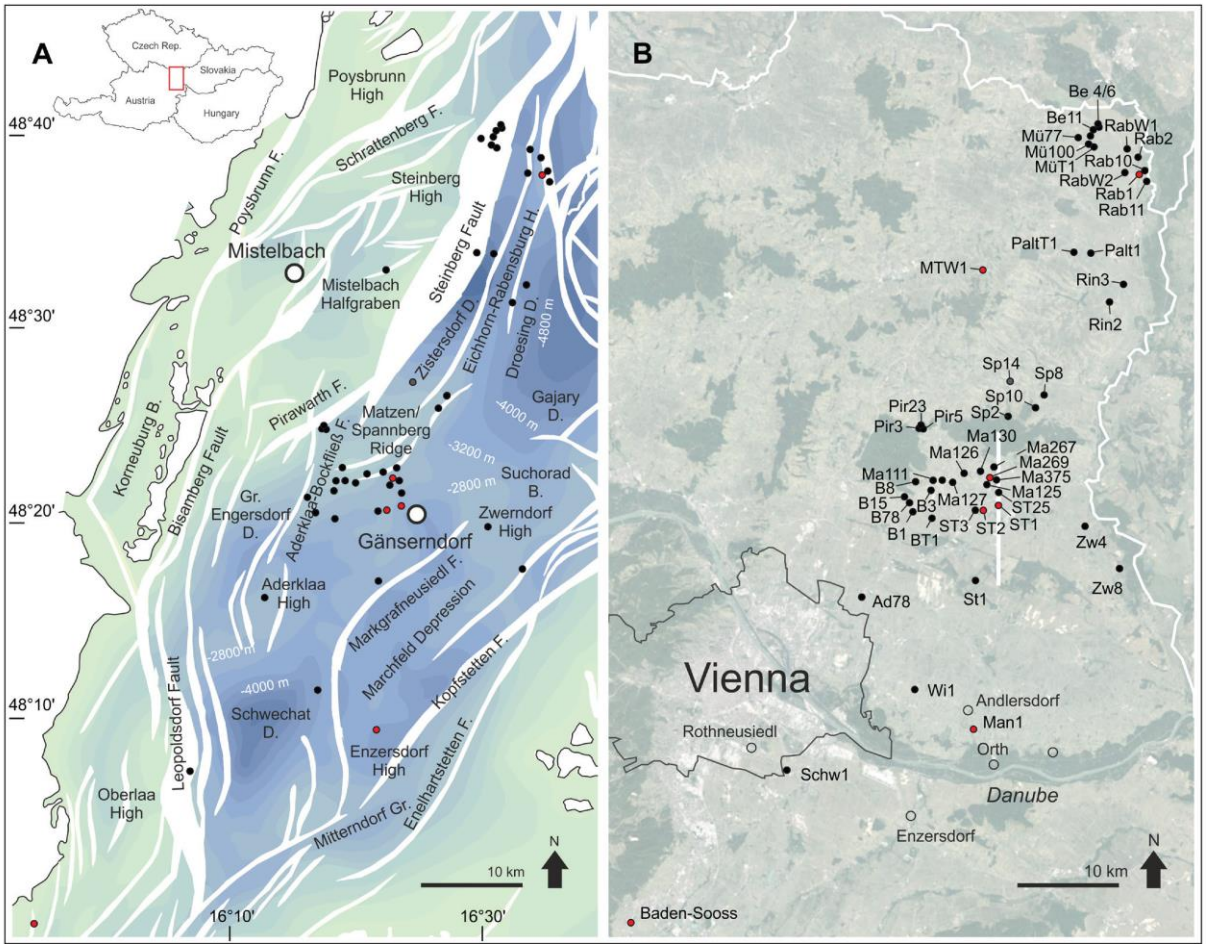

Fig. 3.1: A. Tectonic setting of the central and northern Vienna Basin modified from Kröll and Wessely (1993), Jiříček (2002) and Wessely (2006); black dots correspond to investigated wells. **B.** Position of the mentioned wells, red circles indicate type sections. mentioned in this report. Abbreviations: D: depression; Ad: Aderklaa, B: Bockfließ, Be: Bernhardsthal, Ma: Matzen, Man: Mannsdorf, Mü: Mühlberg, MüT. Mühlberg Tief, Palt: Paltendorf, Pir: Pirawarth, Rab: Rabensburg, Ring: Ringelsdorf, Schw: Schwechat, Sp: Spannberg, ST: Schönkirchen Tief, St: Strasshof, Wi: Wittau, Zw: Zwerndorf. Open circles indicate villages; white line indicates seismic survey shown in Fig. 6 (map generated with Google Earth).

Fossils: The Bockfließ Fm. is rich in fossils, including calcareous nannoplankton, foraminifers, mollusks and decapods. Most data, however, are only available from unpublished internal OMV reports (e.g., Fuchs, 1990) or presented in the unpublished thesis of Hladecek (1965). These data have been re-evaluated by us and supplemented with own results. The foraminiferal assemblages are dominated by *Ammonia tepida* along with elphidiids (e.g., *Elphidium matzenense*) (e.g., Bockfließ 78: 1867–1882 m, Bockfließ 90: 1813–1822 m, 1846–1854 m). Planktonic species are represented by *Globigerina*

ottnangensis, G. praebulloides and *Globoturborotalia woodi* (Matzen 270: 2330–2345 m, Bockfließ 78: 201–2020 m). Typical mollusks are the bivalves *Nuculana* sp., *Ostrea digitalina*, *Papillicardium papillosum*, *Corbula gibba,* and *Macoma elliptica* (e.g., Matzen 269: 2480–2489 m, 2650–2659 m, 2668–2677 m, 2677–2686 m). Similar bivalve assemblages with *Crassostrea gryphoides*, *Parvicardium* sp., *Tellina* sp., *Pitaria* sp., *Venus* sp., *Lutraria* sp., and *Lucina columbella* have been documented from Bockfließ 78 (2006–2014 m), Raggendorf 8 (1897–1902 m, 2015–2018 m, 2225–2231 m), Matzen 267 (2314–2332 m, 2487–2500 m) and Matzen 270 (2357–2366 m). Gastropods are comparatively rare and represented by *Terebralia* sp. (Matzen 269: 2750–2759 m), *Turritella terebralis* (Spannberg 14: 2462–2471 m) and *Nassarius* sp., *Bittium* sp. and *Granulolabium* sp. from Spannberg 14 (2409–2418 m).

Depositional environment: Lagoonal-coastal environments are reflected by the lignite bearing basal parts of the formation, yielding mudflat gastropods, such as *Terebralia* sp. The abundance of infaunal bivalve taxa in most parts of the Bockfließ Fm. documents soft bottom conditions in a fully marine environment. For all mollusk species a depth-range from the shoreface down to the outer shelf is documented (e.g., Marquet, 2004). Typically, however, *Papillicardium papillosum* is found in coastal shallow water environments, such as lagoons, delta-influenced settings and within the rhizome layers of sea grass (Albano and Sabelli, 2012; Giacobbe, 2012; Weber and Zuschin, 2013). *Corbula gibba* is a specialist for instable bottom conditions, being able to withstand dysoxic conditions (Talman and Keough, 2001). Paratethyan assemblages with high contributions of nuculanids are characteristic for shallow to medium deep sublittoral environments (Báldi, 1973). *Ostrea digitalina* was confined to fully marine conditions (Mandic and Harzhauser, 2003) and is documented to have formed bioherms in protected lagoons with level-bottom conditions (Zuschin et al., 2007). Therefore, a fully marine, inner neritic lagoonal environment with occasionally stressed bottom conditions may be expected as depositional environment. Transport of the mollusk shells can be excluded as *Papillicardium* and some tellinds are found articulated in life-position. The lagoon did not become fully isolated from the open

sea, indicated by the sporadic occurrence of globigerinids in upper parts of the formation (e.g., Matzen 270, 2330–2335 m).

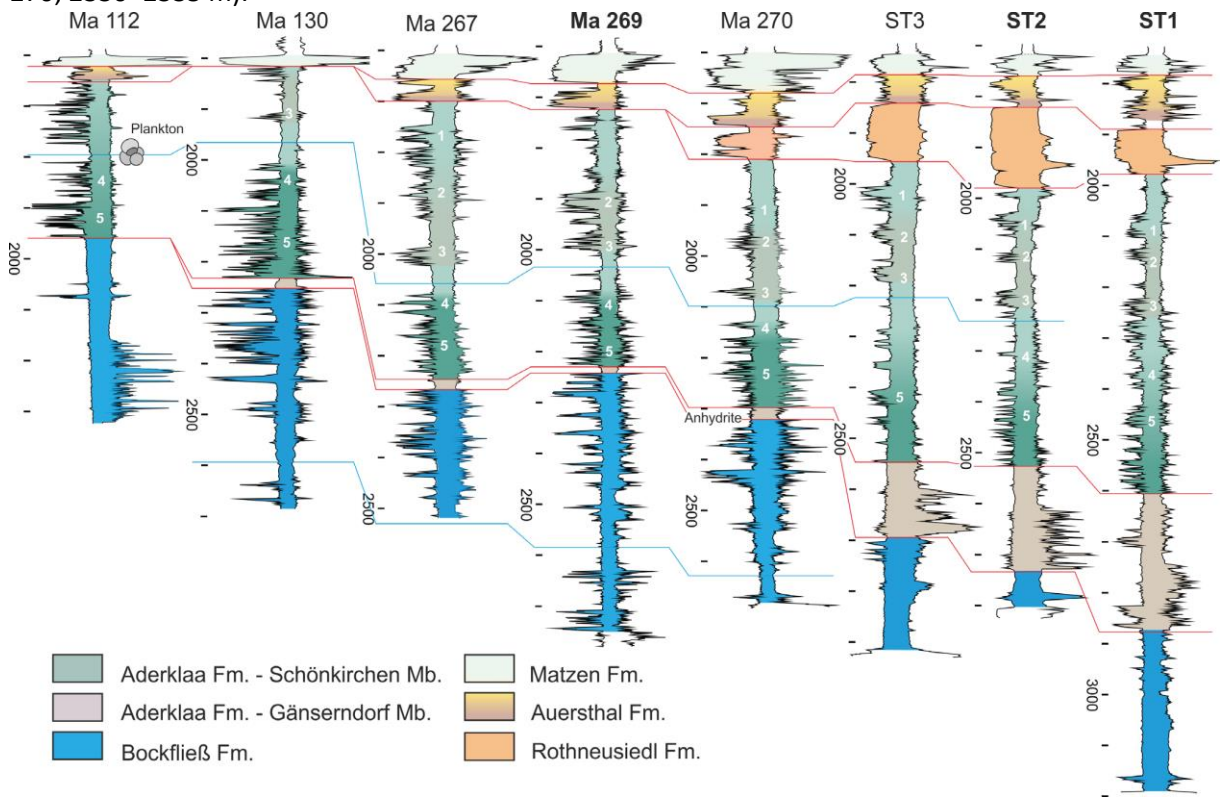

Fig. 3.2 Stratigraphic correlation of Matzen and Schönkirchen wells in the central Vienna Basin. Logs are aligned along the top of the Matzen Fm. Numbers in the Schönkirchen Member correspond to correlative horizons as defined by Hladecek (1965). Red lines indicate sequence boundaries, blue lines are flooding surfaces. Right curve represents the SP-, left curve the RES-log in each well. Pre-Neogene basement is left blank. Type sections are written in bold.

Age: Early Miocene (Burdigalian – early Ottnangian).

Biostratigraphy: The nannoplankton assemblages point to the nannoplankton zones NN3 or lower NN4; *Sphenolithus conicus* has its last occurrence in NN3 (Bergen et al., 2017) and *Sphenolithus belemnos* ranges from the upper NN2 to the lower NN4 (Hilgen et al., 2012). Overall, the assemblage points to an early Ottnangian age. The foraminiferal and mollusk assemblages are of little biostratigraphic significance but do not contradict this interpretation. **Remarks**: The occurrence of the bivalve *Rzehakia*, which was described by Papp et al. (1973) as typical for the Bockfließ Fm., could not be detected herein and was also critically discussed by Schultz (2005). Papp et al. (1973) used the alleged occurrence of *Rzehakia* to correlate the Bockfließ Fm. with the upper Ottnangian "*Rzehakia* beds" of Upper Austria (= Oncophora Formation; Pippèrr et al., 2018; = Pixendorf Group of Gebhardt et al. (2013) in Lower Austria). The presence of this bivalve genus, however, has little biostratigraphic significance as it ranges from the Ottnangian to the Badenian (Schultz, 2005).

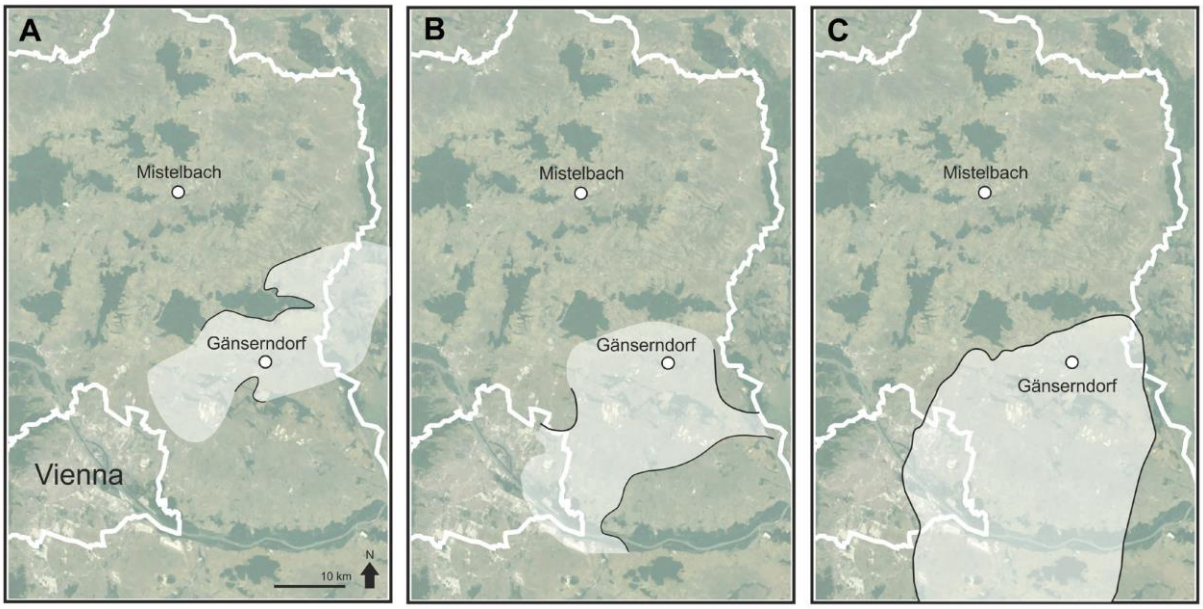

Fig. 3.3: Distribution of the Bockfließ Formation (A), the Gänserndorf Member (B) and the Rothneusiedl Formation (C) based on Hladecek (1965), Weissenbäck (1995) and own data.

Sequence stratigraphy: The Bockfließ Fm. has not been interpreted in terms of sequence stratigraphy so far. Based on its correlation with the Lužice Fm. we assume that the Bockfließ Fm. represents the transgressive systems tract and early high stand systems tract of the 3rd order TB 2.1. cycle of Haq et al. (1988), which is in agreement with Piller et al. (2007).

Underlying units: Pre-Neogene basement (Rhenodanubian Flysch, Mesozoic nappes of the Northern Calcareous Alps).

Overlying units: Aderklaa Fm. south of the Matzen/Spannberg Ridge (Raggendorf-Matzen-Bockfließ-Schönkirchen areas); Badenian units (Matzen Fm., Baden Fm.) north of the Matzen/Spannberg Ridge in the Spannberg area.

Lateral equivalents: The Lužice Fm. of the northern Vienna Basin and Alpine-Carpathian Foredeep is a lateral equivalent and represents more offshore conditions. Based on the nannoplankton, the Bockfließ Fm. is probably a time equivalent of the Mistelbach and Kettlasbrunn members of the Lužice Fm. as defined by Harzhauser et al. (2019).

Geographic distribution: The Bockfließ Fm. is restricted to subsurface drillings in the central Vienna Basin and is documented in numerous wells in the area of Spannberg, Prottes, Matzen, Bockfließ, Raggendorf, Schönkirchen, Straßhof, Deutsch-Wagram, Tallesbrunn, and Glinzendorf. North of the Matzen/Spannberg Ridge, the occurrence is limited to a narrow strip. A continuation in eastern direction into the Gajary Basin on Slovak territory was described by Kováč et al. (2004, fig. 7a). The Aderklaa High and Aderklaa-Bockfließ Fault form the western boundary and into southern direction, the Bockfließ Fm. pinches out in the Gänserndorf area (Figure 3.3A).

Drillings: Bockfließ 78 (1948–1953 m), Matzen 125 (2310–2490 m), Matzen 130 (2270–2680 m), Matzen 269 (2245–2754 m), Matzen 267 (2260–2520 m), Matzen 270 (2325–2685 m), Matzen 375 (2330–2720 m), Schönkirchen T1 (2870–3190 m), Schönkirchen T2 (2730–2810 m), Schönkirchen T25 (2720–2935 m), Schönkirchen T3 (2700–2920 m), Spannberg 8 (2400–2643 m), Spannberg 10 (2150–2290 m), Spannberg 14 (2390–2548.6 m); additional core records: Bockfließ 90 (1813–1822 m), Matzen 100 (2072–2079 m), Prottes 16 (2104–2285 m), Prottes 20 (2170–2171 m), Raggendorf 1 (1963–1968 m), Raggendorf 11 (1885–1891 m), Raggendorf 3 (2010–2051 m), Raggendorf 7 (1873–1876 m), Spannberg 11 (2332–2441 m), Spannberg 4 (2150–-2155 m) (for additional records see Hladecek, 1965).

3.4.1.2. Lužice Formation (Figure 3.4)

Derivation of name: After the village Lužice in the northern Vienna Basin in the Czech Republic (N 48°50'27.19", E 17°4'17.07").

Synonyms: Neusiedl Schlier (Kapounek et al., 1965).

Type section: well Maustrenk MTW1 (1300–1505 m; cores: 7/5 1300.00–1305.00 m, 8/1 1350.00–1355.00 m, 9/5 1380.00–1385.00 m, 10/5 1420.00–1424.70 m, 11/5 1458.00–1463.00 m, 12/6 1480.00–1485.00 m) (N 48° 34' 32.08", E 16° 42' 29.77").

Remark: The Lužice Formation is defined in the Mistelbach Halfgraben by its members: Maustrenk Mb., Mistelbach Mb., Kettlasbrunn Mb. and Hobersdorf Mb. (Harzhauser et al., 2019). The designated type section is also type section of the Mistelbach Mb. For description see (Harzhauser et al., 2019).

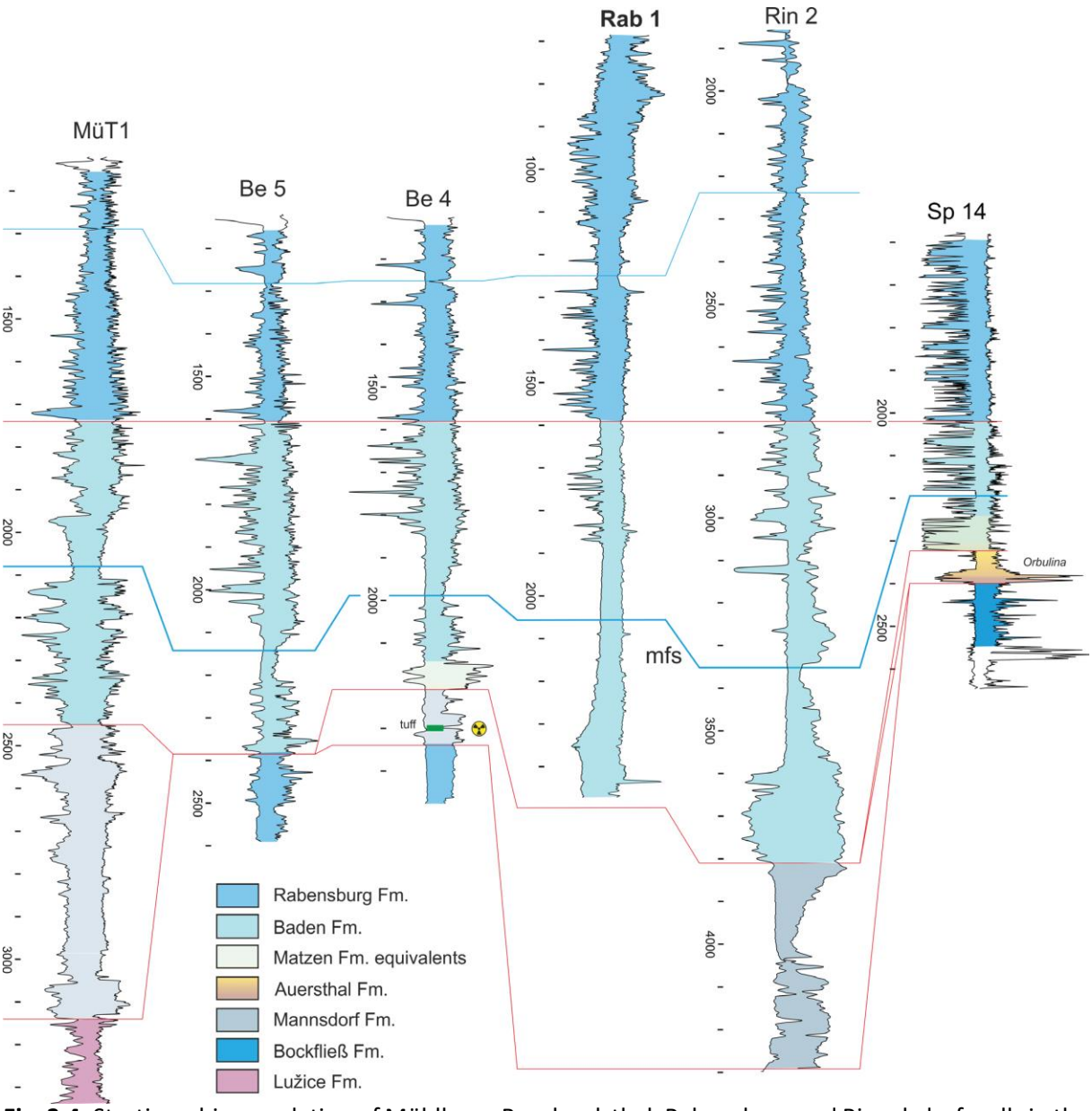

Fig. 3.4: Stratigraphic correlation of Mühlberg, Bernhardsthal, Rabensburg and Ringelsdorf wells in the northern Vienna Basin and a Spannberg well at the northern flank of the Matzen/Spannberg Ridge. Logs are aligned along the boundary between Baden and Rabensburg formations. Red lines indicate sequence boundaries, blue lines are flooding surfaces. Right curve represents the SP-, left curve the RES-log in each well. Pre-Neogene basement is left blank. The maximum flooding surface of the middle Badenian, which is an important marker for OMV correlations is marked as “mfs”. Type sections are written in bold.

Thickness: The maximum thickness of the Lužice Fm. attains about 1000 m in the Mistelbach Halfgraben (Harzhauser et al., 2019). East of the Steinberg Fault, in the northern Vienna Basin, the Lužice Fm. is tilted and strongly eroded. Therefore, only lower parts of the formation are preserved with thicknesses ranging around few hundreds of meters (e.g., ~200 m in the Bernhardsthal field).

Lithology: Laminated grey calcareous clays, silt and siltstones with intercalations of sands, referred to as "Schlier" (Kováč et al., 2004).

Well-log characteristics: Shale-line and low amplitude SP- and RES-log patterns are typical.

Fossils: Rich foraminiferal assemblages with *Bathysiphon taurinensis*, *B. filiformis, Cyclammina praecancellata* along with *Haplophragmoides vasiceki* and *Trilobatus trilobus* (Cicha et al., 1998; see Harzhauser et al., 2015, 2018 for details).

Depositional environment: Open marine pelagic, partly bathyal environments with high nutrient flux and high sedimentation rates (Grunert et al., 2013, Harzhauser et al., 2017). A distinct shallowing trend is indicated by the development of *Lenticulina, Cibicides* and *Elphidium*-dominated foraminiferal assemblages in the upper part of the Lužice Fm**.**

Age: Early Miocene (Burdigalian – early Ottnangian).

Biostratigraphy: Early Ottnangian is based on the co-occurrence of *Bathysiphon filiformis, Cyclammina bradyi* and *Reticulophragmium karpaticum* (Cicha et al., 1998; Harzhauser et al., 2017). An Ottnangian age is also supported by the occurrence of the bivalve *Pecten hornensis* in basal parts of the Lužice Fm. (Harzhauser et al., 2019).

Sequence stratigraphy: The Lužice Fm. comprises a full 3rd order cycle. Based on its age, it is correlated with the TB 2.1. cycle of Haq et al. (1988) and by Piller et al. (2007).

Underlying units: Rhenodanubian Flysch.

Overlying units: The lower Miocene Laa Formation follows in the Mistelbach Halfgraben; in the Austrian part of the northern Vienna Basin, the middle Miocene Mannsdorf or Baden formations discordantly overlay the Lužice Fm.

Lateral equivalents: Bockfließ Fm. in the central Vienna Basin; Wildendürnbach Fm. and Zogelsdorf Fm. in the NACFB (Palzer-Khomenko et al., 2018a, b; Harzhauser et al., 2019).

Geographic distribution: Austrian, Czech and Slovak territories of the northern Vienna Basin and Mistelbach Halfgraben (Buday and Cicha, 1956; Vass, 2002; Kováč et al., 2004; Harzhauser et al., 2018, 2019).

Drillings: Mühlberg T1 (3140–3340 m), Bernhardsthal 4 (2340–275 m), Bernhardsthal 5 (2385–2590 m). For drillings in the Mistelbach Halfgraben see Harzhauser et al. (2017, 2019).

Based on its foraminiferal faunas, the investigated samples from these wells can be correlated with the Mistelbach Mb. and parts of the Kettlasbrunn Mb. of the Lužice Formation.

3.4.2. Karpatian

3.4.2.1. Aderklaa Formation (Figure 3.2)

Derivation of name: After the village Aderklaa in the central Vienna Basin (N 48°17'7.11", E 16°32'18.96").

The deposits of the Aderklaa Fm. were recognized during hydrocarbon exploration in the 1940ies. Originally, these sediments were vaguely termed as “schlierähnliche Serie” (schlier-like series at Aderklaa) (Janoschek, 1942, 1943), “Aderklaaer Schlier (Janoschek, 1951) and “Liegendserie von Aderklaa” (lower series of Aderklaa) (Grill, 1943). Later, Grill (1960) established the term “Schichten von Aderklaa” (Aderklaa beds). These Aderklaa beds were separated by Hladecek (1965) into a basal “terrestrial-lacustric series” and an overlaying “limnic series”. Since Papp et al. (1973), these two units were named Gänserndorfer Schichten (Gänserndorf beds) and Aderklaaer Schichten (Aderklaa beds). Herein, we consider both lithostratigraphic units as members of a single formation for which we propose Aderklaa Fm. as name. We separate the Aderklaa Fm. into a lower and an upper member, which we define as Gänserndorf Member and Schönkirchen Member.

Synonyms: “schlierähnliche Serie” (Janoschek, 1942, 1943), Aderklaaer Schlier (Janoschek, 1951), “Liegendserie von Adlerklaa” (Grill, 1943), Schichten von Aderklaa (Grill, 1960; Janoschek, 1960), Gänserndorfer Schichten p.p. (Papp et al., 1973), Aderklaaer Schichten p.p. (Papp et al., 1973), Aderklaa Formation (Weissenbäck, 1996).

Type section: Designated herein: Well Schönkirchen T1 (1980–2870 m; cores: 4/8 2020.00–2027.00 m, 5/6 2132.00–2137.00 m, 6/6 2227.00–2232.00 m, 7/6 2308.50–2313.50 m, 8/6 2625.00–2630.00 m, 9/5 2730.00–2735.00 m, 10/5 2838.00–2843.00 m) (N 48°21’30.71’’, E 16°43’5.50’’) (Figures 3.1–3.2).

Thickness: The maximum thickness of 1258 m is documented from Wittau Ü1 from the Schwechat Basin. Overall, the thickness varies considerably due to the paleo-relief formed by the underlying Bockfließ Fm. and due to postsedimentary truncation and erosion. A thickness of 500 to 800 m is typical for the Matzen and Schönkirchen areas.

Age: Early Miocene (Burdigalian – Karpatian).

Lithostratigraphic subdivision: The Aderklaa Fm is completely subdivided into the Gänserndorf Member and Schönkirchen Member.

Sequence stratigraphy: The Aderklaa Fm. has not been interpreted in terms of sequence stratigraphy so far. The Karpatian stage has been correlated by Piller et al. (2007) with the 3rd order sea level cycle TB 2.2. of Haq et al. (1988). Herein, we interpret the Gänserndorf Mb. as proximal expression of a lowstand systems tract, whereas the Schönkirchen Mb. represents the transgressive and highstand systems tracts including a marine flooding of the wetlands during the maximum flooding (see Discussion chapter). Based on the large thickness, we tentatively consider the whole sequence as 3rd order cycle.

3.4.2.1.1. Gänserndorf Member (Figure 3.2)

The deposits of the Gänserndorf Member were studied by Hladecek (1965) and termed “terrestrial-lacustric series”. Papp et al. (1973) introduced the term Gänserndorfer Schichten (Gänserndorf beds)

for this unit, which was accepted by subsequent authors (e.g., Grill and Janoschek 1980; Rupp, 1986; Jiřiček and Seifert, 1990; Kreutzer, 1993). Weissenbäck (1995) performed a detailed sedimentological analysis and provided first interpretations of the depositional environment. Kováč et al. (2004) discussed this lithostratigraphic unit at formation rank. Herein we define the Gänserndorf beds as member of the Aderklaa Fm.

Derivation of name: After the town Gänserndorf in the central Vienna Basin (N 48°20'26.31", E 16°43'3.26") (Figure 3.1).

Synonyms: terrestrisch-limnische Schichten (Hladecek, 1965), Gänserndorfer Schichten (Papp et al., 1973), Gänserndorf Formation (Weissenbäck, 1996; Wessely, 2006).

Type section: Designated herein: Well Schönkirchen T1 (2610–2870 m; cores: 8/6 2625.00–2630.00 m, 9/5 2730.00–2735.00 m, 10/5 2838.00–2843.00 m) (N 48°21'30.71'', E 16°43' 5.50'').

Thickness: The unit attains its maximum thickness with 363 m in the well Wittau Ü1. In the Schönkichen Field it attains a thickness of up to 260 m (Schönkirchen T1), becomes reduced to few meters in most Matzen wells (130, 125, 167, 269, 270) and is already completely missing in Raggendorf 8 and Matzen 375. The strongly varying thickness results partly from the paleo-relief that truncated and eroded the underlying Bockfließ Fm.

Lithology: The lithology and sedimentology of the Gänserndorf Mb. was described in detail by Weissenbäck (1995) and is summarized in the following: The deposits are characterized by a rapid alternation of conglomerates, sandstones, marly silty clays and subordinate breccias. Conglomerates are monomictic (dolostones) or polymictic (limestones, dolostones, quartz, schist, sandstones, etc.), poorly sorted and moderately rounded with components of up to 10 cm diameter. The light grey fine to middle sandstone is usually poorly to moderately sorted, often immature and intercalated by mm-thin clay layers. Flaser- and ripple bedding occasionally occurs in the variegated silty marly clay. Characteristic successions consist of fining-upward-units of thick conglomerates passing into sand-silt and marly clay intercalations. Pieces of anhydrite appear at the base of the formation in the wells Matzen 267 and Bockfließ 78. Continuous layers of evaporites, however, have not been documented so far. The Gänserndorf Mb. passes without discordance into the Schönkirchen Member (upper part of the Aderklaa Fm) and is separated from the later by its high amount of coarse grained clastics.

Well-log characteristics: SP-logs are characterized by generally rather low amplitudes, which are opposed by strongly serrated RES patterns with high RES-values. This pattern results from the high degree of compaction and cementation of the conglomerates (Weissenbäck, 1995). Overall, an upsection trend towards lower RES values is seen in the studied logs.

Fossils: The Gänserndorf Mb. is poor in fossils. Wells Matzen 267 (2250–2268 m) and Schönkirchen T1 (2840 m, 2730–2735 m, 2625–2630 m) yielded large ostracods (Candonidae, Cytherideidae), hydrobiid, planorbid and helicid gastropods and oogonia of Characeae (Hladecek, 1965; own data).

Depositional environment: The depositional environment of the Gänserndorf Mb. was interpreted by Weissenbäck (1995) as a transition from alluvial fans in its basal part to a braided river system with the main transport direction from SW to NE. Parts of the succession represent overbank-deposits and probably wetland ponds. This is indicated by the frequent occurrence of hydrobiid gastropods and large freshwater ostracods, which were adapted to lentic environments and did not live in the fast flowing river channels. Paleosol formation and the presence of helicid gastropods clearly indicate terrestrial conditions within the floodplains. Moreover, the formation of anhydrite pebbles is a hint to rather arid climatic conditions.

Age: Early Miocene (Burdigalian – Karpatian).

Biostratigraphy: No biostratigraphic marker species are known from the Gänserndorf Mb. It discordantly overlies the Ottnangian Bockfließ Fm. and passes without discordance into the overlaying Schönkirchen Mb., which is of Karpatian age. Therefore, we assume a Karpatian age for the Gänserndorf Mb. In addition, the indication for rather dry and warm climate is a hint to a Karpatian rather than an Ottnangian age of this formation. As shown by stable isotope data of oyster shells by Harzhauser et al. (2010) and by Kern et al. (2010), based on high resolution pollen analysis, the Karpatian was characterized by very dry and hot summer seasons, thus differing from the still warm but slightly cooler Ottnangian with higher precipitation (Grunert et al., 2014).

Lithostratigraphically higher rank unit: Aderklaa Formation.

Underlying units: In all herein studied wells, the Gänserndorf Mb. discordantly overlies the Bockfließ Fm.

Overlying units: In all herein studied wells, the Gänserndorf Mb. is overlain by the Schönkirchen Mb.

Lateral equivalents: In the Slovak part of the Vienna Basin, the Šaštín Mb. of the Závod Fm. was discussed by Kováč et al. (2004) to be a lateral equivalent based on the occurrence of anhydrite in both units. Harzhauser et al. (2019) defined the Závod Formation as a member (Závod Member) of the Laa Fm.

Geographic distribution: The Gänserndorf Mb. is only known from subsurface drillings. It is restricted to an about 10 to 20 km wide SW-NW trending area in the central Vienna Basin and was drilled mainly in the Schönau, Andlersdorf, Breitenstetten, Breitensee, Matzen, Schönkirchen and Bockfließ wells (Weissenbäck, 1995). It pinches out towards the Matzen/Spannberg Ridge in the north, towards the Aderklaa High in the northwest, towards the Zwerndorf High in the west and disappears in southeastern direction between the Markgrafneusiedl and the Kopfstetten faults. In the west and southwest, the formation reaches into the Schwechat Basin without reaching up to the Oberlaa High. In total, the Gänserndorf Mb. covers roughly 550 km^2 on Austrian territory (Figure 3.3B).

Drillings: Bockfließ T1 (2500–2720 m), Matzen 269 (2230–2268 m), Matzen 270 (2300–2320 m), Schönkirchen T1 (2610–2870 m), Schönkirchen T2 (2530–2730 m), Schönkirchen T3 (2550–2700 m),

Schönkirchen T41 (2611–2618 m); additional core records: Aderklaa 3 (2683–2701 m), Bockfließ 78 (1810–1940 m), Breitenlee 1 (2814–2823, 2888–2893 m), Deutsch Wagram 3 (3022–3027, 3109–3114 m), Fischamend T1 (3038–3043 m), Gänserndorf T1 (2916–2921 m), Glinzendorf T1 (3113–3118 m), Marchegg 1 (2010–2015 m), Markgrafneusiedel NT1 (3150–3155 m), Straßhof T1 (2743–2748 m), Straßhof T2 (2905–2910 m.

3.4.2.1.2. Schönkirchen Member (Figure 3.2)

This lithostratigraphic unit was introduced by Papp et al. (1973) as Aderklaaer Schichten and treated so far as Aderklaa Fm. in the more recent literature (e.g., Weissenbäck, 1995; Kováč et al., 2004). By integrating also, the Gänserndorf Mb. in the Aderklaa Fm., it became necessary to define this unit as new member.

Derivation of name: After the village Schönkirchen in the central Vienna Basin (N 48°21'49.98'', E 16°42'3.09'').

Synonyms: Aderklaaer Schlier p.p. (Janoschek, 1951), Limnische Schichten mit Congerien (Papp et al., 1973), Aderklaaer Schichten (Papp et al., 1973), Aderklaa Formation (Weissenbäck, 1996; Wessely, 2006), ?Grillenberger Kohleserie (Brix and Plöchinger, 1988), ?Hauerbergschichten (Brix and Plöchinger, 1988), Láb beds (Láb Member) in Slovakia (Buday, 1955; Kovac et al., 2004).

Type section: Designated herein: Well Schönkirchen T1 (1980–2610 m; cores: 4/8 2020.00–2027.00 m, 5/6 2132.00–2137.00 m, 6/6 2227.00–2232.00 m, 7/6 2308.50–2313.50 m) (N 48°21'30.71'', E 16°43'5.50'') (Figures 3.1–3.2).

Thickness: A maximum thickness of 1066 m is developed in the Schwechat Basin in well Aderklaa 85 (Weissenbäck, 1995). A very high thickness of 895 m is also documented from the well Wittau Ü1. In the Matzen area, the thickness ranges around 500 m.

Lithology: The lithology and sedimentology of the Schönkirchen Mb. was described in detail by Weissenbäck (1995) and is summarized in the following. Drill cores reveal a rather monotonous alternation of strongly cemented light grey to greenish sandstones with marly silt and marly clay; thin gravel layers are occasionally intercalated. The sand is moderately to moderately well sorted, often with graded bedding and frequent plant debris. Lenticular and flaser bedding are typical. Reworked andesitic tuff within the Schönkirchen Mb. was detected in well Orth 1 (3130-3135 m) by Kapounek and Papp (1969).

Well-log characteristics: SP-logs in the Matzen-Schönkirchen area indicate a subdivision into a strongly serrated basal interval with high amplitudes and an overall bell-shaped outline. Bundles of high-amplitude values form serrated intervals separated by short shale line intercalations (intervals 4 and 5 in Figure 3.2). This lower part is separated by an up to 100 m thick shale line interval from an upper part with at least three high amplitude bundles of cylindrical to funnel-shaped outline (intervals 1, 2

and 3 in Figure 3.2) alternating with shale line intervals. The RES-logs mirror this pattern largely but with lower amplitudes. In the Aderklaa area, this subdivision is less prominent and low amplitude patterns prevail.

Fossils: Large ostracods are the most common fossils in the Schönkirchen Mb. (Candonidae, Cytherideidae, Hemicytheridae). Mollusks are represented by the terrestrial helicid gastropod *Megalotachea silvana* (e.g., Matzen 273: 2070 m). The pachychilid gastropod *Tinnyea lauraea* along with hydrobiids are known from Schönkirchen T1 (2020–2027 m). Hydrobiids are also documented from Matzen 269 (2056–2065 m). The neritid gastropods *Theodoxus crenulatus* and *Vitta pachii* were documented from Raggendorf 8 (1770–1792 m). Bivalves are documented by the dreissenid *Andrusoviconcha neumayri* (e.g., Aderklaa 78: 2757–2766 m, Bockfließ 90: 1770–1779 m, Straßhof 1: 2405–2414 m) and *Trigonipraxis* cf. *kucici* (= *Congeria antecroatica* sensu Papp, 1967) (Aderklaa 78: 2757–2766 m); unidentified dreissenids occur also in Raggendorf 8 (1770–1792 m) (Hladecek, 1965; Papp, 1967; own data). An important finding are marine foraminifera in Matzen 112 (1805 m) comprising *Ammonia beccarii*, *Bulimina schischkinskayae, Globigerina bulloides, Globigerinella regularis, Globorotalia transsylvanica, Hanzawaia buoana,* and *Nonion commune*. Hydrobiid gastropods, dreissenid bivalves and a low diverse foraminiferal fauna was also recorded from the Láb beds on Slovak territory (Fordinál et al., 2012).

Depositional environment: The detailed sedimentological analysis by Weissenbäck (1995) revealed the Schönkirchen Mb. as deposits of a meandering river system with channels and flood plains. The sandy intervals represent largely point-bars and pelitic intervals formed in oxbow lakes. A flood plain depositional environment is also indicated by the fossil content with large sized ostracods and hydrobiids, which might have dwelled in the flood plain lakes. Inhabitants of fluvial environments are represented by the gastropod *Tinnyea*. The most diverse fauna derives from the basal parts of the Schönkirchen Mb. in the Raggendorf 8 well, where dreissenid bivalves, hydrobiids and theodoxids have been detected along with the neritid *Vitta pachii*. This gastropod is occurring in the Korneuburg Basin in coastal mudflats and is unknown from freshwater settings (e.g., Zuschin et al., 2014). A comparable assemblage was described by Harzhauser et al. (2016) from Rupelian marsh land deposits of Turkey, where dreissenids, hydrobiids and *Vitta* co-occurred in the landward part of the mangrove fringe. Therefore, its occurrence in the basal parts of the Schönkirchen Mb. indicates the proximity to the shoreline. At least one short marine flooding of the wetland by the Paratethys Sea is documented by the occurrence of marine foraminifers in the well Matzen 112.

Age: Early Miocene (Burdigalian – Karpatian).

Biostratigraphy: No biostratigraphic marker species are known from the Schönkirchen Mb. Nevertheless, the occurrence of *Vitta pachii* is only known from Karpatian deposits so far (Harzhauser, 2002). In addition, *Andrusoviconcha neumayri* is also recorded from the Karpatian of the Laa Fm.

(Harzhauser and Mandic, 2009) and *Trigonipraxis kucici* is a Karpatian species as well (de Leeuw et al., 2011). The foraminiferal assemblage has little biostratigraphic significance, but the presence of *Globorotalia transsylvanica* and *Globigerinella regularis* excludes an Ottnagnian age (according to the ranges given in Cicha et al., 1998).

Lateral equivalents: The Láb beds (= Láb Ostracod member, Buday and Cicha, 1956) are a lateral equivalent in the Slovak part of the Vienna Basin (Kováč et al., 2004, Fordinál et al., 2012).

The Grillenberger Kohleserie (Brix and Plöchinger, 1988), representing lignites and marls in the area of Grillenberg, Kleinfeld and Jauling (Lower Austria) along the southwestern margin of the Vienna Basin, might be a lateral equivalent of the Schönkirchen Mb. This lignitic series is overlain by the Badenian Gainfarn breccia, which dated as nannoplankton Zone NN4 (Wessely et al., 2007) and would thus support the older Karpatian age of the Grillenberger Kohleserie.

Similarly, the Hauerbergschichten (Brix and Plöchinger, 1988), representing up to 2 m of freshwater limestone at Gainfarn in the southern Vienna Basin might be a time equivalent.

Lithostratigraphically higher rank unit: Aderklaa Formation.

Underlying units: The Schönkirchen Mb. concordantly overlies the Gänserndorf Mb. or discordantly overlies the Bockfließ Fm.

Overlying units: In most of the studied wells, the Schönkirchen Mb. is discordantly overlain by the Aderklaa Conglomerate Fm. In some wells close to the Matzen/Spannberg Ridge, it is overlain directly by the Matzen Fm.

Geographic distribution: The Schönkirchen Mb. is only known from subsurface drillings. In the north, it pinches out along the Matzen/Spannberg Ridge. Towards the east, it reaches via the Suchorad Basin to the Záhorie Lowlands on Slovak territory (= Láb beds), where it is recorded from drillings at Malacky, Láb, Jakubov, Suchohrad, Vysoká pri Morava, and Lozorno (Fórdinal et al., 2012). Thus, the Malé Karpaty mountains form the easternmost border, whereas the Kopfstetten Fault and the Enzersdorf High delimit this member towards the southeast.

In the south, the Schönkichen Mb. reaches into the Schwechat Basin attaining there its maximum thickness. The Aderklaa High and the Leopoldsdorf Fault represent northwestern and western boundaries of the Schönkichen Mb. Strauss et al. (2006) discuss a continuation of the Aderklaa Fm. (undifferentiated) into the southern Vienna Basin down to the northern margin of the Leitha Mountains. These deposits are documented in seismic surveys (Strauss et al., 2006) and drilled by well Wienerherberg 1, where these deposits attain a thickness of about 200 m. Including this southern distribution, the Aderklaa Fm. covers an area of more than 1000 km^2.

Drillings: Aderklaa 78 (2005–2810 m), Bockfließ T1 (2000–2500 m), Matzen 112 (1650–1960 m), Matzen 375 (1885–2330 m), Matzen 269 (1730–2235 m), Matzen 267 (1700–2250 m), Schönkirchen T1 (1980–2600 m), Schönkirchen T2 (1990–2530 m), Schönkirchen T3 (1960–2550 m), Schönkirchen

T25 (1870–2410 m); additional core records: Baumgarten 6 (2578–2581 m), Breitenlee 1 (2435–2667 m), GlinzendorfT1 (2709–3070 m), Maria Ellend 1 (2650–2655 m), Orth 1 (2899–3135 m), Schönau 1 (2704–3021 m).

3.4.3. Badenian

3.4.3.1. Baden Group

The various Badenian deposits of the Vienna Basin were united in the Baden Group on the "Stratigraphic Chart of Austria 2004" (Piller et al., 2004). The chart, however, listed only the most important formations and a formalization was missing so far.

Derivation of name: After the town Baden in the central Vienna Basin (N 48°00'29.00", E 16°14'03.72").

Type section: Designated herein: The 102-m-long scientific core from the abandoned brick yard Baden/Sooss near the town Baden (Lower Austria), south of Vienna (N 47°59'24'', E 16°13'44'') (see Baden Formation below for discussion and references).

Thickness: The maximum thickness of the Baden Group, based on the maximum thicknesses of its formations, ranges around 3300 m.

Lithostratigraphic subdivision: Aderklaa Conglomerate Fm. ("Aderklaaer Konglomerat"), Auersthal Fm. ("Auersthaler Schichten"), Baden Fm., Leitha Fm., Mannsdorf Fm., Matzen Fm. ("Matzen Sand"), Rabensburg Fm., Sandberg Mb.

Informal lithostratigraphic units: Aderklaa bentonite main marker ("Aderklaa Hauptmarker"), Aderklaa Sand ("Aderklaaer Sand"), Andlersdorf Conglomerate ("Andlersdorfer Konglomerat"), Devinska Nová Ves Fm., Enzesfeld Sand ("Enzesfelder Sande"), Gainfarn breccia ("Gainfarner Bekzie"), Gainfarn Sand ("Gainfarner Sande"), Hrušky Fm. ("Hrušecke vrstvy"), Iváň Fm., Jakubov Fm. ("Jakubovske vrstvy"), Kúty Member ("Kutske vrstvy"), Lanžhot Fm. ("Lanzhotske vrstvy"), Lindabrunn Conglomerate ("Lindabrunner Konglomerat"), Matzen bentonite main marker ("Matzen Hauptmarker), Rothneusiedl Conglomerate ("Rothneusiedler Konglomerat"), St. Margarethen limestone ("St. Margarethener Kalksandstein"), Studienka Fm. ("Studienske vrstvy"), Vöslau (Baden) Conglomerate ("Vöslauer (Badener) Konglomerat"), Žižkov beds ("Žižkovske vrstvy"), Zohor Conglomerate, Zwerndorf Sand ("Zwerndorfer Sand").

Fossils: See description of formations below.

Depositional environment: See description of formations below.

Age: Middle Miocene (Badenian, Langhian – early Serravallian).

Biostratigraphy: The Baden Group spans the calcareous nannoplankton zones NN4 (upper part), NN5 and NN6 (Kováč et al., 2004), the foraminiferan plankton zones M5, M6 and M7 (Hohenegger et al.,

2014) and comprises the regional benthic foraminiferal eco-biozones Lower and Upper Lagenidae Zone*, Spirorutilus* Zone and *Bulimina-Bolivina* Zone (Cicha et al., 1998).

Sequence stratigraphy: The Baden Group comprises three 3rd order cycles, termed Ba1, Ba2 and Ba3 by Strauss et al. (2006). These cycles are correlated with the global TB 2.3., TB 2.3.4. and TB 2.5. cycles of Haq et al. (1988) (Strauss et al., 2006; Piller et al., 2007; Hohenegger et al., 2014).

Underlying units: Pre-Neogene Units (e.g., Rhenodanubian Flysch, Magura Flysch, Mesozoic nappes of the Northern Calcareous Alps); Ottnangian formations (Bockfließ Fm., Lužice Formation); Karpatian formations (Aderklaa Fm.).

Overlying units: Sarmatian formations (Holic Fm.) in most of the distribution area; Quaternary deposits along basin margins and the southern Vienna Basin.

Lateral equivalents: Equivalents of the Baden Group are distributed throughout the area of the former Paratethys Sea. Herein we list only equivalents in adjacent depositional areas: Grund Fm. and Mailberg Fm. in the Austrian part of the NACFB (Roetzel, 2009). Baden Clay Fm., Rákos Limestone and Szilàgy Clay Marl Fm. in the Hungarian part of the Eisenstadt-Sopron Basin and the Hungarian Kisaföld basins (Császár, 1997). Špačince Fm. and Báhoň Fm. in the northern Danube Basin in Slovakia (Vass, 2002).

Geographic distribution: Throughout the Vienna Basin.

3.4.3.1.1. Rothneusiedl Formation

Derivation of name: After the village Rothneusiedl, a cadastral district of Vienna, in the central Vienna Basin (N 48°8’27.11’’, E 16°22’28.10’’). This formation was first recognized by Janoschek (1943), who already discussed an unconformity at its base. Later, Janoschek (1951) introduced the terms “Rothneusiedel Konglomerat (Rothneusiedel Conglomerate) and “Aderklaaer Konglomerat” (Aderklaa Conglomerate) for this unit, which are synonyms. The term Aderklaa Conglomerate was adopted by all subsequent authors (e.g., Kapounek et al., 1965; Kapounek and Papp, 1969; Papp et al., 1973; Kreutzer and Hlavaty, 1990). The name Aderklaa Conglomerate Fm., however, is unfavorable as it is nearly eponymous with the Aderklaa Fm. Although the term “Aderklaa Konglomerat” is very well established in the geological literature and widely used in applied geology, we propose to replace it by its synonym Rothneusiedl Fm.

Synonyms: Aderklaaer Konglomerat (Janoschek, 1951), Aderklaa Conglomerate (Weissenbäck, 1996), Aderklaa conglomerate Member (Kovač et al., 2004), Rothneusiedler Konglomerat (Janoschek, 1951).

Type section: Designated herein (Fig. 2): well Schönkirchen T2 (1825–1980 m) (N 48°21’10.84’’, E 16°41’52.24’’) (Fig. 1–2). Papp et al. (1973) mentioned wells Aderklaa 96 and Breitenlee 3 as typical, without designating a formal type section.

Thickness: The maximum thickness was documented from the Schwechat and Marchfeld depressions attaining about 369 m in well Mannsdorf T1 and 350–360 m at Andlersdorf and Breitstetten (Kapounek and Papp, 1969). In the Schönkirchen area, a thickness of up to 150 m is typical, whereas the thickness decreases rapidly towards the Matzen/Spannberg Ridge.

Lithology: The lithology and sedimentology of the Rothneusiedl Fm. was described in detail by Weissenbäck (1995) and is summarized in the following. Moderately cemented to loose, massive, clast-supported conglomerates composed of poorly to moderately rounded, medium to coarse gravel with frequent cobbles. The sediment is polymict with limestones, dolostones and various crystalline components. Intercalations of fine sand and silty marly clay are subordinate but increase in thickness in the Ollersdorf-Prottes area, where sand nearly replaces the conglomerates (Kapounek and Papp, 1969). No bedding and sedimentary structures are recognizable in the conglomerates. The amount of limestones relative to crystalline components increases strongly from SW to NE.

Well-log characteristics: The Rothneusiedl Fm. is recognized easily in well-logs by the sudden increase in SP-logs with sharp boundary towards the underlying Aderklaa Fm. In profile, the SP-logs are either strongly serrated within a high negative amplitude spectrum or cylinder shaped with rare intercalations of lower values, probably correlating with thin sand layers. RES-logs are partly mirroring SP-patterns but often are interrupted by high amplitude intervals, which lack counterpart in the SP-log. These intervals might indicate strongly cemented conglomerate layers. The top of the Rothneusiedl Fm. is often indicated by a sudden transition into shale line logs (socalled Lower Lagenidae Zone in internal OMV-reports).

Fossils: Grill (1943) documented Badenian fully marine lagenid-assemblages from upper parts of the Rothneusiedl Conglomerate in the Oberlaa area. No detailed faunal lists are available.

Depositional environment: The main part of the Rothneusiedl Fm. was interpreted by Weissenbäck (1995) as deposits of a braided river with numerous amalgamating channels and bars. Increasing amount of sand intercalations in its northern distribution area and the decrease of crystalline components in northeastern direction suggests drainage into northern-northeastern direction. Marine influence in this distal area is documented by marine foraminifers in the Oberlaa area (Grill, 1943), heralding the first Badenian transgression.

Age: Middle Miocene (early Langhian – early Badenian). The age of the Rothneusiedl Fm. was discussed controversially. Kapounek et al. (1965), Kapounek and Papp (1969), Papp et al. (1973), and Jiřiček and Seifert (1990) interpreted the unit as terminal phase of the Karpatian, whereas Janoschek (1943, 1951), Kreutzer and Hlavaty (1990), Kreutzer (1992), Kovač et al. (2004), and Strauss et al. (2006) discussed it as basal Badenian. The latter view was supported by seismic data, indicating a major unconformity and hiatus between the Rothneusiedl Fm. and the underlying Bockfließ and Aderklaa formations. Based on sequence stratigraphic models, Weissenbäck (1995, 1996) documented the basal Badenian position of

the Rothneusiedl Fm. In addition, the presence of lagenid-rich foraminiferal assemblages in the upper part of the Rothneusiedl conglomerate proof the Badenian age (Grill, 1943).

Biostratigraphy: Rögl et al. (2008) reported nannoplankton zone NN5 with *Helicosphaera waltrans* from the assumed upper part of Rothneusiedl Fm. in well Aderklaa 40 (2168 –2248 m). This interval, however, is already part of the distinctly younger Auersthal Fm. Based on the stratigraphic position, we assume an early Badenian age for the Rothneusiedl Fm. predating the FOD of *Orbulina* and corresponding to nannoplankton Zone NN4. In respect to the Vienna Basin ecobiostratigraphy it belongs to the Lower Lagenidae Zone.

Sequence stratigraphy: The Rothneusiedl Fm. represents lowstand systems tract deposits of the Badenian Sequence Ba1 of Strauss et al. (2006).

Lithostratigraphically higher rank unit: Baden Group.

Underlying units: Deposits of the Aderklaa Fm. underlay discordantly the Rothneusiedl Fm. in the central Vienna Basin and probably also in the southern Vienna Basin (Strauss et al., 2006).

Lithostratigraphically higher rank unit: Baden Group.

Underlying units: Deposits of the Aderklaa Fm. underlay discordantly the Aderklaa Conglomerate Fm. in the central Vienna Basin and probably also in the southern Vienna Basin (Strauss et al., 2006).

Overlying units: The Aderklaa Conglomerate Fm. is generally overlain by other Badenian deposits. Pelites of the Mannsdorf Fm., usually referred to as “Lower Lagenidae Zone” in internal OMV reports (e.g., Kapounek et al., 1965; Kapounek and Papp, 1969; Weissenbäck, 1995, 1996), overly the Aderklaa Conglomerate Fm. in wells Matzen 375, Aderklaa 78, Wittau 1, Orth 1, and Mannsdorf 1 (among others). In the Matzen and Schönkirchen area, the Aderklaa Conglomerate Fm. is usually overlain by the Matzen Fm.

Lateral equivalents: Within the Vienna Basin, the dolomitic Gainfarn breccia (Wessely et al., 2007) is a proximal and monomictic equivalent along the western margin of the southern Vienna Basin. The about 100-m-thick Rust Fm. in the Rust Range may be an equivalent (Häusler et al., 2014) in the Eisenstadt-Sopron Basin. The unnamed 105-m-thick marine clastics in the Roggendorf 1 well, described by Ćorić and Rögl (2004), is an equivalent in the Alpine-Carpathian Foredeep. The incision and at least parts of the sedimentary fill of the Mistelbach and Iváň canyons, described by Dellmour and Harzhauser (2012) and Harzhauser et al. (2017, 2019), are time equivalents as well. Vass (2002) correlated also the conglomerates and breccias with rare anhydrite of the Kúty Member (Kutske vrstvy; Špička, 1966) in the Kúty Graben in the Slovak Republic with the Aderklaa Conglomerate Fm., but these deposits may also be equivalents of the Auersthal Fm. (see below).

Geographic distribution: The Aderklaa Conglomerate Fm. is only known from subsurface drillings and displays a wide distribution in the central and southern Vienna Basin (Figure 3.3C). In the north, it is delimited by the Matzen/Spannberg Ridge and is already missing in several Matzen wells. It appears

on the Aderklaa High in the northwest and the Zwerndorf High in the northeast. In the west it is largely limited by the Leopoldsdorf Fault, aside from a small occurrence on the Oberlaa High, termed "Rothneusiedler Konglomerat" (Janoschek, 1951). The Aderklaa Conglomerate Fm. covers the Schwechat and Marchfeld basins, crosses the Engelhardstetten Fault in the southeast and pinches out along the Leitha Mountains in the south (Kapounek and Papp, 1969; Weissenbäck, 1995; Strauss et al., 2006). Kröll (1984) reports its distribution in the southern Vienna Basin down to Wiener Neustadt. In total, the Aderklaa Conglomerate Fm. covers an area of at least 950 km^2. Wessely et al. (2007) discussed the presence of the Rothneusiedl Conglomerate even along the western margin of the southern Vienna Basin in the Bad Vöslau area (based on seismic surveys), which might suggest an even much wider distribution of the formation.

Drillings: Aderklaa 78 (1890–2000 m), Bockfließ T1 (1870–1990 m), Matzen 270 (1765–1810 m), Schönkirchen T1 (1895–1980 m), Schönkirchen T2 (1825–1980 m), Schönkirchen T3 (1845–1960 m), Wittau 1 (2690–2700 m); additional core records: Andlersdorf 1 (3111–3407 m), Breitensee Ü1 (1324–1329 m), Eckartsau 1 (1700–1702 m), Glinzendorf T1 (2475–2480 m), Orth 1 (2694–2699 m), Schönau 1 (2475–2580 m), Schönkirchen T26 (1850–1859 m).

3.4.3.1.2. Mannsdorf Formation (Figures 3.4–3.5)

Derivation of name: After the village Mannsdorf an der Donau in the Vienna Basin (N 48°09'09.90'', E 16°39'37.05'').

Synonyms: Tegel, Lower Lagenindae Zone p.p.

Type section: Designated herein: well Mannsdorf 1 (2440–2575 m; cores: 26/3 2477.00–2481.00 m, 27/1 2505.00–2509.00 m, 28/1 2570,00–2572,00 m) (N 48°9'42.97'', E 16°41'3.82'') (Figures 3.1, 3.5).

Thickness: The maximum thickness of 685 m is documented from well Mühlberg T1 followed by well Ringelsdorf 2 with 479 m. Both sections seem to be influenced by synsedimentary subsidence and, therefore, the recorded thickness might be untypical. The preserved thickness varies considerably from well to well ranging from few tens of meters, e.g., Matzen 375 (35 m), Rabensburg 10 (50 m) to < 300 m, e.g., Bernhardsthal 4 (120 m), Wittau 1 (240 m), Aderklaa 78 (280 m) and the formation is even missing in some wells (e.g., in the Matzen area (Fig. 3.2)).

Lithology: Blue-grey clay, marl and silt, partly with thin silt and fine-sand layers ("Tegel"), sandstone layers, rare tuffitic layers are recorded from well Bernhardsthal 4.

Well-log characteristics: Shale-line logs are typical in the central Vienna Basin, indicated by a sudden decrease in SP- and RES-logs from the underlying pre-Neogene units and the high amplitude Aderklaa Conglomerate Fm. Strongly serrated logs, indicating frequent sand layers, may also occur (e.g., Ad 78). Broad cylinder- and funnel-shaped well-logs, suggesting rapid sediment transport, occur at Mühlberg T1 along the Steinberg Fault.

Fossils: The foraminiferan faunal composition is dominated by *Lenticulina inornata*, *Paragloborotalia mayeri, Globigerinella regularis, Tenuitellinata angustiumbilicata, Globoturborotalita druryi, Turborotalia quinqueloba, Lobatula lobatula, Trilobatus trilobus,* and *Globigerina praebulloides.* A subtropical evergreen broadleaved forest was identified from the hinterland of the Vienna Basin at that time (Rybár et al., 2019).

Depositional environment: The foraminiferal fauna suggests an outer neritic to upper bathyal depositional environment with high nutrient content and connection to the open sea. No inner neritic to coastal assemblages were detected in the lower Badenian samples.

Age: Middle Miocene (early Langhian - early Badenian), between c. 15.2 and 14.8 Myr.

An absolute age is available for a tuff layer in well Bernhardsthal 4, which indicates an age of 15.12 Ma (Sant et al., 2020). The Kuchyňa tuff, from a small outcrop along the western part of the Malé Karpaty Mountains at the eastern margin of the Vienna Basin was dated by Rybár et al. (2019) at 15.23 ±0.04 Ma. Based on these data, Sant et al. (2020) discussed a flooding of the Vienna Basin around 15.2 Ma. The position of the Be 4 tuff within the Mannsdorf Fm., however, is unclear and there is no reason to assume that the tuff is in the base of the formation.

An age for the upper boundary of the Mannsdorf Fm. can be expected around 14.8 Ma, based on the absence of *Orbulina* and on the finding of an *in-situ* moldavite at Immendorf in the upper part of the coeval Grund Fm. (Roetzel, 2009). The FOD of *Orbulina* in the Mediterranean is recorded by Iaccarino et al. (2011) at 14.56 Ma. and the Ries Impact, which ejected the moldavite, is dated at around 14.8 Ma (Schmieder et al., 2018).

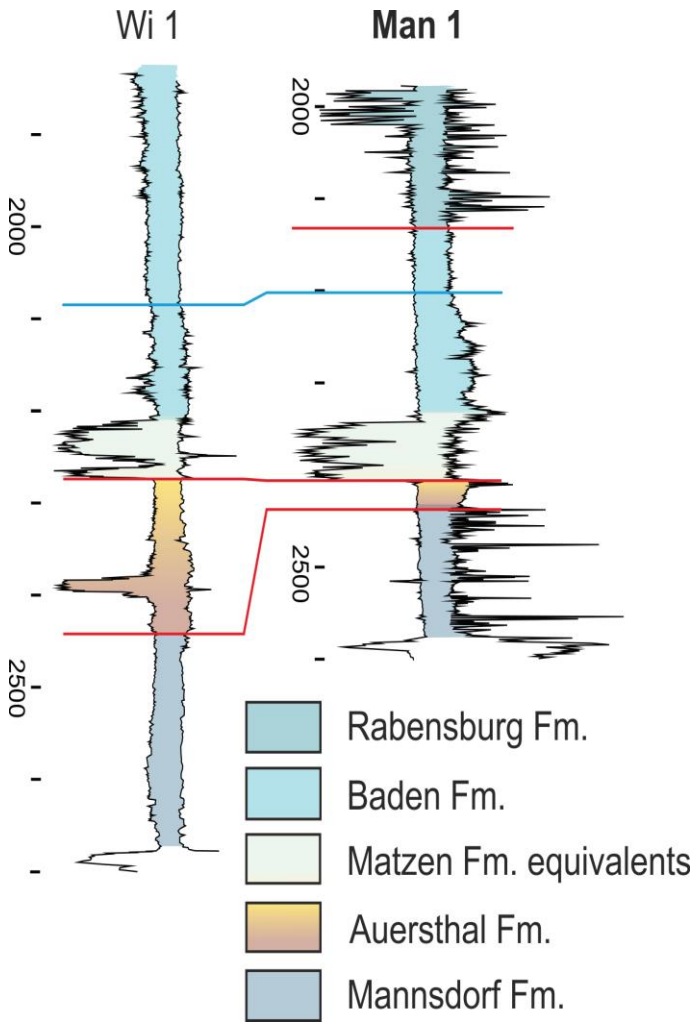

Fig. 3.5: Stratigraphic correlation of Wittau and Mannsdorf wells in the southern part of the central Vienna Basin. Logs are aligned along the top of the Matzen Fm. Red lines indicate sequence boundaries, blue lines are flooding surfaces. Right curve represents the SP-, left curve the RES-log in each well. Pre-Neogene basement is left blank. Type sections are written in bold.

Biostratigraphy: Samples from the Mannsdorf Fm. were the base for the description of the Lanzendorf Fauna by Grill (1941) what later on became the Lower Lagenidae Zone. *Uvigerina macrocarinata* and *Praeorbulina glomerosa circularis* are index fossils for the Lower Lagenidae Zone according to Papp (1963) and Papp et al. (1978) but, in fact, these species are rare and were completely missing in all herein analyzed samples.

Sequence stratigraphy: The Mannsdorf Fm. represents the transgressive systems tract of the Badenian Sequence Ba1 of Strauss et al. (2006).

Lithostratigraphically higher rank unit: Baden Group.

Underlying units: Lower Ottnangian Lužice Fm. in Mühlberg and Bernhardsthal fields; Aderklaa Conglomerate Fm. in Matzen and Aderklaa fields; pre-Neogene basement in Schwechat Field and Mannsdorf area.

Overlying units: Baden Fm., Matzen Fm. in the northern Vienna Basin; Auersthal Fm. in the central Vienna Basin. Between the Mannsdorf Fm. and all overlying formations exists a hiatus.

Lateral equivalents: The Devinska Nová Ves Fm. (Fordinál et al., 2012; Rybár et al., 2019) is a terrestrial equivalent at the eastern margin of the Vienna Basin. The Grund Fm. represents an age equivalent in the North-Alpine Foreland Basin (but not the slightly younger Gaindorf and Mailberg formations).

In the Slovak part of the Vienna Basin, the lowermost Badenian deposits are united in the up to 600-m-thick Lanžhot Formation (Kováč et al., 2004). Fordinál et al. (2012) report *Orbulina suturalis* from basal parts of the Lanžhot Fm. and, therefore, it is most likely not a temporal equivalent of the Mannsdorf Fm. Similarly, Brzobohatý and Stráník (2012) report *Orbulina suturalis* from the Lanžhot Beds in the Sedlec well (Czech Republic).

Geographic distribution: No surface outcrops; the Mannsdorf Fm. occurs in numerous wells in the northern and central Vienna Basin. The distribution area, however, is discontinuous and even close-by wells differ strongly in thickness and cannot be clearly correlated.

Remarks: The distribution of the Mannsdorf Fm. is very patchy. In respect to the outer neritic to upper bathyal depositional environment, such a discontinuous distribution is unlikely, and a much wider original distribution area can be expected. Seismic flattening based on a mid-Badenian maximum flooding surface, revealed the patches as small basins of an early middle Miocene paleorelief. This former geometry was lost thereafter during the mid-Badenian tectonic reorganization of the Vienna Basin.

Drillings: Mannsdorf 1 (2440–2575 m), Wittau 1 (2440–2680 m), Aderklaa 78 (1610–1890 m), Matzen 375 (1790–1825 m), Pirawarth 005 (2020–2100 m), Ringelsdorf 002 (3815–4294 m), Rabensburg 010 (2330–2380 m), Bernhardsthal 4 (2200–2330 m), Mühlberg T1 (2455–3140 m).

3.4.3.1.3. Auersthal Formation (Figures 3.2, 3.5)

Derivation of name: After the market town Auersthal in the central Vienna Basin (N 48°22’25.89’’, E 16°38’10.05’’).

The term “Auerstaler Konglomerat” (Auersthal Conglomerate) has been proposed by Papp et al. (1973, p. 198) for conglomerate and sand with flysch and crystalline components overlaying the Bockfließ, Aderklaa and Aderklaa Conglomerate formations.

Synonyms: Auerstaler Konglomerat (Papp et al., 1973), Auersthaler Schichten (Kröll, 1984; Kreutzer, 1986), Auerstal Member (Kováč et al., 2004), Upper Lagenidae Zone p.p.; Slovakia: Kúty Member of the Lanžhot Fm. (Fordinál et al., 2012).

Type section: Designated herein: well Matzen 269 (1675–1730 m: core: 13/1 1706.00–1708.50 m) (N 48°22’59.37’’, E 16°42’22.09’’) (Figures 3.1–3.2).

Thickness: The maximum thickness of about 160 m is known from the Schwechat Field in Wittau 1. Typically, the Auersthal Fm. attains about 40 to 120 m in the Matzen, Aderklaa and Schönkirchen fields and generally pinches out towards the Matzen/Spannberg Ridge.

Lithology: A succession of conglomerates and sand with marl intercalations; flysch components prevail.

Well-log characteristics: Basal parts are frequently characterized by very broad, blocky cylinder shaped SP-logs, often opposed by strongly serrated RES-logs. Upsection passing abruptly into strongly serrated, amalgamated funnel-shaped logs frequently forming a rough fining upward trend; shale line intervals may also be developed (Wittau 1) suggesting a more distal position.

Fossils: A rich marine microfauna dominated by *Trilobatus (Globigerinoides) trilobus, Spirorutilus carinatus, Heterolepa dutemplei, Lenticulina inornata, Nonion commune, Globigerina bulloides,* and *Orbulina suturalis* was detected in Mannsdorf 1 (2428 m), Matzen 127 (1695 m) and Wittau 1 (2291 m).

Depositional environment: A coastal marine delta with channels (Kreutzer and Hlavatý, 1990; Kreutzer, 1993) shedding into an outer neritic marine habitat. The outer neritic foraminiferal assemblage is in strong contrast to the occurrence of freshwater ostracods reported by Wessely (2006). In respect to the deep erosion of the Auersthal Fm., which truncated parts of the freshwater deposits of the Karpatian Schönkirchen Mb., it is not unlikely that the freshwater fossils have been reworked from Karpatian strata. Similarly, indications for an alternation of marine and limnic conditions (Papp et al., 1973; Wessely, 2006) may result from reworking of Karpatian freshwater deposits.

Age: Middle Miocene (Langhian - middle Badenian); younger than 14.56 Ma based on the frequent occurrence of *Orbulina*.

Biostratigraphy: Nannoplankton zone NN5 with *Helicosphaera waltrans*. In respect to the Vienna Basin ecobiostratigraphy it belongs to the Upper Lagenidae Zone (Papp et al., 1973; Kröll, 1984; Kreutzer, 1986).

Sequence stratigraphy: The Auersthal Fm. represents the lowstand systems tract of the Badenian Sequence Ba2 of Strauss et al. (2006).

Lithostratigraphically higher rank unit: Baden Group.

Underlying units: The Auersthal Fm. has a strong erosive base and displays a clear N-S trend. It rests directly on the Schönkirchen Mb. of the Aderklaa Fm. in the northern Matzen field, on the Aderklaa Conglomerate Fm. in the southern Matzen and Schönkirchen fields and on the lower Badenian Mannsdorf Fm. in the Aderklaa and Schwechat fields. In the Slovak territory, the probably equivalent Kúty beds overlay the Láb beds (=Schönkirchen Mb.) (Fordinál et al., 2012).

Overlying units: In all wells overlain by the Matzen Fm.

Lateral equivalents: No lateral equivalents are known from the Austrian part of the Vienna Basin. Only the Andlersdorf Conglomerate (Kapounek et al., 1965; Kapounek and Papp, 1969) might be a lateral equivalent, but this will need confirmation by seismic data. On Slovak territory, the about 150-m-thick Zohor Conglomerate (Vass et al., 1988) from Devínska Nová Ves, correlated with the Calcareous Nannoplankton Zone NN5 by Fordinál et al. (2012), might be a temporal equivalent. Similarly, the Kúty beds (Kutske vrstvy; Špička, 1966) may represent temporal and genetical equivalents in the northern and central Záhorie Lowlands in Slovakia. Fordinál et al. (2012) describe the Kúty Member as mixture of sandstone, gravel and variegated clays of up to 250 m thickness in the Malacky region. Like the Auersthal Fm., the Kúty Member already contains *Orbulina suturalis* (Fordinál et al., 2012). The Kúty Member grades into the pelites of the Lanžhot Fm.

Geographic distribution: Only subsurface in the central Vienna Basin, spanning from the Matzen/Spannberg Ridge south to the Schwechat Basin and to the Mannsdorf region, where only a thickness of about 30 m is recorded.

Drillings: Auersthal T32 (1765–1840 m), Aderklaa 28 (1740–1810 m), Aderklaa 40 (2168–2248 m), Mannsdorf 1 (2410–2440 m), Matzen 112 (1622–1650 m), Matzen 127 (1670–1790 m), Matzen 127 (1740–1820 m), Matzen 267 (1660–1700 m), Matzen 269 (1675–1730 m), Matzen 270 (1680–1750 m), Matzen 375 (1680–1790 m), Schönkirchen T1 (1785–1870 m), Schönkirchen T2 (1760–1820 m), Schönkirchen T25 (1765–1840 m), Schönkirchen T3 (1790–1845 m), Wittau 1 (2280–2440 m).

Remarks: Since Papp et al. (1973), the Auersthal Fm. has only rarely been mentioned (e.g., Kreutzer and Hlavatý, 1990; Kreutzer, 1986, 1992, 1993; Wessely, 2006). Kreutzer (1992, 1993) discussed the deposits as part of a Badenian lowstand systems tract and as incised valley fill.

3.4.3.1.4. Matzen Formation (Figures 3.2, 3.5)

Due to its economic importance as the most productive play in the Vienna Basin, this unit was discussed in numerous internal OMV reports and papers (e.g., Kölbl, 1959, 1966; Kreutzer and Hlavatý, 1990; Kreutzer, 1986, 1993; Hamilton and Johnson, 1999; Hamilton et al., 2000; Fuchs et al., 2001; Wessely 2006), usually referred to as "Matzen Sand". In older literature, however, it was described as 16th TH (= "sixteenth Tortonian Horizon" based on an erroneous correlation of the Langhian/Serravallian strata of the Vienna Basin with the Mediterranean Tortonian).

Derivation of name: After the village Matzen in the central Vienna Basin (N 48°24'4.38", E 16°41'42.33").

Synonyms: Matzener Sand (Kröll, 1984), 16. Tortonhorizont (16th Tortonian Horizon) (Kreutzer, 1971), Matzen Sand, Zwerndorf Sand (Weissenbäck, 1996), Matzen sands Member (Kováč et al., 2004), Upper Lagenidae Zone – Spiroplectammina Zone p.p., Zwerndorf Member (Kováč et al., 2004).

Type section: Designated herein: well Matzen 269 (1619–1673 m; cores: 8/3 1624.00–1628.00 m, 9/7 1628.00–1636.80 m, 10/10 1636.90–1645.90 m, 11/10 1645.90–1655.00 m,
12/4 1655.00–1664.00 m) (N 48°22'59.37'', E 16°42'22.09'') (Figures 3.1–3.2).

Thickness: The Matzen Fm. typically attains a thickness around 20–50 m in the Bockfließ and Schönkirchen fields and grows to 70 m in the Matzen area (e.g., Matzen 270: 1602–1672 m). It pinches out in S-N direction towards the Matzen/Spannberg Ridge and appears again north of the Matzen/Spannberg Ridge, where it attains a thickness of about 105 m. The maximum thickness of the Matzen Fm. is 140 m (Kreutzer, 1986; Kreutzer and Hlavatý, 1990).

Lithology: Fine to coarse sand, moderately to well sorted, strongly bioturbated, often oil impregnated. Marl layers, silty fine-sand layers and ripple bedding may occur. Intercalations of thin corallincean limestones have been described by Kreutzer (1978).

Well-log characteristics: Broad, blocky cylinder-shaped well logs with moderate serrations. SP-logs may indicate a minor, stepwise fining upward trend, opposed by strong RES-values. The top is distinctly indicated by the abrupt switch to the shale-line interval of the overlaying marls of the Baden Fm.

Fossils: A rather low diverse, marine microfauna with *Heterolepa dutemplei, Lenticulina inornata, Spirorutilus carinatus, Cibicidoides ungerianus, Cibicidoides pachyderma, Martinotiella communis, Anomalinoides badenensis,* and *Melonis pompilioides*. Macrofossils are poorly preserved including frequent plant debris, pectinid and cardiid bivalves, balanids and tubes of *Ditrupa.* A detailed micropaleontological study on the Matzen Fm. was published by Rupp (1986).

Depositional environment: Coastal marine environments with sand dunes and shoreface settings in the sphere of influence of a sand rich braid or fan delta (Fuchs et al., 2001). Rupp (1986) reported an inner neritic depositional environment, whereas the herein studied foraminiferal assemblages suggest a deeper setting in the middle to outer neritic. Rupp (1986), however, reported a rapid deepening within the Matzen Fm. and our samples may derive from its upper parts.

Age: Middle Miocene (Langhian - middle Badenian); younger than 14.56 Ma based on the frequent occurrence of *Orbulina.*

Biostratigraphy: In respect to the Vienna Basin ecobiostratigraphy it belongs to the *Spirorutilus* Zone (Kapounek et al., 1965: Sandschalerzone; Kreutzer, 1986: Sandschalerzone, Spiroplectammina Zone) or the Upper Lagenidae Zone – *Spirorutilus* (*Spiroplectammina*) Zone (Weissenbäck, 1996).

Sequence stratigraphy: The Matzen Fm. represents the initial transgressive systems tract of the Badenian Sequence Ba2 of Strauss et al. (2006).

Lithostratigraphically higher rank unit: Baden Group.

Underlying units: The Matzen Fm. is a transgressive unit overlying older units discordantly from south to north starting with the Auersthal Fm. in the Matzen to Schönkirchen fields, the Bockfließ and Aderklaa formations, in the Bockfließ Field, and even Rhenodanubian Flysch along the Matzen/Spannberg Ridge.

Overlying units: The Matzen Fm. is overlain throughout by marls of the Baden Fm.

Lateral equivalents: The nearly 300-m-thick Zwerndorf Sand is a genetic equivalent of the Matzen Fm. (e.g., Zwerndorf 4: 1518–1800 m). It displays a NW–SE orientation between Dürnkrut and Zwerndorf and was transported from NW (Kreutzer, 1986). Its stratigraphic position is confined by the Matzen bentonite main marker, which lies on the Zwerndorf Sand and also on top of the Matzen Fm. (Kreutzer, 1986). An equivalent of the Matzen Fm. reaches also into the Schwechat Basin (Wittau 1: 2210–2278 m) and the Mannsdorf area (Mannsdorf 1: 2340–2410 m).

A surface outcrop of an equivalent of the Matzen Fm. with huge fossiliferous sand-dunes is exposed in Donnerskirchen at Eisenstadt, representing the distal parts of the Hartl Fm. (Kroh et al., 2003).

A time equivalent in the Slovak territory might be represented by the 150-m-thick Žižkov beds (Buday, 1946), which are described by Fordinál et al. (2012) (as Žižkov Member) as a transgressive unit of gravel, sand and clayey sand, partly with reworked Karpatian fossils. This correlation, however, will need confirmation. The distribution area of the Žižkov beds around Lakšárska Nová Ves and Borský Mikuláš in the Záhorie Lowlands is about 30 km N-E of the distribution of the Matzen Fm. around the Matzen/Spannberg Ridge and both units will most probably represent separate sedimentary bodies.

Geographic distribution: Wide subsurface distribution in the central and southern Vienna Basin. Traditionally, only deposits in the Matzen area have been described as “Matzen Sand”. Herein, however, we include also its equivalents north of the Matzen/Spannberg Ridge (e.g., Spannberg 10: 1960–2066, Spannberg 14: 2233–2340), where the Matzen Fm. attains about 105 m thickness. These units agree in lithology, well-log patterns and lithostratigraphic position.

Drillings: Bockfließ 78 (1615–1660 m), Bockfließ 003 (1632–1660 m), Matzen 112 (1603–1623 m), Matzen 267 (1602–1658 m), Matzen 269 (1619–1673 m), Matzen 270 (1602–1672 m), Matzen 127

(1700–1740 m), Matzen 325 (1607–1680 m), Schönkirchen T1 (1746–1782 m), Schönkirchen T25 (1682–1762 m).

3.4.3.1.5. Baden Formation (Figures 3.4–3.5)

Derivation of name: After the town Baden in the central Vienna Basin (N 48°00'29.00", E 16°14'03.72").

Synonyms: Badener Tegel, Badener Serie (Kapounek et al., 1960; Papp, 1963); Slovakia: Lanžhot Fm. p.p., Jakubov Fm. (Fordinál et al., 2012). Baden Clay Formation in the Hungarian part of the Eisenstadt-Sopron Basin (Császár, 1997).

Type section: Designated herein: The 102-m-long scientific core from the abandoned brick yard Baden/Sooss near the town Baden (Lower Austria), south of Vienna (N 47°59'24'', E 16°13'44''). This core represents only the uppermost part of the formation but is sedimentologically and paleontologically outstandingly well studied and correlated by means of biostratigraphy and astrochronology (Báldi and Hohenegger, 2008; Rupp and Hohenegger, 2008; Hohenegger et al. 2008, 2009a, b, 2014; Hohenegger and Wagreich, 2012).

Remarks: The brick yard Sooss (also: Baden-Sooss), c. 2 km S of the raiway station of Baden, where "Badener Tegel" is outcropping, was designated by Papp (1963, p. 229) as type locality of the "Badener Serie" (former: "Tortonian in the Vienna Basin"). Later, Papp et al. (1978) when reorganizing the stratigraphic system of the Paratethys defined the "Badener Serie" as Badenian Stage. The brick yard Sooss was defined as holostratype for this stage (Papp and Steininger, 1978). The brick yard was abandoned, used as a waste dump and offers currently very poor outcrops. In 2002, in the area of the former clay pit, a scientific core was drilled (Wagreich et al., 2008) (see above).

Reference section: As reference section for the Baden Fm. we designate herein well Ringelsdorf 2 (2770–3815 m; cores: 8/6 2823.00–2828.00 m, 9/6 2937.00–2942.00 m, 10/5 3027.00–3032.00 m, 11/5 3152.00–3157.00 m, 12/5 3243.00–3248.00 m, 13/6 3370.00–3375.00 m, 14/6 3471.00–3476.00 m, 15/6 3541.00–3546.00 m, 16/6 3592.00–3597.00 m, 17/6 3649.00–3654.00 m, 18/6 3767.00–3772.00 m) (N 48°32'11.32'', E 16° 51' 59.90''). This well section represents a full cycle in terms of sequence stratigraphy with a basal lowstand sand, a rapid deepening during the transgressive systems tract culminating in a distinct shale-line interval around the maximum flooding surface and a coarsening upward trend of the highstand systems tract in its upper part. Moreover, underlying (Mannsdorf Fm.) and overlying (Rabensburg Fm.) units are lithostratigraphically and biostratigraphically defined.

Thickness: The maximum thickness of the Baden Fm. ranges around 1120 m in the Rabensburg Field (Rabensburg 2: 1300–2420 m) and around 1045 m in the Ringelsdorf Field (Ringelsdorf 2: 2770-3815 m). In the well Zistersdorf Übertief 2Aa a maximum thickness of 2450 m was recorded (OMV data).

Lithology: Blue-grey to green-grey clay and marl with silt and fine sand intercalations (so-called "Tegel"). Thin corallinacean limestones may be intercalated; bioturbation is frequent.

Well-log characteristics: The Baden Fm. has a characteristic well-log pattern, which allows a correlation across wide areas of the Vienna Basin. It is indicated by an abrupt transition from the blocky patterns of the Matzen Fm. into a long shale line interval with a nearly smooth SP-log and a low amplitude RES-log. Many wells show a clear fining upwards trend within this shale line interval culminating in a distinct incision, marking the maximum flooding surface. This horizon is one of the most characteristic and constant features in the Vienna Basin and is used as marker horizon by OMV geologists. Above follows a rapid coarsening indicated by strongly serrated, high-amplitude SP-logs and serrated RES-logs of somewhat lower amplitudes.

Fossils: This formation contains some of the most outstanding fossiliferous localities of the Vienna Basin, which are emblematic for the Badenian stage of the Central Paratethys. Hundreds of invertebrate and vertebrate species have been recorded since the 19th century from the localities Baden, Bad Vöslau, Baden-Sooss, Gainfarn (Austria) and Mikulov (Czech Republic) (see Papp et al., 1978 and Rögl et al., 2008 for an overview).

Depositional environment: Basinal settings represent normal marine inner to middle neritic environments, often with a rich benthic mollusk fauna; the type section reflects a mean water depth around 250 m (Hohenegger et al., 2008). Outer neritic to upper bathyal environments established along tectonically active zones such as the Steinberg Fault in the Mühlberg area (Harzhauser et al., 2019). Sea grass meadows are typical in nearshore environments (Zuschin et al., 2007; Harzhauser et al., 2019).

Age: Middle Miocene (late Langhian – middle Badenian); younger than 14.91 Ma (Nannoplankton Zone NN5) and younger than 14.56 Ma (Planktonic Foraminifer Zone M6). The type section Baden-Sooss was astronomically tuned to 14.221 and 13.982 Ma by Hohenegger and Wagreich (2012). No absolute dating is available to support this estimate.

The oil bearing plays, called 13th to 15th TH (= "Tortonian Horizons") in OMV reports, are parts of the Baden Fm. (Kreutzer, 1971). The Baden Fm. contains two important bentonite layers. The "Matzen Hauptmarker (MHM)" (= Matzen bentonite main marker) is slightly above the Matzen Fm. in the base of the Baden Fm. (between 16th and 15th TH of OMV nomenclature) and the "Aderklaa Hauptmarker (AHM)" (= Aderklaa bentonite main marker) coincides roughly with the boundary from Lagenidae to *Spirorutilus* Zone (Kreutzer, 1986). Both are recognized easily in well-logs by their high conductivity.

Biostratigraphy: The occurrence of the calcareous nannofossil *Sphenolithus heteromorphus* and the absence of *Helicosphaera ampliaperta* point at NP Zone NN5 (Ćorić and Hohenegger, 2008), the occurrence of *Orbulina suturalis* indicates planktonic foraminiferal zone M6 (Rögl et al., 2008).

In terms of classical ecobiostratigraphy of the Vienna Basin the Upper Lagenidae Zone and the *Spirorutilus* Zone (following the ideas of Grill, 1941) were based on samples of the Baden Fm.

Sequence stratigraphy: The Baden Fm. comprises sediments of the transgressive systems tract and the highstand systems tract of the Badenian Sequence Ba2 of Strauss et al. (2006).

Lithostratigraphically higher rank unit: Baden Group.

Underlying units: Matzen Fm. in the central Vienna Basin, Bockfließ and Mannsdorf formations in northern Vienna Basin.

Overlying units: Rabensburg Fm. in all studied drillings; the Baden Fm. forms the landscape in the Baden region south of Vienna and is partly covered by Quaternary deposits.

At the type locality the Baden Fm. is discordantly overlain by Sarmatian pelitic sediments separated by a fault (Papp and Steininger, 1978, p. 140, Abb. 30).

Lateral equivalents: The "Aderklaaer Sand" (Aderklaa Sand) is a sand rich intercalation within the Baden Fm. It is overlain by the Aderklaa bentonite main marker and bears foraminiferal assemblages typical for the Upper Lagenidae Zone (Kreutzer, 1986; Weissenbäck, 1996).

The "Vöslauer (Badener) Konglomerat" (Vöslau (Baden) Conglomerate) and the "Gainfarner Bekzie" (Gainfarn breccia) (Brix and Plöchinger, 1988) are local coarse clastic equivalents at the western margin of the Vienna Basin. The "Gainfarner Sande" (Gainfarn Sand) and "Enzesfelder Sande" (Enzesfeld Sand) are very fossil rich coastal deposits (Brix and Plöchinger, 1988).

Shallow water carbonate rocks of the Leitha Formation around the southern part of the Leitha Mountains and the margin of the Vienna Basin as well as on paleo-topographic highs in the northern Vienna Basin (e.g., Steinberg area) (see also below).

At least parts of the Lanžhot Fm., as described by Fordinál et al. (2012) and Brzobohatý and Stráník (2012), which are correlated with the Lagenidae Zone and contain *Orbulina suturalis*, are time equivalents or even represent a full equivalent of the Baden Fm. Most probably, this part of the Lanžhot Fm. represents the shale-line interval of the transgressive systems tract of the Baden Fm. The up to 1000-m-thick pelitic Jakubov Fm. (Fordinál et al., 2012) is an equivalent of the Baden Fm. in the Záhorie Lowlands on Slovak territory. It corresponds to the *Spirorutilus carinatus*-dominated interval of the Baden Fm. Important lateral temporal equivalents are the landscape forming corallinacean limestones of the Leitha Fm. In the Czech part of the Vienna Basin, especially in the Mikulov area, the Hrušky Fm. of Picha et al. (2006) and Schultz et al. (2010) corresponds to the Baden Fm.

Geographic distribution: The Baden Fm. has a wide distribution and occurs throughout the investigation area and also in the Mistelbach Halfgraben (e.g., Hohenruppersdorf 24: 270–740 m) as well as in the southern Vienna Basin (where the type locality is located).

Drillings: Mühlberg T1 (1740–2450 m), Bernhardsthal 5 (1610–2385 m), Bernhardsthal 4 (1580–2200 m), Rabensburg 1 (1590–2470 m), Rabensburg 2 (1300–2420 m), Ringelsdorf 2 (2770–3815 m), Matzen 127 (1605–1700 m), Aderklaa 78 (1385–1670 m), Schwechat 1 (1615–2160).

3.4.3.1.6. Leitha Formation

Derivation of name: Named after the hill range called "Leitha Mountains" between the river Leitha and Lake Neusiedl (Lower Austria – Burgenland). The name "Leithakalk" was already mentioned by Keferstein (1828), but he commingled Badenian and Sarmatian limestones. The name was since then widely used and refered to and is restricted to the Badenian corallinacean limestones in the Vienna and Eisenstadt-Sopron basins (e.g., Tollmann, 1955, 1985; Steininger and Papp, 1978; Dullo, 1983; Piller et al., 1996, Wiedl et al., 2012, 2013).

Synonyms: Leithakalk, Nulliporenkalk, Nulliporakalk, Lithothamnienkalk, Lithothamnion limestone, Corallinaceenkalk (e.g., Keferstein, 1828; Fuchs, 1894; Wessely, 1983; Brix and Plöchinger, 1988; Sauer et al., 1992; Piller, 1994). Rákos Limestone Formation in the Eisenstadt-Sopron Basin (Császár, 1997).

Remarks: The term "Leitha Limestone" was also applied to Miocene corallinacean limestones outside the Vienna and Eisenstadt-Sopron basins; e.g., Studencki (1988) used the term to describe the lithofacies of the Polish Pinczow Limestones. Friebe (1990, 1991) was the first author, who applied a strict lithostratigraphic concept and introduced the Weißenegg Fm. as lithostratigraphic unit for the "Leitha Limestones" of the Styrian Basin (see also Riegl and Piller, 2000 for discussion).

Type section: Fenk quarry close to Großhöflein in Burgenland (N 47°50'45.78'', E 16°28'34.60'') (Eisenstadt-Sopron Basin, Burgenland, Austria). This section was proposed by Steininger and Papp (1978) as faciostratotype of the "Leitha Limestone" and described in detail by Riegl and Piller (2000). The Fenk quarry is abandoned but still accessible.

Thickness: According to Tollmann (1985), the Leitha Fm. attains a thickness of up to 50 m based on outcrop data in the southern Leitha Mountains. A maximum subsurface thickness of 120 m is reported by Dlabač (1971) from the Láb region in the Slovak part of the Vienna Basin.

Lithology: The Leitha Fm. is characterized by whitish to light-yellowish, usually well cemented, corallinacean limestones with coralline red algae in various growth forms, ranging from rhodolite facies to maërl-types. Corals are subordinate, forming local coral carpets; *Isognomon/Hyotissa* beds are frequent (Riegl and Piller, 2000), whereas marl intercalations are rare and thin. Some typical microfacies types are bioclastic algal debris facies, bioclastic rhodolite debris, bioclastic algal mollusk, and foraminiferal algal debris (Dullo, 1983; Piller and Kleemann, 1991; Wiedl et al., 2012, 2013).

Fossils: The Leitha Fm. is exceptionally rich in fossils. Coralline red algae, such as *Lithothamnion, Spongites, Mesophyllum, Lithophyllum, Phymatolithon*, and *Sporolithon*, are the most important rock-forming elements (Hrabovský, 2013) along with various foraminifers (e.g., *Amphistegina, Acervulina*,

miliolids, alveolinids) and celleporiform bryozoans. Corals are represented mainly by *Porites*, accompanied by *Tarbellastraea, Caulastrea, Acanthastrea*, and *Stylocora*. Mollusks (*Hyotissa, Isognomon, Macrochlamys, Pinna, Periglypta, LIthophaga, Pholadoma*) and echinoderms (*Clypeaster, Parascutella, Echinolampas)* are further important fossils; see Piller and Kleemann (1991), Riegl and Piller (2000) and Wiedl et al. (2012, 2013) for more detailed surveys.

Depositional environment: Shallow marine, subtropical carbonate ramps and shoals with coral carpets, sea grass meadows, rhodolite pavements and maërl bottoms. The typical depositional depth ranged from <10 m down to ~60 m in a generally low hydrodynamic setting (Riegl and Piller, 1991; Wiedl et al., 2012, 2013).

Age: Middle Miocene (late Langhian - middle Badenian); younger than 14.91 Ma based on correlation with calcareous nannoplankton Zone NN5 (Wiedl et al., 2013).

Biostratigraphy: The presence of the calcareous nannofossil *Sphenolithus heteromorphus* in a marly layer of the Fenk Quarry restricts the type locality to the NPZ NN5 and the Upper Lagenidae – *Spirorutilus* zones (Wiedl et al., 2013). Based on the foraminiferal species *Uvigerina venusta* and *U. liesingensis* Steininger and Papp (1978) placed the Fenk Quarry into the Upper Badenian *Bulimina-Bolivina* zone but the uvigerinid foraminifers seem less reliable markers (compare Haunold, 1995).

Lithostratigraphically higher rank unit: Baden Group.

Underlying units: In many cases, pre-Neogene units form the base of the Leitha Fm., e.g., Lower Austroalpine crystalline and Triassic dolomite in the Leitha Mountains (Pascher and Brix, 1994, Wiedl et al., 2013), Triassic dolomite in Bad Vöslau (Piller and Vavra, 1991) and Rhenodanubian Flysch in the Steinberg area (Grill, 1968). In the Eisenstadt area (Eisenstadt-Sopron Basin), the middle Badenian siliciclastic Hartl Fm. (Kroh et al., 2003) underlays the Leitha Fm. In the Mannersdorf quarries, the Leitha Fm. develops above coarse siliciclastics of Badenian age (Wiedl et al., 2012).

Overlying units: The Leitha Fm. forms the surface of the landscape and overlying units have mostly been eroded aside from lower Sarmatian relics ("detrital Leitha Limestone, Holic Fm., Harzhauser and Piller, 2004).

In subsurface occurrences, the Leitha Fm. is overlain by unnamed upper Badenian deposits (e.g., Göttlesbrunn Horst, Strauss et al., 2006).

Lateral equivalents: The Baden Fm. is a pelitic equivalent in basinal settings. The Jakubov Fm. sensu Fordinál et al. (2012) is the pelitic equivalent on Slovak territory and the limestones of the Stupava Member of the Jakubov Fm. are a full equivalent (Hrabovský and Fordinál, 2013). Further coeval corallinacean limestones are the Mailberg Fm. in the North Alpine Foreland Basin (Mandic, 2004) and the Weißenegg Fm. in the Styrian Basin (Friebe, 1990, 1991).

Geographic distribution: The type area of the Leitha Fm. is situated around the southwestern Leitha Mountains. This occurrence is bound in the east by a roughly N-S striking fault line running from

Mannersdorf in the north to Donnerskirchen in the south (see fig. 9 in Wiedl et al., 2014). The Leitha Fm. occurs also along the margins of the Vienna Basin; e.g., Wöllersdorf, Baden, Bad Vöslau (Austria), Mikulov (Czech Republic), Borský Mikuláš (Slovakia) (Grill, 1968; Čtyroký et al., 1985, Fuchs and Grill, 1984; Fordinál et al., 2012). Further occurrences formed on paleo-topographic highs (e.g., Maustrenk and Prinzendorf in the Steinberg area, Grill, 1968). Subsurface occurrences are documented from the Göttlesbrunn area in the southern Vienna Basin (Strauss et al., 2006).

Outcrops: Central Vienna Basin: Prinzendorf Steinberg-cave (Lower Austria, N 48°35’1.01", E 16°43'13.97") (Mayer et al., 1989); Vrchná hora close to Stupava (Slovakia, N 48°15'39.13", E 17°2'47.87") (Hrabovský, 2013). Southern Vienna Basin: Baden Rauchstallbrunngraben (Lower Austria, N 48°0'0.86", E 16°12'1.79" (Piller and Vavra, 1991, Piller et al., 2007); Mannersdorf (Lower Austria, N 47°58'20.00", E 16°36'51.02") (Wiedl et al., 2012), Loretto Teufelsloch (Lower Austria, N 47°53'47.08", E 16°31'46.21") (own data). Eisenstadt-Sopron Basin: Müllendorf (Burgenland, N 47°51'30.23", E 16°26'54.58") (Wiedl et al., 2013); Großhöflein, Fenk quarry (Burgenland, N 47°50’45.78’’, E 16°28’34.60’’) (Riegl and Piller, 2000).

3.4.3.1.7. Rabensburg Formation (Figures 3.4–3.5)

Derivation of name: After the village Rabensburg in the northern Vienna Basin (N 48°38'59.45", E 16°54'04.27").

Remarks: In the Slovak part of the Vienna Basin this formation is termed Studienske vrstvy (Studienka beds) by Špička, (1966) and Studienka Fm. by Kováč et al. (2004), Hyžný et al. (2012) and Fordinál et al. (2012), which was also adopted by Piller et al. (2004) and Harzhauser et al. (2017, 2019) for the Austrian part of the Vienna Basin. A formalization of the Studienka Fm., however, is lacking so far. A well described section in the Studienka Fm. is a clay-pit at Devinska Nová Ves near Bratislava (Kováčová and Hudáčková, 2009; Košťák et al., 2018). Despite the good accessibility, this only 12-m-thick section is inadequate to serve as a type section for a formation of up to 1000 m thickness. Similarly, the only 20-m-thick section at Walbersdorf near Mattersburg (Burgenland) has been studied in detail by Bachmayer and Weinfurter (1965), Rögl and Müller (1976) and Rupp (1986) but is too short to serve as type section and is now recultivated. Therefore, we prefer to name this formation after the deposits in the Rabensburg and Bernhardsthal fields in the northern Vienna Basin, where the largest thickness is observed.

Synonyms: Badener Serie p.p. (Kreutzer, 1971), Bulimina-Bolivina Zone, Bulimina-Rotalia Zone, Rotalien-Zone, Studienka Formation.

Remarks: The 1st to 10th and maybe also the 12th TH (“Tortonian Horizon”) of OMV nomenclature are part of the Rabensburg Fm. (Kreutzer, 1971).

Type section: Designated herein: well Rabensburg 1 (690–1585 m; cores: 1/1 700.00–705.00 m, 2/1 1060.00–1065.00 m, 3/2 1103.50–1108.50 m, 4/1 1150.00–1155.00 m, 5/1 1200.00–1205.00 m, 6/2 1200.00–1253.50 m, 7/1 1250.00–1253.50 m, 8/2 1290.00–1295.00 m, 9/2 1355.00–1360.00 m, 10/2 1495.00–1500.00 m, 11/1 1530.00–1535.00 m) (N 48°38'53.86'', E 16°54'43.02'') (Figures 3.1, 3.4).

Thickness: A maximum thickness of 1000 m is recorded from the Paltendorf-Ringelsdorf Field and up to 900 m are drilled in the Rabensburg Field; usually, however, strong Sarmatian erosion reduces the thickness considerably. In the Záhorie Lowlands in Slovakia the equivalent Studienka Fm. attains up to 900 m thickness (Fordinál et al., 2012).

Lithology: Dark-grey to green-grey, partly laminated clay, marl and silty marl with sand and numerous corallinacean limestone intercalations (Kreutzer, 1978); gravel intercalations have been described especially from the upper parts in the Matzen Field (Kreutzer, 1974). In the Bernhardsthal field, thin lignite seems and characeen-limestones occur in basal parts of the formation. Anhydrite was found in cuttings of the basal parts of the formation in the Mühlberg Field (Harzhauser et al., 2018).

Well-log characteristics: The Rabensburg Fm. has a characteristic well log pattern consisting of a rapid succession of high amplitude and high frequency SP-logs opposed by similar, only slightly less serrated RES-logs. Shale line intervals are nearly absent and very short.

Fossils: The Rabensburg Fm. is exceptionally rich in marine fossils including numerous foraminifers, mollusks and vertebrates (e.g., Rupp, 1986; Kováčová and Hudáčkova, 2009; Hyžný et al., 2012; Harzhauser et al., 2019; Košťák et al., 2018). Basinal foraminiferal assemblages are characterized by *Bulimina elongata, Bolivina dilatata, Bulimina schischkinskayae, Bolivina antiqua,* and *Bulimina striata*. Lagoonal settings are strongly dominated by *Ammonia*.

Depositional environment: The Rabensburg Fm. comprises a broad range of marine depositional environments. Dysoxic bottom water conditions prevailed in basinal environments, reflected in laminated deposits (Kováčová and Hudáčková, 2009). Periodically, these dysoxic conditions even reached to the surrounding corallinacean shoals (Schmid et al., 2001). Coastal to inner neritic settings were often dominated by mudflats and lagoonal environments with a rich mollusk fauna (Harzhauser et al., 2019) laterally alternating with agitated shoreface and foreshore settings (Hyžný et al., 2012).

Age: Middle Miocene (Serravallian - late Badenian); younger than 13.53 Ma based on NP Zone NN6 (Hudáčková et al., 2000; Jamrich and Halásová, 2010).

Biostratigraphy: Based on *Discoaster exilis* the deposits in Devínska Nová Ves (Slovakia) were correlated with the Calcareous Nannoplankton Zone NN6 (Jamrich and Halásová, 2010).

The frequent occurrence of buliminids and bolivinids were the reason for establishing the upper Badenian ecobiostratigraphic zone "Marine Fauna mit Bolivina dilatata" by Grill (1941) which became lateron the *Bulimina-Bolivina* Zone (Papp and Turnovsky, 1953).

Sequence stratigraphy: The Rabensburg Fm. comprises sediments of the transgressive systems tract and the highstand systems tract of the Badenian Sequence Ba3 of Strauss et al. (2006).

Lithostratigraphically higher rank unit: Baden Group.

Lithostratigraphic subdivision: The heterogenous lithologies (e.g., lignites in the Bernhardsthal area) might justify a definition of members within the Rabensburg Fm. One member was formalized along the western margin of the Malé Karpaty by Baráth et al. (1994) near Devinska Nová Ves (Slovakia) as Sandberg Mb. (of the Studienka Fm.). The Sandberg Mb. comprises coastal marine sand and gravel (Fordinál et al., 2012).

Underlying units: Baden Fm.

Overlying units: Subsurface overlain by the lower Sarmatian Holic Fm. with marked erosive relief; occasionally the upper Sarmatian Skalica Fm. may lie directly with erosional contact on the Rabensburg Fm. Surface outcrops occur around Bratislava.

Lateral equivalents: The unnamed corallinacean limestones in the northeastern part of the Leitha Mountains (Wiedl et al., 2014) and the corallinacean limestones of St. Margarethen in the Rust Mountains (Dullo, 1983; Schmid et al., 2001) are equivalents of the Rabensburg Fm., which formed on agitated shoals (Wiedl et al., 2014). Remark: Schmid et al. (2001) dated the corallinacean limestones of St. Margarethen as NN5, based on the rare occurrence of *Helicosphaera waltrans*. The foraminferal fauna, however, was correlated with the upper Badenian *Bulimina-Bolivina* Zone. Therefore, we assume that the nannoplankton was partly reworked, which is supported by the observed reworking of middle Badenian limestones.

The “Lindabrunner Konglomerat” (Lindabrunn Conglomerate) has been described by Brix and Plöchinger (1988) as coarse grained coastal unit.

Geographic distribution: Wide subsurface distribution throughout the northern and southern Vienna Basin and also in the Mistelbach Halfgraben (e.g., Poysdorf 1: 310–485 m). Surface outcrops are exposed close to Bratislava (Devinska Nová Ves: Jamrich and Halásová, 2010; Hyžný et al., 2012).

Drillings: Mühlberg 77 (1110–1760 m), Mühlberg T1 (1160–1740 m), Mühlberg 100 (1160–1700 m), Bernhardsthal 5 (1160–1700 m), Bernhardsthal 7 (1120–1590 m), Bernhardsthal 6 (1120–1550 m), Rabensburg 1 (690–1585 m), Rabensburg 2 (995–1300 m), Rabensburg 011 (1950–2150 m), Paltendorf 1 (1805–2800 m), Paltendorf T1 (1775–2770 m), Ringelsdorf 2 (1820–2770 m), Spannberg 8 (1560–2010 m), Aderklaa 78 (1320–1385 m), Matzen 126 (1180–1540 m).

3.5. Discussion

The lowermost Neogene units found in the central Vienna Basin can be attributed to the coastal-lagoonal Bockfließ Fm., which is of early Ottnangian age. In the Bernhardsthal-Mühlberg-Rabensburg area in the northern Vienna Basin, the oldest deposits are represented by the open marine Lužice Fm. A transitional position is represented by the Steinberg wells, where deeper marine faunas indicate the transition from the shallow lagoonal conditions of the Bockfließ Fm. towards the open marine Lužice Fm. The geographic gap between both occurrences is most probably a result from heavy erosion during the Styrian Tectonic Phase (Weissenbäck, 1995; Wessely, 2000; Harzhauser et al., 2019). The micro- and macrofaunas of both formations point to fully marine conditions. No indications of a connection to the Ottnangian *Rzehakia* faunas (= *Oncophora* beds in older literature) was detected. These developed in the North Alpine Foreland Basin during the late Ottnangian. At that time the Matzen area was dry land or the respective deposits have been eroded.

No marine deposits of Karpatian age were detected in the wells of the northern Vienna Basin. Such marine sediments are confined to the Korneuburg Basin, the Mistelbach Halfgraben, the adjacent Alpine-Carpathian Foredeep (Harzhauser et al., 2017) and the Slovak part of the north-eastern Vienna Basin (Kováč et al., 2004). In the central and southern Vienna Basin, Karpatian deposits are represented by the Aderklaa Fm., which is strongly tilted (Figure 3.6). The Aderklaa Fm. can be separated into the basal Gänserndorf Mb., reflecting alluvial fans, and the Schönkirchen Mb., which reflects various wetland environments with floodplains, braided rivers and lakes. Despite the geographic gap between the marine and freshwater deposits, both areas most probably formed a continuous distribution area during the Karpatian. This is documented by brackish-marine gastropods in basal parts of the Schönkirchen Mb. and by the occurrence of Karpatian foraminifers in a single horizon of the Schönkirchen Mb. The position of this horizon in the wire-logs suggests a coincidence with a flooding of the wetlands. This in turn, allows for the first time to interpret the Aderklaa Fm. from the viewpoint of sequence stratigraphy. Thus, the Gänserndorf Mb. corresponds to a LST, which passes into the TST of the lower Schönkirchen Mb. This is also reflected by the fining upward trends in the wire-logs. The full flooding of the wetlands is expressed by the maximum flooding surface and the occurrence of marine plankton. The subsequent HST is indicated by the onset of coarsening upward patterns in the wire logs but is frequently truncated by erosion.

The total thickness of this cycle attains up to 1400 m which rivals or even surpasses the thickness of the Karpatian Laa Fm. in the Mistelbach Halfgraben and Alpine-Carpathian Foreland Basin. Therefore, we tentatively assume, that the Aderklaa Fm. spans the entire Karpatian.

After a major erosive phase and considerable tilting of lower Miocene strata during the Styrian Tectonic Phase, sedimentation started with the lower Badenian Aderklaa Conglomerate Fm. (Figure 3.6). The stratigraphic position strongly suggests that these braided river deposits can be linked to the canyon and channel systems of the Mistelbach Halfgraben and North Alpine-Carpathian Foreland Basin, as described by Dellmour and Harzhauser (2012) and Harzhauser et al. (2017, 2019). The Roggendorf conglomerates in the NACFB (Ćorić and Rögl, 2004) are most probably an equivalent, representing a W-E trending feeder.

The Matzen/Spannberg Ridge forms the northern limit of the Aderklaa Conglomerate Fm. Along this tectonic feature the formation pinches out. Therefore, the Matzen/Spannberg Ridge developed during the Styrian Phase and was no barrier towards the central and southern Vienna Basin during the early Miocene as suggested in nearly all stratigraphic schemes (e.g., Kreutzer, 1993).

The lower Badenian Mannsdorf Fm. represents open marine settings, partly indicating even upper bathyal conditions. Its geographic patchiness and the absence of any shallow water deposits, suggests, that only erosional relics of a formerly widely distributed deposit are preserved. Flattening of the marked middle Badenian mfs clearly proofs this interpretation and reveals the remnants as lower Badenian paleobasins.

In terms of sequence stratigraphy, the lower Badenian deposits reflect a LST, represented by the Aderklaa Conglomerate Fm. and the subsequent transgression reflected by the marls of the Mannsdorf Fm. (BA1 sequence of Strauss et al., 2006). A separation into TST, mfs and HST of the Mannsdorf Fm. based only on well-logs is difficult due to the insufficient data available.

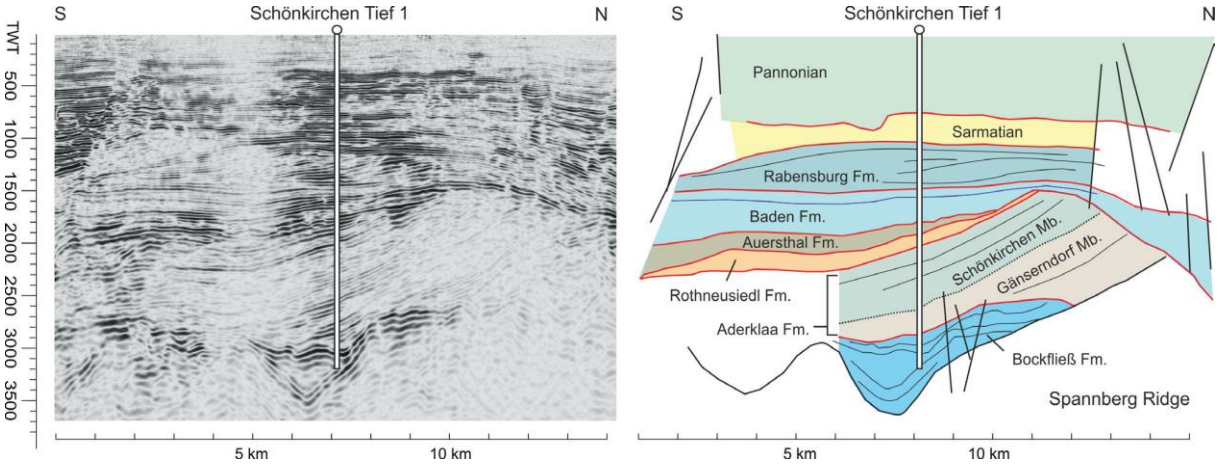

Fig. 3.6. Seismic interpretation of a N-S seismic line showing the tilted lower Miocene strata along the Matzen/Spannberg Ridge; note that the Matzen Fm. is not depictable due to the low thickness.

The age of the early Badenian can be constrained for the first time by the tuff age from the Bernhardsthal Field (15.12 Ma., Sant et al., 2020), the occurrence of a Ries-Impact moldavite at Immendorf (Grund Fm.) in the NAFB (Ries-Impact = 14.8 Ma. Schmieder et al., 2018), and the absence

of *Orbulina* (< 14.56 Ma., Iaccarino et al., 2011). In addition, the age of the Kuchyňa tuff (15.2 Ma.), at the eastern margin of the Vienna Basin supports the estimate (Rybár et al., 2019). This is an enormous advantage, as former correlations of the early Badenian have been mainly conceptual or are overall wrong.

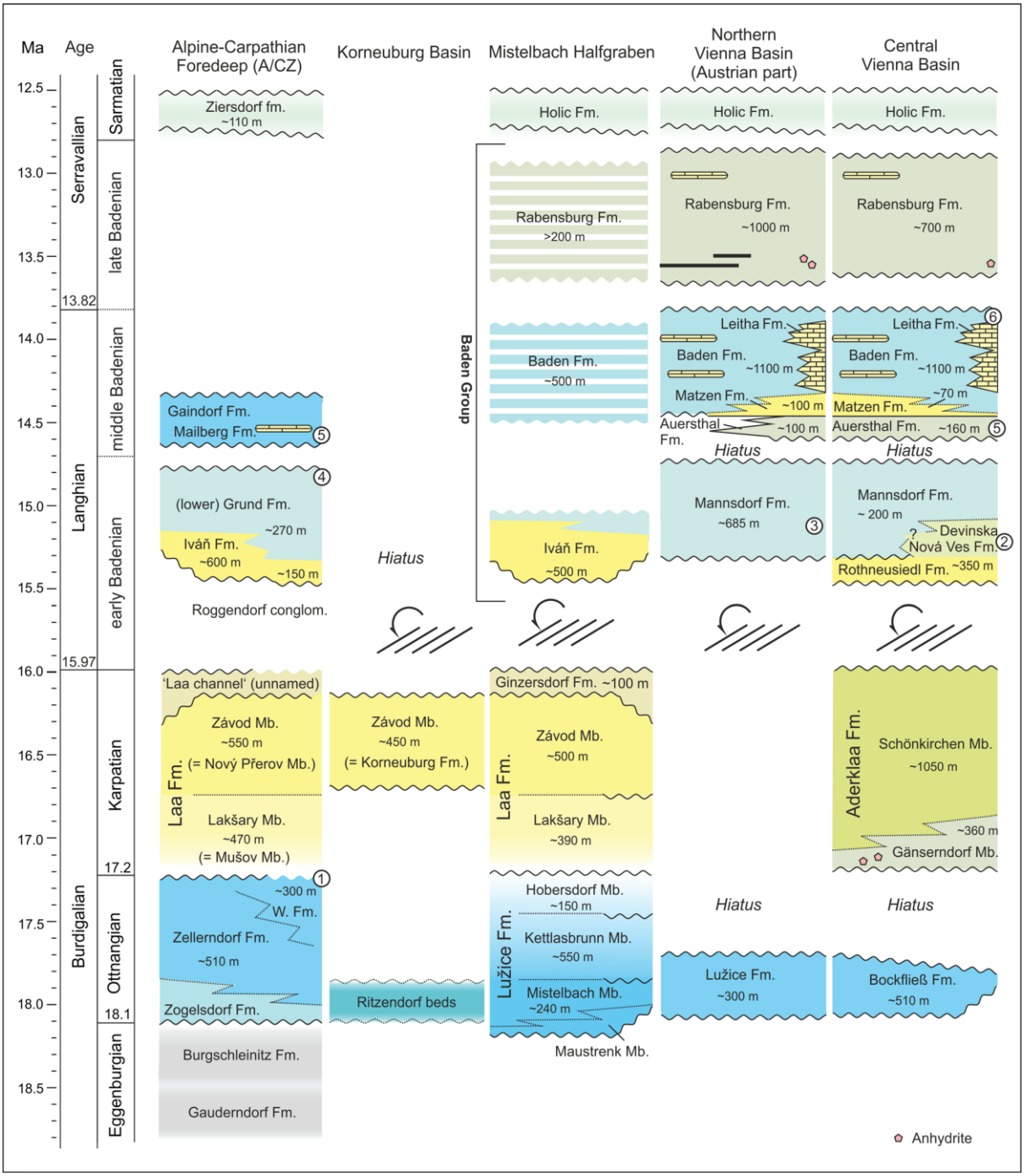

Fig. 3.7. New lithostratigraphic scheme for the Austrian parts of the northern and central Vienna Basin and correlation with adjacent basins (after Harzhauser et al., 2019); W. Fm.: Wildendürnbach Fm. (Palzer-Khomenko et al., 2018a); 1: Straning tuff (Roetzel et al., 2014); 2: Kuchyňa tuff (Rybár et al., 2019); 3: Be 4 tuff (Sant et al., 2020); 4: Ries Impact (Schmieder et al., 2018); 5: FOD Orbulina in the Mediterranean Sea (Iaccarinio et al., 2011); 6: Baden-Soos core (Hohenegger and Wagreich, 2012).

Note that the spatial relation between the marine Mannsdorf Fm. and the terrestrial Devinská Nova Ves Fm. is hypothetical.
Note 1: the Badenian of the Mistelbach Halfgraben is not well resolved yet; during the Badenian, the Mistelbach Halfgraben was an uplifted block and sedimentation was strongly discontinuous.
Note 2: Karpatian deposits are missing in the Austrian part of the northern VB but are represented by the Laa Fm. in the Slovak part of the basin (Kováč et al., 2004).
A hiatus is obvious between the early and middle Badenian; this is indicated by strong erosion and tilting of the lower Badenian Mannsdorf Fm. The middle Badenian cycle starts with the coarse siliciclastics of the Auersthal Fm., which can be dated for the first time to be younger than 14.56 Ma based on the occurrence of *Orbulina*. It is rapidly overlain by the sand of the Matzen Fm., which quickly passes into the pelites of the Baden Fm. The depositional environment of the Baden Fm. ranged from upper bathyal to outer neritic to coastal marine but open marine conditions prevailed in the Vienna Basin. In terms of sequence stratigraphy, the Auersthal Fm. can be explained as LST, overlain by the sands of the initial TST (Ba 2 sequence of Strauss et al., 2006). The rapid deepening is indicated by the long shale line interval seen in all wire-logs, culminating in a pronounced mfs, which is used as marker throughout the Vienna Basin in seismic analysis by OMV. The HST is indicated by the serrated high amplitude SP-logs.
Interestingly, the frequently used ecobiozones Upper Lagenidae Zone and *Spirorutilus* Zone fall both completely within the middle Badenian and are both present in the Baden Fm. These “zones” form an ecological succession due to the deepening of the basin.

The upper Badenian is represented by the up to 1000-m-thick Rabensburg Fm. The depositional environment was generally shallower compared to the middle Badenian and middle to inner neritic settings prevailed. In wire-logs and seismic surveys, it is characterized by high amplitude and high frequency patterns and prograding sigmoidal sedimentary bodies. In terms of sequence stratigraphy, the upper Badenian represents a single cycle (Ba3 of Strauss et al., 2006) with a short TST, moderately developed mfs and thick HST, which is often truncated in thickness by the subsequent Sarmatian deposits. The LST of the upper Badenian cycle is difficult to detect in wire-logs, due to the weak separation from the HST logs of the middle Badenian. Regionally, the occurrence of lignite and anhydrite indicates the onset of the upper Badenian (Harzhauser et al., 2018).

3.5.1. Sedimentation rates

Assuming that the 510-m-thick Bockfließ Fm. spans about half of the Ottnangian, would result in a sedimentation rate of ~ 1.0 m/kyr. This estimate is not unrealistic compared to the sedimentation rate of the Lužice Fm. in the adjacent Mistelbach Halfgraben, which ranges around 0.9 m/kyr (Harzhauser et al., 2019).

Given a duration of the Karpatian of 1.2 Ma, a thickness of 1400 m would result in a gross sedimentation rate of ~1.2 m/kyr. This rate will surely be an overestimate, as the maximum thickness of the alluvial fans of the Gänserndorf Mb., might be local phenomena. Excluding these deposits results still in a high sedimentation rate of ~ 0.9 m/kyr. As the depositional environment was a nearly flat floodplain slightly above sea level, this rate requires a significant subsidence during the piggy-back stage of the Vienna Basin.

We assume that the early Badenian deposition in the central and northern Vienna Basin ranged roughly from ~15.5 to ~14.7 Ma corresponding to a duration of ~ 0.8 Myr. Given a maximum thickness of at least 685 m for the Mannsdorf Fm. results in a sedimentation rate of ~ 0.9 m/kyr. As the total thickness of the Mannsdorf Fm. is most probably underestimated, the sedimentation rate might have been even higher. Applying the assumed age for the early Badenian flooding at 15.2 Ma of Sant et al. (2020) would even require sedimentation rates up to 1.4 m/kyr.

The maximum thickness of middle Badenian deposits in the central Vienna Basin attains ~1300 m. This estimate, however, is based on wells in a tectonically active position and might be untypical. A more representative succession is the Rabensburg 2 well in which the well-logs capture a full succession of LST, TST, mfs and HST. In this well, the middle Badenian attains about 900 m thickness. The middle Badenian in our stratigraphic model has a duration of about 0.8 Myr, which results in a high sedimentation rate of ~1.1 m/kyr. This value is nearly identical with the estimate of Hölzel et al. (2008) but is in contrast with results of Hohenegger and Wagreich (2012), who calculated a sedimentation rate of ~0.5 m/kyr for the upper part of the Baden Fm. in the Baden-Sooss core. This low sedimentation rate would result in a total thickness of about 400 m for the entire Baden Fm., which is an obvious underestimation in respect to the well data (for the northern and central Vienna Basin). Applying the sedimentation rate of Hohenegger and Wagreich (2012) to Rab 2 would result in a duration of 1.8 Myr for the middle Badenian, which is distinctly too long. Thus, the estimate by Hohenegger and Wagreich (2012) may apply only for a short interval or may be based on incorrect astronomical tuning.

The time frame of the late Badenian is constrained by the Langhian/Serravallian boundary at 13.82 Ma and by the Badenian/Sarmatian boundary around 12.8 Ma. Thus, the late Badenian had a maximum duration of ~1 Myr, which results in a sedimentation rate of up to 1 m/kyr in the northern Vienna Basin.

3.6. Conclusions

For the first time, we propose a clear lithostratigraphic scheme for the northern and central Vienna Basin (Figure 3.7). The lower Miocene can be separated into two Ottnangian formations (Lužice Fm., Bockfließ Fm.). Upper Ottnangian deposits seem to be missing either due to non-deposition or

subsequent erosion. The Karpatian is represented in the central Vienna Basin by the Aderklaa Fm. and its members (Gänserndorf Mb., Schönkirchen Mb.) but was eroded largely in the northern Vienna Basin. The middle Miocene Baden Group reveals a complex succession of fluvial, coastal neritic to open marine deposits with distinct and widespread lithologies, which are separated herein into the Aderklaa Conglomerate Fm., the Mannsdorf Fm., the Auersthal Fm., the Matzen Fm., the Baden Fm., the Leitha Fm., and the Rabensburg Fm.

Major disruptions of sedimentation coinciding with tilting and erosion took place during the terminal Ottnangian, the Karpatian/Badenian boundary and the terminal early Badenian. The erosion between the middle and upper Badenian and upper Badenian and Sarmatian are comparatively less severe and sedimentary contacts are generally concordant.

Our results suggest high sedimentation rates ranging roughly around 1 m/kyr for the marine Ottnangian, the lacustrine Karpatian and the marine early, middle and late Badenian. We do not see major differences between the piggy-back stage and the pull-apart stage of the basin. Therefore, these results challenge the subsidence analyses by Hölzel et al. (2008) and Lee and Wagreich (2017), who propose major shifts in sedimentation rates with several “pulses”. The poor biostratigraphic constraints in these analyses might partly have led to misinterpretations.

Concluding, the strict stratigraphic concept as proposed herein is a proper base for new calculations of subsidence histories and may challenge the currently proposed tectonic concepts.

Acknowledgements

We are grateful to Wolfgang Hujer (OMV, Gänserndorf) and his team for help and support during the sampling campaigns. Special thanks to Herwig Peresson and the whole Exploration Austria Team. We greatly acknowledge the very open-minded politics of the OMV-AG to provide access to core material, well-log data, seismic images and internal reports to support geosciences.

Many thanks to Thomas Hofmann (Geological Survey of Austria, Vienna) and his team for providing rare literature.

References

Albano, P.G., Sabelli, B., 2012. The molluscan assemblages inhabiting the leaves and rhizomes of a deep water *Posidonia oceanica* settlement in the central Tyrrhenian Sea. Scientia Marina, 76/4, 721–732. https://doi.org/10.3989/scimar.03396.02C

Bachmayer, F., Weinfurter, E., 1965. *Bregmaceros*-Skelette Pisces mit in situ erhaltenen Otolithen aus den tortonischen Ablagerungen von Walbersdorf. Senckenbergiana Lethaea, 46a, 19–33.

Báldi, K., Hohenegger, J., 2008. Paleoecology of benthic foraminifera of the Baden-Sooss section Badenian, Middle Miocene, Vienna Basin, Austria. Geologica Carpathica, 59/5, 411–424. http://www.geologicacarpathica.com/browse-journal/volumes/59-5/article-455/

Báldi, T., 1973. Mollusc fauna of the Hungarian Upper Oligocene Egerian. Akadémiai Kiadó, Budapest, 511 pp.

Baráth, I., Nagy, A., Kováč, M., 1994. Sandberské vrstvy - vrchnobádenské marginálne sedimenty východného okraja Viedenskej panvy. Geologické práce, Správy, 99, 59–66.

Bartek, V., 1989. Nové litostratigrafické členenie vrchného panónu a pontu v slovenskej časti Viedenskej panvy. Mineralia Slovaca, 21/3, 275–281.

Bergen, J. A., de Kaenel, E., Blair, S., Boesiger, T., Browning, E., 2017. Oligocene-Pliocene taxonomy and stratigraphy of the genus *Sphenolithus* in the circum North Atlantic Basin: Gulf of Mexico and ODP Leg 154. *Journal of Nannoplankton Research*, 37 (2–3), 77–112.

Brix, F., Plöchinger, B., 1988. Erläuterungen zu Blatt 76 Wiener Neustadt. Geologische Karte der Republik Österreich 1:50000. Verlag der Geologischen Bundesanstalt, Wien, 85 pp.

Brzobohatý, R., Stráník, Z., 2012. Paleogeography of the Early Badenian connection between the Vienna Basin and the Carpathian Foredeep. Central European Journal of Geosciences, 4/1, 126–137, https://doi.org/10.2478/s13533-011-0045-z

Buday, T., 1946. Několik poznámek k stratigrafii a paleogeografii tortonu v západní části dolnomoravského úvalu. Věstnik Státniho Geologického Ústavu Československé Republiky, Prague, 21/3–6, 145–152.

Buday, T., Cicha, J., 1956. Nové názory na stratigrafii spodniho a stredniho miocenu Dolnomoravského úvalu a Považi. Geologické práce, Zošit, 43, 5–56.

Cicha, I., Rögl, F., Rupp, C., Čtyroký, J., 1998. Oligocene-Miocene foraminifera of the Central Paratethys. Abhandlungen der Senckenbergischen Naturforschenden Gesellschaft, 549, 1–325.

Ćorić, S., Rögl, F., 2004. Roggendorf-1 borehole, a key-section for Lower Badenian transgressions and the stratigraphic position of the Grund Formation Molasse Basin, Lower Austria. Geologica Carpathica, 55, 165–178.

Ćorić, S., Hohenegger, J., 2008. Quantitative analyses of calcareous nannoplankton assemblages from the Baden-Sooss section Middle Miocene of Vienna Basin, Austria. Geologica Carpathica, 59, 447–460. http://www.geologicacarpathica.com/browse-journal/volumes/59-5/article-457/

Csaszar, G., 1997. Basic lithostratigraphic units of Hungary, charts and short descriptions. Geological Institute of Hungary, Budapest, 114 pp.

Čtyroký, P., 2000. Nové litostratigafické jednotky pannonu vídeòské pánve na Moravì. Vìstník Èeského geologického ústavu, 75, 159–170.

Čtyroký, P., Havlíček, P., Stráník, Z., Pálenský, P., 1995. Geologická a přírodovědná mapa CHKO a BR Pálava. Geologische und naturwissenschaftliche Karte des Landschaftsschutzgebietes (CHKO) und des Biosphärenreservates (BR) Pálava. 1: 25.000. Český geologický ústav, Praha.

De Leeuw, A., Mandic, O., Krijgsman, W., Kuiper, K., Hrvatović, H., 2011. A chronostratigraphy for the Dinaride Lake System deposits of the Livno-Tomislavgrad Basin: the rise and fall of a long-lived lacustrine environment. Stratigraphy, 8, 29–43.

Dellmour, R., Harzhauser, M., 2012. The Iván Canyon, a large Miocene canyon in the Alpine-Carpathian Foredeep. Marine and Petroleum Geology, 38, 83–94. https://doi.org/10.1016/j.marpetgeo.2012.07.001

Dlabač, M., 1971. Dvé studie o sedimentaci v badenu (torton) Vídeňské pánve na Slovensku. Geologické práce, Správy, 56, 89–108.

Dullo, W.C., 1983. Diagenesis of fossils of the Miocene Leitha Limestone of the Paratethys, Austria: An example for faunal modifications due to changing diagenetic environments. Facies, 8, 1–112. https://doi.org/10.1007/BF02536740

Elečko, M., Vass, D., 2001. Litostratigrafické jednotky usadenín sarmatského veku vo viedenskej panve. Mineralia Slovaca, 33, 1–6.

Fodor, L., 1995. From transpression to transtension: Oligocene–Miocene structural evolution of the Vienna Basin and the East Alpine–Western Carpathian junction. Tectonophysics, 242, 151–182. https://doi.org/10.1016/0040-1951(94)00158-6

Fordinál, K., Maglay, J., Elečko, M., Nagy, A., Moravcová, M., Vlačiky, M., Kohút, M., Németh, Z., Bezák, V., Polák, M., Plašienka, D., Olšavský, M., Buček, S., Havrila, M., Hók, J., Pešková, I., Kucharič, L., Kubeš, P., Malík, P., Baláž, P., Liščák, P., Madarás, J., Šefčík, P., Baráth, I., Boorová, D., Uher, P., Zlínska, A., Žecová, K., 2012. Explantions for the geological map of the Vienna Basin, 1:50 000. State Geological institute of Dionýz Štúr, Bratislava, 232 pp. (in Slovak).

Friebe, J.G., 1990. Lithostratigraphische Neugliederung und Sedimentologie der Ablagerungen des Badeniens (Miozän) um die Mittelsteirische Schwelle (Steirisches Becken, Österreich). Jahrbuch der Geologischen Bundesanstalt, 133, 223–257.

Friebe, J.G., 1991. Carbonate sedimentation within a siliciclastic environment: the Leithakalk of the Weißenegg Formation (Middle Miocene, Styrian Basin, Austria). Zentralblatt für Geologie und Paläontologie, 1990/11, 1671–1687.

Fuchs, R., 1990. Multistratigraphische Untersuchungen in den Bockfliesser Schichten des Zentralen Wiener Beckens. OMV-Report, Vienna, 28 pp.

Fuchs, R., Ramberger, R., Veit. C., 2001. Renaissance des größten Öl- und Gasfeldes in Österreich Wiener Becken. Erdöl, Erdgas, Kohle, 117, 528–540.

Fuchs, T., 1894. Ueber abgerollte Blöcke von Nulliporen-Kalk im Nulliporen-Kalk von Kalksteinbruch. Zeitschrift der Deutschen Geologischen Gesellschaft, 46/1, 126–130.

Fuchs, W., Grill, F., 1984. Geologische Karte von Wien und Umgebung 1:200.000. Geologie der Österreichischen Bundesländer. Geologische Bundesanstalt, Wien.

Gebhardt, H., Ćorić, S., Krenmayr, H.-G., Steininger, H., Schweigl, J., 2013. Neudefinition von lithostratigraphischen Einheiten des oberen Ottnangium Untermiozän in der alpin-karpatischen Vortiefe Niederösterreichs: Pixendorf-Gruppe, Traisen-Formation und Dietersdorf-Formation. Jahrbuch der Geologischen Bundesanstalt Wien 153, 1–4, 15–32.

Giacobbe, S., 2012. Biodiversity loss in Sicilian transitional waters: the molluscs of Faro Lake. Biodiversity Journal, 3/4, 501–510.

Grill, R., 1941. Stratigraphische Untersuchungen mit Hilfe von Mikrofaunen im Wiener Becken und den benachbarten Molasse-Anteilen. Oel und Kohle, 37, 595–602.

Grill, R., 1943. Über mikropaläontologische Gliederungsmöglichkeiten im Miozän des Wiener Beckens. Mitteilungen der Reichsanstalt für Bodenforschung, 6, 33–44.

Grill, R., 1960. Untergrenze und Gliederung des Miozäns im Wiener Becken. Mitteilungen der Geologischen Gesellschaft in Wien (Verhandlungen des Comité du Néogène Méditerranéen, 1. Tagung in Wien, 10.-20 Juli 1959), 52 (1959), 15–132.

Grill, R., 1968. Erläuterungen zur geologischen Karte des nord-östlichen Weinviertels und zu Blatt Gänserndorf. Geologische Bundesanstalt, Vienna, 155 pp

Grill, R., Janoschek, W., 1980. Erdöl und Erdgas. In: Oberhauser, R., (Ed.), Der geologische Aufbau Österreichs, Springer Verlag, Wien-New York, pp. 556–574.

Grunert, P., Tzanova, A., Harzhauser, M., Piller, W.E., 2014. Mid-Burdigalian Paratethyan alkenone record reveals link between orbital forcing, Antarctic ice-sheet dynamics and European climate at the verge to Miocene Climate Optimum. Global and Planetary Change, 123, 36–43. https://doi.org/10.1016/j.gloplacha.2014.10.011

Grunert, P., Hinsch, R., Sachsenhofer, R.F., Bechtel, A., Ćorić, S., Harzhauser, M., Piller, W.E., Sperl, H., 2013. Early Burdigalian infill of the Puchkirchen Trough (North Alpine Foreland Basin, Central

Paratethys): Facies development and sequence stratigraphy. Marine and Petroleum Geology, 39, 164–186. https://doi.org/10.1016/j.marpetgeo.2012.08.009

Hamilton, W., Johnson, N., 1999. The Matzen Project; rejuvenation of mature field. Petroleum Geoscience, 5, 119–125, https://doi.org/10.1144/petgeo.5.2.1190

Hamilton, W., Wagner, L., Wessely, G., 2000. Oil and Gas in Austria. Mitteilungen der Österreichischen Geologischen Gesellschaft, 92, 235–262.

Haq, B.U., Hardenbol, J., Vail, P.R., 1988. Mesozoic and Ceno-zoic chronostratigraphy and cycles of sealevel changes. In: Wilgus, C.K., (Ed.), Sea-level changes - an integrated approach. Society of Economic Paleontologists and Mineralogists, Special Publications, 42, pp. 71–108.

Hardenbol, J., Thierry, J., Farley, M.B., Jacquin, T.,Graciansky, P.-C., Vail, P.R., 1998. Mesozoic and Cenozoic Sequence Chronostratigraphic Framework of European Basins. In: Graciansky, C.-P., Hardenbol, J., Jacquin, T., Vail, P.R., (Eds.), Mesozoic and Cenozoic sequence stratigraphy of European basins. Society for Sedimentary Geology Special Publication, 6, 3–13.

Harzhauser, M., 2002. Marine und brachyhaline Gastropoden aus dem Karpatium des Korneuburger Beckens und der Kreuzstettener Bucht Österreich, Untermiozän. Beiträge zur Paläontologie, 27, 61–159.

Harzhauser, M., Mandic, O., 2009. Neogene dreissenids in Central Europe: evolutionary shifts and diversity changes. Chapter 2. In: van der Velde, G., Rajagopal, S., bij de Vaate, A. (Eds.), The Zebra Mussel in Europe. Backhuys Publishers, Leiden/Margraf Publishers, Weikersheim. pp. 11–29.

Harzhauser, M., Piller, W.E., 2004. Integrated stratigraphy of the Sarmatian Upper Middle Miocene in the western Central Paratethys. Stratigraphy, 1/1, 65–86.

Harzhauser, M., Piller, W.E., 2007. Benchmark data of a changing sea. – Palaeogeography, Palaeobiogeography and Events in the Central Paratethys during the Miocene. Palaeogeography, Palaeoclimatology, Palaeoecology, 253, 8–31. https://doi.org/10.1016/j.palaeo.2007.03.031

Harzhauser, M., Daxner-Höck, G. Piller, W. E., 2004. An integrated stratigraphy of the Pannonian Late Miocene in the Vienna Basin. Austrian Journal of Earth Sciences, 9596, 6–19.

Harzhauser, M., Piller, W.E., Müllegger, S., Grunert, P., Micheels, A., 2010. Changing seasonality patterns in Central Europe from Miocene Climate Optimum to Miocene Climate Transition deduced from the *Crassostrea* isotope archive. Global and Planetary Change, 76, 77–84. https://doi.org/10.1016/j.gloplacha.2010.12.003

Harzhauser, M., Theobalt, D., Strauss, P., Mandic, O., Piller, W. E., 2019. Seismic-based lower and middle Miocene stratigraphy in the northwestern Vienna Basin Austria. Newsletter on Stratigraphy, 52, 221–224. https://doi:10.1127/nos/2018/0490

Harzhauser, M., Mandic, O., Büyükmeriç, Y., Neubauer, T.A., Kadolsky, D., Landau, B.M., 2016. A Rupelian mangrove swamp mollusc fauna from the Thrace Basin in Turkey. Archiv für Molluskenkunde, 145, 23–58.

Harzhauser, M., Theobalt, D., Strauss, P., Mandic, O., Carnevale, G., Piller, W. E., 2017. Miocene biostratigraphy and paleoecology of the Mistelbach Halfgraben in the northwestern Vienna Basin Lower Austria. Jahrbuch der Geologischen Bundesanstalt, 157, 57–108.

Harzhauser M., Grunert P., Mandic O., Lukeneder P., García Gallardo Á., Neubauer T.A., Carnevale G., Landau B.M., Sauer R., Strauss P., 2018. Middle and Late Badenian palaeoenvironments in the northern Vienna Basin and their potential link to the Badenian Salinity Crisis. Geologica Carpathica, 69, 129–168. https://doi.org/10.1515/geoca-2018-0009

Haunold, T.G., 1995. Zur Taxonomie, Systematik und stratigraphischen Bedeutung uvigerinider Foraminiferen im Neogen des Wiener Beckens und benachbarter Gebiete – 40 Jahre nach Papp and Turnovsky (1953). Jahrbuch der Geologischen Bundesanstalt, 138, 67–87.

Häusler, H., Scheibz, J., Chwatal, W., Kohlbeck, F., 2014. Coeval Lower Miocene subsidence of the Eisenstadt Basin and relative updoming of its Austroalpine frame: implications from high-resolution geophysics at the Oslip section (Northern Burgenland, Austria). International Journal of Earth Science, 104, 475–493. https://doi.org/10.1007/s00531-014-1084-8

Hedberg, H.D., 1976. International stratigraphic guide. John Wiley, New York, 200 pp.

Hilgen, F.J., Lourens, L.J., Van Dam, J.A., 2012. The Neogene Period. In: Gradstein, F.M., Ogg, J.G., Schmitz, M.D., Ogg, G.M. (Eds.), The Geologic Time Scale 2012, Volume 1. Elsevier, Amsterdam, pp. 923–978.

Hinsch, R., Decker K., Peresson, H., 2005. 3-D seismic interpretation and structural modeling in the Vienna Basin: implications for Miocene to recent kinematics. Austrian Journal of Earth Sciences, 97, 38–51.

Hladecek, K., 1965. Zur Schichtfolge und Lagerung des Helvets von Matzen. PhD-Thesis, University of Vienna, 106 pp.

Hohenegger, J., 2005. Estimation of environmental paleogradient values based on presence/absence data: a case study using benthic foraminifera for paleodepth estimation. Palaeogeography, Palaeoclimatology, Palaeoecology, 217, 115–130. https://doi.org/10.1016/j.palaeo.2004.11.020

Hohenegger, J., Wagreich, M., 2012. Time calibration of sedimentary sections based on insolation cycles using combined cross-correlation: dating the gone Badenian stratotype Middle Miocene, Paratethys, Vienna Basin, Austria as an example. International Journal of Earth Sciences, 101, 339–349. https://doi.org/10.1007/s00531-011-0658-y

Hohenegger, J, Ćorić, S., Wagreich, M., 2014. Timing of the Middle Miocene Badenian Stage of the Central Paratethys. Geologica Carpathica, 65/1, 55–66. https://doi.org/10.2478/geoca-2014-0004

Hohenegger, J., Pervesler, P., Uchman, A., Wagreich, M., 2009b. Upper bathyal trace fossils document palaeoclimate changes. Terra Nova, 21, 229–236. https://doi.org/10.1111/j.1365-3121.2009.00878.x

Hohenegger, J., Andersen, N., Báldi, K., Ćorić, S., Pervesler, P., Rupp, C., Wagreich, M., 2008. Paleoenvironment of the Early Badenian Middle Miocene in the southern Vienna Basin Austria – multivariate analysis of the Baden-Sooss section. Geologica Carpathica, 59, 461–487. http://www.geologicacarpathica.com/browse-journal/volumes/59-5/article-458/

Hohenegger, J., Ćorić, S., Khatun, M., Pervesler, P., Rögl, F., Rupp, C., Selge, A., Uchman, A., Wagreich, M., 2009a. Cyclostratigraphic dating in the Lower Badenian Middle Miocene of the Vienna Basin Austria: the Baden-Sooss core. International Journal of Earth Sciences, 98, 915–930. https://doi.org/10.1007/s00531-007-0287-7

Hölzel, M., Wagreich, M., Faber, R., Strauss, P., 2008. Regional subsidence analysis in the Vienna Basin (Austria). Austrian Journal of Earth Sciences, 101, 88–98.

Hölzel, M., Decker, K., Zámolyi, A., Strauss, P., Wagreich, M., 2010. Lower Miocene structural evolution of the central Vienna Basin (Austria). Marine and Petroleum Geology 27, 666–681. https://doi.org/10.1016/j.marpetgeo.2009.10.005

Hrabovský, J., 2013. Negenikulátne koralinné riasy (Corallinales, Sporolithales, Rhodophyta) z litotamniových vápencov lokality Vrchná hora pri Stupave (Viedenská panva, Slovensko). Mineralia Slovaca, 45, 23–34.

Hrabovský, J., Fordinál, K., 2013. Paleoekologické zhodnotenie riasových vápencov z lokality Stupava-Vrchná hora (Viedenská panva, Slovensko). Mineralia Slovaca, 45, 11–22.

Hyžný, M., Hudáčková, N., Biskupič, R., Rybár, S., Fuksi, T., Halásová, E., Zágoršek, K., Jamrich, M., Ledvák P., 2012. Devínska Kobyla – a window into the Middle Miocene shallow-water marine environments of the Central Paratethys (Vienna Basin, Slovakia). Acta Geologica Slovaca, 4/2, 95–111.

Iaccarino, S.M., Di Stefano, A., Foresi, L.M., Turco, E., Baldassini, N., Cascella, A., Da Prato, S., Ferraro, L., Gennari, R., Hilgen, F.J., Lirer, F., Maniscalco, R., Mazzei, R., Riforgiato, F., Russo, B., Sagnotti, L., Salvatorini, G., Speranza, F., Verducci, M., 2011. High-resolution integrated stratigraphy of the upper Burdigalian-lower Langhian in the Mediterranean: the Langhian historical stratotype and new candidate sections for defining its GSSP. Stratigraphy, 8/2–3, 199–215.

Jamrich, M., Halásová, E., 2010. Vývoj spoločenstiev vápnitých nanofosílií Viedenskej panvy ako odraz paleoenvironmentálnych zmien počas vrchného bádenu (Devínska Nová Ves – tehelňa). Acta Geologica Slovaca, 2, 2, 123–140.

Janoschek, R., 1942. Die bisherigen Ergebnisse der erdölgeologischen Untersuchungen im inneralpinen Wiener Becken. Oel und Kohle, 38, 125–150.

Janoschek, R., 1943. Das Inneralpine Wiener Becken. In: Schaffer, F.X. (Ed.), Geologie der Ostmark, Franz Deuticke, Wien, pp. 427–514.

Janoschek, R., 1951. Das Inneralpine Wiener Becken. In: Schaffer, F.X. (Ed.), Geologie von Österreich, 2. Auflage, Franz Deuticke, Wien, pp. 525–693.

Jiříček, R., 2002. The evolution of the Molasse in the Alpine-Carpathian Foredeep and the Vienna Basin. Exploration Geophysics, Remote sensing and environment, 9, 179 p.

Jiříček, R., Seifert, P., 1990. Palaeogeography of the Neogene in the Vienna Basin and the adjacent part of the foredeep. In: Minaříková, D., Lobitzer, H., (Eds.), Thirty Years of Geological Cooperation between Austria and Czechoslovakia. Cesky Geologicky Ustav, Praha, pp. 89–105.

Jiříček, R., Tomek, Č., 1981. Sedimentary and structural evolution of the Vienna Basin. Earth Evolution Science, 3–4, 195–204.

Kapounek, J., Papp, A., 1969. Der Vulkanismus in der Bohrung Orth 1 und die Verbreitung von Grobschüttungen zwischen dem Spannberger Rücken und der Donau. Verhandlungen der Geologischen Bundesanstalt, 1969, 114–123.

Kapounek, J., Kröll, A., Papp, A., Turnovsky, K., 1965. Die Verbreitung von Oligozän, Unter- und Mittelmiozän in Niederösterreich. Erdoel-Erdgas-Zeitschrift, 81/4, 109–115.

Keferstein, C., 1828. Beobachtungen und Ansichten über die geognostischen Verhältnisse der nördlichen Kalk-Alpenkette in Oesterreich und Baiern. Teutschland, geognostisch-geologisch dargestellt und mit Charten und Durchscnittszeichnungen. Verlag des Landes-Industrie-Comptoirs. Weimar, 5/3, 425 pp.

Kern, A., Harzhauser, M., Mandic, O., Roetzel, R., Ćorić, S., Bruch, A.A., Zuschin, M., 2010. Millennial-scale vegetation dynamics in an estuary at the onset of the Miocene Climate Optimum. Palaeogeography, Palaeoclimatology, Palaeoecology, 304, 247–261. https://doi.org/10.1016/j.palaeo.2010.07.014

Kölbl, L., 1959. Art und Verteilung der Sedimentkörper im Torton des Erdölfeldes Matzen Wiener Becken. Eclogae Geologicae Helvetiae, 51/3, 999–1009.

Kölbl, L., 1966. Geologische Studie über die Bildung der tortonen Zwischenhorizonte von Matzen und die Entstehung ihrer Lagerstätten. Erdöl-Erdgas Zeitschrift, 82, 45–65.

Košťák, M., Schlögl, J., Culkac, A., Tomašových, A., Mazucha, M., Hudáčková, N., 2018. The unique preservation of Sepia soft tissues in the Miocene deposits Serravallian, Vienna Basin: Implications for the origin of microbodies in the fossil record. Palaeogeography Palaeoclimatology Palaeoecology, 493, 111–118. https://doi.org/10.1016/j.palaeo.2018.01.005

Kováč, M., Baráth, I., Harzhauser, M., Hlavatý, I., Hudáčková, N., 2004. Miocene depositional systems and sequence stratigraphy of the Vienna Basin. Courier des Forschungs-Instituts Senckenberg, 246, 187–212.

Kováčová, P., Hudáčkova, N., 2009. Late Badenian foraminifers from the Vienna Basin Central Paratethys: stable isotope study and paleoecological implications. Geologica Carpathica, 60/1, 59–70. https://doi.org/10.2478/v10096-009-0006-3

Kreutzer, K., 1971. Mächtigkeitsuntersuchungen im Neogen des Ölfeldes Matzen, Nieder-Österreich. Erdöl-Erdgas-Zeitschrift, 87, 38–49.

Kreutzer, N., 1974. Lithofazielle Gliederung einiger Sand- und Schotter-Komplexe des Sarmatien und obersten Badenien im Raume von Matzen und Umgebung (Wiener Becken). Erdoel-Erdgas-Zeitschrift, 90, 114–127.

Kreutzer, N., 1978. Die Geologie der Nulliporen (Lithothamnien)-Horizonte der miozänen Badener Serie des Ölfeldes Matzen (Wiener Becken). Erdoel-Erdgas-Zeitschrift, 94, 129–145.

Kreutzer, N., 1986. Die Ablagerungssequenzen der miozänen Badener Serie im Feld Matzen und im zentralen Wiener Becken. Erdöl, Erdgas, Kohle, 102/11, 492–503.

Kreutzer, N., 1992. Matzen Field – Austria. Vienna Basin. A field study for the Treatise of Petroleum Geology. AAPG, Tulsa, 57–97.

Kreutzer, N., 1993. Das Neogen des Wiener Beckens. In: Brix, F., Schultz, O., (Eds.), Erdöl und Erdgas in Österreich. Naturhistorisches Museum Wien und F. Berger, Horn., pp. 232–248.

Kreutzer, K., Hlavatý, V., 1990. Sediments of the Miocene mainly Badenian in the Matzen area in Austria and in the southern part of the Vienna Basin in Czechoslovakia. In: Minarikove, D., Lobitzer, H., (Eds.), Thirty years of geological cooperation between Austria and Czechoslovakia. UUG, Praha, pp. 110–123.

Kroh, A., Harzhauser, M., Piller, W.E., Rögl, F., 2003. The Lower Badenian Middle Miocene Hartl Formation Eisenstadt-Sopron Basin, Austria. Österreichische Akademie der Wissenschaften, Schriftenreihe Erdwissenschaftliche Kommissionen, 16, 87–109.

Kröll, A., 1984. Die Erdöl- und Erdgasregion Matzen/Schönkirchen aus geologischer Sicht. Erdöl-Erdgas, 100, 185–195.

Kröll A., Wessely G., 1993. Strukturkarte - Basis der tertiären Beckenfüllung 1:200.000. Erläuterung zu den Karten über den Untergrund des Wiener Beckens und der angrenzenden Gebiete. Geologische Bundesanstalt, Wien.

Lankreijer, A., Kováč, M., Cloetingh, S., Pitoňák, P., Hlôška, P., Biermann, C., 1995. Quantitative subsidence analysis and forward modelling of the Vienna and Danube basins: thin-skinned versus thick-skinned extension. Tectonophysics, 252, 433–451. https://doi.org/10.1016/0040-1951(95)00099-2

Lee, E.J., Wagreich, M., 2017. Polyphase tectonic subsidence evolution of the Vienna Basin inferred from quantitative subsidence analysis of the northern and central parts. International Journal of Earth Sciences, 106, 687–705. https://doi.org/10.1007/s00531-016-1329-9

Mandic, O., 2004. Foraminiferal paleoecology of a submarine swell - the Lower Badenian (Middle Miocene) of the Mailberg Formation at the Buchberg in the Eastern Alpine Foredeep: initial report. Annalen des Naturhistorischen Museums in Wien, 105A, 161–173.

Mandic, O., Harzhauser, M., 2003. Molluscs from the Badenian Middle Miocene of the Gaindorf Formation Alpine Molasse Basin, NE Austria - taxonomy, paleoecology and biostratigraphy. Annalen des Naturhistorischen Museums Wien, 104A, 85–127.

Marquet, R., 2004. Ecology and evolution of Pliocene bivalves from the Antwerp Basin. Bulletin de l'Institut Royal des Sciences Naturelles de Belgique, Sciences de la Terre, 74 Supplementum, 205–212.

Mayer, A., Pavuza, R., Wirth, J., 1989. Die Höhlen des Steinberges im Weinviertel (Niederösterreich). Die Höhle. Zeitschrift für Karst- und Höhlenkunde, 40/2, 37–49.

Palzer-Khomenko, M., Wagreich, M., Knierzinger, W., Meszar, M.-E., Gier, S., Kallanxhi, M.-E., Soliman, A., 2018a. A calcite crisis unravelling Early Miocene (Ottnangian) stratigraphy in the North Alpine-Carpathian Foreland Basin: A litho- and chemostratigraphic marker for the Rzehakia Lake System. Geologica Carpathica, 69/4, 315–334. https://doi.org/10.1515/GEOCA-2018-0019

Palzer-Khomenko, M., Wagreich, M., Kallanxhi, M.-E., Soliman, A., Knierzinger, W., Meszar, M.-E., Gier, S., 2018b. Facies, palaeogeography and stratigraphy of the lower Miocene Traisen Formation and Wildendürnbach Formation (former "Oncophora Beds") in the Molasse Zone of Lower Austria. Austrian Journal of Earth Sciences, 111/1, 75–091. https://doi.org/10.17738/ajes.2018.0006

Papp, A., Küpper, K., 1952. Über die Entwicklung der Heterosteginen im Torton des Wiener Beckens. – Anzeiger der mathematisch-naturwissenschaftlichen Klasse der Österreichischen Akademie der Wissenschaften, 89/10, 110–118.

Papp, A., Turnovsky, K., 1952. Die Entwicklung der Uvigerinen im Vindobon (Helvet und Torton) des Wiener Beckens. – Jahrbuch der Geologischen Bundesanstalt, 96, 117–142.

Papp, A., 1963. Die biostratigraphische Gliederung des Neogens im Wiener Becken. Mitteilungen der Geologischen Gesellschaft Wien, 56, 1, 225–317.

Papp, A., 1967. Mollusken aus dem Aderklaaer Schlier. Annalen des Naturhistorischen Museums in Wien. 71, 341–346.

Papp, A., Steininger, F., 1978. Holostratotypus des Badenien. In: Papp, A., Cicha, I., Senes, J., Steininger, F., (Eds.), M4 Badenien (Moravien, Wielicien, Kosovien). Chronostratigraphie und Neostratotypen: Miozän der zentralen Paratethys. Verlag der Slowakischen Akademie der Wissenschaften, Bratislava, 6, pp. 138–145.

Papp A., Rögl F., Seneš J., 1973. M2, Ottnangien: Die Innviertler, Salgótarjáner, Bántapusztaer Schichtengruppe und die *Rzehakia* Formation. Chronostratigraphie und Neostratotypen: Miozän der zentralen Paratethys. Verlag der Slowakischen Akademie der Wissenschaften, 3, 841 pp.

Papp, A., Cicha, I., Senes, J., Steininger, F., 1978. M4, Badenien Moravien, Wielicien, Kosovien. Chronostratigraphie und Neostratotypen: Miozän der zentralen Paratethys. Verlag der Slowakischen Akademie der Wissenschaften, Bratislava, 6, 594 pp.

Pascher, G.A., Brix, F., 1994. Geologische Karte der Republik Österreich ÖK 77 Eisenstadt 1:50.000. Geologische Bundesanstalt, Wien.

Picha, F.J., Stráník, Z., Krejčí, O., 2006. Geology and hydrocarbon resources of the Outer Western Carpathians and their foreland, Czech Republic. In: Golonka, J., Picha, F.J. (Eds.), The Carpathians and their foreland: Geology and hydrocarbon resources. AAPG Memoir, 84, 49–175.

Piller, W.E., 1994. *Nullipara ramosissima* Reuss, 1847 - a re-discovery. Beiträge zur Paläontologie, 19, 181–189.

Piller, W.E., Kleemann, K., 1991. Middle Miocene Reefs and related fades in Eastern Austria. I) Vienna Basin. VI. International Symposium on Fossil Cnidaria including Archaeocyatha and Porifera. Excursion-Guidebook, Excursion B4, Geologisch-Paläontologisches Institut und Museum Münster, Münster, 28 pp.

Piller, W.E, Vavra, N., 1991. Das Tertiär im Wiener- und Eisenstädter Becken. In: Roetzel, R., Nagel, D., (Eds.), Exkursionen im Tertiär Österreichs, Molassezone – Waschberg Zone – Korneuburger Becken – Wiener Becken – Eisenstädter Becken. Österreichische Paläontologische Gesellschaft, Wien, pp. 161–216.

Piller, W.E., Decker, K., Haas, M., 1996. Sedimentologie und Beckendynamik des Wiener Beckens. Exkursionsführer SEDIMENT'96, 11. Sedimentologentreffen Wien, Exkursion A1. Berichte der Geologischen Bundesanstalt, 33, 41 pp.

Piller, W.E., Harzhauser, M., Mandic, O., 2007. Miocene Central Paratethys stratigraphy - current status and future directions. Stratigraphy, 4, 2/3, 151–168.

Piller, W.E., Kroh, A., Mandic, O., 2007. Der Rauchstallbrunngraben – ein alter Exkursionspunkt. In. Hoffmann, T. (Ed.), Wanderungen in die Erdgeschichte 22 – Wien, Niederösterreich, Burgenland Friedrich Pfeil, München, 141–143.

Piller, W. E., Egger, H., Erhart, C.W., Gross, M., Harzhauser, M., Hubmann, B., Van Husen, D., Krenmayr, H.G., Krystyn, L., Lein, R., Lukeneder, A., Mandl, G.W., Rögl, F., Roetzel, R., Rupp, C., Schnabel, W., Schönlaub, H.P., Summesberger, H., Wagreich, M., Wessely, G., 2004. Die stratigraphische Tabelle von Österreich 2004 sedimentäre Schichtfolgen. Poster, Österreichische Stratigraphische Kommission; Österreichische Akademie der Wissenschaften, Kommission für die paläontologische und stratigraphische Erforschung Österreichs.

Pippérr, M., Reichenbacher, B., Kirscher, U., Sant, K., Hanebeck, H., 2018. The middle Burdigalian in the North Alpine Foreland Basin (Bavaria, SE Germany) – a lithostratigraphic, biostratigraphic and magnetostratigraphic re-evaluation. Newsletters on Stratigraphy, 51/3, 285–309.

Reuss, A.E., 1847.1. Die fossilen Polyparien des Wiener Tertiärbeckens. Ein monographischer Versuch. Naturwissenschaftliche Abhandlungen (ed. Haidinger, W.), 2,1–109.

Riegl, B., Piller, W.E., 2000. Biostromal Coral Facies: a Miocene Example from the Leitha Limestone (Austria) and its actualistic Interpretation. Palaios, 15, 399–413. https://doi.org/10.1669/0883-1351(2000)015<0399:BCFAME>2.0.CO;2

Roetzel, R., 2009. Erläuterungen zu Blatt 23 Hadres. Geologische Karte der Republik Österreich 1 : 50000. Geologische Bundesanstalt, Wien, 150 pp.

Roetzel, R., De Leeuw, A., Mandic, O., Márton, E., Nehyba, S., Kuiper, K.F., Scholger, R., Wimmer-Frey, I., 2014. Lower Miocene (upper Burdigalian, Karpatian) volcanic ash-fall at the south-eastern margin of the Bohemian Massif in Austria – New evidence from 40Ar/39Ar-dating, palaeomagnetic, geochemical and mineralogical investigations. Austrian Journal of Earth Sciences, 107, 2–22.

Rögl, F., Müller, C., 1976. Das Mittelmiozän und die Baden-Sarmat Grenze in Walbersdorf (Burgenland). Annalen des Naturhistorischen Musuems in Wien, 80, 221–232.

Rögl, F., Ćorić, S., Harzhauser, M., Jimenez-Moreno, G., Kroh, A., Schultz, O., Wessely, G., Zorn, I., 2008. The Middle Miocene Badenian stratotype at Baden-Sooss, Lower Austria. Geologica Carpathica, 59, 367–374. http://www.geologicacarpathica.com/browse-journal/volumes/59-5/article-452/

Royden, L.H., 1985. The Vienna Basin: a thin-skinned pull-apart basin. In: Biddle, K.T., Christie-Blick, N., (Eds.), SEPM Special Publications 37, pp 319–338.

Rybár, S., Šarinová, K., Sant, K., Kuiper, K.F., Kováčová, M., Vojtko, R., Reiser, M.K., Fordinál, K., Teodoridis, V., Nováková, P., Vlček, T., 2019. New 40Ar/39Ar, fission track and sedimentological data on a middle Miocene tuff occurring in the Vienna Basin: Implications for the north-western Central Paratethys region. Geologica Carpathica, 70/5, 386–404. https://doi.org/10.2478/geoca-2019-0022

Salvador, A., 1994. The International Stratigraphic Guide: A guide to stratigraphic classification terminology, and procedure. John Wiley, New York, 214 pp.

Sant, K., Kuiper, K.F., Rybár, S., Grunert, P., Harzhauser, M., Mandic, O., Jamrich, M., Šarinová, K., Hudáčková, N., Krijgsman, W., 2020. 40Ar/39Ar geochronology using high sensitivity mass spectrometry: Examples from middle Miocene horizons of the Central Paratethys. Geologica Carpathica, 71/ 2, 166–182. https://doi.org/10.31577/GeolCarp.71.2.5

Sauer, R., Seifert, P. Wessely, G., 1992. Guidebook to excursions in the Vienna Basin and the adjacent Alpine-Carpathian thrustbelt in Austria. Mitteilungen der Geologischen Gesellschaft, 85, 264 pp.

Schmid, H.P., Harzhauser, M., Kroh, A., 2001. Hypoxic Events on a Middle Miocene Carbonate Platform of the Central Paratethys Austria, Badenian, 14 Ma. Annalen des Naturhistorischen Museums in Wien, 102A, 1–50.

Schmieder, M., Kennedy, T., Jourdan, F., Buchner, E., Reimold, W.U., 2018 A high-precision 40Ar/39Ar age for the Nördlinger Ries impact crater, Germany, and implications for the accurate dating of terrestrial impact events. Geochimica et Cosmochimica Acta, 220, 146–157. https://doi.org/10.1016/j.gca.2017.09.036

Schultz, O., 2005. Bivalvia neogenica Solenoidea – Clavagelloidea. Catalogus Fossilium Austriae, Österreichische Akademie der Wissenschaften, Wien, 1/3, 691-1212.

Schultz, O., Brzobohatý, R., Kroupa., O., 2010. Fish teeth from the Middle Miocene of Kienberg at Mikulov, Czech Republic, Vienna Basin. Annalen des Naturhistorischen Museums in Wien, 112, 489–506.

Špička, V., 1966. Palaeogeografie a tektonogeneze Vídeňské pánve a příspěvek k její naftově-geologické problematice. Rozpravy Československé Akademie Věd, Řada matematickýchpřírodopisných Věd, 76, 12, 3–118.

Steininger, F., Papp, A., 1978. 9. Faziostratotypus: Gross Höflein NNW, Steinbruch “Fenk”, Burgenland, Österreich. In: Papp, A., Cicha, I., Senes, J., Steininger, F., (Eds.), M4 Badenien (Moravien, Wielicien, Kosovien). Chronostratigraphie und Neostratotypen: Miozän der zentralen Paratethys. Verlag der Slowakischen Akademie der Wissenschaften, Bratislava, 6, pp. 194–203.

Steininger, F.F., Piller, W.E., 1999. Empfehlungen (Richtlinien) zur Handhabung der stratigraphischen Nomenklatur. Courierier des Forschungs-Institutes Senckenberg, 209, 1–19.

Strauss, P., Harzhauser, M., Hinsch, R., Wagreich, M., 2006. Sequence stratigraphy in a classic pull-apart basin Neogene, Vienna Basin. A 3D seismic based integrated approach. Geologica Carpathica, 57/3, 185–197.

Studencki, W., 1988. Facies and sedimentary environment of the Pinczow Limestones (Middle Miocene; Holy Cross Mountains, Central Poland. Facies, 18, 1–26.

Talman, S.G., Keough, M.J., 2001. Impact of an exotic clam, *Corbula gibba*, on the commercial scallop, *Pecten fumatus*, in Port Phillip Bay, south-east Australia: evidence of resource-restricted growth in a subtidal environment. Marine Ecology Progress Series, 221, 135–143. https://doi.org/10.3354/meps221135

Tollmann, A., 1955. Das Neogen am Nordwestrand der Eisenstädter Bucht. Wissenschaftliche Arbeiten aus dem Burgenland, 10, 75 pp.

Tollmann, A., 1985. Geologie von Österreich. Band II. Außerzentralalpiner Anteil. Deuticke, Wien, 710 pp.

Vass, D., 2002: Litostratigrafia Západných Karpát: neogén a budínsky paleogén. Štátny geologický ústav D. Štúra, Bratislava, 202 pp.

Vass, D., Nagy, A., Kohút, M., Kraus, I., 1988. Devínskonovoveské vrstvy: Hruboklastické sedimenty na juhovýchodnom okraji Viedenskej panvy. Minerlia Slovaka, 20/2, 109–122.

Weber, K., Zuschin, M., 2013. Delta-associated molluscan life and death assemblages in the northern Adriatic Sea: implications for paleoecology, regional diversity and conservation. Palaeogeography, Palaeoclimatology, Palaeoecology, 370, 77–91. https://doi.org/10.1016/j.palaeo.2012.11.021

Weissenbäck, M., 1995. Ein Sedimentationsmodell für das Unter- bis Mittelmiozän Karpatien-Badenien des zentralen Wiener Beckens. Dissertation am Geologischen Institut der Universität Wien, 154 pp.

Weissenbäck, M., 1996. Lower to Middle Miocene sedimentation model of the central Vienna Basin. In: Wessely, G., Liebl, W., (Eds.), Oil and Gas in alpidic thrustbelts and basins of Central and Eastern Europe. European Association of Geoscientists and Engineers EAGE, Special Publications 5, pp. 355–363.

Wessely, G., 1983. Zur Geologie und Hydrodynamik im südlichen Wiener Becken und seiner Randzone: Mitteilungen der Österreichischen Geologischen Gesellschaft, 76, 27–68.

Wessely, G., 2000. Sedimente des Wiener Beckens und seiner alpinen und subalpinen Unterlagerung. Mitteilungen der Gesellschaft für Geologie und Bergbaustudenten Österreichs, 44, 191–214.

Wessely, G., 2006. Niederösterreich. Geologie der Österreichischen Bundesländer. Geologische Bundesanstalt Wien, 416 pp.

Wessely, G., Ćorić, S., Rögl, F., Zorn, I., 2007a. Stratigraphy of the Thermal Water Area Baden - Bad Vöslau at the Western Border of the Southern Vienna Basin. Scripta Facultatis Scientiarum Naturalium Universitatis Masarykianae Brunensis, Geology, 36, 39–44.

Wessely, G., Ćorić, S., Rögl, F., Draxler, I., Zorn, I., 2007b. Geologie und Paläontologie von Bad Vöslau (Niederösterreich). Jahrbuch der Geologischen Bundesanstalt, 147, 419–448.

Wiedl, T., Harzhauser, M., Piller, W.E., 2012. Facies and synsedimentary tectonics on a Badenian carbonate platform in the southern Vienna Basin Austria, Central Paratethys. Facies, 58, 523–548. https://doi.org/10.1007/s10347-011-0290-0

Wiedl, T., Harzhauser, M., Kroh, A., Ćorić, S., Piller, W.E., 2013. Ecospace variability along a carbonate platform at the northern boundary of the Miocene reef belt Upper Langhian, Austria Palaeogeography, Palaeoclimatology, Palaeoecology, 370, 232–246, http://dx.doi.org/10.1016/j.palaeo.2012.12.015

Wiedl, T., Harzhauser, M., Kroh, A., Ćorić, S., Piller, W.E., 2014. From biologically to hydrodynamically controlled carbonate production by tectonically induced palaeogeographic rearrangement

Middle Miocene, Pannonian Basin. Facies, 60, 865–881. https://doi.org/10.1007/s10347-014-0408-2

Zuschin, M., Harzhauser, M., Mandic, O., 2007. The stratigraphic and sedimentologic framework of fine-scale faunal replacements in the Middle Miocene of the Vienna Basin Austria. Palaios, 22, 285–295. https://doi.org/10.2110/palo.2005.p05-023r

Zuschin, M., Harzhauser, M., Hengst, B., Mandic, O., Roetzel, R., 2014. Long-term ecosystem stability in an Early Miocene estuary. Geology, 42, 1–4. https://doi.org/10.1130/G34761.1

Chapter 4

Early and middle Miocene paleobathymetry of the Vienna Basin (Austria)

Matthias Kranner[1,2]*, Mathias Harzhauser[1], Oleg Mandic[1], Philipp Strauss[3], Wolfgang Siedl[3], Werner E. Piller[2]

1) Geological-Paleontological Department, Natural History Museum Vienna, Burgring 7, 1010 Vienna, Austria; matthias.kranner@nhm-wien.ac.at; mathias.harzhauser@nhm-wien.ac.at; oleg.mandic@nhm-wien.ac.at
2) Institute of Earth Sciences (Geology and Paleontology), NAWI Graz Geocenter, University of Graz, Heinrichstr. 26, 8010 Graz, Austria; werner.piller@uni-graz.at
3) OMV Exploration and Production GmbH, Trabrennstraße 6-8, 1020 Vienna, Austria; philipp.strauss@omv.com; wolfgang.siedl@omv.com

*) Corresponding author: matthias.kranner@nhm-wien.ac.at; phone +43 1 52177 255

Abstract

The Vienna Basin (VB) originated during the early Miocene and represents one of the largest onshore oil and gas field in Europe. The VB is composed of several horst and graben structures forming different subbasins, each with its own geodynamic evolution and deviating paleobathymetric developments during the Miocene. We present an analysis of water depth evolution along a NE-SW transect by applying a transfer function for benthic foraminifers. We document dramatic changes in the depth profile through time, which coincide with shifts of prevailing tectonic regimes. Bathyal conditions were established during the early Miocene piggy-back stage and the early middle Miocene extensional phase. A clear shallowing trend from upper bathyal to inner neritic conditions occurred during the middle Miocene extensional tectonic phase.

All lowstand systems of relative sea level in the VB coincide with global Mi-events. The observed maxima of the relative sea level in the VB are vaguely in phase with the global record from the Ottnangian (late early Miocene) to the middle Badenian (middle Miocene) but exceed the range of global sea level rise by three to four times, suggesting a strong tectonic amplification. Fluctuations of the relative sea level during the late Badenian and Sarmatian (Serravallian, middle Miocene) range well within the global signal, documenting ceasing influence of tectonics.

Keywords

Miocene, Paratethys Sea, Vienna Basin, subsidence, tectonics, sea level

4.1. Introduction

The Vienna Basin (VB) contents one of the largest onshore oil and gas fields in Europe (Hamilton et al., 2000; Arzmüller et al., 2006; Boote et al., 2018; Rupprecht et al., 2019). Consequently, the VB is one of the best studied Neogene Basins within Europe with thousands of conducted drillings by different oil companies. During the last decades the OMV AG is leading in the investigation of the northern and central VB and numerous boreholes with up to 8500 m depth (Zistersdorf ÜT 2a) were studied (mostly unpublished OMV internal reports). Still, the correlation of Neogene deposits throughout the basin remained ambiguous, due to the complex fault systems of the VB. A major obstacle for correlations is the Spannberg Ridge (Fig. 4.1), a west-east trending tectonic high in the central VB, which separates today the northern parts of the Neogene basin fill from those in the central and southern VB (Kreutzer, 1992; Hamilton et al., 2000; Fuchs et al., 2001; Wessely, 2006; Hölzel et al., 2010; Siedl et al., 2020). To resolve this correlation problem, the OMV initiated detailed stratigraphic analyses of major oil fields in the northern and central VB (Fig. 4.1), integrating biostratigraphic, lithological, seismic and well-log data. Paleontological analyses with main focus on micropaleontology, in particular on foraminifers, of 52 wells (717 samples) of the northern and central VB have been conducted.

Recently the Miocene lithostratigraphy of the Vienna Basin was described in detail by Harzhauser et al. (2020), who provide definitions of all lithostratigraphic units and their lithology as used herein. Harzhauser et al. (2020) established a formalized lithostratigraphic scheme for the VB and provided basic information on the depositional environments and the thicknesses of the lithostratigraphic units. These authors discuss also the history of investigation of the Vienna Basin and explain synonyms of lithostratigraphic units. The paleoenvironments represented by these lithostratigraphic units was outlined by Harzhauser et al. (2019, 2020), based on micro- and macrofossils.

Siedl et al. (2020) described the evolution of Badenian depositional environments in the northern Vienna Basin, based on modern 3D seismic and thousands of well data. These results showed three distinct phases of basin evolution (Kováč et al., 2004; Hinsch et al., 2005; Strauss et al., 2006, Salcher et al., 2012; Beidinger and Decker, 2016): 1. an E-W trending piggyback basin on top of the Alpine thrust belt, which is referred to herein as proto-Vienna Basin; 2. an extensional basin stage with high local extensional fault tectonic activities, shaping the VB since the early middle Miocene; 3. a recent rhombic basin with certain pull-apart kinematics.

Rupp (1986), Báldi and Hohenegger (2008) and Harzhauser et al. (2017, 2018) provided paleoecological information for the Austrian part of the VB on a smaller geographically scale and with focus on certain stratigraphic intervals. Rupp (1986) made first paleo-bathymetrical interpretations for the middle Badenian of the Matzen area (Matzen and Baden formations) based on the P/B ratio and depth

preferences of benthic species gathered from the literature. Báldi and Hohenegger (2008) estimated paleo-water depths for the Baden Formation.

For the Slovak part of the VB several analyses were conducted on upper Badenian deposits, mainly using foraminifers and calcareous nannoplankton as proxies for depth estimations (e.g., Kováčová and Hudáčková, 2009; Hyžný et al., 2012; Pivko et al., 2017; Košťák et al., 2018). Additionally, one study by Schlögl et al. (2017) calculating paleo-water depth using the formula of Hohenegger (2005) was conducted on Karpatian sediments. Further, Brzobohatý and Stráník (2012) calculated water depth based on otoliths for the lower Badenian of the Czech part of the VB at the junction to the Moravian part of the Carpathian Foredeep. A slightly broader regional scale was discussed in Harzhauser et al. (2017) for the lower and middle Miocene basin fill of the Mistelbach Halfgraben in the northern VB and by Harzhauser et al. (2018), who described the middle/upper Badenian transition in the Bernhardsthal-Mühlberg fields. For both areas, rough estimates of the paleo-bathymetry were provided based on a huge amount of quantified data on foraminiferal faunas. Nevertheless, these authors did not apply statistical methods to derive depositional depth estimates. All these studies revealed detailed paleoenvironmental information but focused on discrete time slices and limited geographic areas within the VB.

Surprisingly, however, nobody has attempted so far to calculate the changing water depth in different subbasins of the VB throughout the Miocene. Therefore, we provide the first comprehensive data set of hundreds of investigated foraminiferal samples from a NE to SW trending succession of subbasins in the Vienna Basin spanning c. 6 Myr from the Ottnangian (late early Miocene) to the Sarmatian (late middle Miocene), aiming to shed light on the complex basin evolution and the effect of local tectonics versus global sea-level fluctuations.

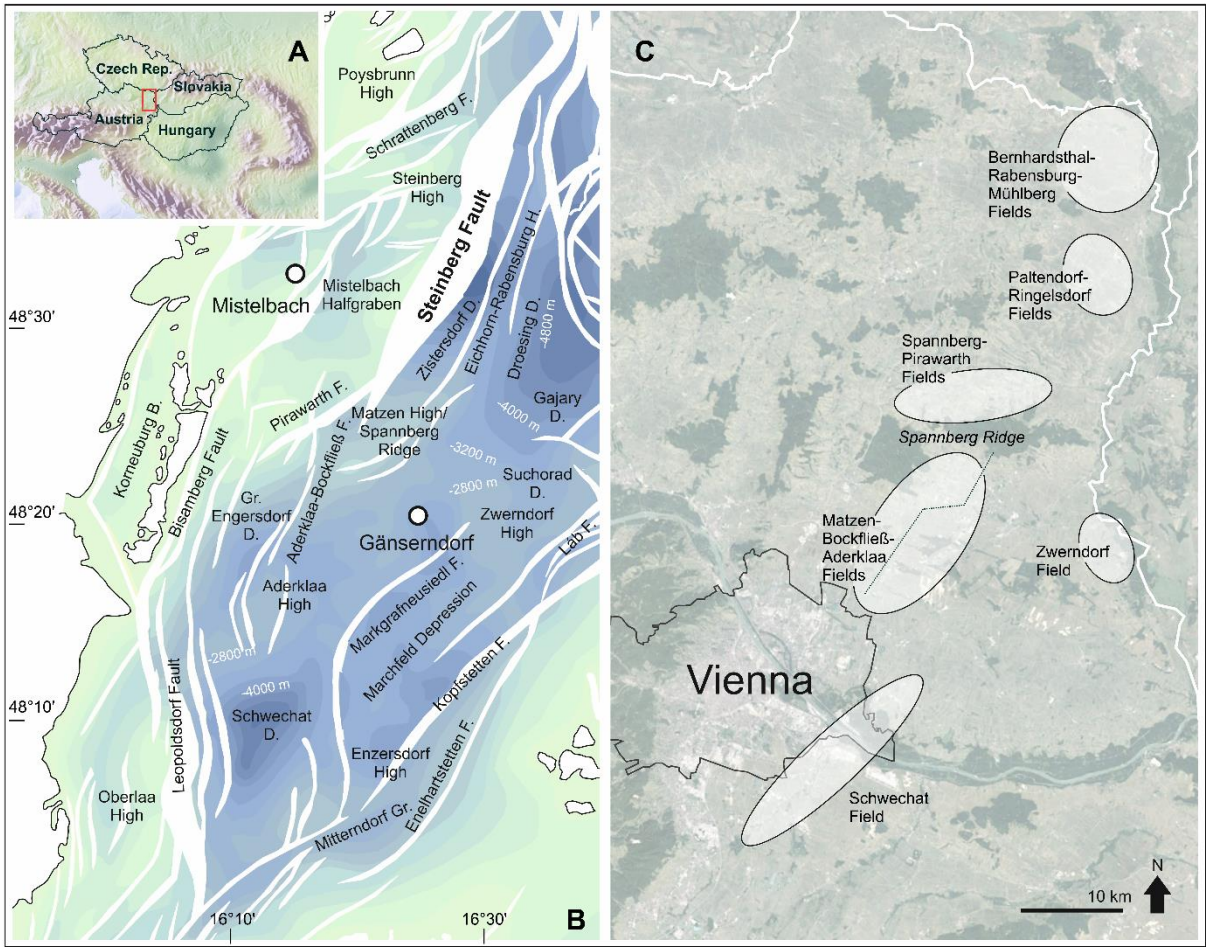

Fig. 4.1 A. Location of the Vienna Basin within central Europe. **B.** Tectonic setting of the central and northern Vienna Basin modified after Harzhauser et al. (2020) (B = basin, D = depression, F = fault, H = high). **C.** Position of the investigated oil fields. Dotted line within Matzen-Aderklaa Fields represents position of seismic line in Figure 2 (modified after Harzhauser et al., 2020).

4.2. Geological setting

The Vienna Basin is an about 200 km long and 55 km wide, rhomboid pull-apart basin (Royden, 1985; Wessely, 1988, 2006), covering large parts of eastern Austria and extending northwards into the Czech Republic and eastwards to Slovakia (Fig. 4.1A) (Kováč et al., 2004; Wessely, 2006). The studied area is situated in the Austrian part of the northern and central part of the Vienna Basin (Fig. 4.1). The development of a series of small piggy-back basins on the frontal part of the N- to NW-propagating thrust belt of the Eastern Alps marks the initial phase of the (proto-)Vienna Basin during the early Miocene (Fodor, 1995; Decker, 1996; Lee and Wagreich, 2017). Sedimentation commenced in the northern and central VB around 18.1 Ma during the early Miocene (Ottnangian; for Central Paratethys terminology see Fig. 4.2) (Harzhauser et al., 2019) and covered Cretaceous to Paleogene Penninic and Austroalpine units, separated by an angular unconformity (Hölzel et al., 2010). For the early Miocene proto-VB, Lee and Wagreich (2017) calculated a rather slow basement subsidence rate of up to 300 m/myr. At around 17.0 Ma, during the Karpatian, the subsidence rate increased up to 1 km/myr (Lee and Wagreich, 2017; Harzhauser et al., 2020). Alongside, a series of high zones and graben structures developed within the basin in the Rabensburg, Matzen, Aderklaa and Bockfließ areas during the middle Miocene (Hamilton et al., 2000).

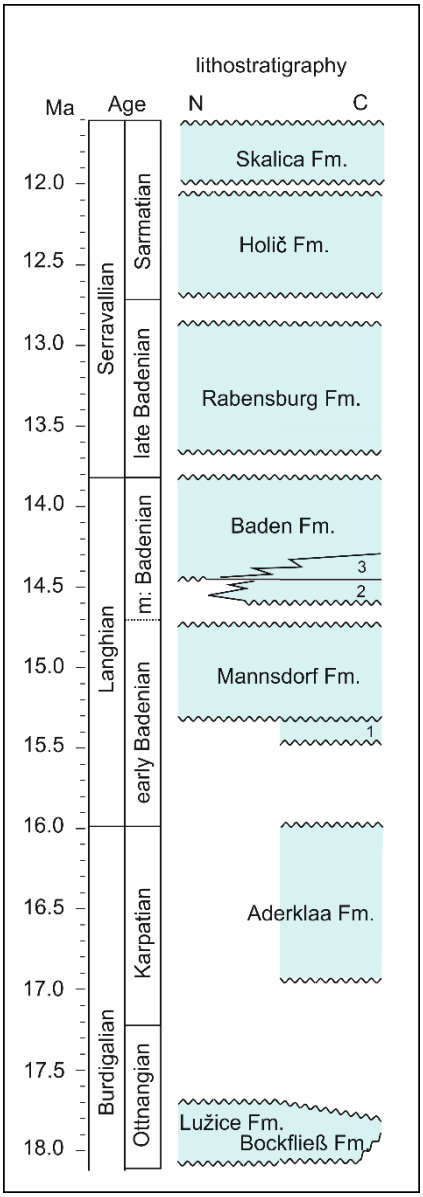

Figure 4.2. Correlation of the Vienna Basin lithostratigraphy with the Mediterranean and Central Paratethys ages after Hilgen et al. (2012); modified from Harzhauser et al. (2020) (1 = Rothneusiedel Fm., 2 = Auersthal Fm., 3 = Matzen Fm.).

Tectonic activity around the Karpatian-Badenian boundary at roughly 16 Ma, termed Styrian Tectonic Phase (Stille, 1924; Rögl et al., 2007; Hohenegger et al., 2009), coincided with strong uplift and tilting of lower Miocene strata. New depocenters formed in the northern and central VB and marine sedimentation extended southwards during the middle Miocene (e.g., Harzhauser et al., 2020; Siedl et al., 2020). The Styrian tectonic phase terminated the piggy-back phase and extensional tectonics dominated since the early Badenian (roughly 16 Ma) (Siedl et al., 2020).

Until recently pull-apart kinematics were supposed to have shaped the VB during the middle and late Miocene (e.g., Royden, 1985, 1988; Fodor, 1995; Decker, 1996; Hölzel et al., 2010) but

recent seismic interpretations by the OMV AG Exploration (Austria) could only detect extensional processes during that time of basin evolution (Hinsch et al., 2005; Beidinger and Decker, 2016; Siedl et al., 2020).

Due to lateral extrusion of the Eastern Alps (Royden, 1985, 1988; Fodor, 1995; Decker, 1996; Hölzel et al., 2010; Lee and Wagreich, 2017) the area of the VB was embossed by extensional tectonic. Consequently, complex fault systems developed, which subdivided the Vienna Basin into a series of horst and graben systems with uplifted blocks at the margins, separated from depressions by major faults (Kröll and Wessely, 1993; Hamilton et al., 2000; Wessely, 2006; Hölzel et al. 2010). With a displacement of up to 6000 m, the ESE dipping Steinberg fault (Fig. 4.1B) is amongst the most prominent faults within Europe (Hamilton et al., 2000).

4.2.1. Investigation area

Herein, we investigate several hydrocarbon production fields in the central and northern Vienna Basin of Austria. These target areas are arranged roughly in NNE–SSW direction (Fig. 4.1C).If we refer to "northern" and "central" hereinafter, we specifically mean of the Austrian part of the Vienna Basin.

4.2.1.1. Bernhardsthal, Rabensburg and Mühlberg fields*:* these are the northernmost fields of the investigation area. The region represents the junction between the Mistelbach Halfgraben in the west with the Steinberg High as boundary (Fig. 4.1B), the Zistersdorf Depression in the south and the Moravian Central Depression in the north. To the east it is bounded by the northern spur of the Eichhorn-Rabensburg High, where most of the Rabensburg drillings are situated. The thickness of Neogene deposits may reach more than 3300 m in the Mühlberg area (Harzhauser et al., 2020).

4.2.1.2. Palterndorf-Ringelsdorf fields*:* situated about 10 km south of the Bernhardsthal-Rabensburg-Mühlberg fields; this region is bounded by the Mistelbach Halfgraben and the Steinberg fault to the west, the Zistersdorf Depression to the south and the Droesing Depression to the east. The wells are situated directly on the Steinberg fault, the Zistersdorf Basin and at the junction between Eichhorn-Rabensburg Horst and Droesing Depression. The maximum thickness of Neogene deposits in the analyzed wells attains at least 4295 m.

4.2.1.3. Spannberg-Pirawarth fields: situated about 20 km SW of the Palterndorf-Ringelsdorf fields. The Spannberg-Pirawarth fields lie directly north of the Spannberg Ridge and Matzen High. The area is bounded to the NW by the Pirawarth Fault and reaches via the Zistersdorf Depression to the southern spur of the Eichhorn-Rabensburg High in the east. The maximum thickness of Neogene deposits in the studied wells attains up to 2640 m.

4.2.1.4. Bockfließ-Matzen fields*:* situated south of the Matzen High and the Spannberg Ridge. The Matzen Field is the most productive and most important oilfield in the Vienna Basin (Kreutzer, 1992; Fuchs et al., 2001). It is bounded to the west by the Aderklaa-Bockfließ Fault. Most drillings are concentrated south of the Matzen High and north of the city of Gänserndorf. The maximum thickness of Neogene deposits in the studied wells attains 3200 m in the Schönkirchen area (Fig. 4.3) (for detailed seismic interpretation see Siedl et al., 2020).

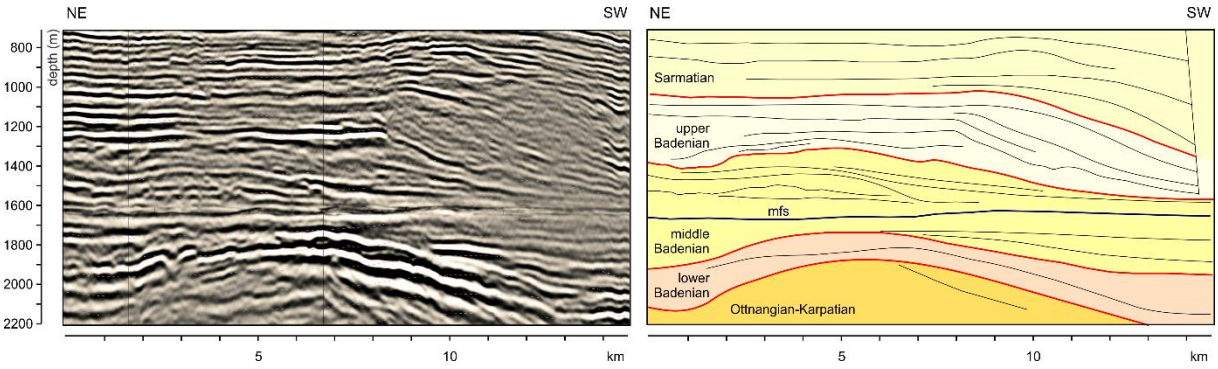

Fig. 4.3. Seismic interpretation of a NE-SW oriented seismic line crossing the Matzen-Aderklaa Field. Seismic profile flattened on the maximum flooding surface (mfs) of the Ba2-sequence as defined by Siedl et al. (2020) (blue line).

4.2.1.5. Aderklaa Field*:* situated about 10 km SW of the Matzen Field and directly NE of the City of Vienna. The well Ad78 is positioned on the Aderklaa High, which is bounded to the west by the southern branches of the Aderklaa-Bockfließ fault system. The thickness of Neogene deposits attains 2812 m. This field is discussed herein together with the Bockfließ-Matzen fields.

4.2.1.6. Zwerndorf Field*:* situated about 15 km ESE of the Matzen Field at the Austrian/Slovak border. The wells are drilled on the Zwerndorf High, which is bounded by the Markgrafneusiedl Fault in the west, the Marchfeld Depression in the south, the Láb Fault in the east and the Suchohrad Depression in the north. The base of the Neogene was not reached in the analyzed wells, which suggests a thickness of Neogene deposits of at least 1900 m.

4.2.1.7. Schwechat Field*:* spanning an area from Laxenburg 6 km south of Vienna to Wittau 5 km east of Vienna. The analyzed wells form a NE–SW cross section from the Schwechat Basin across the Leopoldsdorf Fault to the Oberlaa High. To the east, the Schwechat Depression is bounded by the Markgrafneusiedl Fault and the Enzersdorf High, on which Man1 was drilled. The thickness of Neogene deposits varies considerably ranging from less than 900 m on the Oberlaa High to more than 5000 m in the Schwechat Depression.

4.2.2. Lithostratigraphy

The Miocene lithostratigraphy of the Vienna Basin has been recently formalized in detail by Harzhauser et al. (2020) within the Austrian Vienna Basin (Fig. 4.2). All wells discussed herein have also been analyzed by Harzhauser et al. (2020) and therefore all samples can be clearly assigned to a discrete lithostratigraphic unit. These are the lower Miocene Ottnangian Lužice and Bockfließ formations (~middle Burdigalian), the lower Miocene Karpatian Aderklaa Fm. (~upper Burdigalian) and the formations of the middle Miocene Badenian Baden group (Langhian to lower Serravallian), which comprise the lower Badenian Rothneusiedl and Mannsdorf formations, the middle Badenian Auersthal, Matzen and Baden formations and the upper Badenian Rabensburg formations. The Sarmatian (upper Serravallian) is represented by the Holíč and Skalica formations. A brief description of the lithologic units in stratigraphic order, according to these authors is provided here (for detailed description see Harzhauser et al., 2020). The Bockfließ Fm. is characterized by light and dark grey, micra-rich marly clay with sand intercalations and sporadic Flysch clasts in the base, whereas the Lužice Fm. consists of laminated gray calcareous clays, silt and siltstone with intercalations of sand. The Aderklaa Fm. is subdivided into the Gänserndorf Member and the Schönkirchen Member. The Gänserndorf Mb. is characterized by a rapid alternation of conglomerates, sandstones, marly silty clays and subordinate breccias, whereas the Schönkirchen Mb. displays a monotonous alternation of strongly cemented light grey to greenish sandstones with marly silt and marly clay and intercalations of thin gravel layers. The Rothneusiedl Fm. is characterized by massive, clast-supported conglomerates composed of poorly to moderately rounded, medium to coarse gravel with frequent cobbles with loose intercalations of fine sand and silty marly clay. The Mannsdorf Fm. consists of blue-grey clay, marl and silt, partly with thin silt and fine-sand layers, sandstone layers, rare tuffitic layers. The Auersthal Fm. displays a succession of conglomerates and sand with marl intercalations with prevailing Flysch components. The Matzen Fm. is characterized by bioturbated, often oil impregnated fine to coarse sand, whereas the Baden Fm. consists of bioturbated blue-grey to green-grey clay and marl with silt, fine sand and sporadic corallinacean limestone intercalations. The Rabensburg Fm. is characterized by dark-grey to green-grey, partly laminated clay, marl and silty marl with sand and numerous corallinacean limestone intercalations with rare occurrence of Anhydrite in the basal parts. The Sarmatian lithology of the studied area was described by Harzhauser and Piller (2004) as pelitic-siliciclastic for the Holíč Fm. and siliciclastic-oolitic for the Skalica Fm. All investigated sediments were deposited in marine environments except for the Aderklaa Fm., which represents fluvial and lacustrine depositional environments (e.g., Hladecek, 1965; Weissenbäck, 1995, 1996). A short-termed marine flooding, however, was detected by Harzhauser et al. (2020) in the Matzen Field. Therefore, this formation is included herein.

Due to the different tectonic settings, the thicknesses of the formations differ from field to field (Fig. 4.4). Post-sedimentary tilting and erosion have affected the lower Miocene formations. Therefore, lower Miocene deposits are lacking in the northern VB (Mühlberg-Bernhardsthal, Rabensburg and Palterndorf-Ringelsdorf and Spannberg-Pirawarth fields) and are rapidly pinching out towards the Spannberg Ridge in the Bockfließ-Matzen-Aderklaa fields (Fig. 4.4). Similarly, the lower Badenian deposits have been strongly affected by tectonics and form discontinuous occurrences in former paleobasins, which are separated now by the Spannberg Ridge and the Palterndorf High (Siedl et al., 2020; Harzhauser et al., 2020). The distribution of all subsequent formations corresponds roughly to their original depositional area and the Baden, Rabensburg and Holíč formations have been deposited continuously throughout the VB.

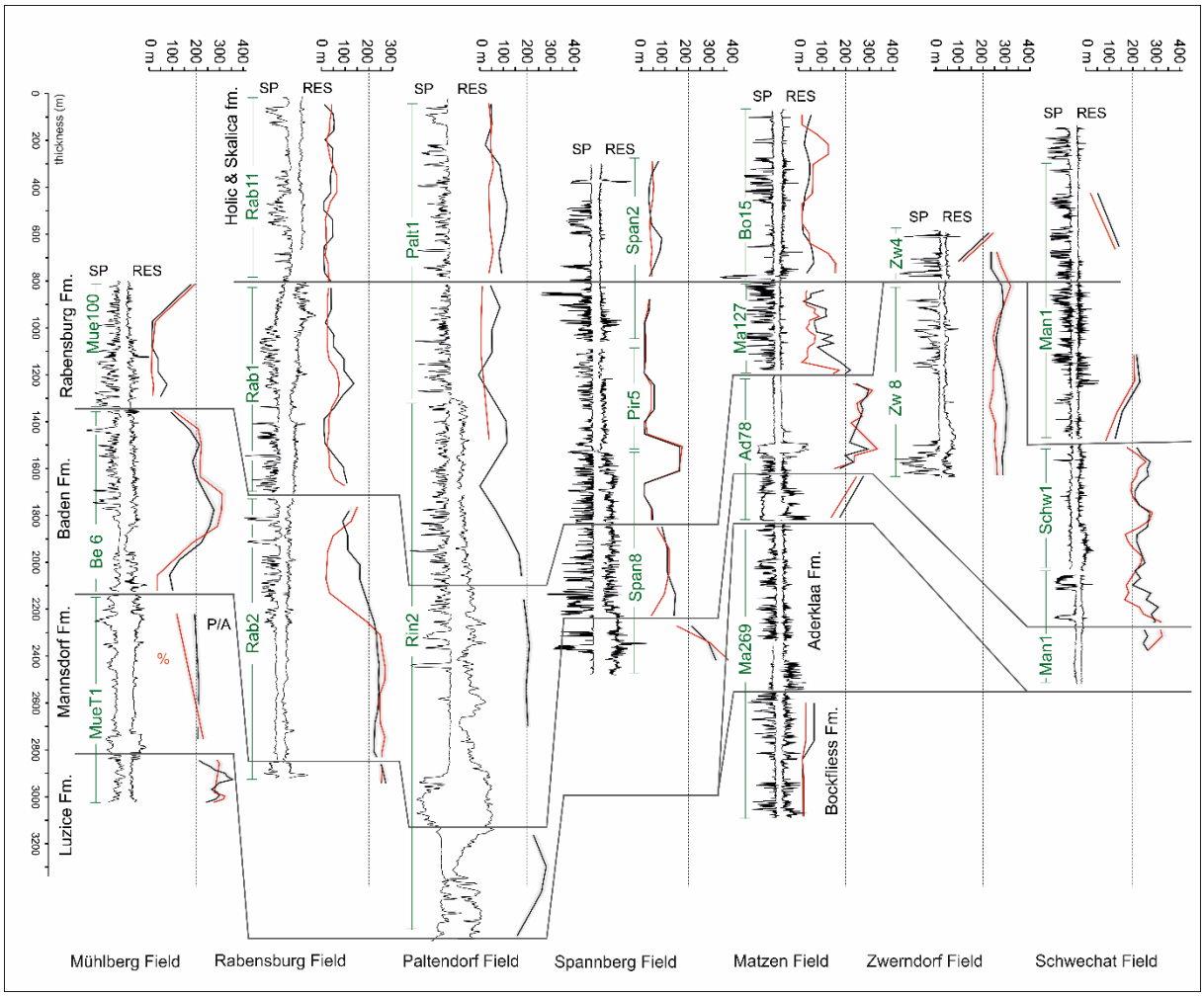

Fig. 4.4. Composite wire-logs for each investigated area with relative position of analyzed foraminiferal samples. Water depth estimates are based on abundance data (red line) and presence/absence data (black line), grey interval corresponds to 95% confidence intervals (SP = spontaneous potential, RES = Resistivity; green letters correspond to well acronyms).

The thickness of the Bockfließ Fm. ranges from 150–250 m in the Spannberg-Pirawarth fields to 150–500 m in the Aderklaa-Bockfließ-Matzen field and zero in all other fields (Fig. 4.4). The Lužice Fm. is

only found in the northernmost field (Mühlberg-Bernhardsthal) and spans from roughly 150–200 m. Within all other fields Ottnangian deposits are lacking completely due to postsedimentary erosion (Fig. 4.4).

Similarly, Karpatian deposits are lacking due to postsedimentary erosion in the Austrian part of the northern VB being restricted to the southern fields. The Aderklaa Fm. pinches out in the central VB along the Spannberg Ridge in the Bockfließ-Matzen-Aderklaa fields attaining up to 900 m in thickness. In all other fields the Aderklaa Fm. is not present (Fig. 4.4). Marine Karpatian deposits, however, are preserved in the Korneuburg and Mistelbach halfgrabens along the western margin of the VB (Fig. 4.1B) (Zuschin et al., 2014; Harzhauser et al., 2019).

The Rothneusiedl Fm., which represents the lowermost Badenian deposits (e.g., Kováč et al., 2004; Strauss et al., 2006; Harzhauser et al., 2020), covers the Aderklaa Fm. in the Bockfließ-Matzen-Aderklaa fields with about 50–100 m thickness but is lacking in all northern fields.

The Mannsdorf Fm. has only a patchy distribution in tectonically formed paleobasins (Siedl et al., 2020). It attains up to 700 m in the Mühlberg-Bernhardsthal fields, around 500 m in the Palterndorf-Ringelsdorf fields but only 100 m and less in the Rabensburg, Spannberg-Pirawarth and Aderklaa-Bockfließ-Matzen fields (Fig. 4.4). The Auersthal Fm. ranges from 80–90 m in the Spannberg-Pirawarth fields, from 50–120 m in the Bockfließ-Matzen-Aderklaa fields and 20–170 m in the Mannsdorf-Schwechat-Wittau fields. It was not developed in the Strasshof-Zwerndorf, Palterndorf-Ringelsdorf, Rabensburg and Mühlberg-Bernhardsthal fields. The Matzen Fm. typically overlies the Auersthal Fm. and is found in the same fields ranging from 20–50 m in the Spannberg-Pirawarth fields to 70 m in the Bockfließ-Matzen-Aderklaa fields and up to about 100 m in the Strasshof-Zwerndorf fields. Within the Mannsdorf-Schwechat-Wittau fields in the south it accounts for only 50–70 m.

The Baden Fm. covers the entire investigated area with varying thicknesses ranging around 300–1200 m in the northern fields (Bernhardsthal-Mühlberg, Rabensburg and Ringelsdorf-Palterndorf). Within the Pirawarth-Spannberg fields the deposits of the Baden Fm. account for up to 300 m, whereas in the Matzen Depression they account generally for less than 300 m. To the south east (Strasshof-Zwerndorf fields and Schwechat depressions) the thickness increases again to 200–600 m (Fig. 4.4).

The Rabensburg Fm. overlies the Baden Fm. in the whole area with varying thicknesses from about 100–1000 m with generally thicker deposits in the northern VB, than in the central part (Fig. 4.4).

The Holíč Fm. covers the investigated area from the Rabensburg Field southwards with thicknesses from 200–400 m and can be found in most drillings. The Skalica Fm. covers the whole area with varying thicknesses of 300–500 m (Fig. 4.4).

4.2.3. Depositional settings

For all formations basic data on their depositional environments are available. Hence, the Bockfließ Fm. is interpreted by Harzhauser et al. (2020) to have formed in shallow lagoonal settings, whereas the Lužice Fm. represents deep, open marine environments within the studied area (Grunert et al., 2013; Harzhauser et al., 2017). The Aderklaa Fm. represents wetland deposits encompassing lacustrine and riverine deposits with a short-lived marine incursion. The Rothneusiedl Fm. was mostly deposited in a braided river system (Weissenbäck, 1995), which became rapidly flooded during a marine transgression and covered by shallow marine deposits (Grill, 1943). The Mannsdorf Fm. represents outer neritic to upper bathyal depositional environments (Harzhauser et al., 2020). The Auersthal Fm. was controversially discussed either as a coastal marine delta with channels (Kreutzer and Hlavatý, 1990; Kreutzer, 1993) or as an alternation of marine and limnic conditions, due to the occurrence of freshwater ostracods (Papp et al., 1973; Wessely, 2006). The overlaying Matzen Fm. was interpreted as coastal marine with sand dunes and shoreface environments of a sand rich braid or fan delta (Fuchs et al., 2001).

Open marine depositional environments prevailed in the central Vienna Basin during deposition of the Baden Fm. (Hohenegger et al., 2008). In the tectonically strongly structured Mühlberg Field, Harzhauser et al. (2018) documented outer neritic to bathyal settings in depocenters and shallow marine environments with seagrass meadows along the margins (Zuschin et al., 2007; Harzhauser et al., 2019).

A comparable range of marine environments is documented for the Rabensburg Fm. Basinal settings were dominated by dysoxic bottom conditions (Kováčová and Hudáčková, 2009), corallinacean shoals developed in topographic highs (Schmid et al., 2001; Pivko et al., 2017), agitated shoreface and foreshore settings are recorded from coastal settings (Ruman and Hudáčková, 2010; Hyžný et al., 2012) and extensive mudflats developed in lagoonal embayments (Harzhauser et al., 2019). The Sarmatian Holíč Fm. represents shallow marine environments partly with seagrass meadows (e.g., Schütz et al., 2007; Koubová and Hudáčková, 2010; Zlinská et al., 2010) whereas the Skalica Fm. is characterized by oolite shoals (Harzhauser and Piller, 2004; Harzhauser et al., 2018).

4.3. Methods

284 Miocene samples have been taken from 42 boreholes in the Austrian part of the VB. All samples were treated with diluted H_2O_2 (12%) for several hours and sieved with tap water through a standard set of sieves (500, 250, 125 and 63 µm) and later on oven dried at 40 °C and split with a microsplitter (Rupp, 1986). Foraminifers were picked of all size fractions until at least 300 specimens were found or

all splits of each fraction were analyzed. For identification of foraminifers several monographs and publications were used (e.g.: Papp et al., 1973; Loeblich and Tappan, 1987; Cicha et al., 1998; Rögl and Spezzaferri, 2003; Bubík and Kaminski, 2004; Kaminski and Gradstein, 2005; Murray et al., 2011; Bindiu-Haitonic et al., 2017). If at least 100 specimens could be identified of a sample, we considered the data to be sufficient for statistical analyses. All gathered data were first transferred into percentages (per sample), before an arcsin-root-transformation was applied for variance stabilization and to ensure a better comparability for further statistical processing (Linder and Berchtold, 1976; Zuschin and Hohenegger, 1998). To detect temporal bathymetric trends in each field, the samples of all wells of each field were ordered according to their relative stratigraphic position from oldest to youngest. This relative positions of the samples within the lithostratigraphic units was deduced by seismic-aided correlation. In addition, wire-logs (Spontaneous Potential, Resistivity) have been used for cross-correlations. This allows to construct an idealized log for each field in which all samples are placed in their relative temporal succession (Fig. 4.4).

To determine paleo-bathymetry, depth ranges of extant benthic foraminifers were gathered from numerous publications (e.g.: Sgarrella and Moncharmont Zei, 1993; Altenbach et al., 2003; Hohenegger, 2005; Rasmussen, 2005; Spezzaferri and Tamburini, 2007; Sen Gupta et al., 2009; Phipps et al., 2010; Milker and Schmiedl, 2012) and used as limits (Table 1) in the paleo water depth calculations after Hohenegger (2005) and Báldi and Hohenegger (2008) with following formulas:
First the gradient value is calculated with:

$$\sqrt{\frac{\sum_{j=1}^{m} l_j a_j d_j^{-1}}{\sum_{j=1}^{m} a_j d_j^{-1}}}$$

Where l_j stands for the location parameter represented by the geometric mean ($\sqrt{x_{j\,min} * x_{j\,max}}$), whereas the weighting factor d_j in this equation was calculated with ($x_{j\,max} - x_{j\,min}$) and a_j represents the abundance of the species. This is than applied in the dispersion (σ_g) formula:

$$\left(\sqrt{\frac{\sum_{j=1}^{m}\left(l_j - g\right)^2 d_j^{-1}}{\sum_{j=1}^{m} d_j^{-1}}}\right)^{1/2}$$

Which leads to the calculated paleo-water depth using a 95% confidence interval (Y=95%, see Zar, 1999):

$$g \pm t_{\frac{1-Y}{2},n-1}\sqrt{\sigma_g^2/m}$$

For comparative reasons the same formula was also applied for presence/absence data (see Hohenegger, 2005).

Planktonic foraminifers are absent from many samples. Therefore, the Plankton/Benthos (P/B) ratio can only be derived for a limited number of samples. The (P/B) ratio is calculated using the formula of Van der Zwaan (1990), because it takes into account the presence of stress markers (S):

$$P(\%) = \frac{P}{(P + B - S)})$$

$$\mathrm{Depth(m)} = \mathrm{e}^{3.58718} + 0.03534 * \mathrm{P(\%)}$$

The software PAST (Paleontological Statistics, version 3.25, Hammer et al., 2001) and R (R-software, version 3.6.1, R-Development Core Team, 2005) were used for the statistical analyses and visualization. To eliminate redeposited foraminifers of the dataset, broken specimens (less than 60% of the test intact) as well as specimens showing significant differences in preservation (e.g., abrasion) were excluded. Further, using the formula of Báldi and Hohenegger (2008) relativizes the effect of any potential redeposited specimens by taking in account the abundance of the species.

We apply the bathymetric categories defined by Adegoke et al. (2017): inner neritic = shoreface down to ca. 40 meters, middle neritic = 40–100 meters, outer neritic = 100–200 meters, bathyal = below 200 meters.

4.3.1. Limitations

The P/B ratio formula was developed by Van der Zwaan (1990) for oceanic settings where reasonable numbers of planktic foraminifers occur in the samples. Consequently, this approach works well in open marine environments (e.g.: Kouwenhoven and Van der Zwaan, 2006) but its results have to be interpreted with caution in the Vienna Basin, which was a semi-enclosed basin of a semi-enclosed epicontinental sea with limited connections to the proto-Mediterranean Sea.

The formula of Hohenegger (2005), using presence/absence (P/A) values, lacks a weighing factor. Consequently, rare species are treated like frequent species and may bias the results. Therefore, depth estimates based on P/A data are only considered when no abundance data were available (wells Rin2 and Be11). Some bias may also occur in estimates based on abundance data. For example, low bottom oxygenation and high nutrient flux may lead to an overestimation of the depositional depths due to the high abundances of bolivinids and buliminids. These are typically found in deeper marine environments due to their preferences of low oxygen areas with a high nutrient availability but may spread to shallow environments if ecological parameters are adequate.

The formulas derive absolute depth in meters. In the following paragraphs we list these values rounded to the nearest ten but we are aware that the values are only guidelines and must not be taken literally.

4.4. Results

In total, about 65.000 foraminiferal specimens have been picked from 284 samples, identified and assigned to 309 species-level taxa (238 Miocene species). A list of all identified species and their relative abundance per sample are provided in the online Supplementary (Tab.1). For 26 samples (Rin2 and Be11 well) only presence/absence data are available (online Supplementary, Tab.2). In addition, data for the Mistelbach Halfgraben (online Supplementary, Tab. 3) have been used from Harzhauser et al. (2017).

In the following, characteristic foraminiferal assemblages, which have been entered in the formulas for depth range estimates are discussed for each field.

Applying the formula of Hohenegger (2005) and Báldi and Hohenegger (2008) reveals different paleobathymetric developments for each oilfield during the early and middle Miocene. Water depth fluctuations per field based on abundance and P/A data are shown along idealized wire-logs of each field (Fig. 4.4). Mean water depths per field are graphically shown in boxplot diagrams separated into time intervals (Fig. 4.5). To follow offshore developments through time in the VB, all data per time interval are combined in Fig. 4.6. Nearshore samples are excluded in these calculations.

A selection of important foraminifers, used in the water depth calculations, is shown on Fig. 4.7. In the following the faunal compositions and paleobathymetrical changes of each discrete oilfield are described.

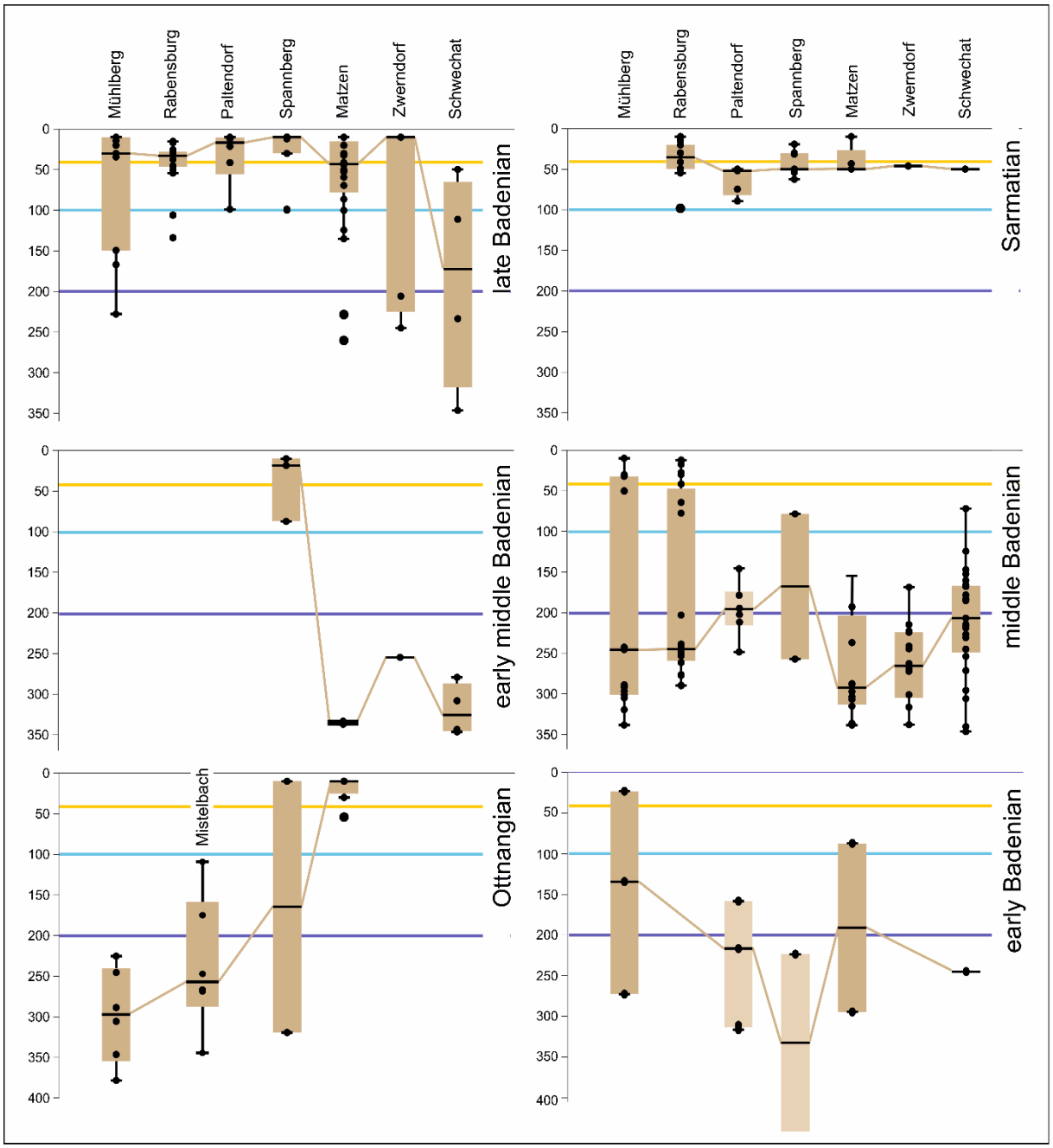

Fig. 4.5. Boxplots of water depth estimates separated in time slices and oil fields, including Ottnangian data from the Mistelbach Halfgraben provided by Harzhauser et al. (2017). Yellow line indicates transition from inner to middle neritic, light blue line indicates transition from middle to outer neritic and dark blue line indicates boundary to bathyal depths. All estimates are based on abundance data except for the early Badenian of the Palterndorf and Spannberg fields, for which only presence/absence data are available (P/A data shown in light brown).

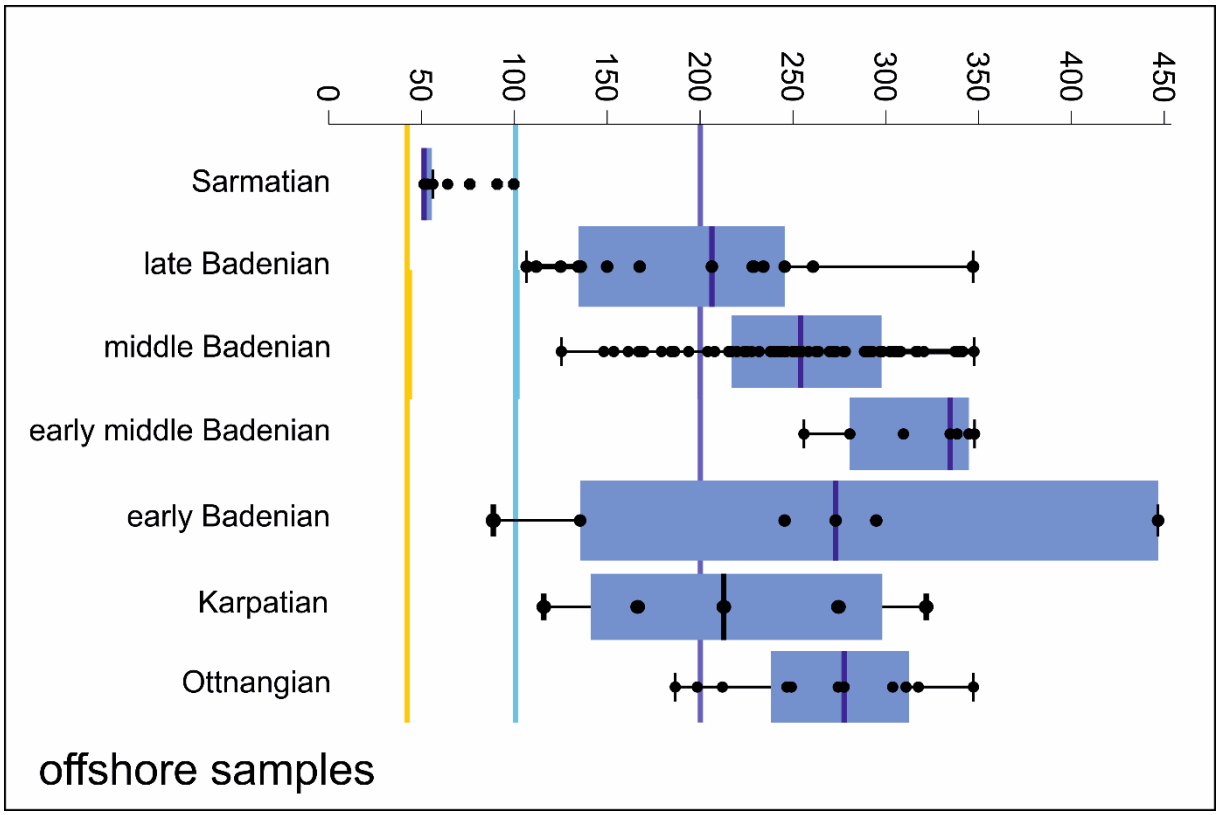

Figure 6. Boxplots uniting abundance data of all offshore samples per time slice, including data from the Mistelbach Halfgraben provided by Harzhauser et al. (2017).

4.4.1. Mühlberg-Bernhardsthal fields

Paleontological data of 44 core samples of wells Be4, Be5, Be6, Be7, Be11, BeS2, BeS3 and Mue77, Mue100, Mue 110 and MueT1 were gathered and assigned to the following lithostratigraphic units:

4.4.1.1. Faunal description

4.4.1.1.1. Lužice Formation*:* 15 samples of the Mühlberg-Bernhardsthal fields derived of the Lužice Fm. (Be4/2245.5, 2347.5, 2414, 2478, Be5/2400, Be11/2344, 2405, 2480, 2497.4, 2570, 2582, 2585, 2585.8 and 2712.5 and MueT1/3300). The samples are characterized by a highly diverse foraminiferal fauna of up to 62 species. The most important species in these samples, accounting for up to 39.8% of the assemblages, are *Bathysiphon taurinensis, Spirorutilus carinatus* (Fig. 4.7L)*, Pullenia bulloides, Planularia* sp., *Martinotiella karreri, Lenticulina inornata* (Fig. 4.7P–Q)*, Lenticulina melvilli, Heterolepa dutemplei, Bolivina hebes, Bolivina trunensis, Cibicides pachyderma, Haplophragmoides vasiceki,* and several species of globigerinids, which may account for up to 60% (e.g., Be4/2245.5).

4.4.1.1.2. Mannsdorf Formation*:* three samples are derived from the Mannsdorf Fm. (MueT1/2480, 2737, 3127). Samples MueT1/3127 and 2737 show high abundances of agglutinated foraminifers (c. 31%), with a slight dominance of *Bathysiphon taurinensis* in 3127 and higher amounts of *Spirorutilus carinatus* in MueT1/2737. Further, sample 3127 contains 32.1% of *Heterolepa dutemplei*, whereas sample MueT1/2737 shows 13% planktonics (*Globigerinoides* div. sp.) and both contain a significant

number of *Lenticulina inornata* (9.8 and 9.4%). The uppermost sample MueT1/2480 is less diverse and is dominated by *Ammonia beccarii* (87%; Fig. 4.7A–B) accompanied by *Reophax scorpiurus* (7.5%).

4.4.1.1.3. Baden Formation*:* 15 samples of the Baden Fm. yielded foraminifers (Mue100/1745, 1820, 1825, 1900, 1980, 1983, 1990, Mue110/1803, 1855, Be4/2078.5, 2141, Be6/2091, Be7/1900, BeS2/1706, BeS3/1746.8). The lowermost samples (Be4/2141, 2078.5, Be6/2091) are dominated by *Ammonia beccarii* (up to 87.5%) accompanied by *Elphidium crispum* (11% in Be4/2141).

Samples Mue100/1820-1990 show high abundances of *Spirorutilus carinatus* (70.2% in 1900) or dominance by *Pullenia bulloides* (67.3%) (Mue100/1980; Fig. 4.7S). These are frequently accompanied by *Grigelis pyrula* (up to 23.1% in Mue100/1980). In the upper samples, the faunal composition changes to *Ammonia beccarii* dominated assemblages (Mue100/1745, Mue 110/1803, 1855) accompanied by *Astegerinata* sp. (24%, Mue 110/1855) and *Quinqueloculina* sp. (58.3%, Mue100/1745).

4.4.1.1.4. Rabensburg Formation*:* nine of eleven samples of the Rabensburg Fm. display a low diverse fauna of 10 or less species (Be6/1406 and 1509, Be7/1429 and 1434.5, BeS3/1599.5 and Mue100/1570, 1590, 1615 and 1650). The samples are generally dominated by *Ammonia beccarii* (80-100%). The exception is sample Be 7/1434.5, which is dominated by *Cycloforina* div sp. (60.7%) and elphidiids (35.7%). The two stratigraphic highest samples (Mue77/1234, 1343) show a higher diversity of 15 and 25 species. Sample Mue77/1343 yields 57.6% planktonic foraminifers with *Globigerina bulloides* as main component (35.8%) accompanied by the benthic *Nonion commune* (10%; Fig. 4.7H) and *Heterolepa dutemplei* (7.4%). The planktonic abundance decreases in sample Mue77/1234 to 3%

and the benthic *Globulina gibba* (24.8%), *Heterolepa dutemplei* (19%) and *Cibicidoides ungerianus* (15.3%) are predominant.

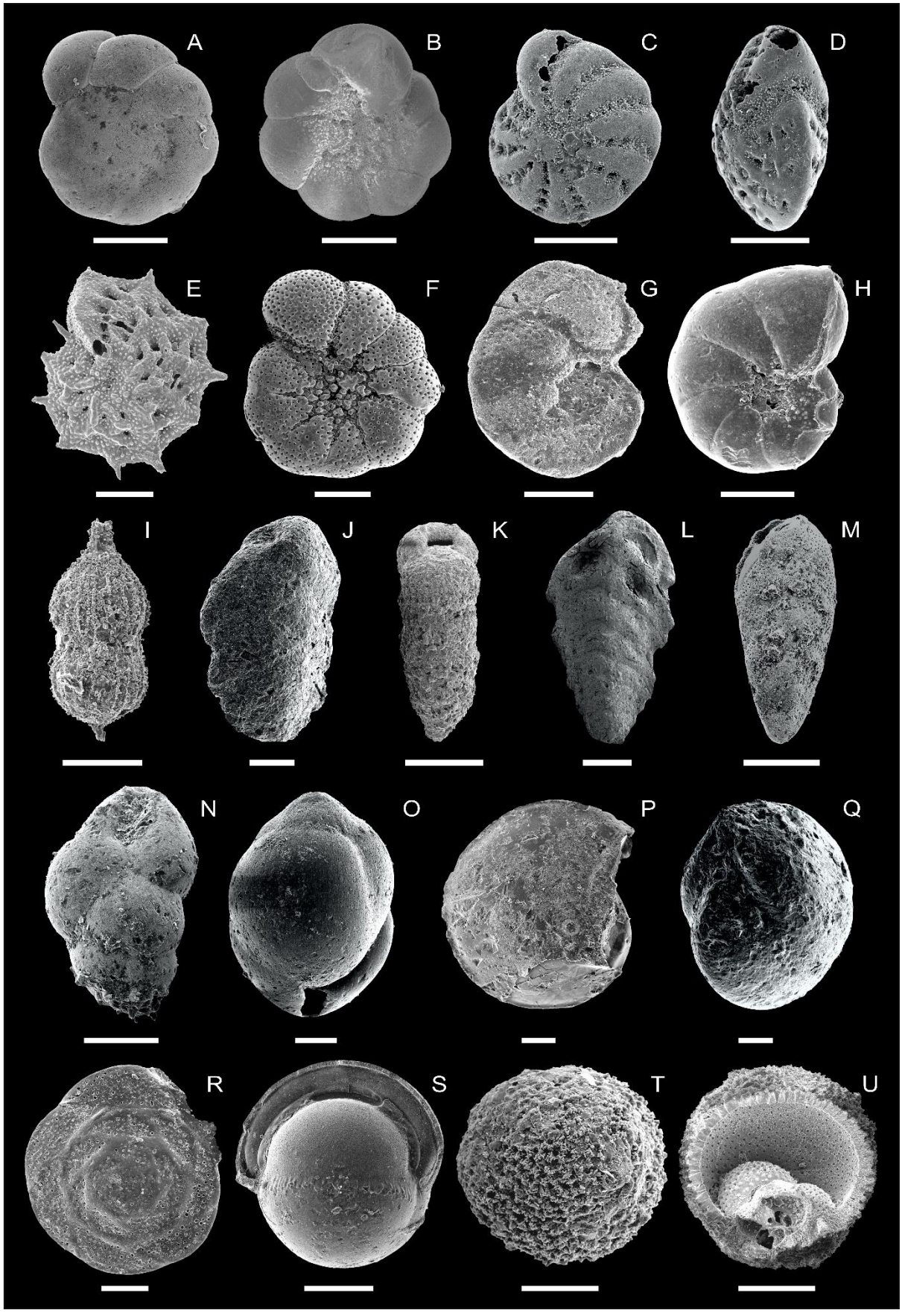

Fig. 4.7 A-B: *Ammonia beccarii* (Linne, 1758); **C-D:** *Elphidium rugosum* (d'Orbigny, 1846); **E:** *Elphidium aculeatum* (d'Orbigny, 1846); **F:** *Porosononion granosum* (d'Orbigny, 1846); **G:** *Lobatula lobatula* Walker and Jacob, 1798; **H:** *Nonion commune* (d'Orbigny, 1846); **I:** *Amphicoryna badenensis* (d'Orbigny, 1846); **J:** *Textularia gramen* d'Orbigny, 1846; **K:** *Textularia laevigata* d'Orbigny, 1826; **L:** *Spirorutilus carinatus* (d'Orbigny, 1846); **M:** *Bolivina dilatata* Reuss, 1850; **N:** *Bulimina subulata* (Cushman and Parker, 1937); **O:** *Globobulimina pyrula* (d'Orbigny, 1846); **P-Q:** *Lenticulina inornata* (d'Orbigny, 1846); **R:** *Heterolepa dutemplei* (d'Orbigny, 1846); **S:** *Pullenia bulloides* (d'Orbigny, 1846); **T-U:** *Orbulina suturalis* Brönnimann, 1951
Scale bar = 100 µm.

4.4.1.2. Paleobathymetry

4.4.1.2.1. Ottnangian*:* the foraminiferal faunas of this northernmost oilfield indicate a bathyal setting with a water depth ranging between 230 and 380 m (Fig. 4.5) based on abundance data (Table 1). Using only P/A data results in a broader range from 180 to 450 m for the Lužice Fm. Similar values of 200 and 440 m are deduced from samples with rich and well preserved planktonic faunas (Be4/2245.5, Be4/2478), for which the P/B ratio formula of Van der Zwaan (1990) can be reliably applied. These values confirm the allocation to offshore bathyal conditions as suggested by Harzhauser et al. (2019, 2020).

4.4.1.2.2. Early Badenian*:* after a hiatus of several million years (Karpatian sediments are missing), the early Badenian (MueT/3127) starts with bathyal settings with a calculated water depth of 270 m (250 m with P/A) and water depth decreases to outer and inner neritic depths at the end of the early Badenian. E.g., an outer neritic water depth of 130 m (190 m with P/A) is calculated for MueT1/2737 followed to a drop down of 20 m in MueT1/2480 coinciding with a predominance of *Ammonia beccarii*.

4.4.1.2.3. Middle Badenian*:* shallow inner neritic environment of 30 to 50 m water depth became established with the onset of the middle Badenian with samples yielding mostly *Ammonia beccarii.* These shallow marine conditions were rapidly replaced by outer neritic to bathyal settings during the middle Badenian flooding, which is used as an important marker throughout the Vienna Basin (Harzhauser et al., 2020, Siedl et al., 2020). These samples are dominated by agglutinated foraminifers (mostly *Spirorutilus carinatus*) indicating water depths of 250 to 340 m. The terminal middle Badenian is marked by a distinct sea level drop to inner neritic conditions resulting in a water depth of about 10 m.

4.4.1.2.4. Late Badenian*:* near shore inner neritic shallow water conditions prevailed at the beginning of the late Badenian with a water depth ranging around 30 m. A marked transgression is reflected in the upper part of the upper Badenian deposits in the Mühlberg-Bernhardsthal fields resulting in outer neritic to upper bathyal conditions with a calculated water depth of 150 to 230 m (e.g., Mue77/1343 and 1234).

Sarmatian samples were not available from these fields.

4.4.2. Rabensburg Field

64 samples of the Rabensburg Field from wells Rab1, Rab2, Rab10, Rab11, RabW1 and RabW2 contained foraminiferal faunas and could be assigned to following formations:

4.4.2.1. Faunal description

4.4.2.1.1. Mannsdorf Formation*:* the lowermost sample (Rab10/2374) contains a moderately diverse fauna of evenly distributed 18 species. Most abundant are *Trochammina* sp. (16.3%), *Paragloborotalia mayeri* (14.9%) and *Globigerinella regularis* (12.8%). In total 59.5% of the total assemblage are planktonic foraminifers.

4.4.2.1.2. Baden Formation*:* 23 samples derived of the Baden Fm. The stratigraphically lowest samples (Rab11/2200, 2237.5, 2296) contain a moderately diverse to diverse fauna of 13-34 species with evenly distributed species. Most abundant are *Spirorutilus carinatus* (24% in Rab11/2200), *Uvigerina semiornata* (13.7% in Rab11/2237.5), *Pullenia bulloides* (13.1% in Rab11/2237.5) and *Psammosiphonella discreta* (10.4% in Rab11/2296). Planktonics are scarcely found but may attain up to 11.8% in few samples (Rab11/2237.5, 2296). Up section, the faunal composition changes to assemblages dominated by *Heterolepa dutemplei*, frequently accompanied by *Pullenia bulloides*, *Spirorutilus carinatus* and *Amphicoryna badenensis* (Fig. 4.7I) (Rab1/1980, 2020 and 2122, Rab2/2110, 2050, 2191, 2237, Rab10/1970, RabW2/2500, 2505, 2570, 2580). The planktonic *Orbulina suturalis* (Fig. 4.7T–U) is frequently present, too (Rab1/1980, 2020 and Rab2/2050, 2191).

The uppermost samples of the Baden Fm. in the Rabensburg Field are dominated by *Ammonia beccarii* up to 95.7% (Rab1/1640, Rab2/1370, 1525, 1568, 1615, 1695, 1715 and 1770), frequently accompanied by *Nonion commune* (up to 37.4% in Rab2/1770). Sample Rab2/1460 is dominated by planktonic species (35.7% *Turborotalita quinqueloba* and 14.3% *Globorotalia transsylvanica*) accompanied by *Cibicides pachyderma* (21.4%).

4.4.2.1.3. Rabensburg Formation*:* the faunas of this formation (Rab1/700, 900, 1060, 1103.5, 1150, 1200, 1290, 1355, 1495 and 1530, Rab2/1020, 1050, 1100, 1230 and 1300, Rab11/1956.3, 1977.6 and 2026) consist mostly of hyaline (70.8-100%), benthic specimens (> 99.2%). The samples show a generally high amount of *Ammonia beccarii*, which may account for up to 92.7% (Rab2/1100). *Porosononion granosum* (Rab1/1103.5, 54%; Fig. 4.7F), *Elphidium rugosum* (Rab1/1530, 73%; Fig. 4.7C–D), *Anomalinoides badenensis* (Rab2/1300, 44.4%) and *Cycloforina hauerina* (Rab11/1956.3, 38.9%) are further important constituents of the fauna. Planktonics are rare in most samples but may account for up to 14.85% (*Globigerinella regularis,* Rab11/1956.37) and 11.5% (*Globigerina bulloides*, Rab11/1956.37).

4.4.2.1.4. Holíč Formation*:* samples Rab10/1000 and Rab11/1848, 1853, 1859 and 1943 yield only benthic foraminifers with a diversity of 2-7 species. Samples Rab10/1000, Rab11/1848 and Rab11/1859 are strongly dominated by *Ammonia beccarii* (90.3-98.3%), the fauna of Rab11/1853 still has 44% *Ammonia beccarii* but yields also 22.5% of *Cycloforina hauerina* and 20.4% of *Varidentella sarmatica*. Sample only contained 28.6% *Ammonia beccarii* and shows a dominance of different elphidiids may account for large parts of the samples (66.3%, Rab11/1943; 43%, Rab11/1805).

4.4.2.1.5. Skalica Formation*:* the topmost samples of the Rabensburg Field are either dominated by *Porosononion granosum* (up to 61.7% in samples Rab2/710 and 920, Rab11/1202, 1213.58, 1227.52, 1235.75, 1360, 1372.36, 1410, 1421.3, 1438,92, 1451.42, 1500 and 1580) or by *Ammonia beccarii* (84.9% in sample Rab2/920). Elphidiids may account for up to 38.8% (Rab11/1235.75).

4.4.2.2. Paleobathymetry

4.4.2.2.1. Early Badenian*:* the oldest samples of the Rabensburg Field derive from the Mannsdorf Fm. (Rab10/2374.1) and was deposited in a deep marine, upper bathyal setting. The calculated water depth of 250 m, using the formula of Báldi and Hohenegger (2008) is slightly shallower than the P/B ratio calculation, which results in 320 m.

4.4.2.2.2. Middle Badenian*:* the sequence starts with bathyal deposits with a water depth varying from 200 to 290 m (e.g., Rab1/1980, 2020, 2122, Rab2/2010, 2050, 2191, 2237, Rab10/1970, Rab11/2200, 2237.5, 2296). This deep marine interval is followed by a shallowing to 80 - 10 m (e.g., Rab1/1640, Rab2/1525, 1565, 1615, 1695, 1715).

4.4.2.2.3. Late Badenian: inner to middle neritic conditions of 20 to 50 m water depth prevailed during the late Badenian in the Rabensburg Field (e.g., Rab1/700, 900, 1060, 1103.5, 1150, Rab2/1020, 1050, 1100, Rab11/1956.3, 1977.6). Only samples Rab2/1300 suggest slightly deeper conditions of more than 100 m due to the high abundance of *Anomalinoides badenensis*, which might cause a slight overestimation of the depositional depth.

4.4.2.2.4. Sarmatian*:* inner neritic conditions prevailed throughout the Sarmatian with water depths ranging around 10 to 50 m with no significant difference between the Holíč Fm. (e.g., Rab11/1805, 1848, 1853, 1859, 1953) and the Skalica Fm. (e.g., Rab2/710, 920, Rab10/1000, Rab11/1202, 1213.8, 1227.5, 1235.7, 1360, 1580). Only sample Rab11/1438.9 indicates deeper conditions of about 100 m due to the large amount of *Nonion commune* and *Porosononion granosum*.

4.4.3. Palterndorf-Ringelsdorf fields

34 samples of the wells Palt1, Rin2 and 3 contain foraminifers and were allocated to the following formations. The Mannsdorf and Baden Fm. are only represented by samples of the Rin2 and 3 wells, of which only P/A were acquired.

4.4.3.1. Faunal description

4.4.3.1.1. Mannsdorf Formation*:* samples Rin2/3832, 3923, 4056, 4143 and 4295 display low diverse assemblages dominated by benthic species, amongst which *Bolivina antiqua, Schlumbergerina transilvaniae, Cibicides pachyderma* and *Martinotiella karreri* show the highest abundances. Only sample Rin2/2495 yields also planktonic species (*Globigerina bulloides, Trilobatus trilobus*).

4.4.3.1.2. Baden Formation*:* the succession from Rin2/3027, 3152, 3243, 3370, 3471, 3541 and 3592 to Rin3/4124 shows samples that are dominated by *Spirorutilus carinatus* and in all samples *Bulimina elongata* is frequently present. Other important species are *Textularia gramen* (Fig. 4.7J)*, Cibicides pachyderma, Melonis pompilioides, Bathysiphon taurinensis*, *Trilobatus trilobus, Globobulimina pyrula* (Fig. 4.7O) and *Heterolepa dutemplei.*

4.4.3.1.3. Rabensburg Formation*:* the samples (Palt1/1825, 2111, 2140, 2245, 2382 and 2452, Rin2/2160, 2287, 2668 and 2713) are generally dominated by *Ammonia beccarii* (up to 96.9%) only sample Palt1/2140 displays a high abundance of *Cyclammina* cf. *compressa* (24.3%). Scarce planktonic species, such as *Trilobatus trilobus* and *Globigerinella obesa*, can be detected throughout.

4.4.3.1.4. Holíč Formation*:* samples Palt1/1460, 1687, 1760 and 1790 contain low diverse assemblages of benthic foraminifers. The most abundant species are *Ammonia beccarii* (up to 50% in Palt1/1460), *Nonion tumidulus* (up to 43.5% in Palt1/1760)*, Cycloforina contorta* (up to 26.7% in Palt1/1687), *Cycloforina hauerina* (up to 13.3% in Palt1/1687) and *Cycloforina fluviata* (11.3% in Palt1/1687).

4.4.3.1.5. Skalica Formation*:* the studied interval shows samples dominated by *Porosononion granosum* 67.7-96% (Palt1/1175, 1210, 1240 and 1300) and one (Palt1/1060) dominated by *Ammonia beccarii* (55%), accompanied by *Elphidium crispum* (14.7%) and *Porosononion granosum* (11%).

4.4.3.2. Paleobathymetry

4.4.3.2.1. Early Badenian*:* Only P/A data were acquired for the samples from the Mannsdorf Fm. in the Ringelsdorf area. These data suggest outer neritic conditions of about 160 m for the lowermost samples (Rin2/4143, 4295) and a shift towards upper bathyal conditions ranging from 220 to 320 m for the following samples (Rin2/3832, 3923, 4065).

4.4.3.2.2. Middle Badenian*:* slightly shallower but still outer neritic to upper bathyal conditions ranging around 200 m water depth are indicated for the middle Badenian. The topmost sample is dominated by *Ammonia beccarii* and indicates inner neritic conditions around 10 m water depth.

4.4.3.2.3. Late Badenian*:* all samples indicate shallow inner neritic conditions with water depths ranging from 10 to 50 m (e.g., Palt1/1825, 2122, 2140, Rin2/2160, 2287, 2668).

4.4.3.2.4. Sarmatian*:* middle and inner neritic depositional environments of 20 to 100 m water depth prevailed during the early Sarmatian. Deepest conditions of about 100 m are recorded for samples Palt1/1687, 1760 and 1790. Middle neritic settings of 50 to 90 m water depth are also calculated for the late Sarmatian.

4.4.4. Spannberg-Pirawarth fields

39 samples of the Span2, 8, 10 and Pir3, 5 and 23 were analyzed and allocated to following formations.

4.4.4.1. Faunal description

4.4.4.1.1. Bockfließ Formation*:* the lowermost sample Span8/2640 is dominated by *Ammonia beccarii* (96.6%) but a drastic faunistic change can be observed to sample Span8/2450, which yields a low diverse fauna with *Spirorutilus carinatus* (36.4%) and *Cycloforina badenensis* (27.3%.)

4.4.4.1.2. Mannsdorf Formation*:* only two samples are available (Pir5/2043, Pir5/2059) with a low diverse fauna dominated by more than 89% of *Lenticulina inornata*.

4.4.4.1.3. Matzen Formation*:* three samples were acquired of the Matzen Fm. Samples Pir5/1956 and 1995.6 are dominated by *Ammonia beccarii* (95-100%), whereas sample Pir5/2007.6 is dominated by *Bulimina elongata* (67.2%) accompanied by *Nonion commune* (29.9%).

4.4.4.1.4. Baden Formation*:* two samples are available (Span8/2071, Span8/2275). Span8/2275 is dominated by *Heterolepa dutemplei* (43.5%, Fig. 4.7R) accompanied by *Nonion commune* (21.6%) whereas Span8/2071 shows a dominance of *Ammonia beccarii* (58.3%).

4.4.4.1.5. Rabensburg Formation*:* 17 samples (Pir3/1337 and 1570, Pir5/1300, 1327, 1717, 1722, 1905, 1914, 1922, and 1948.8, Pir23/1700, 1712 and 1782, Span2/1593 and 1620, Span8/1750 and Span10/1540) yield faunas with an overall dominance of *Ammonia beccarii* (63-100%). In few samples *Elphidium crispum* is frequently present(33.33% in Span2/1620 and dominating with 79.2% in Span2/1593), as well as miliolids (e.g., *Cycloforina hauerina* in Span10/1540 with 10.3%). Sample Pir23/1770 is completely dominated by *Lenticulina inornata* and Pir23/1700 is the only sample also yielding planktonic foraminifera (20% *Globigerinella regularis*).

4.4.4.1.6. Holíč Formation*:* seven samples (Pir5/1255, Span2/1320 and 1420, Span8/1380, 1450 and 1550 and Span10/1430) of the Holíč Fm. revealed faunas with high amounts of *Anomalinoides dividens* (up to 74% in Span8/1550), frequent abundances of *Biasterigerina planorbis* (up to 33.3% in Span2/1420) and *Ammonia beccarii*. Sample Span8/1380 is dominated by *Varidentella reussi* (78.9%) and *Varidentella sarmatica* (9.6%).

4.4.4.1.7. *Skalica Formation:* the samples (Pir5/765 and Span2/880, 1000 and 1100) show high numbers of *Porosononion granosum* (98.7% in Pir5/765 and 17.6-51.7% in all Span2 samples). Sample Span2/1100 contains also high numbers of *Cycloforina hauerina* (29.4%) and Span2/880 of *Varidentella reussi* (49.4%).

4.4.4.2. Paleobathymetry

4.4.4.2.1. Ottnangian*:* the few Ottnangian samples from the Spannberg-Pirawarth fields document a transition from coastal to outer marine environments. Faunas from sample Span8/2640 indicate very shallow conditions around 10 m water depth which are rapidly replaced by upper bathyal conditions

and a water depth of about 320 m (Span8/2450), in which deep-water species like *Lenticulina inornata, Spirorutilus carinatus* and *Bulimina elongata* dwelled.

4.4.4.2.2. Early Badenian*:* only two samples are available for this interval (Pir5/2034.6, 2059). The foraminiferal assemblages indicate deep, bathyal settings with a water depth of about 450 m.

4.4.4.2.3. Middle Badenian: the initial marine phase of the middle Badenian is represented in the Spannberg-Pirawarth fields by the sandy Matzen Fm. (Pir5/1956, 1995.6 and 2007.6). Its foraminiferal assemblages indicate inner to middle neritic conditions and a water depth ranging from 10 to 90 m. The Baden Fm. is represented in this area by a short succession. The available samples suggest middle neritic water depth of about 80 m (Span8/2071) to upper bathyal conditions of up to 260 m water depth (e.g., Span8/2275). Using only P/A values results in similar calculations of 130 to 180 m.

4.4.4.2.4. Late Badenian*:* a long succession of samples from the Rabensburg Fm. reveals predominately inner neritic conditions (e.g., Pir3/1337, 1570, Pir5/1300, 1327, 1717, Span2/1593, 1620, Span8/1750) with a calculated water depth varying from 10 to 30 m. The maximum water depth of about 100 m is indicated by samples Span10/1540 and Pir5/1939.

4.4.4.2.5. Sarmatian*:* Shallow marine, inner to middle neritic conditions of 20 to 50 m prevailed during the early Sarmatian (e.g., Pir5/1255, Span 2/1320, Span8/1380,1450, Span10/1430) with a shallowing trend. Only slightly deeper conditions of 30 to 60 m water depth characterized the late Sarmatian in the Spannberg-Pirawarth fields.

4.4.5. Aderklaa-Bockfließ-Matzen fields

68 analyzed samples of the wells Ad78, Bo3, 8 and 15, and Ma111, 112, 125, 126, 127 and 269 yielded foraminiferal faunas and could be assigned to following formations:

4.4.5.1. Faunal description

4.4.5.1.1. Bockfließ Formation*:* the fauna of all samples (Bo3/2172.7, Bo8/1900 and 2000, Ma269/2315, 2659, 2677 and 2715) is dominated by *Ammonia beccarii* (43.8-100%). Only two samples yield significant numbers of other species: 56.2% of *Nonion tumidulus* in Ma269/2659 and 30.4% of *Globulina granulosa* in Bo3/2280.

4.4.5.1.2. Aderklaa Formation*:* A single sample in the otherwise fluvial-lacustrine Schönkirchen Mb. revealed autochthonous foraminifers (see Harzhauser et al. 2020). Sample Ma112/1805.5 yields a low diverse fauna with 58.3% planktonics (*Globorotalia transsylvanica, Globigerinella regularis* and *Globigerina bulloides*) accompanied by the benthic *Caucasina schischkinskayae*, *Ammonia beccarii, Nonion commune* and *Hanzawaia boueana*.

4.4.5.1.3. Mannsdorf Formation*:* sample Ad78/1829 contained a moderate diverse evenly distributed assemblage of 14 species. Most abundant are *Heterolepa dutemplei* (16.7%)*, Globigerina bulloides* (14.3%), *Globobulimina pyrula* and *Bathysiphon taurinensis* (both 11.9%).

4.4.5.1.4. Auersthal Formation*:* two samples (Ad78/1742.1 and Ma112/1620) derived from the Auersthal Fm. Ma112/1620 yields only *Porosononion granosum* and *Nonion commune*, whereas Ad78/1742 shows an evenly distributed fauna of 21 species with highest abundances of *Lenticulina inornata* (20.9%)*, Martinotiella communis* (13.4%) and *Reophax nodulosa brevior* (6%).

4.4.5.1.5. Matzen Formation*:* two samples (Ad78/1706.1 and Ma125/1645) contain foraminifers. Ma125/1645 is dominated by *Ammonia beccarii* (100%), whereas Ad78/1706.1 yields a moderate diverse, evenly distributed fauna of 23 species with highest abundances of *Cibicidoides* div sp. (16.1%), buliminids (15.3%) and *Martinotiella communis* (11.9%).

4.4.5.1.6. Baden Formation*:* eleven samples (Ad78/1420, 1500 and 1665, Bo8/1740, Ma111/1656 and 1663, Ma125/1482, Ma126/1655 and 1665 and Ma127/1610 and 1695) contained mainly agglutinated foraminifers (mostly *Spirorutilus carinatus, Bathysiphon taurinensis, Alveolophragmium crassum, Alveolophragmium obliquicameratum* and textulariids like *Textularia laevigata*, Fig. 4.7K) and *Heterolepa dutemplei* accompanied by rare planktonics. Some samples, however, display high contributions by *Orbulina suturalis* (e.g., 34.2% in Ad78/1420 with 34.2%). Sample Ma125/1482 is an outlier, which is dominated by *Anomalinoides badenensis* and *Cibicidoides ungerianus* (46.2 and 38.5%).

4.4.5.1.7. Rabensburg Formation*:* the 23 samples (Bo8/1500, 1560, 1655 and 1676, Ma111/1368, 1420, 1490 and 1515, Ma112/1317 and 1362, Ma125/1250, 1255, 1317, 1356 and 1405, Ma126/1490 and 1510, Ma127/1365, 1451 and 1552 and Ma269/1376, 1393.8 and 1425.8) are generally dominated by *Ammonia beccarii,* frequently accompanied by elphidiids (mostly *Elphidium rugosum* and *Elphidium aculeatum,* Fig. 4.7E), *Nonion commune* and *Nonion tumidulus*. Exceptions are sample Ma111/1368, which is dominated by *Triloculina gibba* (36.9%) accompanied by 20 equally distributed miliolid and hyaline species (≤ 10%) *Lobatula lobatula* (Fig. 4.7G) and sample Ma125/1405, which is dominated by *Bulimina elongata* (57.3%) accompanied by *Cycloforina contorta* (15%).

4.4.5.1.8. Holíč Formation*:* most samples (Ad78/1080, 1296 and 1303, Bo15/1669 and 1720, Ma111/1144 and 1170, Ma112/1040 and Ma127/1140 and 1185) are dominated by *Ammonia beccarii* (up to 100% in Bo15/1669 and 1720) accompanied by *Elphidium hauerinum*. Similarly, Ad78/1080 is dominated by a single species (98.8% *Anomalinoides dividens*). Only sample Ma127/1140 displays a more diverse assemblage with *Articulina gibbosula* (25.7%), *Elphidium reginum* (23%), *Elphidium crispum* (21.7%) and *Triloculina gibba* (11%).

4.4.5.1.9. Skalica Formation*:* the samples Ad78/885, Bo15/1360, 1475 and 1530 and Ma112/792 are dominated by *Porosononion granosum*, rarely accompanied by *Varidentella reussi* (18.2% in

Bo15/1530). Samples Ma125/920 and 1010 lack *Porosononion granosum* but are dominated by *Ammonia beccarii*.

4.4.5.2. Paleobathymetry

4.4.5.2.2. Ottnangian: samples from the Bockfließ Fm. (e.g., Bo3/2172.7, Bo8/1900, 2000, Ma269/2315, 2695, 2677) formed in inner neritic settings with calculated water depths ranging around 10 to 30 m characterize this interval. Only sample Bo3/2280 represents slightly deeper conditions of about 50 m.

4.4.5.2.3. Karpatian*:* thick deposits of the limnic Aderklaa Fm. formed in the Matzen subbasin during the Karpatian. Consequently, foraminifers were lacking in those samples, but within sample Ma112/1805.5 a foraminiferal assemblage with planktonic species indicated a short period flooding of the Matzen area. The high percentage of planktonic foraminifers (58%) would provide a water depth calculation of 280 m according to P/B ratio. This value is highly unrealistic of course but shows the close vicinity of the area to open marine environments.

4.4.5.2.4. Early Badenian*:* only two samples are available revealing different bathymetric conditions. Sample Ma112/1620 was deposited in the middle neritic in a water depth of about 90 m whereas Ad78/1829 indicates bathyal depths of about 300m. This difference might reflect the paleotopography of the area. Well Ad78 lies several km to the south of well Ma112 and seems to represent an offshore setting. Due to the strong tectonics, however, the original relation between these depositional areas cannot be reliably reconstructed.

4.4.5.2.5. Middle Badenian*:* already the lowermost samples from the Auersthal and Matzen formations indicate deep marine bathyal conditions (e.g., Ad78/1742.17, Ma125/1645, Ad78/1706) down to 340 m water depth, contradicting the interpretation of Rupp (1986) of the Matzen Fm. as inner neritic deposits. Few samples within this deep-water interval (e.g., Ma125/1645) are outliers indicating shallow inner neritic conditions ranging around 10 m water depth. These samples are interpreted to derive from intercalations of shallow marine sediment or from reworking. The open marine conditions continued throughout the middle Badenian and samples from the Baden Fm. (e.g., Ad78/1420, 1500 and 1665, Ma125/1482, Ma126/1655, Ma127/1641, 1695) yield foraminiferal assemblages that dwelled in water depths between 200 and 340 m.

4.4.5.2.6. Late Badenian*:* much shallower conditions were established during the late Badenian in the Aderklaa-Bockfließ-Matzen fields. The stratigraphically oldest samples of the Rabensburg Fm. indicate the deepest depositional conditions ranging to the upper bathyal (e.g., Ma125/1405: 260 m, Bo8/1676: 230 m). The following samples (e.g., Bo8/1500, 1560, 1655, Ma111/1368, 1420, Ma112/1317 Ma125/1250, 1255, 1317, Ma126/14900, Ma127/1365, 1451, Ma269/1376, 1425.8) suggest water depths of 10 to 140 m and therefore represent inner to outer neritic conditions. This pattern documents a rapid shallowing during the late Badenian.

4.4.5.2.7. Sarmatian*:* inner to middle neritic conditions and water depths ranging from 10 to 100 m prevailed during the early Sarmatian (e.g., Ad78/1080, 1276, 1303, Bo15/1669, 1720, Ma111/1144, Ma112/1040, Ma125/920, Ma127/1140) coinciding with a general shallowing trend. Inner neritic conditions with a calculated water depth of 10 to 50 m is also documented for the late Sarmatian.

4.4.6. Zwerndorf-Strasshof fields

21 samples of the Zw4 and 8 and Str1 wells contained foraminiferal faunas and were allocated to following formations.

4.4.6.1. Faunal description

4.4.6.1.1.Matzen Formation*:* sample Zw4/1560 revealed a low diverse fauna of 14 species dominated by *Heterolepa dutemplei* (59.2%) and *Spirorutilus carinatus* (16.4%).

4.4.6.1.2. Baden Formation*:* ten samples (Str1/1680, 1750, 1792 and 1820, Zw4/1240, 1325, 1430, 1445, 1460 and 1500 and Zw8/1445, 1480 and 1710) contained evenly distributed faunas with frequent abundances of planktonics (mostly *Globigerina bulloides*, up to 38.5% in Zw4/1325 and *Orbulina suturalis* up to 9.9% in Str1/1680). The benthic fauna is characterized by high abundances of *Heterolepa dutemplei* (up to 31.5% in Str1/1820) along with several agglutinated foraminifers (e.g.: *Spirorutilus carinatus, Haplophragmoides vasiceki, Haplophragmoides carinatus* and *Reophax nodulosa brevior*) and uvigerinids (*Uvigerina venusta, Uvigerina pudica, Uvigerina brunnensis* and *Pappina parkeri*). Only sample Zw4/1325 is dominated by *Bolivina dilatata* (41.5%; Fig. 4.7M) and *Globigerina bulloides* (38.5%).

4.4.6.1.3. Rabensburg Formation*:* samples Str1/1440 and 1550 yielded faunas dominated by buliminids (55.2%; *Bulimina elongata, Bulimina elongata longa, Bulimina gutsulica* and *Caucasina. schischkinskayae*) accompanied by *Globobulimina pyrula* (20.8%). Up section, samples Str1/1280, Zw4/1150 and Zw8/1120 and 1200 are dominated by *Ammonia beccarii* (to 100% in Zw8/1120 and 1200).

4.4.6.1.4. Skalica Formation*:* sample Zw4/1010 has a moderately diverse fauna (25 species) dominated by of *Ammonia beccarii* (45.2%) accompanied by *Elphidium crispum* (17.1%).

4.4.6.2. Paleobathymetry

4.4.6.2.1. Middle Badenian*:* bathyal conditions down to 340 m water depth are indicated already by the lowermost sample Zw4/1560, which marks the transition from the Matzen Fm. to the Baden Fm., coinciding with the middle Badenian transgression. The bathyal conditions with calculated water depths from 220 to 320 m persisted in the Zwerndorf-Strasshof fields throughout the middle Badenian (e.g., Str1/1680, 1792, 1820, Zw4/1240, 1325, 1430, Zw8/1445, 1480). Only sample Str1/1750 was deposited in slightly shallower, outer neritic settings with a water depth of about 170 m.

4.4.6.2.2. Late Badenian*:* deeper marine conditions ranging between 210 and 250 m water depth prevailed also during the late Badenian (e.g., Str1/1440 and 1550). These values might be overestimated due to the high abundance of bolivinids and buliminids, which typically dwell in deeper environments, linked to an increased nutrient supply and lowered oxygen values (e.g., Eichler et al., 2014). If shallow areas develop a high nutrient supply accompanied by low oxic conditions, bolivinids and buliminids account for large numbers of the association but this is not further subject of this work.
4.4.6.2.3. Sarmatian*:* Only a single sample is available (Zw4/1010) from the Skalica Fm., which indicates inner neritic conditions with a water depth around 50 m.

4.4.7. Schwechat Field

In total, 39 samples were collected from wells Him1, Man1, Schw1 and Wit1.

4.4.7.1. Faunal description

4.4.7.1.1. Mannsdorf Formation*:* sample Man1/2570 yields a low diverse fauna with four evenly distributed species (*Cibicides pachyderma, Heterolepa dutemplei, Laevidentalina elegans* and *Vaginulina legumen*).

4.4.7.1.2. Auersthal Formation*:* three samples (Man1/2428 and Wit1/2291 and 2388) derived from the Auersthal Fm. and yielded moderately diverse to diverse faunas of 8-29 species. These assemblages are highly influenced by planktonic species like *Trilobatus trilobus* (dominating in Wit1/2291 with 59%) and *Orbulina suturalis* (37.8% in Man1/2428), most important benthic species for reconstructing paleobathymetry are *Lenticulina inornata, Heterolepa dutemplei* and *Cyclammina vulchoviensis*.

4.4.7.1.3. Matzen Formation*:* sample Wit1/2260, yielded a low diverse fauna of 6 species, dominated by *Lenticulina inornata* (59.1%) and *Heterolepa dutemplei* (32.3%).

4.4.7.1.4. Baden Formation*:* 25 samples (Him1/1310, 1695, 1800, 1850, 1908, 1950 and 2003.5, Man1/2180, 2230, 2296 and 2340, Schw1/1650, 1765, 1825, 1909, 1962, 2025 and 2141.5 and Wit1/1844, 1900, 1965, 2021, 2056, 2146 and 2173) yielded foraminiferal assemblages. All samples contain significant numbers of planktonics, mostly *Globigerina bulloides*, *Globigerinella obesa* and *Trilobatus trilobus* accompanied by *Orbulina suturalis*; benthic assemblages consist mainly of agglutinated foraminifers (*Spirorutilus carinatus*, *Bathysiphon taurinensis* and *Reophax nodulosa brevior*) and *Heterolepa dutemplei*. Samples Him1/1310, 1695 and 1800 displayed relatively low numbers of planktonic specimens (<12%) and are consequently dominated by benthic species. This general pattern varies in sample Him1/1695 by higher contributions of elphidiids (19.7%) and *Heterolepa dutemplei* (10.2%) and in sample Him1/1800 by a high abundance of *Bulimina elongata* (46.5%). Another assemblage type is represented by sample Him1/1310 in which *Ammonia beccarii* is the most abundant species (24.7%) along with few planktonics (e.g., *Orbulina suturalis*).

4.4.7.1.5. Rabensburg Formation*:* five samples (Man1/2055 and 2128 and Schw1/1420, 1515 and 1580) yielded foraminiferal assemblages with low diverse faunas (2-8 species), except for sample Man1/2128 with 20 species. In the low diverse samples, the most important species are *Anomalinoides badenensis, Ammonia beccarii, Elphidium crispum, Bolivina dilatata, Bulimina subulata* (Fig. 4.7N) and *Globigerina bulloides*. Within sample Man1/2128 no species is clearly dominating; most abundant are *Sphaeroidina bulloides* (24.2%), *Heterolepa dutemplei* (15.1%), *Bulimina striata* (13.1%).

4.4.7.1.6. Holíč Formation*:* sample Him1/1100 contains mostly miliolid specimens (96.7%), dominated by *Varidentella reussi* (65.6%) accompanied by *Varidentella sarmatica* (10.5%) and *Cycloforina contorta* (8.2%).

4.4.7.1.7. Skalica Formation*:* Sample Man1/1510 is dominated by *Porosononion granosum* (77.8%).

4.4.7.2. Paleobathymetry

4.4.7.2.1. Early Badenian*:* Only a single sample is available (Man1/2570) suggesting a bathyal setting with a calculated water depth of 250 m.

4.4.7.2.2. Middle Badenian*:* upper bathyal conditions and a water depth of 280 to 350 m were already established during the initial early Badenian represented by the samples from the Auersthal and Matzen formations (Man1/2428, Wit1/2291, 2388 Wit1/2260). Outer neritic to upper bathyal conditions persisted during the interval of middle Badenian, which is represented by numerous samples from the Baden Fm. (e.g., Him1/1695, 1800, 1850, 1908, 1950, Man1/2180, 2230, 2296, Schw1/1650, 1765, 11825, 1909, Wit1/1844, 1900, 1965, 2021, 2056). A water depth range from 120 to 350 m is calculated for these samples. A shallowing is indicated by the top-most sample (Him1/1310), which revealed middle neritic conditions with a calculated water depth of 70 m.

4.4.7.2.3. Late Badenian*:* middle to outer neritic settings with calculated water depths of 50 to 110 m established during the early phase of the late Badenian (e.g., Schw1/1515, 1580). Stratigraphically younger samples (e.g., Man1/2128, Schw1/1420) suggest a rapid deepening culminating in bathyal water depths of 230 and 350 m. These estimates might be slightly biased by the frequent occurrence of buliminids, *Nonion commune* and *Sphaeroidina bulloides.*

4.4.7.2.4. Sarmatian: Only two samples represent the early and late Sarmatian in the area (Him1/1100, Man1/1510), which both indicate show inner neritic settings in 30 to 50 m water depth.

4.5. Discussion

4.5.1. Relative sea level of the Miocene Vienna Basin

Kováč et al. (2004, 2018), Strauss et al. (2006) and Siedl et al. (2020) analyzed the sequence stratigraphy of the Vienna Basin and defined six 3rd order cycles spanning from the Ottnangian to the Sarmatian, based on seismic data (Figs. 3). Of these the three Badenian cycles are well resolved in 3D seismic with clearly defined lowstand systems tract, transgressive systems tract and highstand systems tract deposits (Siedl et al., 2020). The 3rd order cycles of the VB have been correlated with the global 3rd order cycles of Haq et al. (1987, 1988) by Kováč et al. (2004, 2018), Strauss et al. (2006), Piller et al. (2007) and Siedl et al. (2020).

Similarly, Hardenbol et al. (1998) correlated the cycles, which they observed in the Pannonian Basin, with the Haq-cycles. Sant et al. (2017) and Kováč et al (2018), in contrast, assumed that the tectonic reorganization of the Central European basins was the dominant factor to explain regional floodings in the Central Paratethys and that global sea level fluctuations were of subordinate relevance. Moreover, the sea level estimates of Haq et al. (1987, 1988) turned out to be unrealistically high (Miller et al., 2011; Cramer et al., 2011). Miller et al. (2017, 2020) constrained the amplitude of global sea level fluctuations during the early and middle Miocene Mi-events to about 20 to 50 m. Herein, we present estimates of the amplitude of the sea level changes in the VB (Figs. 5, 6) and compare match and mismatch with global signals (Fig. 4.8).

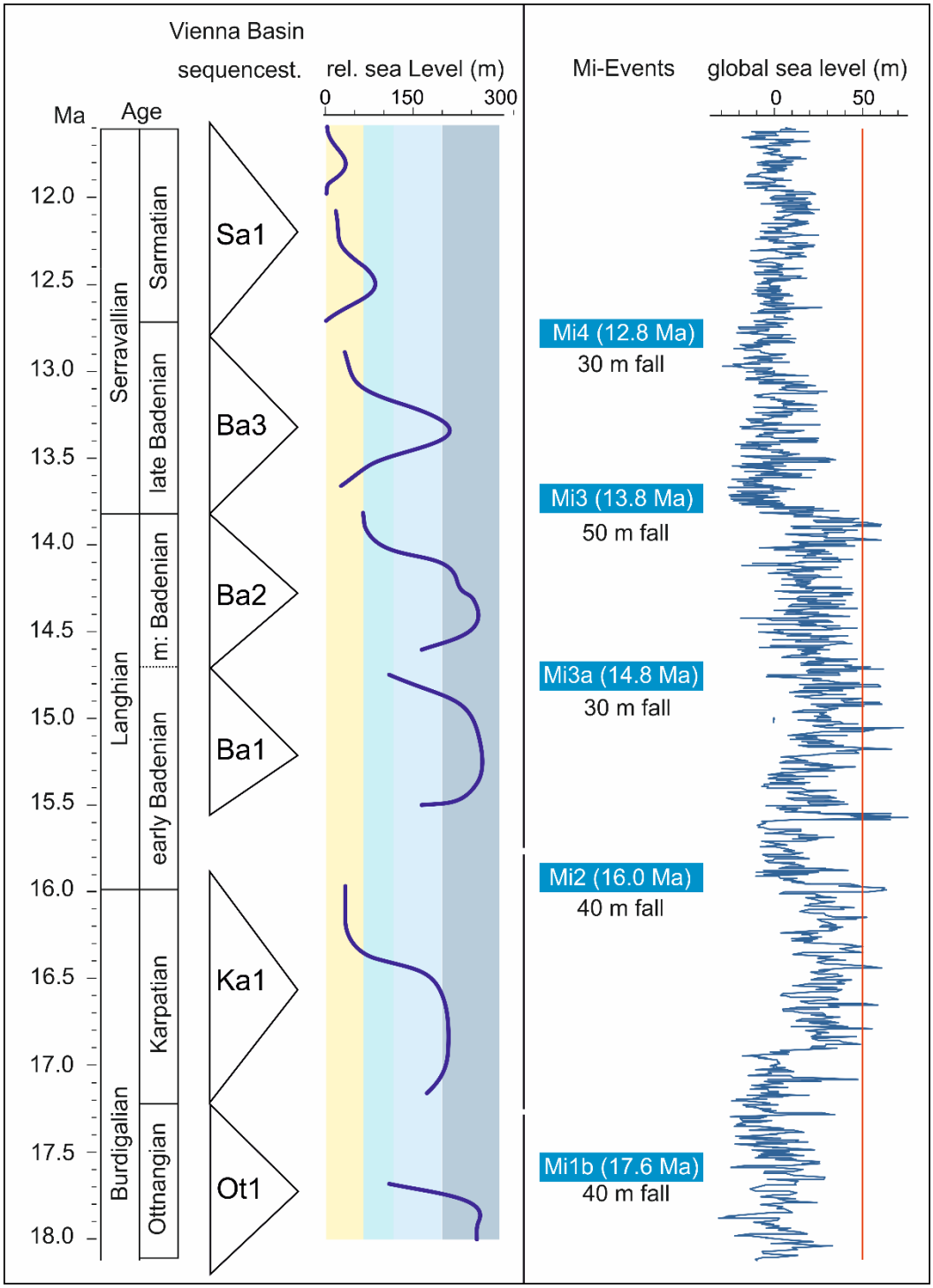

Fig. 4.8 Correlation of the Vienna Basin sequence stratigraphy and relative sea level with the Mediterranean and Central Paratethys ages after Hilgen et al. (2012); modified from Harzhauser et al. (2020) and Siedl et al. (2020). Age of Mi-Events and associated sea level fall amplitudes after Miller et al. (2017, 2020). Global sea level curve (red line marks 50 m) obtained from $\delta^{18}O$ and Mg/Ca values from Pacific cores and the corresponding benthic foraminiferal $\delta^{18}O$ splice after Miller et al. (2017, 2020).

4.5.1.1. Ot1-sequence, early Miocene (Ottnangian): the first marine flooding of the proto-Vienna Basin occurred during the Ottnangian around 18.1 Ma (Harzhauser et al., 2019) and was interpreted by Piller et al. (2007) to correlate with the TB 2.1. cycle of Haq et al. (1988) and the Bur 3 cycle of Hardenbol et al. (1998). Our data document a quick transgression, which entered a strongly structured basin separated into a shallow embayment in the central Vienna Basin and a deep marine basin in the northern VB. Inner neritic conditions became established in the central VB with mean values ranging around 20 m, indicated by the assemblages from the Bockfließ Fm. (Fig. 4.9). The transition into deep marine environments occurred in the Spannberg-Pirawarth area, where the lagoonal conditions of the Bockfließ Fm. graded rapidly into upper bathyal settings of the Lužice Fm. (Fig. 4.9). A water depth down to 300 m was developed in the Bernhardsthal-Mühlberg fields. Thus, the maximum net-rise of the relative sea level in the Vienna Basin would have ranged around 300 m.

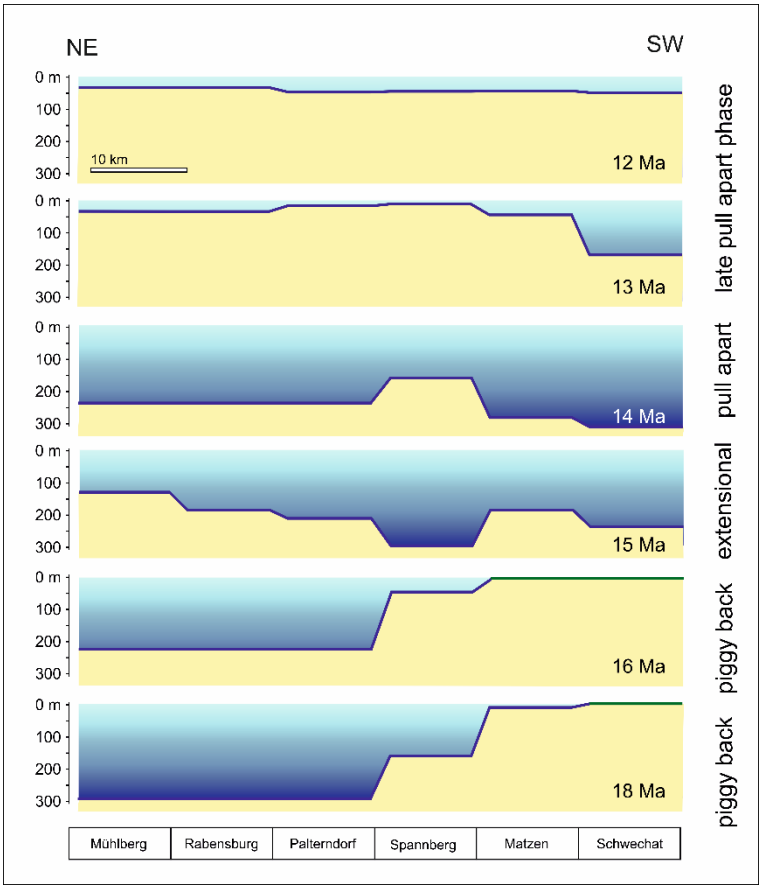

Fig. 4.9. Sketch summarizing the paleobathymetric evolution of the Vienna Basin along a NE-SW transect in relation with the prevailing tectonic regime. Note that these reconstructions focus solely on mean water depth estimates as shown in Figs. 4 and 5 and do not integrate paleogeographic information provided by Siedl et al. (2020) (e.g., deltaic bodies, incised valleys).

Similarly, deep water conditions prevailed in the Mistelbach Halfgraben with water depth up to 340 m during the early Ottnangian (based on data from the Mistelbach Fm. in Harzhauser et al., 2017). These data document continuous deep marine environments in the northern VB (Figs. 5, 6).

A rapid shallowing occurred during the late Ottnangian (Palzer-Khomenko et al, 2018, Harzhauser et al., 2019). The timing of this shallowing coincides with the Mi1b event at 17.6 Ma, which resulted in a fall of the global sea level of about 40 m (Miller et al., 2017, 2020). The magnitude of this sea level drop would easily account for the cessation of marine sedimentation in the central Vienna Basin and would still allow the continuation of marine deposition in the deep northern parts, which lead onto the Carpathian Foredeep. The deep marine deposits of the Mistelbach Fm. in the Mistelbach area, are covered by the shallow marine Kettelsbrunn Mb. which was deposited in an inner-middle neritic setting, hardly exceeding 100 m of water depth (Fig. 4.5).

4.5.1.2. Ka1-sequence, early Miocene (Karpatian): sedimentation between the Ottnangian and Karpatian was discontinuous in the Vienna Basina marked by a major erosive reflector in the seismic surveys (e.g., Matzen area: Hladecek, 1965, Mistelbach Basin: Harzhauser et al., 2019). It is unclear if this erosion occurred under subaeral conditions or in a marine environment. The timing correlates with a global sea level drop around 17.0 Ma followed by a marked sea level rise of about 50 m (Fig. 4.8). Still, a marked bathymetric south-north gradient was characterizing the Vienna Basin (Fig. 4.9). Terrestrial depositional environments prevailed in the central Vienna Basin, represented by the Aderklaa Fm. (Harzhauser et al., 2020). The coeval deposits have been eroded in the Austrian part of the VB but are preserved in two halfgrabens along the northwestern margin of the VB (Korneuburg Basin: Zuschin et al., 2014; Mistelbach Basin: Harzhauser et al., 2019). In addition, open marine deposits are preserved along the eastern margin of the VB on Slovak territory (Kováč et al., 2004; Schlögl et al., 2011). We have integrated bathymetric data from these regions for our reconstructions (Fig. 4.9). Faunas of the estuarine Korneuburg Basin indicate inner neritic settings (Zuschin et al., 2014). In the adjacent Mistelbach Basin, the Karpatian transgression led to outer neritic to upper bathyal conditions with water depths based on benthic foraminifers down to 320 m (Fig. 4.6). A single marine flooding into the wetlands of the central VB is documented by our data for the Matzen field. Miller et al. (2017) documented a marked negative excursion in the $\delta^{18}O$ record between Mi1b and Mi2 around 16.5–16.6 Ma, which correlates with a global sea level rise of 40–60 m. This global event may well be reflected in the observed flooding of the central VB. An alternative explanation would be a short pulse of increased subsidence rate in the central VB, which ranged around 1 m/kyr on average during the Karpatian (Harzhauser et al., 2020).

4.5.1.3. Ba1-sequence, middle Miocene (early Badenian): after a major tectonic reorganization of the VB around the early/middle Miocene boundary, the Vienna Basin was flooded again. Tilting and heavy erosion of lower Miocene strata is documented for the central Vienna Basin, the Korneuburg Basin and the Mistelbach Basin, suggesting that the area fell dry (Harzhauser et al., 2019, 2020). The initial flooding is reflected in the central and southern VB by the marine reworking of the conglomerates of the lacustrine Rothneusiedel Fm. (Kováč et al., 2004; Strauss et al., 2006; Harzhauser et al., 2020). In the northern Pannonian Basin, the Carpathian Foredeep and the Transylvanian Basin this marine flooding resulted in deep marine conditions with the high abundance of *Praeorbulina sicana* and *Praeorbulina glomerosa* (Oszczypko and Oszczypko-Clowes, 2012; De Leeuw et al., 2013; Holcová et al., 2018; Hudáčková et al., 2020). In the northern and southern VB, the invading sea entered a strongly structured landscape with several deep subbasins (Siedl et al., 2020). On average, the relative seal level in the VB ranged around 270 m during the early Badenian. In deepest parts, water depth may have exceeded even 400 m. This flooding correlates with a strong positive trend in the global sea level record (Fig. 4.8). The maximum amplitude of the global signal, however, does not exceed 60 m. The observed bathymetry during the early Badenian is therefore best explained by rapid subsidence during the early extensional phase of the VB, which was amplified by the overall high global sea level.

4.5.1.4. Ba2-sequence, middle Miocene (middle Badenian): the early/middle Badenian boundary coincides with the Mi3a event of Miller (2020), which resulted in a global sea level fall of about 30 m. The strong discordance between the lower Badenian and the middle Badenian, however, is clearly related to tectonic activity (Siedl et al., 2020: Fig. 4.4) marking the onset of extensional tectonics. Thus, tectonics may have considerably enhanced the global sea level signal.

The middle Badenian transgression is reflected by sandy deposits of the Auersthal and Matzen formations. Our data document a very rapid rise of the relative sea level leading to bathyal conditions down to 340 m water depth during the early phase of the middle Badenian. These results clearly contradict previous interpretation of the Matzen Formation as shallow inner neritic coastal sand (Harzhauser et al., 2020; Siedl et al. 2020). The middle Badenian flooding is an excellent marker in all subbasins of the Vienna Basin expressed as long shale-line interval in well logs and as distinct maximum flooding surface in seismic surveys (Siedl et al., 2020; Harzhauser et al., 2020) (Fig. 4.3). This flooding is documented in all major Central Paratethyan Basins (e.g., Bicchi et al., 2003; Filipescu, 2004; Peryt, 2013; Filipescu and Filipescu, 2014; Sant et al., 2019). Holcová et al. (2015) recorded marine outer shelf to upper bathyal conditions from the Moravian part of the Carpathian Foredeep and traced the flooding in numerous drillings from the Carpathian Foredeep into the northern Pannonian Basin, correlating it to the TB 2.4 cycle of Haq et al. (1988) (Holcová et al., 2018; Šarinová et al., 2018; Hudáčková et al., 2020). The average water depth in the VB ranged around 250 m during this phase.

These data are in line with water depth estimates of Báldi and Hohenegger (2008), who, however, analyzed only a short core interval from Baden-Sooss. The water depth estimates are well constrained by the maximum accommodation for deposition as revealed by flattening the seismic data of the Ba2-sequence along its maximum flooding surface (Fig. 4.3). This method limits the water depth between lowstand deposits and maximum flooding surface to roughly 300 m (without backstripping calculations). The subsequent shallowing trend during the middle Badenian is most likely related to the ceasing accommodation due to high sedimentation rates as reconstructed by Lee and Wagreich (2017) and Harzhauser et al. (2020).

The observed middle Badenian fluctuations of the relative sea level in the VB exceed the amplitude of the global sea level rise between Mi3 and Mi3a, which ranged around 50 m (Fig. 4.8; Miller et al. 2020). Sant et al. (2019) linked this middle Badenian transgression mainly to the subsidence of the Pannonian Basin Complex (PBC). This flooding, however, is also recorded outside the PBC. Mandic (2004) documented the mid-Badenian flooding also in the North Alpine Foreland Basin, which at that time was rather uplifted than subsiding (Kováč et al., 2017). Moreover, markedly increasing subsidence rates in the PBC might rather be expected to have caused backstepping and forced regressions instead of transgressions. Therefore, we assume that the observed flooding is strongly enhanced by the major global sea level rise, between the Mi3 and Mi3a events.

4.5.1.5. Ba3-sequence, middle Miocene (late Badenian): the global sea level drop at the Langhian/Serravallian boundary, coinciding with the Mi3 event (13.8 Ma), is constrained to have ranged around 50 m (John et al., 2004; Westerhold et al., 2005; Miller et al., 2017, 2020). A marked sea level drop is also documented from Paratethyan Basins. Middle Badenian corallinacean shoals became exposed in the southern Vienna Basin (Strauss et al., 2006), paralic coal swamps developed in parts of the northern VB (Harzhauser et al., 2018), a distinct shallowing occurred in the southern Pannonian Basin System (Bakrač et al., 2010; Pezelj et al. 2013; Mandic et al., 2019; Hudáčková et al., 2020), the Slovakian Danube Basin (Šarinová et al., 2018; Holcová et al., 2019) and in the Carpathian Foredeep (Peryt, 2013; Nehyba et al., 2016). Evaporite formation took place during that time in several Paratethyan basins (e.g., Mărunţeanu, 1999; Chira, 2000; Andreyeva-Grigorovich et al., 2003; Babel, 2004; Peryt et al., 2004; Peryt, 2006; Báldi et al., 2017), Recently, Badenian anhydrite was also detected in the Bernhardsthal Field in the northern Vienna Basin (Harzhauser et al. 2019) but no detailed information on its distribution is available. Incised valleys formed in the Alpine-Carpathian Foredeep (Gebhardt and Roetzel, 2013). The subsequent transgression peaked in the VB in a maximum water depth of about 210 m in deep depressions, such as the Schwechat depression (Fig. 4.9). Middle neritic water depths prevailed in the northern VB.

The global sea level rise following the Mi3 event ranged around 60 m (Fig. 4.8). This amplitude could easily account for the observed relative sea level rise in the VB. Tectonically active parts subsided to outer neritic and even bathyal water depth whereas uplifted or stable areas were only shallowly flooded, reflecting the global signal.

4.5.1.6. Sa1-sequence, middle Miocene (Sarmatian): the Badenian/Sarmatian boundary at 12.7 Ma is close to the Mi4 event at 12.8, which caused a global sea level fall of about 30 m (Miller et al., 2020). This amplitude explains the observed erosion between the Badenian Rabensburg Fm. and the Sarmatian Holíč Fm. The subsequent rise of the global sea level of up to 50 m (Fig. 4.8) explains the re-establishment of inner neritic water depths of about 20 to 50 m in most parts of the VB during the Sarmatian.

4.5.2. Subsidence rates

At first sight, the subsidence rates might be suspected to have governed the water depth evolution in the various subbasins of the VB. Such differentiated subsidence rates for single subbasins have been calculated by Hölzel et al. (2008) and Lee and Wagreich (2017). Similarly, Harzhauser et al. (2020) discussed net-rates of subsidence based on maximum thicknesses of the lower and middle Miocene formations in relation to available time of deposition. During the middle Miocene subsidence rates in the northern and central Vienna Basin ranged around 1 m/kyr (Harzhauser et al., 2020) but were low to nearly stationary on tectonic highs (0.2 m/kyr) (Lee and Wagreich, 2017). Locally, subsidence was strongly influenced by the then active Steinberg fault (Wessely, 2006). The average subsidence rate would theoretically allow a rise of the water depth of 100 m within 100 kyr. Seismic geometries as presented by Siedl et al. (2020), however, document that subsidence was more or less balanced by synchronous sedimentation in most areas. Only in tectonically active areas, such as the Mühlberg Field along the Steinberg fault and the Schwechat depression, submarine basins formed. Therefore, tectonics resulted in the development of deep subbasins but fails to explain the repeatedly observed rapid shifts of hundred and more meters in geological short time from coastal settings to outer neritic or even bathyal depths and vice versa.

4.6. Conclusions

Each of the investigated oilfields represents a small subbasin within the Vienna Basin and each subbasin experienced its own geodynamic development. Based on our data it is possible to search for

common developments, which can be traced in all subbasins and to distinguish these from local developments, which may be explained by regional tectonics.

The proto-Vienna Basin was flooded for the first time during the Ottnangian at around 18.1 Ma peaking in maximum water depth down to 300 m. Bathyal, open marine conditions became established in the northern Vienna Basin, whereas the central VB was characterized by lagoonal, neritic environments at that time. During the Karpatian fluvial/limnic conditions prevailed in the central VB with a short marine flooding, flushing planktonic foraminifers into the central VB during the global sea level high around 16.5 Ma. Deep water conditions prevailed in the northern VB (e.g., Mistelbach Halfgraben) attaining more than 300 m in water depth. The simple N-S basin architecture during the early Miocene, as shown in Fig. 4.9, is linked to the piggy-back stage of the tectonic evolution of the VB.

Basin geometry changed dramatically at the early/middle Miocene boundary. The tectonic regime changed from piggy-back to extensional and the early Badenian transgression entered new and deep paleobasins (Siedl et al., 2020) with water depths down to 400 m. The middle Badenian transgression corresponds to the wide-spread mid-Langhian flooding of Sant et al. (2019). Initially, the relative sea level in the VB attained 350 m but soon shifted to around 250 m due to cessation of accommodation by high sedimentation rates. With the middle Badenian, the tectonic regime switched to an extensional regime, which persisted into the late Badenian and Sarmatian. Consequently, deeper marine conditions developed only in tectonically active subbasins, whereas inner to middle neritic conditions prevailed in most areas of the VB until the Sarmatian.

All lowstand systems in the relative sea level of the Austrian VB coincide with global sea level lows during Mi-events (Fig. 4.8. The global sea level fall during the Mi3, at the Langhian/Serravallian boundary, is an outstanding example for this coincidence with dramatic change of paleoenvironments in the VB. Therefore, we propose a causal link between both patterns. For the observed transgressions, the link to the global sea level is less straightforward. Peaks in water depth of the VB can roughly be correlated with maxima in the global record but the observed amplitudes exceed those of the global record three to four times. This is especially true during the early Miocene and the early middle Miocene. Therefore, we postulate a strong tectonic amplification of the global signal during the piggy-back and extensional phases of the VB. The fluctuations of the relative sea level in the VB during the late Badenian and Sarmatian, in contrast, range well within the amplitude of the global records. Therefore, we assume that subsidence was roughly balanced by sedimentation during the extensional stage of tectonic evolution in the VB basin allowing for a more reliable record of the global sea level signal.

Acknowledgements

We thank the OMV Exploration Austria working group, led by Herwig Peresson, for their cooperation and Wolfgang Hujer (OMV, Gänserndorf) and his team for help and support during the sampling campaign. Many thanks to the preparators of the NHM Vienna, Anton Engelbert, Anton Fürst and specifically to Iris Feichtinger, for preparing, washing and sieving of the enormous number of samples in a short time period. Further, we want to address our gratitude to Dr. Diego Antonia Garcia Ramos (University of Vienna) for his help with operating the R-Software.

We greatly acknowledge the very open-minded politics of the OMV-AG to provide access to core material, well-log data, seismic images and internal reports to support geosciences.

This project was financed by the OMV.

Finally, we want to thank our reviewers, Natália Hudáčková (Comenius University in Bratislava, Slovakia), Sorin Filipescu (Babeş-Bolyai University, România) and associate editor Ernesto Schwarz (University of La Plata, Argentina) for professional and helpful remarks to improve this work.

References

Adegoke, A.K., Abdullah, W.H., Yandoka, B.M.S., 2017. Provenance and paleoenvironment of organic matter within the Fika sediments in Chad (Bornu) Basin, northeastern Nigeria: An integrated organic geochemical and palynofacies approach. International Journal of Coal Geology, 173, 94–109. https:// doi.org/10.1016/j.coal.2017.02.007

Altenbach, A.V., Lutze, G.F., Schiebel, R., Schönfeld, J., 2003. Impact of interrelated and interdependent ecological controls on benthic foraminifera: an example from the Gulf of Guinea. Palaeogeography, Palaeoclimatology, Palaeoecology, 197(3–4), 213–238. https://doi.org/10.1016/S0031-0182(03)00463-2

Andreyeva-Grigorovich, A.S., Oszczypko, N., Savitskaya, N.A., Ślączka, A., Trofimovich, N.A., 2003. Correlation of Late Badenian salts of the Wieliczka, Bochnia and Kalush areas (Polish and Ukrainian Carpathian Foredeep). Annales Societatis Geologorum Poloniae 73(2), 67–89.

Arzmüller, G., Buchta, S.B., Ralbovsky, E., Wessely, G., 2006. The Vienna Basin. In: Golonka, J., Picha, F.J. (Eds.), The Carpathians and their foreland: Geology and hydrocarbon resources. American Association of Petroleum Geologists Memoir, 84, pp. 191–204. https:// doi.org/10.1306/M84985

Babel, M., 2004. Badenian evaporite basin of the northern Carpathian Foredeep as a drawdown salina basin. Acta Geologica Polonica 54, 317–337.

Báldi, K., Hohenegger, J., 2008. Paleoecology of benthic foraminifera of the Baden-Sooss section Badenian, Middle Miocene, Vienna Basin, Austria. Geologica Carpathica, 59(5), 411–424. http://www.geologicacarpathica.com/browse-journal/volumes/59-5/article-455/

Báldi, K., Velledits, F., Ćorić, S., Lemberkovics, V., Lőrincz, K., Shevelev, M., 2017. Discovery of the Badenian evaporites inside the Carpathian Arc: implications for global climate change and Paratethys salinity. Geologica Carpathica, 68(3), 193–206.

Bakrač, K., Hajek-Tadesse, V., Miknić, M., Grizelj, A., Hećimović, I., Kovačić, M., 2010. Evidence for Badenian local sea level changes in the proximal area of the North Croatian Basin. Geologia Croatica, 63(3), 259–269. https://doi.org/104154/gc.2010.21

Beidinger, A., Decker, K., 2016. Paleogene and Neogene kinematics of the Alpine-Carpathian fold-thrust belt at the Alpine-Carpathian transition. Tectonophysics, 690, 263–287. https://doi.org/10.1016/j.tecto.2016.09.002

Bicchi, E., Ferrero, E., Gonera, M., 2003. Palaeoclimatic interpretation based on Middle Miocene planktonic foraminifera: the Silesia Basin (Paratethys) and Monferrato (Tethys) records. Palaeogeography, Palaeoclimatology, Palaeoecology, 196 (3–4), 265–303. https://doi.org/10.1016/S0031-0182(03)00368-7

Bindiu-Haitonic, R., Niculici, S., Filipescu, S., Bălc, R., Aroldi, C., 2017. Biostratigraphy and palaeoenvironments of the Eocene deep-water deposits of the Tarcău Nappe Eastern Carpathians, Romania based on agglutinated foraminifera and calcareous nannofossil assemblages. In: Kaminski, M.A., Alegret, L. Eds.: Proceedings of the Ninth International Workshop on Agglutinated Foraminifera Grzybowski Foundation Special Publication, 22, 17–37.

Boote, D.R.D., Sachsenhofer, R.F, Tari, G., Arbouille, D., 2018. Petroleum provinces of the Paratethyan region. Journal of Petroleum Geology, 41(3), 247–297. https://doi.org/10.1111/jpg.12703

Brzobohatý, R., Stráník, Z., 2012. Paleogeography of the Early Badenian connection between the Vienna Basin and the Carpathian Foredeep. Central European Journal of Geosciences, 4(1), 126–137, https://doi.org/10.2478/s13533-011-0045-z

Bubík M., Kaminski M.A., 2004 Eds. Proceedings of the Sixth International Workshop on Agglutinated Foraminifera Grzybowski Foundation Special Publication, 8, 486 pp.

Cícha, C., 2000. Nannoplancton calcaros si moluste Miocene din Transilvania, Romania. Carpatica, Cluj-Napoca, 183 pp.

Cícha, I., Rögl, F., Rupp, C., Čtyroký, J., 1998. Oligocene-Miocene foraminifera of the Central Paratethys. Abhandlungen der senckenbergischen naturforschenden Gesellschaft, 549, 325 pp.

Cramer, B.S., Miller K.G., Barrett, P.J., Wright, J.D., 2011. Late Cretaceous–Neogene trends in deep ocean temperature and continental ice volume: Reconciling records of benthic foraminiferal geochemistry (δ18O and Mg/Ca) with sea level history. Journal of Geophysical Research: Oceans, 116, C12, https://doi.org/10.1029/2011JC007255.

Decker, K., 1996. Miocene tectonics at the Alpine–Carpathian junction and the evolution of the Vienna Basin. Mitteilungen der Gesellschaft der Geologie und Bergbaustudenten Österreichs, 41, 33–44.

De Leeuw, A., Filipescu, S., Maţenco, L., Krijgsman, W., Kuiper, K., Stoica, M., 2013. Paleomagnetic and chronostratigraphic constraints on the Middle to Late Miocene evolution of the Transylvanian Basin (Romania): Implications for Central Paratethys stratigraphy and emplacement of the Tisza–Dacia plate. Global and Planetary Change, 103, 82–98.

Eichler, P.P., Pimenta, F.M., Eichler, B.B., Vital, H., 2014. Living Bulimina marginata in the SW Atlantic continental margin: effect of the subtropical shelf front and South Atlantic central water. Continental Shelf Research, 89, 88–92.

Filipescu, S., 2004. Bogdanowiczia pocutica Pishvanova in the Middle Miocene of Transylvania – Paleoenvironmental and stratigraphic implications. In: Codrea V., Petrescu I. Dica P., (Eds.), Acta Palaeontologica Romaniae 4, 113–117.

Filipescu, R., Filipescu, S., 2014. New data on the Early–Middle Badenian transition in the NW Transylvanian Basin (Romania) revealed by the planktonic foraminifera assemblages. Studia Universitatis Babes-Bolyai Geologia 59, 39–44. https://doi.org/10.5038/1937-8602.59.1.3

Fodor, L., 1995. From transpression to transtension: Oligocene–Miocene structural evolution of the Vienna Basin and the East Alpine–Western Carpathian junction. Tectonophysics, 242, 151–182. https://doi.org/10.1016/0040-1951(94)00158-6

Fuchs, R., Ramberger, R., Veit. C., 2001. Renaissance des größten Öl- und Gasfeldes in Österreich Wiener Becken. Erdöl, Erdgas, Kohle, 117, 528–540.

Gebhardt, H., Roetzel, R., 2013. The Antarctic viewpoint of the Central Paratethys: cause, timing, and duration of a deep valley incision in the Middle Miocene Alpine–Carpathian Foredeep of Lower Austria. International Journal of Earth Sciences, 102(4), 977–987. https://doi.org/10.1007/s00531-012-0841-9

Grill, R., 1943. Uber mikropalaontologische Gliederungsmoglichkeiten im Miozän des Wiener Beckens. Mitteilungen der Reichsanstalt für Bodenforschung, 6, 33–44.

Grunert, P., Hinsch, R., Sachsenhofer, R.F., Bechtel, A., Ćorić, S., Harzhauser, M., Piller, W.E., Sperl, H., 2013. Early Burdigalian infill of the Puchkirchen Trough (North Alpine Foreland Basin, Central Paratethys): Facies development and sequence stratigraphy. Marine and Petroleum Geology, 39, 164–186. https://doi.org/10.1016/j.marpetgeo.2012.08.009

Hamilton, W., Wagner, L., Wessely, G., 2000. Oil and Gas in Austria. Mitteilungen der Österreichischen Geologischen Gesellschaft, 92, 235–262.

Hammer, Ø., Harper, D.A.T., Ryan, P.D., 2001. PAST: paleontological statistics software package for education and data analysis. Palaeontologia Electronica. 4(1), 1–9.

Haq, B.U., Hardenbol, J., Vail, P.R., 1987. Chronology of fluctuating sea levels since the Triassic. Science, 235, 1156–1166.

Haq, B.U., Hardenbol, J., Vail, P.R., 1988. Mesozoic and Cenozoic chronostratigraphy and cycles of sealevel changes. In: Wilgus, C.K., (Ed.), Sea-level changes - an integrated approach. Society of Economic Paleontologists and Mineralogists, Special Publications, 42, pp. 71–108.

Hardenbol, J., Thierry, J., Farley, M.B., Jacquin, T.,Graciansky, P.-C., Vail, P.R., 1998. Mesozoic and Cenozoic Sequence Chronostratigraphic Framework of European Basins. In: Graciansky, C.-P., Hardenbol, J., Jacquin, T., Vail, P.R., (Eds.), Mesozoic and Cenozoic sequence stratigraphy of European basins. Society for Sedimentary Geology Special Publication, 6, pp. 3–13.

Harzhauser, M., Piller, W.E., 2004. Integrated stratigraphy of the Sarmatian Upper Middle Miocene in the western Central Paratethys. Stratigraphy, 1(1), 65–86.

Harzhauser, M., Theobalt, D., Strauss, P., Mandic, O., Carnevale, G., Piller, W.E., 2017. Miocene biostratigraphy and paleoecology of the Mistelbach Halfgraben in the northwestern Vienna Basin (Lower Austria). Jahrbuch der Geologischen Bundesanstalt, 157, 57–108.

Harzhauser, M., Grunert, P., Mandic, O., Lukeneder, P., Garcia Gallardo, A., Neubauer, T.A., Carnevale, G., Landau, B.M., Sauer, R., Strauss, P., 2018. Middle and Late Badenian palaeoenvironments in the northern Vienna Basin and their potential link to the Badenian Salinity Crisis. Geologica Carpathica, 69, 129–168. https://doi.org/10.1515/geoca-2018-0009.

Harzhauser, M., Theobalt, D., Strauss, P., Mandic, O., Piller, W.E., 2019. Seismic-based lower and middle Miocene stratigraphy in the northwestern Vienna Basin Austria. Newsletter on Stratigraphy, 52, 221–224. https://doi:10.1127/nos/2018/0490

Harzhauser, M., Kranner, M., Mandic, O., Strauss, P., Siedl, W., Piller, W.E., 2020. Miocene lithostratigraphy of the northern and central Vienna Basin (Austria). Austrian Journal of Earth Sciences, 113(1), 169–199. https://doi.org/10.17738/ajes.2020.0011

Hilgen, F.J., Lourens, L.J., Van Dam, J.A., 2012. The Neogene Period. In: Gradstein, F.M., Ogg, J.G., Schmitz, M., Ogg, G., (Eds.), A Geologic Time Scale 2012. pp. 923–978, (Elsevier) Amsterdam

Hinsch, R., Decker, K., Peresson, H., 2005. 3D seismic interpretation and structural modeling in the Vienna Basin: implication for Miocene to recent kinematics, Austrian Journal of Earth Science, 97, 38–50.

Hladecek, K., 1965. Zur Schichtfolge und Lagerung des Helvets von Matzen. PhD-Thesis, University of Vienna, 106 pp.

Hohenegger, J., 2005. Estimation of environmental paleogradient values based on presence/absence data: a case study using benthic foraminifera for paleodepth estimation. Palaeogeography, Palaeoclimatology, Palaeoecology, 217, 115–130. https://doi.org/10.1016/j.palaeo.2004.11.020

Hohenegger, J., Andersen, N., Báldi, K., Ćorić, S., Pervesler, P., Rupp, C., Wagreich, M., 2008. Paleoenvironment of the Early Badenian Middle Miocene in the southern Vienna Basin Austria –

multivariate analysis of the Baden-Sooss section. Geologica Carpathica, 59, 461–487. http://www.geologicacarpathica.com/browse-journal/volumes/59-5/article-458/

Hohenegger J., Rögl F., Ćorić S., Pervesler P., Lirer F., Roetzel R., Scholger R., Stingl K., 2009. The Styrian Basin: a key to the Middle Miocene (Badenian/Langhian) Central Paratethys transgressions. Austrian Journal of Earth Sciences, 102, 102–132.

Holcová, K., Brzobohatý, R., Kopecká, J., Nehyba, S., 2015. Reconstruction of the unusual Middle Miocene (Badenian) palaeoenvironment of the Carpathian Foredeep (Lomnice/Tisnov denudational relict, Czech Republic). Geological Quarterly, 59(4) 654–678. https://doi.org/10.7306/gq.1249

Holcová, K., Doláková, N., Nehyba, S., Vacek, F., 2018. Timing of Langhian bioevents in the Carpathian Foredeep and north ern Pannonian Basin in relation to ocean o graphic, tectonic and climatic processes. Geological Quarterly, 62(1), 3–17. https://doi.org/10.7306/gq.1399

Holcová, K., Dašková, J., Fordinál, K., Hrabovský, J., Milovský, R., Scheiner, F., Vacek, F., 2019. A series of ecostratigraphic events across the Langhian/Serravallian boundary in an epicontinental setting: the northern Pannonian Basin. Facies, 65(3), 36. https://doi.org/10.1007/s10347-019-0576-

Hölzel, M., Wagreich, M., Faber, R., Strauss, P., 2008. Regional subsidence analysis in the Vienna Basin (Austria). Austrian Journal of Earth Sciences, 101, 88–98.

Hölzel, M., Decker, K., Zamolyi, A., Strauss, P., Wagreich, M., 2010. Lower Miocene structural evolution of the central Vienna Basin (Austria). Marine and Petroleum Geology, 27, 666–681. https://doi.org/10.1016/j.marpetgeo.2009.10.005

Hyžny, M., Hudáčková, N., Biskupič, R., Rybár, S., Fuksi, T., Halásová, E., Zágoršek, K., Jamrich, M., Ledvák P., 2012. Devínska Kobyla – a window into the Middle Miocene shallow-water marine environments of the Central Paratethys (Vienna Basin, Slovakia). Acta Geologica Slovaca, 4(2), 95–111.

John, C.M., Karner,G.D., Mutti M., 2004. $\delta^{18}O$ and Marion Plateau backstripping: Combining two approaches to constrain late middle Miocene eustatic amplitude. Geology, 32, 829–832. https://doi.org/10.1130/G20580.1

Kaminski, M.A., Gradstein, F.M., 2005. Atlas of Paleogene cosmopolitan deep-water agglutinated foraminifera. Grzybowski Foundation Special Publication, 10, 547 pp.

Košťák, M., Schlögl, J., Culkac, A., Tomašových, A., Mazucha, M., Hudáčková, N., 2018. The unique preservation of Sepia soft tissues in the Miocene deposits Serravallian, Vienna Basin: Implications for the origin of microbodies in the fossil record. Palaeogeography Palaeoclimatology Palaeoecology, 493, 111–118. https://doi.org/10.1016/j.palaeo.2018.01.005

Koubová, I., Hudáčková, N., 2010. Foraminiferal successions in the shallow water Sarmatian sediments from the MZ 93 borehole (Vienna Basin, Slovak part). Acta Geologica Slovaca. 2, 1, 47–58

Kouwenhoven, T.V., Van der Zwaan, G.J., 2006. A reconstruction of late Miocene Mediterranean circulation patterns using benthic foraminifera. Palaeogeography, Palaeoclimatology, Palaeoecology, 238(1–4), 373–385. https://doi.org/10.1016/j.palaeo.2006.03.035

Kováč, M., Baráth, I., Harzhauser, M., Hlavatý, I., Hudáčková, N., 2004. Miocene depositional systems and sequence stratigraphy of the Vienna Basin. Courier des Forschungs-Instituts Senckenberg, 246, 187–212.

Kováč, M., Márton, E., Oszczypko, N., Vojtko, R., Hók, J., Králiková, S., Plašienka, D., Klučiar, T., Hudáčková, N., Oszczypko-Clowes, M., 2017 Neogene palaeogeography and basin evolution of the Western Carpathians, Northern Pannonian domain and adjoining areas. Global and Planetary Change, 155, 133–154. https://doi.org/10.1016/j.gloplacha.2017.07.004

Kováč, M., Halásová, E., Hudáčková, N., Holcová, K., Hyžný, M., Jamrich, M., Ruman, A., 2018. Towards better correlation of the Central Paratethys regional time scale with the standard geological time scale of the Miocene Epoch. Geologica Carpathica, 69(3), 283–300. https://doi.org/10.1515/geoca-2018-0017

Kováčová, P., Hudáčková, N., 2009. Late Badenian foraminifers from the Vienna Basin Central Paratethys: stable isotope study and paleoecological implications. Geologica Carpathica, 60(1), 59–70. https://doi.org/10.2478/ v10096-009-0006-3

Kreutzer, N., 1992. Matzen Field – Austria. Vienna Basin. A field study for the Treatise of Petroleum Geology. American Association of Petroleum Geologists, Tulsa, 57–97.

Kreutzer, N., 1993. Das Neogen des Wiener Beckens. In: Brix, F. Schultz, O. (Eds.), Erdöl und Erdgas in Österreich. Naturhistorisches Museum Wien und F. Berger, Horn., pp. 232–248.

Kreutzer, K., Hlavatý, V., 1990. Sediments of the Miocene mainly Badenian in the Matzen area in Austria and in the southern part of the Vienna Basin in Czechoslovakia. In: Minart´íková, D., Lobitzer, H. (Eds.), Thirty years of geological cooperation between Austria and Czechoslovakia. UUG, Praha, pp. 110–123.

Kröll, A., Wessely, G., 1993. Strukturkarte - Basis der tertiären Beckenfüllung 1:200.000. Erläuterung zu den Karten über den Untergrund des Wiener Beckens und der angrenzenden Gebiete. Geologische Bundesanstalt, Wien.

Lee, E.J., Wagreich, M., 2017. Polyphase tectonic subsidence evolution of the Vienna Basin inferred from quantitative subsidence analysis of the northern and central parts. International Journal of Earth Sciences, 106, 687–705. https://doi.org/10.1007/s00531-016-1329-9

Linder, A., Berchtold, W., 1976. Statistische Auswertung von Prozentzahlen: Probit-und Logitanalyse mit EDV, Stuttgart: Birkhäuser, 232 pp.

Loeblich, A.R., Tappan, L., 1987. Foraminiferal genera and their classification. Van Nostrand Reinhold Company Inc., New York, 2 vols, 847 plates, 970 pp.

Mandic, O., 2004. Foraminiferal paleoecology of a submarine swell – the Lower Badenian (Middle Miocene) of the Mailberg Formation at the Buchberg in the Eastern Alpine Foredeep: initial report. Annalen des Naturhistorischen Museums Wien 105A, 161–174.

Mandic, O., Sant, K., Kallanxhi, M.-E., Ćorić, S., Theobalt, D., Grunert, P., De Leeuw, A., Krijgsman, W., 2019. Integrated bio-magnetostratigraphy of the Badenian reference section Ugljevik in southern Pannonian Basin - implications for the Paratethys history (middle Miocene, Central Europe). Global and Planetary Change, 172, 374–395. https://doi.org/10.1016/j.gloplacha.2018.10.010

Mărunţeanu, M., 1999. Litho- and biostratigraphy (calcareous nannoplankton) of the Miocene deposits from the Outer Moldavides. Geologica Carpathica, 50(4) 313–324.

Miller, K.G., Baluyot, R., Wright, J.D., Kopp, R.E., Browning, J.V., 2017. Closing an early Miocene astronomical gap with Southern Ocean $\delta^{18}O$ and $\delta^{13}C$ records: Implications for sea level change, Paleoceanography, 32, 600–621, https://doi.org/10.1002/2016PA003074

Miller, K.G., Browning, J.V., Schmelz, W.J., Kopp, R.E., Mountain, G.S., Wright, J.D., 2020. Cenozoic sea level and cryospheric evolution from deep-sea geochemical and continental margin records. Science Advances 6: eaaz1346. https://doi.org/10.1126/sciadv.aaz1346

Miller, K.G., Mountain, G.S., Wright, J.D., Browning, J.V., 2011. A 180-million-year record of sea level and ice volume variations from continental margin and deep-sea isotopic records. Oceanography 24(2), 40–53. https://doi.org/10.5670/oceanog.2011.26

Milker, Y., Schmiedl, G., 2012. A taxonomic guide to modern benthic shelf foraminifera of the western Mediterranean Sea. Palaeontologia Electronica, 15(2), 1–134. https://palaeo-electronica.org/content/pdfs/271.pdf

Murray, J. W., Alve, E., Jones, B.W., 2011. A new look at modern agglutinated benthic foraminiferal morphogroups: their value in palaeoecological interpretation. Palaeogeography, Palaeoclimatology, Palaeoecology, 309(3–4), 229–241.

Nehyba, S., Holcová, K., Gedl, P., Doláková N., 2016. The Lower Badenian transgressive-regressive cycles—a case study from Oslavany (Carpathian Foredeep, Czech Republic). Neues Jahrbuch für Geologie und Paläontologie, 279, 209–238. https://doi.org/10.1127/njgpa/2016/0548

Oszczypko, N., Oszczypko-Clowes, M., 2012. Stages of development in the Polish Carpathian Foredeep Basin. Central European Journal of Geosciences, 4: 138–162. https://doi.org/10.2478/s13533-011-0044-0

Palzer-Khomenko, M., Wagreich, M., Kallanxhi, M.E., Soliman, A., Knierzinger, W., Meszar, M.E., Gier, S., 2018. Facies, palaeogeography and stratigraphy of the lower Miocene Traisen Formation and Wildendurnbach Formation (former “Oncophora Beds”) in the Molasse Zone of Lower Austria. Austrian Journal of Earth Sciences, 111(1), 75–91. https://doi.org/10.17738/ajes.2018.0006

Papp, A., Rögl, F., Seneš, J., 1973. M2, Ottnangien: Die Innviertler, Salgotarjaner, Bantapusztaer Schichtengruppe und die Rzehakia Formation. Chronostratigraphie und Neostratotypen: Miozän der zentralen Paratethys. Verlag der Slowakischen Akademie der Wissenschaften, 3, 841 pp.

Peryt, D., 2013. Foraminiferal record of marine transgression during deposition of the Middle Miocene Badenian evaporites in Central Paratethys (Borków section, Polish Carpathian Foredeep). Terra Nova 25, 298–306. https://doi.org/10.1111/ter.12036

Peryt, T.M., 2006. The beginning, development and termination of the Middle Miocene Badenian salinity crisis in Central Paratethys. Sedimentary Geology, 188, 379–396. https://doi.org/10.1016/j.sedgeo.2006.03.014

Peryt, T.M., Poberezhskyy, A.V., Jasionowski, M., Peryt, D.,Petrychenko, O.Y., Lyzun, S.O., Turchinov, I.I., 2004. Korelat-siya badeńskikh sulfatnykh vikladiv Naddnistrov'ya. Geologia iGeokhimia Horyuchykh Kopalyn, 56–69.

Pezelj, Đ., Mandic, O., Ćorić, S., 2013. Paleoenvironmental dynamics in the southern Pannonian Basin during initial Middle Miocene marine flooding. Geologica Carpathica, 6, 81–100.

Phipps, M.D., Kaminski, M.A., Aksu, A.E., 2010. Calcareous benthic foraminiferal biofacies along a depth transect on the southwestern Marmara shelf (Turkey). Micropaleontology, 377–392. https://doi.org/10.2307/40959490.

Piller, W.E., Harzhauser, M., Mandic, O., 2007. Miocene Central Paratethys stratigraphy - current status and future directions. Stratigraphy, 4, 2(3), 151–168. https://doi.org/0.1016/j.palaeo.2007.03.031

Pivko, D., Hudáčková, N., Hrabovský, J., Sládek, I., Ruman, A., 2017. Palaeoecology and sedimentology of the Miocene marine and terrestrial deposits in the “Medieval Quarry” on Devínska Kobyla Hill (Vienna Basin). Geological Quarterly, 61(3), 549–568.

R Development Core Team, 2005. R: a language and environment for statistical computing. R Foundation for Statistical Computing, Vienna, Austria, www.R-project.org.

Rasmussen, T.L., (2005). Systematic paleontology and ecology of benthic foraminifera from the Plio-Pleistocene Kallithea Bay section, Rhodes, Greece. Cushman Foundation Special Publication, 39, 53–157.

Rögl, F., Spezzaferri. S., 2003. Foraminiferal paleoecology and biostratigraphy of the Mühlbach section. Gaindorf Formation, Lower Badenian, Lower Austria. Annalen des Naturhistorischen Museums in Wien, 104A, 23–75.

Rögl, F., Ćorić, S., Hohenegger, J., Pervesler, P., Roetzel, R., Scholger, R., Spezzaferri, S., Stingl, K., 2007. The Styrian Tectonic Phase – A series of events at the Early/Middle Miocene boundary revised and stratified (Styrian Basin, Central Paratethys). Joannea Geologie, Paläontologie, 9, 89–91.

Royden, L.H., 1985. The Vienna Basin: a thin-skinned pullapart basin. In: Biddle, K., Christie-Blick, N. (Eds.), Strike Slip Deformation, Basin Formation and Sedimentation. Society of Economics Palaeontologists and Mineralogists Special Publication, 37, pp. 319–338. https://doi.org/10.2110/pec.85.37.0319

Royden, L.H., 1988. Late Cenozoic tectonics of the Pannonian basin system. In: Royden, L.H., Horvath, F. (Eds.), The Pannonian Basin – A Study in Basin Evolution. American Association of Petroleum Geologists Memoir, 45, pp. 27–48. https://doi.org/10.1306/M45474C3

Ruman, A., Hudáčková, N., 2015. Middle Miocene chitons (Polyplacophora) from the Slovak part of the Vienna Basin and the Danube Basin (Central Paratethys), Acta Geologica Slovaca, 7, 2, 155–173.

Rupp, C., 1986. Paläoökologie der Foraminiferen in der Sandschalerzone Badenien, Miozän des Wiener Beckens. Beiträge zur Paläontologie von Österreich, 12, 180 pp.

Rupprecht, B.J., Sachsenhofer, R.F., Zach, C., Bechtel, A., Gratzer, R., Kucher, F., 2019. Oil and Gas in the Vienna Basin: hydrocarbon generation and alteration in a classical hydrocarbon province. Petroleum Geoscience, 25, 3–29. https://doi.org/10.1144/petgeo2017-056

Salcher, B.C., Meurers, J., Smit, J., Decker, K., Hölzel, M., Wagreich, M., 2012. Strike-slip tectonics and Quaternary basin formation along the Vienna Basin fault system inferred from Bouguer gravity derivatives. Tectonics, 31, TC3004, https://doi.org/10.1029/2011TC002979

Sant, K., Palcu, D., Mandic, O., Krijgsman, W., 2017. Changing seas in the Early–Middle Miocene of Central Europe: a Mediterranean approach to Paratethyan stratigraphy. Terra Nova, 29, 273–281 https://doi.org/10.1111/ter.12273

Sant, K., Palcu, D.V., Turco, E., Di Stefano, A., Baldassini, N., Kouwenhoven, T., Kuiper, K.F., Krijgsman, W., 2019. The mid-Langhian flooding in the eastern Central Paratethys: integrated stratigraphic data from the Transylvanian Basin and SE Carpathian Foredeep. International Journal of Earth Sciences, 108(7), 2209–2232. https://doi.org/10.1007/s00531-019-01757-z

Schmid, H.P., Harzhauser, M., Kroh, A., 2001. Hypoxic Events on a Middle Miocene Carbonate Platform of the Central Paratethys Austria, Badenian, 14 Ma. Annalen des Naturhistorischen Museums in Wien, 102A, 1–50.

Schütz, K., Harzhauser, M., Rögl, F., Ćorić, S., Galović, I., 2007. Foraminifera and Phytoplankton from the Lower Sarmatian of the Southern Vienna Basin (Petronell, Lower Austria). Jahrbuch der Geologischen Bundesanstalt, 147(1–2), 449–488.

Sen Gupta, B., Smith, L.E., Machain-Castillo, M.L., 2009. Foraminifera of the Gulf of Mexico. In: Felder, D.L., Camp, D.K. (Eds.), Gulf of Mexico–Origins, Waters, and Biota. Biodiversity. Texas A and M Press College Station, Texas pp. 87–129.

Sgarrella, F., Moncharmont Zei, M., 1993. Benthic foraminifera of the Gulf of Naples (Italy): systematics and autoecology. Bollettino della Società Paleontologica Italiana, 32(2), 145–264.

Siedl, W., Strauss, P., Sachsenhofer, R.F., Harzhauser, M., Kuffner, T., Kranner, M., 2020. Revised Badenian (middle Miocene) depositional systems of the Austrian Vienna Basin based on a new sequence stratigraphic framework. Austrian Journal of Earth Sciences, 113(1), 87–110. https://doi.org/10.17738/ajes.2020.0006

Spezzaferri, S., Tamburini, F., 2007. Paleodepth variations on the Eratosthenes Seamount Eastern Mediterranean: sea level changes or subsidence? eEarth Discuss, 2, 115–132. https://doi.org/10.1029/2004PA001071

Stille, H., 1924. Grundfragen vergleichender Tektonik. Borntraeger, Berlin, 443 pp.

Strauss, P., Harzhauser, M., Hinsch, R., Wagreich, M., 2006. Sequence stratigraphy in a classic pull-apart basin Neogene, Vienna Basin. A 3D seismic based integrated approach. Geologica Carpathica, 57(3), 185–197.

Van der Zwaan, G.J., Jorissen, F.J. Stigter, H.C., 1990. The depth dependency of planktonic/benthic foraminiferal ratios: constrains and applications. Marine Geology, 95, 1–16.

Weissenbäck, M., 1995. Ein Sedimentationsmodell für das Unter- bis Mittelmiozän Karpatien-Badenien des zentralen Wiener Beckens. Dissertation am Geologischen Institut der Universität Wien, 154 pp.

Weissenbäck, M., 1996. Lower to Middle Miocene sedimentation model of the central Vienna Basin. in: Wessely, G., Liebl, W., (Eds.): Oil and Gas in alpidic thrustbelts and basins of Central and Eastern Europe. European Association of Geoscientists and Engineers EAGE, Special Publications 5, pp. 355–363.

Wessely, G., 1988. Structure and Development of the Vienna Basin in Austria. In: Royden, L.H., Horvath, F., (Eds.), The Pannonian System. A study in basin evolution. American Association Petroleum Geologists Memoir, 45, 333–346.

Wessely, G., 2006. Niederösterreich. Geologie der Österreichischen Bundesländer. Geologische Bundesanstalt Wien, 416 pp.

Westerhold, T., Bickert, T., Röhl, U., 2005. Middle to late Miocene oxygen isotope stratigraphy of ODP site 1085 (SE Atlantic): new constrains on Miocene climate variability and sea level fluctuations. Palaeogeography, Palaeoclimatology, Palaeoecology, 217(3–4), 205–222. https://doi.org/10.1016/j.palaeo.2004.12.001

Zlinská, A. Hudáčková, N. Koubová, I., 2010: Lower Sarmatian foraminifera from marginal marine environments in the Malacky vicinity (Vienna Basin). Geologické výzkumy na Moravě a ve Slezsku. 17, 1–2, 104–106.

Zuschin, M., Hohenegger, J., 1998. Subtropical coral-reef associated sedimentary facies characterized by molluscs (Northern Bay of Safaga, Red Sea, Egypt). Facies, 38(1), 229–254.

Zuschin, M., Harzhauser, M., Mandic, O., 2007. The stratigraphic and sedimentologic framework of fine-scale faunal replacements in the Middle Miocene of the Vienna Basin Austria. Palaios, 22, 285–295. https://doi.org/10.2110/palo.2005.p05-023r

Zuschin, M., Harzhauser, M., Hengst, B., Mandic, O., Roetzel, R., 2014. Long-term ecosystem stability in an Early Miocene estuary. Geology, 42, 1–4. https://doi.org/10.1130/G34761.1

Supplementary

Table S4.1

List of all identified foraminiferal species-level taxa, their extant depth limits (gathered of literature) and their relative abundance per sample of all investigated oilfields in alphabetic order.

Table S4.2

Presence/absence data-list of all identified foraminiferal species-level taxa, their extant depth limits (gathered of literature) of the wells Be11 and Rin2.

Table S4.3

List of all identified foraminiferal species-level taxa, their extant depth limits (gathered of literature) of the Karpatian and Ottnangian and their relative abundance per sample of the Mistelbach area in alphabetic order (Data from Harzhauser et al., 2017).

Chapter 5

Trends in temperature, salinity and productivity in the Vienna Basin (Austria) during the early and middle Miocene

Matthias Kranner[1,2*], Mathias Harzhauser[1], Oleg Mandic[1], Philipp Strauss[3], Wolfgang Siedl[3], Werner E. Piller[2]

[1)] Geological-Palaeontological Department, Natural History Museum Vienna, Burgring 7, 1010 Vienna, Austria; mathias.harzhauser@nhm-wien.ac.at; oleg.mandic@nhm-wien.ac.at

[2)] Institute of Earth Sciences (Geology and Palaeontology), NAWI Graz Geocenter, University of Graz, Heinrichstr. 26, 8010 Graz, Austria; werner.piller@uni-graz.at

[3)] OMV Exploration and Production GmbH, Trabrennstraße 6-8, 1020 Vienna, Austria; philipp.strauss@omv.com; wolfgang.siedl@omv.com

*) Corresponding author: matthias.kranner@nhm-wien.ac.at; phone +43 1 52177 255

Abstract

The Neogene Vienna Basin (VB) is a major hydrocarbon reservoir resulting in detailed information from extensive drilling programs. Based on the quantitative analysis of hundreds of foraminiferal samples from 52 drillings, we present the first continuous paleoenvironmental reconstruction of the VB from the early Miocene to the middle Miocene spanning 6.4 million years. Our analyses comprise reconstructions of Sea Surface Temperature (SST), bottom water temperature (BWT), salinity, trophic levels, stress indicators, mode of life, feeding preferences and diversity indices (Fisher α, dominance and equitability) based on a transfer function and applied statistics (e.g., box plots and ternary diagrams). Bottom water temperatures indicate a cooling during the early and middle Badenian (Langhian), which seemingly contradicts the global warming of the Middle Miocene Climate Optimum and a subsequent warming, which contrasts the expected trend following the cooling of the Miocene Climate Transition. Both trends are discussed as result from bathymetric evolution of the VB and intense upwelling during the early and middle Badenian. Repetitive alternations of *Orbulina*-rich assemblages, indicating a warm and stratified waterbody, with globigerinid-dominated assemblages, indicating upwelling and high productivity, are discussed in the light of a yet undescribed waxing and waning of upwelling intensity on a decadal to millennial scale. The applied formula for SST-calculations seems to underestimate real temperatures. Nevertheless, it reveals a distinct warming of about 3°C

from the early to the middle Miocene. In contrast to previous interpretations, we document normal marine conditions from the Ottnangian to the Sarmatian (middle Burdigalian to Serravallian) with a slight increase in salinity during the late Sarmatian.

5.1. Introduction

The Vienna Basin (VB) (Fig. 5.1) is amongst the largest onshore oil and gas provinces of Europe (Hamilton, 2000; Arzmüller et al., 2006; Boote et al., 2018; Rupprecht et al., 2019). Consequently, the VB is one of the most intensely studied Neogene European Basins with thousands of explorative boreholes. Detailed analyses were conducted of numerous drillings by the OMV AG during the last decades (mostly unpublished OMV internal reports). Moreover, the VB is among the key areas for the understanding of the evolution of the Central Paratethys Sea during the early and middle Miocene (e.g., Papp and Steininger, 1978; Harzhauser and Piller, 2004; Kováč et al. 2004; Sant et al. 2017, Harzhauser et al. 2020). The deposits in the VB generally capture its marine history, which lasted from the mid-Burdigalian (Ottnangian) to the Serravallian (Sarmatian) and was succeeded by the lacustrine environments of Lake Pannon during the late Miocene (Tortonian/Pannonian) (Kováč et al. 2004; Harzhauser et al. 2020, Siedl et al. 2020). Sparked by new 3D seismic data and intense paleontological analyses of hundreds of wells, the paleoenvironments and depositional settings of the VB have been recently interpreted by Harzhauser et al. (2019) and Siedl et al. (2020), who provided detailed paleogeographic maps. Based on

Fig. 5.1. Topographic map of the Vienna Basin (white lines represent borders between countries) with the positions of the investigated wells (open circles with well acronyms; see Table 5.2-Supplementary).

these data, Kranner et al. (2021) reconstructed the paleobathymetric evolution of the VB as interplay of global sea level fluctuations and local tectonics.

Foraminifers have been utilized for modern paleoecological interpretations of Vienna Basin deposits only in surprisingly few papers such as Rupp (1986), Piller and Harzhauser (2005), Schütz et al. (2007), Báldi and Hohenegger (2008), Hohenegger et al. (2008), Kováčová et al. (2008), Rupp and Hohenegger (2008), Hyžný et al. (2012), Harzhauser et al. (2017, 2018a, b, 2019) and Kranner et al. (2019, 2021). In addition, Spezzaferri and Ćorić (2001), Rögl and Spezzaferri (2002), Spezzaferri et al. (2002), Mandic (2004), Grunert et al. (2010) and Brzobohatý and Stráník (2012), focused on Ottnangian, Karpatian and Badenian assemblages from the adjacent parts of the North Alpine-Carpathian Foredeep.

Except for Báldi and Hohenegger (2008) and Rupp and Hohenegger (2008), these faunistic interpretations are descriptive and lack statistical analysis based on quantitative data. Most papers focus on biostratigraphy and paleobathymetry (e.g., Harzhauser et al., 2018a), whereas ecological parameters such as salinity, bottom water temperature (BWT), nutrient flux, stress indicators and dissolved oxygen are only briefly discussed. Moreover, all these studies focus on short time slices and restricted geographic areas and differ in their methods, which hampers comparability.

Therefore, we provide the first comprehensive dataset based on hundreds of samples from a NNE to SSW trending succession through the northern and central Vienna Basin, spanning from the late early Miocene (Ottnangian) to the late middle Miocene (Sarmatian). The aim of this task is to quantify the ecological parameters salinity, BWT, bottom water oxygenation and nutrient flux for the time bins Ottnangian (18.1–17.2 Ma), Karpatian (17.2–16.0 Ma), early Badenian (15.8–15.5 Ma), middle Badenian (15.4–13.8 Ma), late Badenian (13.8–12.7 Ma), early Sarmatian (12.7–12.0 Ma) and late Sarmatian (12.0–11.6 Ma) (Fig. 5.2) (ages correspond to time spans, which are represented by deposits).

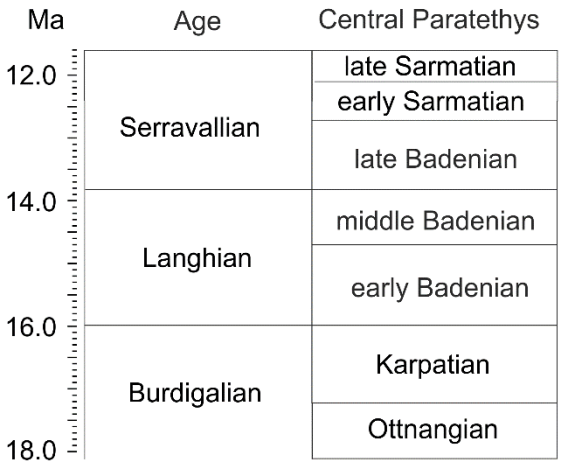

Fig. 5.2. Stratigraphic table showing the correlation of regional Central Paratethyan ages with the international standard scale (after Gradstein et al., 2012 and Harzhauser et al., 2020).

5.2. Geological setting

The Vienna Basin (VB) is an about 200 km long and 55 km wide, rhomboid extensional basin (Royden, 1985; Wessely, 1983, 2006), covering large parts of eastern Austria and extending northwards into the

Czech Republic and eastwards to Slovakia (Kováč et al., 2004; Wessely, 2006). The study area is situated in the Austrian part of the northern and central part of the VB targeting several hydrocarbon production fields roughly arranged in NNE to SSW direction (Fig. 5.1).

The evolution of the Vienna Basin started during the early Miocene as a series of small piggy-back sub-basins on the frontal part of the N- to NW-propagating thrust belt of the Eastern Alps (Jiřiček and Seifert, 1990; Fodor, 1995; Decker, 1996; Lee and Wagreich, 2017). Within these piggy-back basins, marine sedimentation commenced during the mid-Burdigalian (= Ottnangian) (Harzhauser et al., 2019) overlaying Cretaceous to Paleogene Penninic and Austroalpine units with a marked angular unconformity (Hölzel et al., 2010; Kranner et al., 2019). During the late early Miocene, the Vienna Basin become accentuated by the Styrian tectonic phase (Wessely, 2006) and depocenters developed in the northern and central Vienna Basin. During the early Miocene (= piggy-back stage of basin evolution) the VB is referred to as proto-Vienna Basin. Marine sedimentation prevailed in the northern proto-VB during the early Miocene and extended into the S during the middle Miocene. During the middle and late Miocene, the Vienna Basin was embossed by extensional tectonics, due to the lateral extrusion of the Eastern Alps (Royden, 1985, 1988; Fodor, 1995; Decker, 1996; Decker et al., 2005; Hölzel et al., 2008, 2010; Lee and Wagreich, 2016). Consequently, complex fault systems developed, which subdivided the Vienna Basin into a series of horst and graben systems with uplifted blocks at the margins, separated from depressions by major faults (Kröll and Wessely, 1993; Hamilton et al., 2000; Wessely, 2006; Hölzel et al. 2010). Due to these structural elements, the Neogene basin-fill is an important target for hydrocarbon exploration (Hamilton and Johnson, 1999).

5.3. Material and Methods

Three hundred thirteen (313) Miocene samples have been taken from 52 boreholes in the Austrian part of the VB (Fig. 5.1). Micropaleontological analyses with main focus on benthic and planktic foraminifers revealed ~65.000 specimens assigned to 309 species-level taxa. All washed samples were treated with diluted H_2O_2 (12%) for several hours and sieved with tap water through a standard set of sieves (500, 250, 125 and 63 µm) and later on oven dried at 40 °C and split with a microsplitter (as described in Rupp, 1986). For identification of foraminifers several taxonomic monographs and publications were used (e.g.: Papp et al., 1973; Loeblich and Tappan, 1987; Cicha et al., 1998; Rögl and Spezzaferri, 2003; Bubík and Kaminski, 2004; Kaminski and Gradstein, 2005; Bindiu-Haitonic et al., 2017).

Biostratigraphic dating and position within lithostratigraphic units have been established for all samples in Harzhauser et al. (2017, 2020) and are indicated in the Supplementary (Table 5.1).

To obtain paleoecological proxy records univariate statistics were applied and Fisher's Alpha (α) (Fisher et al., 1943), equitability and dominance have been computed for the whole dataset (Fig. 5.3). The Fisher alpha index (α) diminishes the influence of sample size and number of individuals (Murray, 1991) and the Equitability (J) reflects the distribution of species within the assemblage and expresses the similarity between species contributions (Hammer and Harper, 2007; Murray, 1991). High J values reflect a more even distribution of individuals among taxa present. The Dominance index expresses the dominance of a particular species within a sample. Therefore, D=0 means equally distributed taxa in the sample, whereas D=1 means the complete dominance of one species (Hammer and Harper, 2007). For statistical analyses the software PAST (Paleontological Statistics, version 4.03, Hammer et al. 2001) was used.

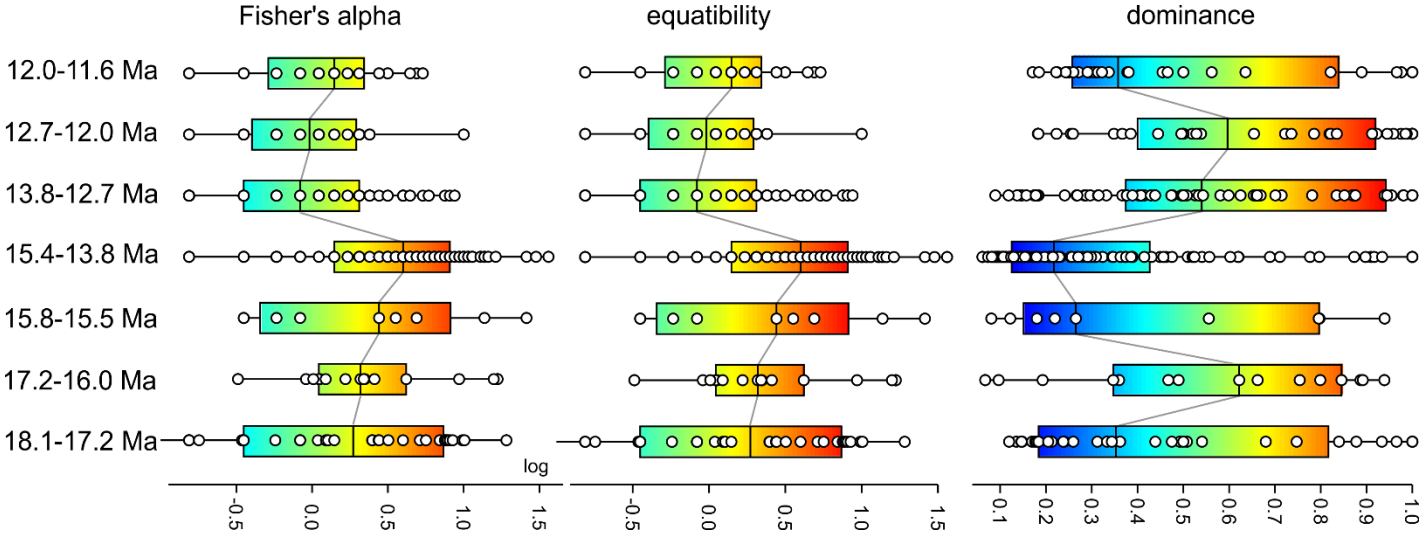

Fig. 5.3. Boxplots illustrating the evolution of diversity indices (Fisher´s Alpha, equitability and dominance) during the early and middle Miocene in the proto-VB and VB. Calculations are based on abundance data of benthic foraminifers.

Ecological ranges of extant foraminifers were gathered from numerous publications to determine the ecological parameters salinity, bottom and surface water temperature, preferred feeding strategies (deposit, suspension and herbivore feeding), preferred mode of life (infaunal, epifaunal, semi-infaunal), nutrient availability (based on trophic desiderata of planktonic foraminifers) and stress tolerance (based on benthic foraminifers and their tolerance to oxic, salinity and nutrient stress; e.g.: Murray, 1991, 2006; Sgarrella and Moncharmont Zei, 1993; Altenbach et al., 2003; Hohenegger, 2005; Kaminski and Gradstein, 2005; Rasmussen, 2005; Bicchi et al., 2006; Spezzaferri and Tamburini, 2007; Hohenegger et al., 2008; Sen Gupta et al., 2009; Phipps et al., 2010; Milker and Schmiedl, 2012; Holcová et al., 2015, 2018; Székely et al., 2017; Ilies et al., 2020).

Some important foraminifers for paleoenvironmental reconstruction are illustrated in Fig. 5.4 A–Q.

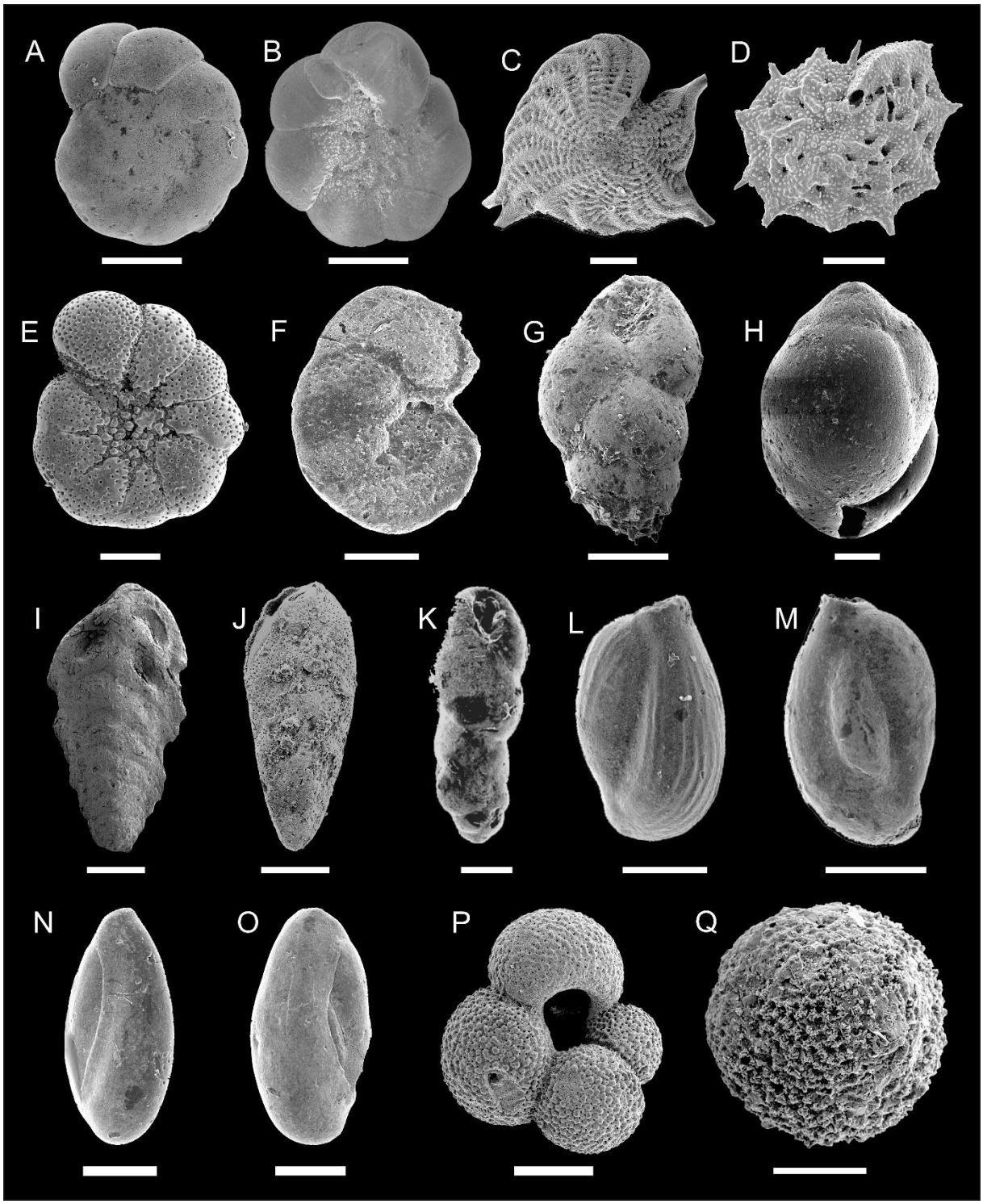

Fig. 5.4. Important foraminifers for ecological interpretations. **A**–**B**: *Ammonia beccarii* (Linne, 1758); **C**: *Elphidium reginum* (d'Orbigny, 1846); **D**: *Elphidium aculeatum* (d'Orbigny, 1846); **E**: *Porosononion granosum* (d'Orbigny, 1846); **F**: *Lobatula lobatula* Walker and Jacob, 1798; **G**: *Bulimina subulata* (Cushman and Parker, 1937); **H**: *Praeglobobulimina pyrula* (d'Orbigny, 1846); **I:** *Spirorutilus carinatus* (d'Orbigny, 1846); **J**: *Bolivina dilatata* Reuss, 1850; **K**: *Bulimina elongata* d'Orbigny, 1826; **L**–**M**: *Cycloforina fluviata* (Venglinsky, 1958); **N**–**O**: *Pseudotriloculina consobrina* (d'Orbigny, 1846); **P**: *Globigerina bulloides* d'Orbigny, 1826; **Q**: *Orbulina suturalis* Brönnimann, 1951

Scale bar = 100 μm.

5.3.1. Salinity, bottom water temperature (BWT) and sea surface temperature (SST)

Range values for salinity, BWT (based on benthos) and sea surface temperature (based on planktic foraminifers) have been used as limits in the calculations after Hohenegger (2005) and Báldi and Hohenegger (2008) with following formulas:

First the gradient value is calculated with:

$$\sqrt{\frac{\sum_{j=1}^{m} l_j a_j d_j^{-1}}{\sum_{j=1}^{m} a_j d_j^{-1}}}$$

Where l_j stands for the location parameter represented by the arithmetic mean ($\frac{x_{j\,min}+x_{j\,max}}{2}$), whereas the weighting factor d_j in this equation was calculated with ($x_{j\,max} - x_{j\,min}$) and a_j represents the abundance of the species. This is than applied in the dispersion (σ_g) formula:

$$\left(\sqrt{\frac{\sum_{j=1}^{m}\left(l_j - g\right)^2 d_j^{-1}}{\sum_{j=1}^{m} d_j^{-1}}}\right)^{1/2}$$

Which leads to the calculated salinity or BWT or SST (depending on the used parameter) using a 95% confidence interval (Y=95%, see Zar, 1999):

$$g_{-}^{+} t_{\frac{1-\mathrm{Y}}{2},\mathrm{n}-1}\sqrt{\sigma_g^2/m}$$

Salinity, BWT and SST values are illustrated as box plot through time (Figs 5–6).

5.3.2. Mode of life, feeding strategies and oxygenation

To determine the mode of life, feeding strategies and oxygenation of benthic foraminifers, data were transferred to percentages per sample and plotted in a ternary diagram, combined with a density map, after their gathered preferences (Figs 7–8). To obtain oxygen values, benthic foraminifers were grouped into three categories, oxic (1.5–6.0 ml/l), suboxic (0.3–1.5 ml/l) and dysoxic (0.1–0.3 ml/l).

5.3.3. Trophic level

The trophic level was plotted in a ternary diagram (Fig. 5.9), the same way as oxygenation, feeding strategies and mode of life but using planktic foraminifers.

5.4. Results

All identified species and their relative abundance per sample (including full well names) are given in the Supplementary, Table 5.1. Herein, we describe the ecologically relevant results ordered within their assigned stratigraphic age from oldest to youngest.

5.4.1. Ottnangian

36 samples are assigned to the Ottnangian. The majority of samples indicates suboxic and eutrophic to mesotrophic conditions (Figs 7, 9), predominated by infaunal herbivores (mean: 56%). Oxic conditions are correlated with abundant epifaunal species (mean: 31%).

Some samples show moderate abundances of deposit feeders and high abundances of suspension feeders (Be4/2347.5, 2414; Ah1/520; GI2/1084; Ka2/1020; Mi1/1373.5; MtW1/1130, 1380, 1480).

Stress markers are rarely found in Ottnangian samples and usually do not exceed 5% of the faunal composition (Fig. 5.5). All samples were of marine origin (33–36 PSU, Fig. 5.5). The BWT ranges from 10–18°C with a mean temperature of about 13°C (Fig. 5.6).

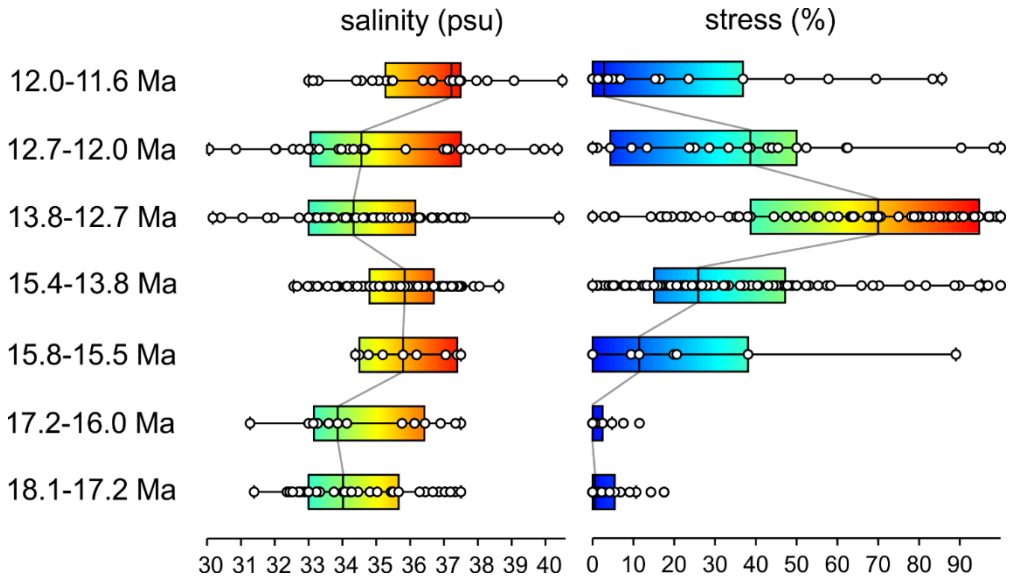

Fig. 5.5. Boxplots illustrating the evolution of salinity (PSU) and stress (%) during the early and middle Miocene in the proto-VB and VB. Calculations are based on abundance data of benthic and planktic foraminifers and the formulas of Hohenegger (2005) and Báldi and Hohenegger (2008).

Samples did not contain sufficient numbers of planktic foraminifers to calculate reliable SST levels for the Ottnangian.

Fisher α values of the Ottnangian samples show a mean value of 3.7 but vary considerably from sample to sample. 14 values lie between 0 and 0.8, whereas 12 samples show values >5 (Fig. 5.3).

Dominance and Equitability levels (Fig. 5.3) fluctuate considerably from sample to sample with a mean of 0.6 (J) and 0.5 (D). Samples Bo3/2172.7; Bo8/1900, 2000; Ma269/2715 and Ka2/1380 are completely dominated by a single species (D=1) and six other samples (Span8/2640; Ma269/2315, 2677; Ah1/460;

Ka2/1080 and Mi1/1373.5) show dominance values >0.6. Samples with low dominance values show high equitability levels (mean of 0.8).

5.4.2.Karpatian

The 16 Karpatian samples indicate oligotrophic conditions (Fig. 5.9) with suboxic to low oxic assemblages (mean: 89%) with predominantly shallow infaunal herbivore species (Fig. 5.7).

All samples yielding foraminifers show marine PSU values from 31–38 (Fig. 5.5). The BWT shows a mean value of 15°C and varies from 7–18°C (Fig. 5.6). Nearly no stress indicators could be detected within the samples (11% within Ah1/310, other samples 0–8%; Fig. 5.5). Planktic foraminifers are scarce and do not allow reliable SST calculations.

The mean Fisher α value of the Karpatian samples is 4.2 (Fig. 5.3). The majority of the samples shows values between 1.0–4.2. Two samples (Ka1/500 and 795) display values lower than 1, whereas 3 samples show high numbers (Ah1/250 with 9.3, 280 with 16.3 and 819 with 15.8). Eight samples display high dominance values >0.6 (Hrd25/740; Ka1/500, 550, 701, 750, 795, 895 and Si3/1250). Consequently, samples Ah1/250, 280, 310 and Hrd19/819) have high J values over 0.6 with low D values <0.36.

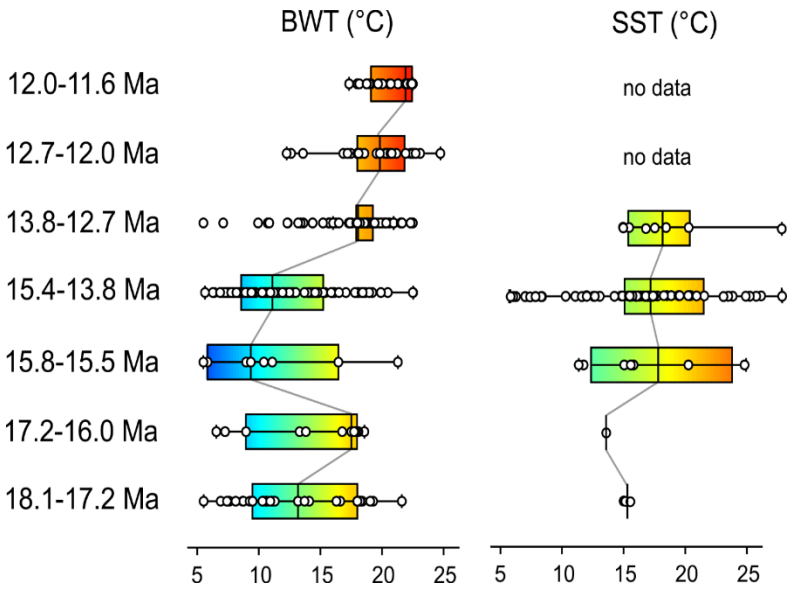

Fig. 5.6. Boxplots illustrating the evolution of bottom water temperature (BWT) and sea surface temperature (SST) during the early and middle Miocene in the proto-VB and VB. Calculations are based on abundance data of benthic and planktic foraminifers and the formulas of Hohenegger (2005) and Báldi and Hohenegger (2008).

5.4.3. Early Badenian

Nine samples represent the early Badenian, suggesting prevailing oligo- to mesotrophic conditions (Fig. 5.9). The ternary diagram (Fig. 5.7) reveals more variation concerning oxygenation, mode of life and food preferences compared to the Ottnangian and Karpatian samples. Samples Pir5/2043.6, Pir5/2059 and MueT1/2480 contain 89–100% suboxic indicators and sample MueT1/2737 is also dominated by suboxic indicators (55%). Only two samples contain considerable amounts of dysoxic indicators (Ad78/1829: 45%, Rab10/2374.1: 61%) and oxic indicators are dominant in samples Ma112/1620 and Man1/2570. Epifaunal species predominate nearly all samples (up to 97%) accompanied by deep infaunal ones (up to 38%) except for sample MueT1/2480, which contains 89% shallow infaunal species.

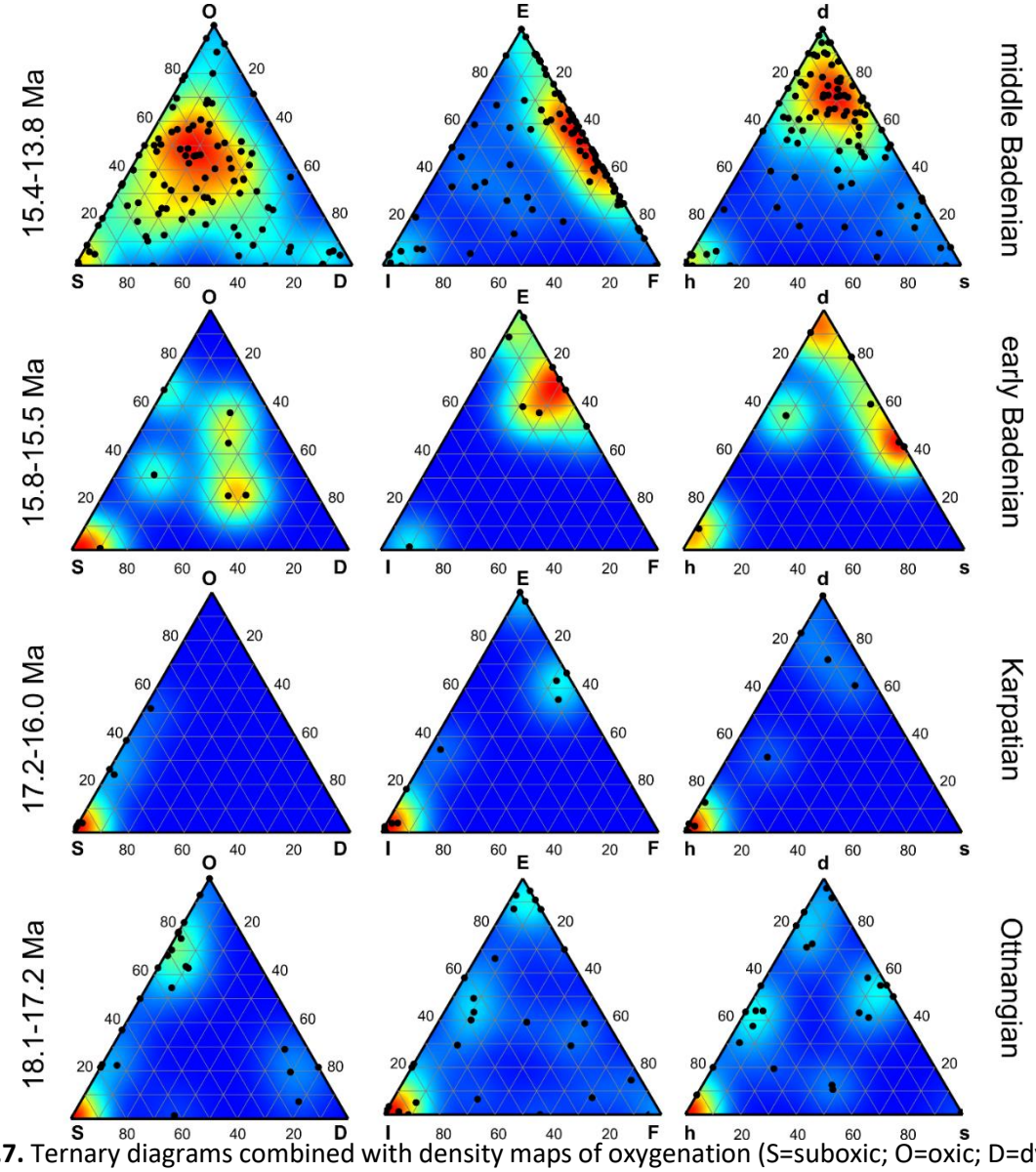

Fig. 5.7. Ternary diagrams combined with density maps of oxygenation (S=suboxic; O=oxic; D=dysoxic) and preferred mode of life (I=shallow infaunal; E=epifaunal; F=deep infaunal) and feeding strategies (h=herbivore; d=deposit; s=suspension) using abundance values of benthic foraminifers; Ottnangian to middle Badenian.

Three samples contain high numbers of suspension feeders (Ad78/1829: 36%, Man1/2570: 57%, MueT1/3127: 54%). Samples MueT1/2480 (89%) and MueT1/2737 (36%) show significant numbers of herbivores, the other samples yield mostly deposit feeders.

PSU values for all samples vary from 35–37 and the mean BWT is 11°C (varying from 5.5–21°C; Fig. 5.5, 6). Four samples indicate high stress (Ad78/1829, MueT1/2737, MueT1, 2127, Rab10/2374.1: 11–38%) and sample MueT1/2480 is even dominated by stress markers (89%; Fig. 5.5).

Calculations using planktic foraminifers showed a mean SST of 17.7°C (±2.9; Fig. 5.6).

Four samples show low Fisher α values (≤0.8), three samples (Ad78/1829; MueT1/2480 and Rab10/2374.1) display values from 2.8–4.9 and two show high values (MueT1/2737 with 26 and 3127 with 13.7; Fig. 5.3).

Dominance levels of samples Ma112/1620, MueT1/2480, Pir5/2043.6 and 2059 are higher than 0.55, whereas the others are below 0.3. Except for samples MueT1/2480, Pir 5 2043.6 and Pir 2059 the equitability levels are higher than 0.6 (Fig. 5.3).

5.4.4. Middle Badenian

101 samples were collected from middle Badenian deposits, revealing a broad range of trophic levels with a slight tendency to eutrophic conditions, mixed with mesotrophic conditions and some samples that point to more oligotrophic conditions (Fig. 5.9). The broad range is also indicated for the other parameters (Figs 4–7). Hence, a rather balanced relation between oxic indicators (34.3%), suboxic (41.3%) and dysoxic (24.4%) is recorded although strong fluctuations are obvious for certain samples (e.g., 95% oxic indicators in Zw8/1480, 90% dysoxic indicators in Zw4/1325 and 99% suboxic indicators in Rab2/1615). Most of the fauna consists of deposit feeders that lived either epifaunal or deep infaunal.

PSU values range from 30 to 43 with a mean of 36 and the mean BWT is about 12°C (varying from 6–23°C). Stress markers are dominating in some samples (e.g., Bo8/1700, 1740; Pir5/1995.6, Rab2/1525, 1565, 1615, 1695 and 1715 with 70–95%) but only on average stress markers attain about 33% (Fig. 5.5).

The SST based on planktic foraminifers has ranges around 17.9 °C (±0.7; Fig. 5.6).

The mean Fisher α value (Fig. 5.3) during the middle Badenian is 5.7 with major fluctuations spanning from 0.2 and 36.3. 18 samples (Ma111/1663; Ma125/1482, 1645; Man1/2296, 2340; Mue100/1745, 1980; Mue110/1803; Pir5/1956, 1995.6, 2007.6; Rab1/1640; Rab2/1460, 1525, 1695; Rin3/4124;

Schw1/1650 and Zw8/1480) have values below 1. 15 samples (Ad78/1500; Be7/1900; Him1/1695; Ma126/1665, 1695; Mue100/1980; Rab2/2010, 2050, 2191; Schw1/1825; Str1/1750; Wit1/1900, 2146, 2291 and Zw8/1710) have values ≥10. Three samples are completely dominated by a single species (D=1; Ma125/1645; Man1/2296 and Pir5/1956) and 12 other samples show high dominance values exceeding 0.6 (Be4/2141; Be6/2091; Mue100/1980; Pir5/1995.6; Rab2/1525, 1565; 1615, 1695, 1715; Schw1/1650; Zw4/1325 and Zw8/1480) with relatively low J values (not exceeding 0.4), except Mue100/1980 which hast an equitability value of 0.8. All other samples have relatively high J values (higher than 0.5) with a mean of 0.8 (Fig. 5.3).

5.4.5. Late Badenian

89 samples represent the late Badenian. Trophic levels vary considerably from sample to sample. Some indicate eutrophic, some oligotrophic and some mesotrophic conditions (Fig. 5.9). The ternary plots of benthic foraminifers (Fig. 5.8) show mostly shallow infaunal suboxic herbivores with some samples yielding high numbers of deep infaunal sub-dysoxic deposit feeders (e.g., Bo8/1676 and Str1/1550).

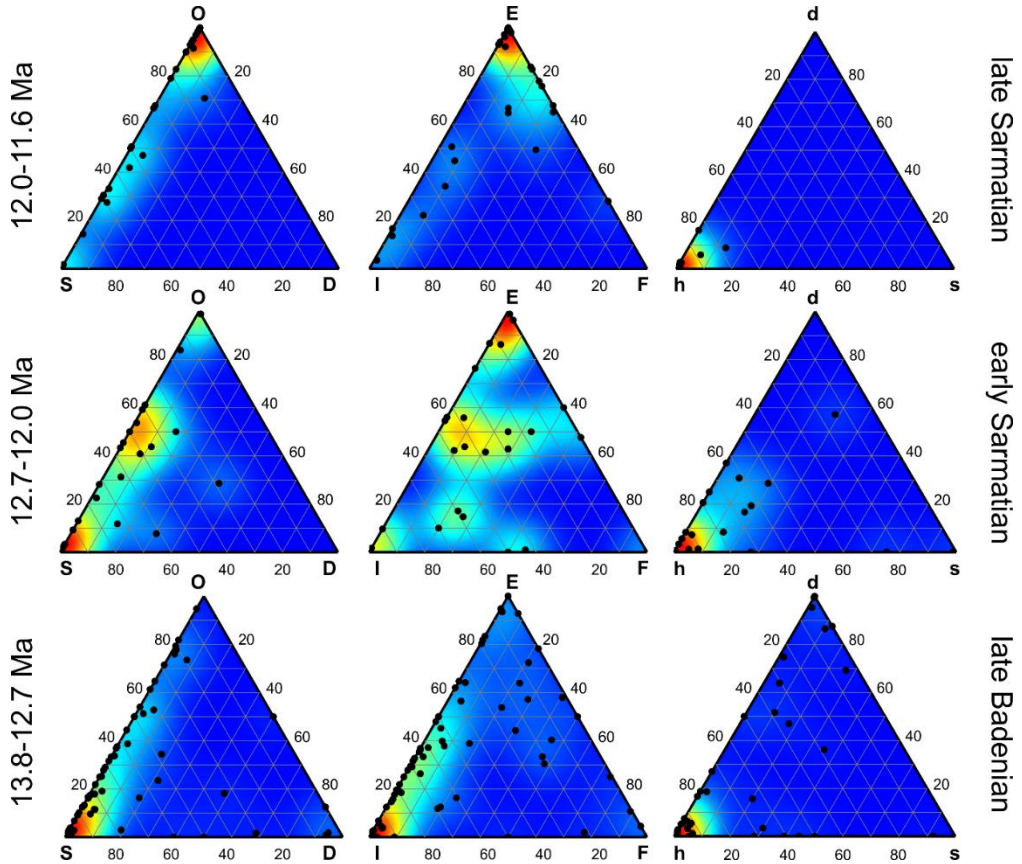

Figure 5.8. Ternary diagrams combined with density maps of oxygenation (S=suboxic; O=oxic; D=dysoxic) and preferred mode of life (I=shallow infaunal; E=epifaunal; F=deep infaunal) and feeding strategies (h=herbivore; d=deposit; s=suspension) using abundance values of benthic foraminifers; late Badenian to late Sarmatian.

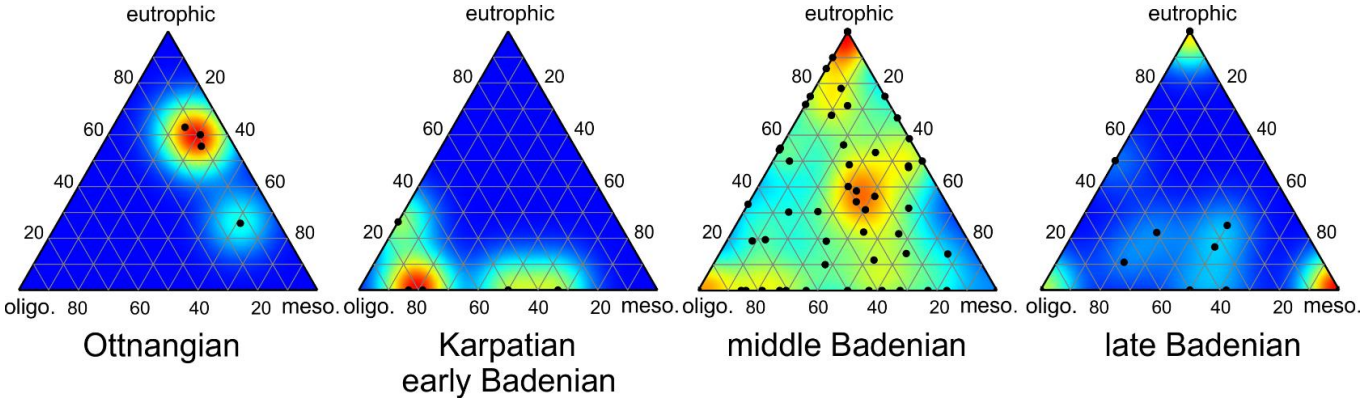

Figure 5.9. Ternary diagrams combined with density maps of trophic levels (oligo-, meso- and eutrophic) based on abundance values of planktic foraminifers, separated in time slices.

PSU values vary from 31–40 with the mean of 35 (Fig. 5.5). The calculated mean BWT is 18°C varying from 7–23°C (Fig. 5.6).

During the late Badenian stress markers are dominating most of the samples with a mean average of 65% throughout the succession (Fig. 5.5).

SST reconstruction resulted in a mean average of 18.2 °C (±1.0; Fig. 5.6).

The mean Fisher α value (Fig. 5.3) of the late Badenian is 1.6 with variations from 0.2–8.7. Fifteen samples (BeS3/1599.5; Bo8/1676; Ma111/1368, 1490; Ma112/1317; Ma127/1451; Ma269/1376; Man1/2128; Mue77/1234, 1343; Rab1/700, 1060, 1355; Str1/1550 and Span10/1540) exceed values more than 3 and 29 samples (Ad78/1350; Be6/1406, 1509; Be7/1429, 1434.5; Bo8/1560; Ma111/1515; Ma125/1255, 1317, 1356, 1405; Ma127/1552; Ma269/1425.8; Palt1/1825, 2140, 2452; Pir5/1939; Rab1/900, 1103.5, 1200, 1495, 1530; Rab11/1977.6, 2026;Rab2/1020, 1050, 1100, 1230 and Schw1/1515) show values between 1 and 2, whereas the remaining 45 samples show values below 1. 18 Samples are completely dominated by one species (D=1; Bo8/1500; Ma126/1510; Mue100/1590, /1615; Palt1/2245; Pir23/1700, 1712, 1770; Pir3/1337; Pir5/1327, 1717, 1722, 1905, 1914, 1922¸Str1/1280; Zw8/1120 and1200) and another 31 samples (Be6/1406, 1509; Bo8/1655; Ma112/1362; Ma125/1250; Ma269/1393.8; Man1/2055; Mue100/1570, 1650; Palt1/1825, 2111, 2382; Pir3/1570; Pir5/1300, 1948.8; Pir23/1782; Rab1/700, 900, 1150, 1290, 1495, 1530; Rab11/1956.37, 1977.6, 2026; Rab2/1020, 1100, 1230; Schw1/1580; Span2/1593 and Span8/1750) show high dominance values >0.5. Five samples (Bo15/2000; Ma111/1420, Ma126/1490, Schw1/1420 and Str1/1440) display two equally distributed species (J=1, D=0.5) and the remaining 35 samples show equitability levels >0.5 with dominance values <0.5 (Fig. 5.3).

5.4.6. Early Sarmatian

30 analyzed samples represent the early Sarmatian. Due to the lack of planktic foraminifers no trophic levels and SST can be calculated.

A slight shift from suboxic (56%) to more oxic (39%) epifaunal indicators could be realized in the ternary diagrams (Fig. 5.8). The mean PSU value is 35 varying from sample to sample from 31–40 (Fig. 5.5) while the BWT shows a mean of 19 °C ranging from 14–25°C (Fig. 5.6). Stress markers are represented with a mean value of 38% (Fig. 5.5), with only three samples dominated by stress indicators (Ad78/1276: 52%; Ma112/1040: 62%, Rab11/1859: 98%).

The mean Fisher α value for the early Sarmatian is 1.6 with variations from 0.2–5.4 (Fig. 5.3). Seven samples (Ma 112/1040; Ma 127/1140; Ma 125/920, 1010; Palt1/1460, 1687and Span 8/1550) show high values >2, whereas 10 (Ad 78/1080, 1303; Bo 15/1669, 1720; Ma 127/1185; Palt1/1790; Pir 5/1255; Rab 11/1859; Span 2/1320 and Span 8/1450) samples have values <1 and the other 12 lie between 1 and 2. Four samples are completely dominated by one species (D=1; Bo 15/1669, 1720; Palt1/1790 and Span 8/1450), another 6 samples (Ad 78/1080, 1303; Rab 11/1848, 1859; Span 8/1380 and 1550) show high dominance values ≥0.6 with corresponding low equitability levels (<0.5). The other samples display relatively high J values (>0.5) with a mean of 0.8. and dominance not exceeding 0.5 (Fig. 5.3).

5.4.7. Late Sarmatian

32 samples cover the late Sarmatian. No trophic levels and SST were calculated because of the lack of planktic foraminifers.

Ternary diagrams (Fig. 5.8) show the complete shift to oxic, epifaunal herbivore dominated faunas.

The mean PSU value is 37, ranging from 33 to 41 (Fig. 5.5) and the mean BWT is 21°C ranging from 17 to 22 °C (Fig. 5.6). Stress markers are represented with about 21% but dominate four samples (Rab10/1000: 95%, Rab11/1360: 83%, Rab11/1580: 96%, Rab2/920: 86%; Fig. 5.5).

Fisher α values of the late Sarmatian vary from 0.2–10 and show a mean of 1.3 (Fig. 5.3). The highest Fisher α values shows sample Zw4/1010, another 15 samples (Palt1/1060, 1210, 1240; Pir5/0765; Rab10/1000; Rab11/1235.75, 1372.36, 1438.92, 1500; Rab2/710, 920; RabW1/1101; Span 2/880, 1000 and Span2/1100) have values from 1.1–2.4, whereas the remaining samples display values <1. Only 2 samples (Bo15/1360 and 1475) are completely dominated by one species but also only 10 samples (Bo15/1530; Palt1/1060, 1300; Rab11/1235.75, 1438.92; Rab2/710, 880, 1000, 1100 and Zw 4/1010) display dominance values <0.5 (Fig. 5.3). Nearly half of the samples (Ad78/0885; Bo15/1360, 1475;

Ma112/0792; Palt1/1240; Pir5/0765; Rab10/1000; Rab11/1202, 1372.36, 1410, 1421.3, 1451.42, 1500; Rab2/920 and RabW1/1101) show low equitability levels <0.5, the others ≥0.6 (Fig. 5.3).

5.5. Discussion

In the following, we discuss all ecological results mentioned above in stratigraphic order, from old to young.

5.5.1. Ottnangian

26 samples derived of the Ottnangian Lužice Fm. from the northern and north-western Vienna Basin (see Supplementary, Table 5.1). These samples were deposited under eutrophic to mesotrophic, suboxic to oxic conditions (Figs 7, 9), which is similar to the results of Harzhauser et al. (2017) for the adjacent Mistelbach Halfgraben. The majority of the assemblage lived epifaunal to shallow infaunal and shows a moderate to high diversity (Fisher α) with high equitability (mean ~0.7) and low dominance levels (Fig. 5.3) pointing to relatively stable conditions.

Relatively cool bottom water conditions prevailed with a mean of 12 °C (Fig. 5.6). This estimate is in agreement to data by Grunert et al. (2010) from the close-by North Alpine-Carpathian Foreland Basin (NACFB). The relatively scarce abundance of planktic foraminifers in the samples impede with a reliable interpretation of SST, but the few available planktic data point to relatively cool SST ~15°C (Fig. 5.6), which agrees with the cool SST results of Grunert et al. (2010) for the NACFB. This temperature regime and the eutrophic to mesotrophic conditions (Fig. 5.9) is in line with slight upwelling conditions, which prevailed in the NACFB (Grunert et al., 2010).

The other 10 Ottnangian samples derived of the Bockfließ Fm. in the central VB. The faunas show much higher dominance values with lower Fisher α and equitability levels than those of the Lužice Fm. All samples display slightly oxic to suboxic conditions (Fig. 5.7) with high nutrient input, indicating close vicinity to the shoreline. The shallower depositional setting correlates with higher BWTs (mean of 17°C) compared to the open marine conditions of the northern VB. These correspond well to the interpretations of Harzhauser et al. (2020) and Kranner et al. (2021), who describe the Bockfließ Fm. as near shore equivalent of the offshore Lužice Fm.

Salinity values decreases slightly from deposits of the open marine Lužice Fm. (mean of 35 PSU; Fig. 5.5) to those of the lagoonal Bockfließ Fm. (mean of 33 PSU; Fig. 5.5) indicating, however, normal marine salinity throughout the Ottnangian in the VB.

Our data suggest similar conditions from the northern part of the proto-VB to those of the adjacent NACFB, with upwelling conditions and consequently cool bottom and surface waters (Grunert et al., 2010), grading into the shallow, nearshore environments of the Bockfließ Fm. of the southern proto-VB.

5.5.2. Karpatian

The Karpatian samples of the northern proto-VB indicate low oxic to suboxic conditions (Fig. 5.7) with an overall moderate to high diversity and higher dominance values than in the Ottnangian (Fig. 5.3). Compared to the Mistelbach Halfgraben (Harzhauser et al., 2017), no indication for upwelling conditions could be detected. The few planktic foraminifers rather indicate oligotrophic conditions (Fig. 5.9). The mean salinity value of 35 PSU (Fig. 5.5) indicates normal marine conditions for all samples yielding foraminifers.

Spezzaferri et al. (2002) reconstructed dysoxic cool to temperate water conditions for the nearby North Alpine-Carpathian Foreland Basin (NACFB) during the Karpatian whereas warm conditions prevailed in the shallow marine estuary of the Korneuburg Basin (Zuschin et al., 2014). Our data suggest BWTs ranging around 17°C (Fig. 5.6) for the proto-VB, which would be in agreement with its rather coastal transitional position between the open marine NACFB and the estuarine Korneuburg Basin and the terrestrial wetlands of the central and southern proto-VB (Harzhauser et al., 2020; Siedl et al., 2020; Kranner et al., 2021).

5.5.3. Early Badenian

Only a limited number of early Badenian samples was available. Therefore, our results must be interpreted with caution. Generally, the samples show oligo-mesotrophic conditions (Fig. 5.9), similarly to the Karpatian but the mean BWT drops severely (~11°C; Fig. 5.6). This temperature estimate is surprising, given that the early Badenian corresponds to parts of the Miocene Climatic Optimum (MCO; Zachos et al., 2001, 2008; Holbourn et al., 2015; Sant et al., 2017; Miller et al., 2020; Westerhold et al., 2020). Coeval assemblages from the adjacent NACFB, however, suggest similar slightly dysoxic and relatively cool bottom water conditions (Rögl and Spezzaferri, 2002). The low BWTs are contrasted by relatively warm SST values with a mean of 17.7 ($\pm$2.9)°C (Fig. 5.6). The drop form the Karpatian to the

early Badenian in BWTs, contrasting the global record, correlates to the deepening of the studied area described by Kranner et al. (2021) and might therefore be more a consequence of this or the limited number of samples.

A part of the samples suggests oxic to suboxic conditions with large amounts of epifaunal herbivores (Fig. 5.7), which point to shallow marine conditions with seagrass meadows as described by Harzhauser et al. (2017) from the adjacent Mistelbach Halfgraben.

All analyzed early Badenian samples indicate normal marine conditions (mean PSU ~ 36; Fig. 5.5) with moderate to high diversity and low dominance levels (Fig. 5.3).

5.5.4. Middle Badenian

A broad range of environmental variables is captured by the large number of samples from the middle Badenian, which suggests heterogenous and manifold marine paleoenvironments with oscillating diversity indices (Fig. 5.3). This is expressed by a rather even distribution of bottom water oxygenation indicators and a mixture of epi- and deep infaunal species (Fig. 5.7). Deposit feeding predominates among the feeding types indicating a high nutrient supply and environments at the lower boundary or even below the photic zone (Murray, 1991, 2006; Armstrong and Brasier, 2005). Nevertheless, herbivores or suspension feeders may account for large parts of the assemblages in some samples (Fig. 5.7). The high abundance of herbivores suggests environments within the photic zone with high abundance of plant nourishment (Murray, 1991, 2006) like seagrass meadows with oxic to suboxic conditions, similar to the reconstructions of Mandic (2004) of the NACFB. These samples may have been transported into deeper environments by storms. High water energy is also in line with the high number of suspension feeders (like *Lobatula lobatula*, Fig. 5.4 F) suggesting strong movement of water masses, like currents (Haward and Haynes, 1967; Dobson and Haynes, 1973; Linke and Lutze, 1993; Semeniuk, 2000; Schönfeld, 2002; Kaminski and Niessen, 2015; Garcia-Gallardo et al., 2017).

The mean SST (17.9 $\pm$0.7°C) and the mean BWT (12°C) are higher during the middle Badenian compared to the early Badenian (Fig. 5.6). This pattern coincides with the final stages of the global Middle Miocene Climatic Optimum (e.g., Zachos et al., 2001, 2008; Holbourn et al., 2015; Miller et al., 2020; Westerhold et al., 2020) as well as with the interpretation of Holcová et al. (2015, 2018), who linked the common presence of *O. suturalis* and the absence of *Praeorbulina* div. sp. with a rise in SST and more eutrophic conditions during the middle Badenian.

About one third of the analyzed samples yields *Orbulina suturalis* (Fig. 5.4 Q) which is most common in warm, stratified water columns with eutrophic conditions (Fig. 5.9) (Bé, 1977; Hemleben et al., 1989;

Schiebel and Hemleben, 2005; Holcová et al., 2015, 2018). In addition, many samples display high abundances of four-chambered globigerinids, such as *G. bulloides* (Fig. 5.4 P)*, G. praebulloides, G. concinna* and *Globigerina* sp., which are characteristic for sub-surface waters with high productivity (Schiebel et al., 1997) and are frequently associated with open-ocean and/or coastal upwelling (Naidu and Malmgren 1996; Kincaid et al. 2000; Mohiuddin et al. 2005; Storz et al. 2009; Holcová et al. 2019).

These differences in the planktic fauna suggests oscillations in the SSTs with concomitant high nutrient flux. Similar oscillations of ecological parameters were observed by Holcová et al. (2015, 2018) and Ilies et al. (2020) for middle Badenian occurrences of the Carpathian Foredeep, the northern Pannonian Basin and the Transylvanian Basin. Ilies et al. (2020) linked these oscillations to seasonal cold currents or upwelling events. Given the resolution of the samples, which cover several years to decades we consider it very unlikely that the difference between *Orbulina*-rich samples versus globigerinid-rich samples can be explained by seasonality. Instead, we assume that a yet undescribed decadal to millennial change of upwelling intensity is responsible for the observed pattern. Changing intensities of upwelling on a sub-Milankovitch scales are documented for the California Current (Chhak and Di Lorenzo, 2007), the northern Canary Current (Santos et al., 2005; Relvas et al., 2009), the Iberian upwelling system (Miranda at al., 2012) and the Benguela upwelling system (Tim et al., 2015) as well as NACFB (Auer et al., 2014, 2015). McGregor et al. (2007) discussed similar fluctuations in presence and intensity of the northwest African upwelling system during the last 2500 years. Typically, wind stress and changes in air temperature with coherent changes in the land-sea-pressure gradients are discussed as important factors influencing upwelling intensity (Santos et al., 2005; McGregor et al., 2007; Miranda et al., 2012; Tim et al., 2015). In addition, decadal-scale basin-wide processes, such as variations in the North Atlantic Oscillation may result in changing upwelling intensities (Santos et al., 2005). The driving forces behind these observations, however, are still poorly known. Even more so, our spotty data do not allow to link the observed pattern with potential forces such as solar cycles.

Upwelling is also indicated by the benthic assemblages, which are dominated by taxa indicating high nutrient availability, like *Spirorutilus carinatus* (Fig. 5.4 I) (Spezzaferri et al., 2002; Ćorić and Rögl, 2004; Grunert et al., 2010; Pezelj et al., 2013; Székelý et al., 2017). Similarly, high numbers of suspension feeders in deep water environments are usually linked to strong currents and/or costal upwelling (Mullineaux, 1988; Linke and Lutze, 1992; Schönfeld, 1997, 1998, 2002, García-Gallardo et al., 2017).

Salinity values fluctuate more compared to the other time slices (30–43 PSU) but do not vary much compared to the other ecological parameters described above. Consequently, normal marine

conditions with a mean PSU value of 36 (Fig. 5.5) prevailed despite the considerable diversity of paleoenvironments during the middle Badenian.

5.5.5. Late Badenian

The late Badenian is dominated by suboxic conditions settled by shallow infaunal herbivores (Fig. 5.8). Most samples are characterized by a high abundance of *A. beccarii*, whereas plankton is scarce. Several samples, however, show a high abundance of buliminids (e.g., *Bulimina subulata*, Fig. 5.3 G; *Bulimina elongata*, Fig. 5.3 K and *Praeglobobulimina pyrula*, Fig. 5.4 H) and bolivinids (e.g., *Bolivina dilatata*, Fig. 5.4 J), suggesting high nutrient availability with reduced oxygen values (Murray, 1991, 2006). Samples dominated by buliminids and bolivinids can also be found in recent settings in Oxygen Minimum Zones (OMZs) in various parts of the world (e.g., Arabian Sea, Indian Ocean, Gulf of Mexico, Mississippi Delta) and different water depths from shallow to deep marine (e.g., Hermelin and Shimmield, 1990; Denne and Sen Gupta, 1991; Gooday and Rathburn, 1999; Glock et al., 2013). These conditions are also indicated by the low Fisher α values, the high dominance values (Fig. 5.3) and the high amount of stress indicators (Fig. 5.5). This pattern indicates two dominant environmental types covered by our samples: shallow marine lagoonal and slightly deeper poorly oxygenated bottoms. Similarly, Harzhauser et al. (2019) documented lagoonal and mudflat environments in the northwestern Vienna Basin during the late Badenian and Kováčová and Hudáčková (2009) described dysoxic conditions from basinal deposits. Compared to the middle Badenian, the salinity values drop slightly, but with a mean of 35 PSU (Fig. 5.5), normal marine conditions prevail throughout the late Badenian, too.

Hence, there is a considerable shift in prevailing ecological parameters from the middle to the late Badenian. This is most probably related to a major shallowing trend in the Vienna Basin (see Kranner et al., 2021). This shallowing may also explain the warmer SSTs, which ranged around 18.2 $\pm$1.0°C during the late Badenian and the relatively warmer BWT, which raised to a mean of 18°C (Fig. 5.6), overprinting the global cooling during the Middle Miocene Climatic Transition (MMCT) following the MCO (Zachos et al., 2001; Holbourn et al., 2005; Miller et al., 2020; Westerhold et al., 2020).

5.5.6. Early Sarmatian

During the early Sarmatian a general shift to oxic conditions with epifaunal and herbivorous species occurred (Fig. 5.8). The assemblages point to widespread seagrass meadows, based on the elphidiid-dominated assemblage (e.g., *Elphidium reginum*, Fig 3. C and *Elphidium aculeatum*, Fig. 5.4 D) and their affiliation to seagrasses (e.g., Langer, 1993) as documented for fossil (e.g., Betzler et al., 2000; Puga-

Bernabéu et al., 2007; Harzhauser et al., 2018) and recent faunas (e.g., of the Mediterranean of the Philippines; Langer et al., 1998; Lacuna and Gayda, 2014; Mateu-Vincens et al., 2014).

During the early Sarmatian the BWT continues to rise compared to the Badenian to a mean of 19°C (Fig. 5.6). These high temperatures are in contrast to the expected influence of the global cooling during the MMCT (e.g., Zachos et al., 2001; Holbourn et al., 2005; Miller et al., 2020; Westerhold et al. 2020) and can be explained due to the marginal setting of the area and the continuing shallowing trend (Kranner et al., 2021). Further, the Vienna Basin was completely restricted from the Mediterranean Sea (e.g., Popov et al., 2004; Harzhauser and Piller, 2007; Kováč at al., 2017a) and harbored a highly endemic fauna (Harzhauser and Piller, 2004; Piller and Harzhauser, 2005; Schütz et al., 2007; Palcu et al., 2015) resulting in the low species diversity and high dominance values (Fig. 5.3). The mean PSU value of 35 (Fig. 5.5) supports the interpretation of the Sarmatian sea to be fully marine by Piller and Harzhauser (2005) and Schütz et al. (2007). Schütz et al. (2007) discussed coastal upwelling during the early Sarmatian based on the occurrence of diatomites. This cannot be confirmed nor rejected, due to the lack of planktic foraminifers.

5.5.7. Late Sarmatian

The late Sarmatian is characterized by well oxygenated conditions and seagrass meadows, reflected by a dominance of epifaunal herbivores (Fig. 5.8). An additional increase in BWT with a mean of 21°C (Fig. 5.4) may be caused by the continuous shallowing trend (Kranner et al., 2021) but may also be linked to a slight global warming trend as suggested by the stable isotope data of Westerhold et al. (2020). The late Sarmatian salinity ranged around 37 PSU (Fig. 5.5) correlating with marine to slightly hypersaline conditions. This is in agreement with the assumptions of Piller and Harzhauser (2005) and agrees with the widespread oolite formation during the late Sarmatian (Harzhauser and Piller, 2004, 2010; Piller and Harzhauser, 2005; Cornée et al., 2009), contrasting the reconstruction of Palcu et al. (2015) assuming the Sarmatian to be the brackish transition from the Badenian to the Pannonian. The interpretation of Palcu et al. (2015), however, was revised by Silye and Filipescu (2016), stating that the identified benthic foraminiferal species (especially cycloforinids) rather suggest hypersaline lagoons or marshes than brackish conditions, which aligns with our results.

The analyzed assemblages suggest two predominating environmental types during the late Sarmatian. Most samples show a low diversity (Fig. 5.3) and are dominated by *Porosononion granosum* (Fig. 5.4 E) and point to normal marine conditions (Langer, 1993) with moderate abundances of seagrass meadows (see also Harzhauser et al., 2018). Less frequent, samples with slightly higher diversity (Fig. 5.3), yielding high amounts of miliolids (like *Cycloforina fluviata*, Fig. 5.4 L–M and *Pseudotriloculina consobrina*, Fig. 5.4 N–O), accompanied by elphidiids or *Ammonia beccarii* (Fig. 5.4 A–B), suggest

hypersaline conditions (Murray, 1991, 2006; Armstrong and Brasier, 2005). Comparable assemblages can be found in recent settings within the Red Sea (Hariri ,2008; Abu-Zied and Bantan, 2013) and in the Persian Gulf (Murray, 1970; Basson and Murray, 1995; Amao et al., 2016). These two assemblage types reflect different depositional environments: coastal-lagoonal (miliolid-dominated) versus inner to middle neritic (*Porosononion granosum*-dominated).

5.5.8. General trends

The calculated SSTs indicate a positive shift of about 3°C from the early to the middle Miocene. This warming agrees with the global MCO. The absolute values derived from the herein applied transfer function, however, seem to be underestimates. Throughout the middle Miocene, the SST values range around 18°C (17.7–18.2°C; Fig. 5.6). This value is below the annual average SST of the modern Mediterranean Sea, which ranges around 19.7 ±1.3 °C (Shaltout and Omstedt, 2014). Given the tropical biota of the middle Badenian with its reefs and thermophilic mollusc faunas (Zuschin et al., 2005, 2006; Harzhauser et al., 2007; Piller et al., 2007), a distinctly higher SST can be expected. Thus, the currently used formula of Hohenegger (2005) and Báldi and Hohenegger (2008) will need refinements. Nevertheless, it reveals general trends within the dataset such as the observed warming.

BWTs display considerably changes during the observed time interval with a distinct drop from early to middle Miocene and severe warming of about 7°C from the middle to the late Badenian and a continuation of that trend throughout the Sarmatian. This pattern opposes global climate trends, which indicate a warming during the MCO and a cooling during the MMCT. On a regional scale near-tropical conditions are evident during the middle Badenian, followed by a drop of mean annual temperature of about 7°C during the late Badenian (Böhme, 2003). Therefore, we assume that local conditions governed the temperature of the bottom water. Upwelling transported relatively cool water masses into the bathymetrically deep Vienna Basin during the early and middle Badenian. Ceasing accommodation space resulted in a distinct shallowing of the basin during the late Badenian (Kranner et al., 2021) and upwelling conditions were lost in favor of an estuarine circulation. Similarly, the very shallow marine conditions during the Sarmatian allowed for a warming of the bottom water. Moreover, a short global warm spell during the late Serravallian, as seen in the isotope data of Westerhold et al (2020) might have amplified this trend, leading to the warm and hypersaline late Sarmatian conditions.

Indicators for stress are rather scarce in early Miocene assemblages but rise in number during the early and middle Badenian when *Spirorutilus*-dominated assemblages became widespread (Fig. 5.5). A dramatic increase of stress indicators is seen during the late Badenian. This change in ecological

conditions was related to the rise of the OMZ close to the sea bottom and the spread of dysoxic conditions. A switch of the prevailing circulation system from antiestuarine to estuarine was discussed by Báldi et al. (2006) and Kováč et al. (2017b) as trigger for this development. Stress levels clearly calmed down during the Sarmatian when well oxygenated environments dominated (Fig. 5.5, 8).

Salinity stayed within fully marine ranges throughout the investigated time span. Nevertheless, an increase in salinity from ~34 to ~36 PSU (Fig. 5.5) is observed from early to middle Miocene, which might be related to the increased evaporation during the MCO. A slight drop of salinity followed during the late Badenian coinciding with the global cooling of the MMCT and a change in Paratethyan circulation patterns (Báldi et al., 2006). Another major rise in salinity of about 3 PSU occurred from the early to the late Sarmatian resulting in hypersaline conditions.

5.6. Conclusions

Our data document that the environmental conditions during the early Miocene in the northern part of the proto-VB were identical to those of the adjacent NACFB, where upwelling conditions brought cool bottom and surface waters (Grunert et al., 2010). This strongly suggests that the northern proto-VB was only an embayment of the North Alpine-Carpathian Foreland Basin during the Ottnangian, grading into the shallow, nearshore environments of the Bockfließ Fm. of the southern proto-VB. This is in line with the slight increase in bottom water temperature (BWT) and reduction in diversity along a north-south transect (Fig. 5.3, 6). During the Karpatian the northern proto-VB represented the transition between the estuarine Korneuburg Basin and the terrestrial wetlands of the central and southern proto-VB towards the open marine NACFB. Relatively warm bottom water conditions prevailed (~17°C; Fig. 5.6).

Early Badenian deposits of the VB are scarce and therefore, a detailed reconstruction is hampered. Nevertheless, a cooling trend in BWT is observed, contradicting the expected influence of the global warming associated with Miocene Climatic Optimum. This cooling might reflect the deepening of the area as described by Kranner et al. (2021) and upwelling of cool bottom water. Shallow water environments with seagrass meadow developed in the north-western VB with moderate to high diversity (Fig. 5.3), similar to those of the adjacent Mistelbach-Halfgraben.

Considerable oscillations in SST, nutrient flux, oxygenation and diversity occurred during the middle Badenian (Fig. 5.3, 6, 7, 9). Phases of high productivity sparked high abundances of four-chambered globigerinids, whereas phases with warm bottom water currents and a stratified water column are reflected by blooms of *Orbulina suturalis* (Fig. 5.4 Q). This repetitive ecologic succession may be explained by periodic intensification of upwelling followed by sluggish conditions and stratification on

a decadal to millennial scale as described by Auer et al. (2014, 2015) for the early Miocene of Europe as well as by McGregor et al. (2007), Chhak and Di Lorenzo (2007), Santos et al. (2005), Relvas et al. (2009), Miranda at al. (2012) and Tim et al. (2015) from modern upwelling systems.

The late Badenian represents mostly shallow, nearshore environments. The shallowing coincided with increasing BWT, locally counterbalancing the influence of the global cooling during the MMCT. In many parts of the basin, the foraminiferal assemblages lived in or close to the OMZ, suggesting widespread dysoxic, stressed conditions in deeper parts of the VB (Fig. 5.5, 5.8).

Fully marine conditions with widespread seagrass meadows providing well oxygenated habitats for low diverse benthic foraminifers prevailed during the Sarmatian (Fig. 5.3, 5.5). The lack of planktic species impedes with reconstructing SSTs, but a continued rising of BWT is observed during the Sarmatian. From the early to the late Sarmatian, the change from elphidiid-dominated to *P. granosum*-dominated assemblages indicates a loss of seagrass meadows. Further, the high abundance of miliolids, as well as the calculated PSU values suggests a distinct increase in salinity from the early to the late Sarmatian (Fig. 5.5), which fits to the widespread formation of oolites at that time.

Acknowledgements

We are grateful to Wolfgang Hujer (OMV, Gänserndorf) and his team for help and support during the sampling campaigns. Special thanks to Herwig Peresson and the whole Exploration Austria Team. Many thanks to the preparators of the NHM Vienna, Anton Engelbert, Anton Fürst and specifically to Iris Feichtinger, for preparing, washing and sieving the enormous number of samples in a short time period. We greatly acknowledge the very open-minded politics of the OMV-AG to provide access to core material, well-log data, seismic images and internal reports to support geosciences.

References

Abu-Zied, R.H., Bantan, R.A., 2013. Hypersaline benthic foraminifera from the Shuaiba Lagoon, eastern Red Sea, Saudi Arabia: Their environmental controls and usefulness in sea-level reconstruction. Marine Micropaleontology, 103, 51–67.

Altenbach, A.V., Lutze, G.F., Schiebel, R., Schönfeld, J., 2003. Impact of interrelated and interdependent ecological controls on benthic foraminifera: an example from the Gulf of Guinea. Palaeogeography, Palaeoclimatology, Palaeoecology, 197(3–4), 213–238. https://doi.org/10.1016/S0031-0182(03)00463-2

Amao, A.O., Kaminski, M.A., Setoyama, E., 2016. Diversity of Foraminifera in a shallow restricted lagoon in Bahrain. Micropaleontology, 62(3), 197–211.

Armstrong, H.A., Brasier, M.D., 2005. Microfossils. Blackwell Publishing. 305 pp.

Arzmüller, G., Buchta, S.B., Ralbovsky, E., Wessely, G., 2006. The Vienna Basin. In: Golonka, J., Picha, F.J. (Eds.), The Carpathians and their foreland: Geology and hydrocarbon resources. American Association of Petroleum Geologists Memoir, 84, pp. 191–204. https:// doi.org/10.1306/M84985

Auer, G., Piller, W.E., Harzhauser, M., 2014. High-resolution calcareous nannoplankton palaeoecology as a proxy for small-scale environmental changes in the Early Miocene. Marine micropaleontology, 111, 53–65.

Auer, G., Piller, W.E., Harzhauser, M., 2015. Two distinct decadal and centennial cyclicities forced marine upwelling intensity and precipitation during the late Early Miocene in central Europe. Climate of the Past, 11(2), 283–303.

Báldi, K ., 2006. Paleoceanography and climate of the Badenian (Middle Miocene, 16.4–13.0 Ma) in the Central Paratethys based on foraminifera and stable isotope ($\delta^{18}O$ and $\delta_{13}C$) evidence. International Journal of Earth Science, 95, 119–142. https://doi.org/10.1007/s00531-005-0019-9

Báldi, K., Hohenegger, J., 2008. Paleoecology of benthic foraminifera of the Baden-Sooss section Badenian, Middle Miocene, Vienna Basin, Austria. Geologica Carpathica, 59(5), 411–424. http://www.geologicacarpathica.com/browse-journal/volumes/59-5/article-455/

Basson, P.W., Murray, J.W., 1995. Temporal variations in four species of intertidal foraminifera, Bahrain, Arabian Gulf. Micropaleontology, 41, 69–76.

Bé, A.W.H., 1977. An ecological, zoogeographic and taxonomic review of Recent planktonic foraminifera. Academic Press, London. 100 pp.

Betzler, C., Martın, J.M., Braga, J.C., 2000. Non-tropical carbonates related to rocky submarine cliffs (Miocene, Almerıa, southern Spain). Sedimentary Geology, 131, 51–65.

Bicchi, E., Dela Pierre, F., Ferrero, E., Maia, F., Negri, A., Pirini Radrizzani, C., Radrizzani, S., Valleri, G., 2006. Evolution of the Miocene Carbonate Shelf of Monferrato (North-western Italy). Bollettino della Societa Paleontologica Italiana 45, 171–194.

Bindiu-Haitonic, R., Niculici, S., Filipescu, S., Bălc, R., Aroldi, C., 2017. Biostratigraphy and palaeoenvironments of the Eocene deep-water deposits of the Tarcău Nappe Eastern Carpathians, Romania based on agglutinated foraminifera and calcareous nannofossil assemblages. In: Kaminski, M.A., Alegret, L., (Eds.), Proceedings of the Ninth International Workshop on Agglutinated Foraminifera Grzybowski Foundation Special Publication, 22, 17–37.

Böhme, M., 2003. The Miocene Climatic Optimum: evidence from ectothermic vertebrates of Central Europe. Palaeogeography, Palaeoclimatology, Palaeoecology, 195, 389–401. https://doi.org/10.1016/S0031-0182(03)00367-5

Boote, D.R.D., Sachsenhofer, R.F, Tari, G., Arbouille, D., 2018. Petroleum provinces of the Paratethyan region. Journal of Petroleum Geology, 41(3), 247–297. https://doi.org/10.1111/jpg.12703

Brzobohatý, R., Stráník, Z., 2012. Paleogeography of the Early Badenian connection between the Vienna Basin and the Carpathian Foredeep. Central European Journal of Geosciences, 4(1), 126–137, https://doi.org/10.2478/s13533-011-0045-z

Bubík M., Kaminski M.A., 2004 (Eds.), Proceedings of the Sixth International Workshop on Agglutinated Foraminifera Grzybowski Foundation Special Publication, 8, 486 pp.

Chhak, K., Di Lorenzo, E., 2007. Decadal variations in the California Current upwelling cells. Geophysical Research Letters, 34 (14). https://doi.org/10.1029/2007GL030203

Cicha, I., Rögl, F., Rupp, C., Čtyroký, J., 1998. Oligocene-Miocene foraminifera of the Central Paratethys. Abhandlungen der senckenbergischen naturforschenden Gesellschaft, 549, 325 pp.

Ćorić, S., Rögl, F., 2004. Roggendorf-1 borehole, a key-section for Lower Badenian transgressions and the stratigraphic position of the Grund Formation Molasse Basin, Lower Austria. Geologica Carpathica, 55, 165–178.

Cornée, J.J., Moissette, P., Saint Martin, J.J., Kázmér, M., Tóth, E., Görög, A., Dulai, A., Müller, P., 2009. Marine carbonate systems in the Sarmatian (Middle Miocene) of the Central Paratethys: the Zsámbék Basin of Hungary. Sedimentology, 56(6), 1728–1750.

Decker, K., 1996. Miocene tectonics at the Alpine–Carpathian junction and the evolution of the Vienna Basin. Mitteilungen der Gesellschaft der Geologie und Bergbaustudenten Österreichs, 41, 33–44.

Denne, R.A., Gupta, B.K.S., 1991. Association of bathyal foraminifera with water masses in the northwestern Gulf of Mexico. Marine Micropaleontology, 17(3–4), 173–193.

Dobson, M., Haynes, J., 1973. Association of foraminifera with hydroids on the deep shelf. Micropaleontology, 19, 78–90.

Fodor, L., 1995. From transpression to transtension: Oligocene–Miocene structural evolution of the Vienna Basin and the East Alpine–Western Carpathian junction. Tectonophysics, 242, 151–182. https://doi.org/10.1016/0040-1951(94)00158-6

García-Gallardo, Á., Grunert, P., Van der Schee, M., Sierro, F.J., Jiménez-Espejo, F.J., Zarikian, C.A.A., Piller, W.E., 2017. Benthic foraminifera-based reconstruction of the first Mediterranean-Atlantic exchange in the early Pliocene Gulf of Cadiz. Palaeogeography, Palaeoclimatology, Palaeoecology, 472, 93–107.

Glock, N., Schönfeld, J., Eisenhauer, A., Hensen, C., Mallon, J., Sommer, S., 2013. The role of benthic foraminifera in the benthic nitrogen cycle of the Peruvian oxygen minimum zone. Biogeosciences, 10(7), 4767–4783.

Gooday, A.J., Rathburn, A.E., 1999. Temporal variability in living deep-sea benthic foraminifera: a review. Earth-Science Reviews, 46, 187–212.

Gradstein, F.M., Ogg, J.G., Schmitz, M.D., Ogg, G.M., 2012. The Geological Time Scale 2012. Elsevier, Amsterdam, 2 vols., 1144 pp.

Grunert, P., Soliman, A., Harzhauser, M., Müllegger, S., Piller, W., Roetzel, R., Rögl, F., 2010. Upwelling conditions in the Early Miocene Central Paratethys Sea. Geologica Carpathica, 61(2), 129–145.

Hamilton, W., Johnson, N., 1999. The Matzen Project; rejuvenation of mature field. Petroleum Geoscience, 5(2), 119–125. https://doi.org/10.1144/petgeo.5.2.1190

Hamilton, W., Wagner, L., Wessely, G., 2000. Oil and Gas in Austria. Mitteilungen der Österreichischen Geologischen Gesellschaft, 92, 235–262.

Hammer, Ø., Harper, D.A.T., Ryan, P.D., 2001. PAST: paleontological statistics software package for education and data analysis. Palaeontologia Electronica. 4(1), 1–9.

Hammer, Ø., Harper, D.A.T., 2007. Paleontological Data Analysis, Blackwell Publishing, Oxford, 351 pp.

Hariri, M.S., 2008. Effect of hydrographic conditions on the ecology of benthic foraminifera in two different hypersaline lagoons, eastern Red Sea coast, Kingdom of Saudi Arabia. Journal of KAU Marine Sciences, 19, 3–13.

Harzhauser, M., Piller, W.E., 2004. Integrated stratigraphy of the Sarmatian Upper Middle Miocene in the western Central Paratethys. Stratigraphy, 1(1), 65–86.

Harzhauser, M., Piller, W.E., 2007. Benchmark data of a changing sea. - Palaeogeography, Palaeobiogeography and Events in the Central Paratethys during the Miocene. Palaeogeography, Palaeoclimatology, Palaeoecology, 253, 8–31. https://doi.org/10.1016/j.palaeo.2007.03.031

Harzhauser, M., Piller, W.E., 2010. Molluscs as a major part of subtropical shallow-water carbonate production–an example from a Middle Miocene oolite shoal (Upper Serravallian, Austria). Carbonate systems during the Oligocene–Miocene climatic transition, 42, 183–200.

Harzhauser, M., Theobalt, D., Strauss, P., Mandic, O., Carnevale, G., Piller, W.E., 2017. Miocene biostratigraphy and paleoecology of the Mistelbach Halfgraben in the northwestern Vienna Basin (Lower Austria). Jahrbuch der Geologischen Bundesanstalt, 157, 57–108.

Harzhauser, M., Grunert, P., Mandic, O., Lukeneder, P., Garcia Gallardo, A., Neubauer, T.A., Carnevale, G., Landau, B.M., Sauer, R., Strauss, P., 2018a. Middle and Late Badenian palaeoenvironments in the northern Vienna Basin and their potential link to the Badenian Salinity Crisis. Geologica Carpathica, 69, 129–168. https://doi.org/10.1515/geoca-2018-0009.

Harzhauser, M., Mandic, O., Kranner, M., Lukeneder, P., Kern, A.K., Gross, M., Carnevale, G., Jawecki, C., 2018b. The Sarmatian/Pannonian boundary at the western margin of the Vienna Basin (City of Vienna, Austria). Austrian Journal of Earth Sciences, 111, 26–247. https://doi.org/10.17738/ajes.2018.0003

Harzhauser, M., Theobalt, D., Strauss, P., Mandic, O., Piller, W.E., 2019. Seismic-based lower and middle Miocene stratigraphy in the northwestern Vienna Basin Austria. Newsletter on Stratigraphy, 52, 221–224. https://doi:10.1127/nos/2018/0490

Harzhauser, M., Kranner, M., Mandic, O., Strauss, P., Siedl, W., Piller, W.E., 2020. Miocene lithostratigraphy of the northern and central Vienna Basin (Austria). Austrian Journal of Earth Sciences, 113(1), 169–199. https://doi.org/10.17738/ajes.2020.0011

Haward, N.J.B., Haynes, J.R., 1967. Clamys opercularis (Linnaeus) as a mobile substrate for Foraminifera. Journal of Foraminiferal Research, 6, 30–38.

Hemleben, C., Spindler, M., Anderson, O.R., 1989. Modern Planktonic Foraminifera. Springer, New York.

Hermelin, J.O.R., Shimmield, G.B., 1990. The importance of the oxygen minimum zone and sediment geochemistry in the distribution of Recent benthic foraminifera in the northwest Indian Ocean. Marine Geology, 91(1–2), 1–29.

Hohenegger, J., 2005. Estimation of environmental paleogradient values based on presence/absence data: a case study using benthic foraminifera for paleodepth estimation. Palaeogeography, Palaeoclimatology, Palaeoecology, 217, 115–130. https://doi.org/10.1016/j.palaeo.2004.11.020

Hohenegger, J., Andersen, N., Báldi, K., Ćorić, S., Pervesler, P., Rupp, C., Wagreich, M., 2008. Paleoenvironment of the Early Badenian Middle Miocene in the southern Vienna Basin Austria – multivariate analysis of the Baden-Sooss section. Geologica Carpathica, 59, 461–487. http://www.geologicacarpathica.com/browse-journal/volumes/59-5/article-458/

Holbourn, A., Kuhnt, W., Schulz, M., Erlenkeuser, H. (2005). Impacts of orbital forcing and atmospheric carbon dioxide on Miocene ice-sheet expansion. Nature, 438(7067), 483–487. https://doi.org/10.1038/nature04123

Holbourn, A., Kuhnt, W., Kochhann, K.G., Andersen, N., Sebastian Meier, K.J., 2015. Global perturbation of the carbon cycle at the onset of the Miocene Climatic Optimum. Geology, 43(2), 123–126. https://doi.org/10.1130/G36317.1

Holcová, K., Brzobohatý, R., Kopecká, J., Nehyba, S., 2015. Reconstruction of the unusual Middle Miocene (Badenian) palaeoenvironment of the Carpathian Foredeep (Lomnice/Tisnov denudational relict, Czech Republic). Geological Quarterly, 59(4) 654–678. https://doi.org/10.7306/gq.1249

Holcová, K., Doláková, N., Nehyba, S., Vacek, F., 2018. Timing of Langhian bioevents in the Carpathian Foredeep and northern Pannonian Basin in relation to ocean o graphic, tectonic and climatic processes. Geological Quarterly, 62(1), 3–17. https://doi.org/10.7306/gq.1399

Holcová, K., Dašková, J., Fordinál, K., Hrabovský, J., Milovský, R., Scheiner, F., Vacek, F., 2019. A series of ecostratigraphic events across the Langhian/Serravallian boundary in an epicontinental setting: the northern Pannonian Basin. Facies, 65(3), 36. https://doi.org/10.1007/s10347-019-0576

Hölzel, M., Wagreich, M., Faber, R., Strauss, P., 2008. Regional subsidence analysis in the Vienna Basin (Austria). Austrian Journal of Earth Sciences, 101, 88–98.

Hölzel, M., Decker, K., Zamolyi, A., Strauss, P., Wagreich, M., 2010. Lower Miocene structural evolution of the central Vienna Basin (Austria). Marine and Petroleum Geology, 27, 666–681. https://doi.org/10.1016/j.marpetgeo.2009.10.005

Hyžný, M., Hudačkova, N., Biskupič, R., Rybar, S., Fuksi, T., Halasova, E., Zagoršek, K., Jamrich, M., Ledvak P., 2012. Devinska Kobyla – a window into the Middle Miocene shallow-water marine environments of the Central Paratethys (Vienna Basin, Slovakia). Acta Geologica Slovaca, 4(2), 95–111.

Ilies, I., A., Oltean, G., Haitonic, R.B., Filipescu, S., Miclea, A., Jipa, C., 2020. Early middle Miocene paleoenvironmental evolution in southwest Transylvania (Romania): Interpretation based on foraminifera. Geologica Carpathica, 71, 5, 444–461. https://doi.org/10.31577/GeolCarp.71.5.5

Jiřiček, R., Seifert, P., 1990. Palaeogeography of the Neogene in the Vienna Basin and the adjacent part of the foredeep. In: Minařikova, D. and, Lobitzer, H., (Eds.), Thirty Years of Geological Cooperation between Austria and Czechoslovakia. Cesky Geologicky Ustav, Praha, pp. 89–105.

Kaminski, M.A., Gradstein, F.M., 2005. Atlas of Paleogene cosmopolitan deep-water agglutinated foraminifera. Grzybowski Foundation Special Publication, 10, 547 pp.

Kaminski, M.A., Niessen, F., 2015. Modern agglutinated Foraminifera from the Hovgård Ridge, Fram Strait, west of Spitsbergen: evidence for a deep bottom current. In Annales Societatis Geologorum Poloniae, 85, 309–320. https://doi.org/10.14241/asgp.2015.006

Kincaid, E., Thunell, R.C., Le, J., Lange, C.B., Weinheimer, A.L., Reid, F.M., 2000. Planktonic foraminiferal fluxes in the Santa Barbara Basin: response to seasonal and interannual hydrographic changes. Deep Sea Research Part II: Topical Studies in Oceanography, 47(5–6), 1157–1176.

Kováč, M., Barath, I., Harzhauser, M., Hlavaty, I., Hudačkova, N., 2004. Miocene depositional systems and sequence stratigraphy of the Vienna Basin. Courier des Forschungs-Instituts Senckenberg, 246, 187–212.

Kováč, M., Márton, E., Oszczypko, N., Vojtko, R., Hók, J., Králiková, S., Plašienka, D., Klučiar, T., Hudáčková, N., Oszczypko-Clowes, M., 2017a. Neogene palaeogeography and basin evolution of the Western Carpathians, Northern Pannonian domain and adjoining areas. Global and Planetary Change, 155, 133–154. https://doi.org/10.1016/j.gloplacha.2017.07.004

Kováč, M., Hudáčková, N., Halásová, E., Kováčová, M., Holcová, K., Oszczypko-Clowes, M., Báldi, K., Less, G., Nagymarosy, A., Ruman, A., Klučiar, T., Jamrich, M., 2017b. The Central Paratethys palaeoceanography: A water circulation model based on microfossil proxies, climate, and changes of depositional environment. Acta Geologica Slovaca, 75–114.

Kováčová, P., Hudačkova, N., 2009. Late Badenian foraminifers from the Vienna Basin Central Paratethys: stable isotope study and paleoecological implications. Geologica Carpathica, 60(1), 59–70. https://doi.org/10.2478/v10096-009-0006-3

Kováčová, P., Emmanuel, L., Hudáčková, N., Renard, M., 2008. Central Paratethys paleoenvironment during the Badenian (Middle Miocene): evidence from foraminifera and stable isotope (δ13C and δ18O) study in the Vienna Basin (Slovakia). International Journal of Earth Sciences, 98, 5, 1109–1127. https://doi.org/10.1007/s00531-008-0307-2

Kranner, M., Harzhauser, M., Rögl, F., Ćorić, S., Strauss, P., 2019. Biostratigraphic constraints for a Lutetian age of the Harrersdorf Unit (Rhenodanubian Zone): Implication for basement structure of the northern Vienna Basin (Austria). Geologica Carpathica, 70(5), 405–417. https://doi.org/10.2478/geoca-2019-0023

Kranner, M., Harzhauser, M., Mandic, O., Strauss, P., Siedl, W., Piller, W.E., 2021. Early and middle Miocene paleobathymetry of the Vienna Basin (Austria). Marine and Petroleum Geology. Under review

Kröll, A., Wessely, G., 1993. Strukturkarte - Basis der tertiären Beckenfüllung 1:200.000. Erläuterung zu den Karten über den Untergrund des Wiener Beckens und der angrenzenden Gebiete. Geologische Bundesanstalt, Wien.

Lacuna, M.L. Gayda, K.A., 2014. Benthic foraminiferal assemblage on a mixed stands of seagrass and macroalgae in Kauswagan, Lanao del Norte, Southern Philippines. Animal Biology and Animal Husbandry, 6, 102–116.

Langer, M.R., 1993. Epiphytic foraminifera. Marine Micropaleontology 20, 235–265.

Langer, M.R., Frick, H., Silk, M.T., 1998. Photophile and sciaphile foraminiferal assemblages from marine plant communities of Lavezzi Islands (Corsica. Mediterranean Sea). Revue de Paléobiologie, 17, 525–530.

Lee, E.J., Wagreich, M., 2017. Polyphase tectonic subsidence evolution of the Vienna Basin inferred from quantitative subsidence analysis of the northern and central parts. International Journal of Earth Sciences, 106, 687–705. https://doi.org/10.1007/s00531-016-1329-9

Linke, P., Lutze, G. F., 1993. Microhabitat preferences of benthic foraminifera—a static concept or a dynamic adaptation to optimize food acquisition? Marine micropaleontology, 20(3–4), 215–234. https://doi.org/10.1016/0377-8398(93)90034-U

Loeblich, A.R., Tappan, L., 1987. Foraminiferal genera and their classification. Van Nostrand Reinhold Company Inc., New York, 2 vols, 847 plates, 970 pp.

Lacuna, M.L., Gayda, K.A., 2014. Benthic foraminiferal assemblage on a mixed stands of seagrass and macroalgae in Kauswagan, Lanao del Norte, Southern Philippines. Animal Biology and Animal Husbandry, 6, 102–116.

Mandic, O., 2004. Foraminiferal paleoecology of a submarine swell – the Lower Badenian (Middle Miocene) of the Mailberg Formation at the Buchberg in the Eastern Alpine Foredeep: initial report. Annalen des Naturhistorischen Museums Wien 105A, 161–174.

Mateu-Vicens, G., Khokhlova, A., Sebastián-Pastor, T., 2014. Epiphytic foraminiferal indices as bioindicators in Mediterranean seagrass meadows. Journal of Foraminiferal Research, 44(3), 325–339. https://doi.org/10.2113/gsjfr.44.3.325

McGregor, H.V., Dima, M., Fischer, H.W., Mulitza, S., 2007. Rapid 20th-century increase in coastal upwelling off northwest Africa. Science, 315 (5812), 637–639. https://doi.org/10.1126/science.1134839

Miller, K.G., Browning, J.V., Schmelz, W.J., Kopp, R.E., Mountain, G.S., Wright, J.D., 2020. Cenozoic sea level and cryospheric evolution from deep-sea geochemical and continental margin records. Science Advances 6: eaaz1346. https://doi.org/10.1126/sciadv.aaz1346

Milker, Y., Schmiedl, G., 2012. A taxonomic guide to modern benthic shelf foraminifera of the western Mediterranean Sea. Palaeontologia Electronica, 15 (2), 1–134. https://palaeo-electronica.org/content/pdfs/271.pdf

Miranda, P. M.A., Alves, J.M.R., Serra, N., 2013. Climate change and upwelling: response of Iberian upwelling to atmospheric forcing in a regional climate scenario. Climate dynamics, 40 (11–12), 2813–2824. https://doi.org/10.1007/s00382-012-1442-9

Mohiuddin, M.M., Nishimura, A., Tanaka, Y., 2005. Seasonal succession, vertical distribution, and dissolution of planktonic foraminifera along the Subarctic Front: Implications for

paleoceanographic reconstruction in the northwestern Pacific. Marine Micropaleontology, 55 (3–4), 129–156.

Mullineaux, L.S., 1988. The role of settlement in structuring a rad-substratum community in the deep sea. Journal of Experimental Marine Biology and Ecology, 120, 247–261.

Murray, J.W., 1970. The Foraminiferida of the Persian Gulf: 6. Living forms in the Abu Dhabi Region. Journal of Natural History, 4, 55–67.

Murray, J.W., 1991. Ecology and Paleoecology of Benthic Foraminifera. Longman Scientific and Technical, Essex, UK, 1-365.https://doi.org/10.1017/S0025315400053650

Murray, J.W., 2006. Ecology and Applications of Benthic Foraminifera. Cambridge University Press, Cambridge, 438 pp. https://doi.org/10.1017/CBO9780511535529

Naidu, P.D., Malmgren, B.A., 1996. Relationship between late Quaternary upwelling history and coiling properties of Neogloboquadrina pachyderma and Globigerina bulloides in the Arabian Sea. The Journal of Foraminiferal Research, 26, 64–70.

Palcu, D.V., Tulbure, M., Bartol, M., Kouwenhoven, T.J., Krijgsman, W., 2015. The Badenian–Sarmatian Extinction Event in the Carpathian foredeep basin of Romania: Paleogeographic changes in the Paratethys domain. Global and Planetary Change, 133, 346–358.

Papp, A., Steininger, F., 1978. Holostratotypus des Badenien: Baden-Sooss. – In: Papp, A., Cicha, I., Senes, J., Steininger, F., (Eds.), M4 Badenien (Moravien, Wielicien, Kosovien). – Chronostratigraphie and Neostratotypen, 6, 138–145, Bratislava.

Papp, A., Rögl, F., Seneš, J., 1973. M2, Ottnangien: Die Innviertler, Salgotarjaner, Bantapusztaer Schichtengruppe und die Rzehakia Formation. Chronostratigraphie und Neostratotypen: Miozän der zentralen Paratethys. Verlag der Slowakischen Akademie der Wissenschaften, 3, 841 pp.

Pezelj, Đ, Mandic, O, Ćorić, S., (2013) Paleoenvironmental dynamics in the southern Pannonian Basin during initial Middle Miocene marine flooding. Geologica Carpathica, 6, 81–100.

Phipps, M.D., Kaminski, M.A., Aksu, A.E., 2010. Calcareous benthic foraminiferal biofacies along a depth transect on the southwestern Marmara shelf (Turkey). Micropaleontology, 377–392. https://doi.org/10.2307/40959490.

Piller, W.E., Harzhauser, M., 2005. The myth of the brackish Sarmatian Sea. Terra Nova, 17(5), 450–455. https://doi.org/10.1111/j.1365-3121.2005.00632.x

Piller, W.E., Harzhauser, M., Mandic, O., 2007. Miocene Central Paratethys stratigraphy - current status and future directions. Stratigraphy, 4, 2(3), 151–168. https://doi.org/0.1016/j.palaeo.2007.03.031

Popov, S.V., Rögl, F., Rozanov, A.Y., Steininger, F.F., Shcherba, I.G., Kováè, M., 2004. Lithological-paleogeographic maps of Paratethys. 10 Maps Late Eocene to Pliocene. Courier Forschungsinstitut Senckenbergiana, 250 pp.

Puga-Bernabéu, Á., Braga, J.C., Martín, J.M., 2007. High-frequency cycles in Upper-Miocene ramp-temperate carbonates (Sorbas Basin, SE Spain). Facies, 53(3), 329–345.

Rasmussen, T.L., 2005. Systematic paleontology and ecology of benthic foraminifera from the Plio-Pleistocene Kallithea Bay section, Rhodes, Greece. Cushman Foundation Special Publication, 39, 53–157.

Relvas, P., Luis, J., Santos, A.M.P., 2009. Importance of the mesoscale in the decadal changes observed in the northern Canary upwelling system. Geophysical Research Letters, 36 (22). https://doi.org/10.1029/2009GL040504

Rögl, F., Spezzaferri. S., 2002. Foraminiferal paleoecology and biostratigraphy of the Mühlbach section. Gaindorf Formation, Lower Badenian, Lower Austria. Annalen des Naturhistorischen Museums in Wien, 104A, 23–75.

Royden, L.H., 1985. The Vienna Basin: a thin-skinned pullapart basin. In: Biddle, K., Christie-Blick, N. (Eds.), Strike Slip Deformation, Basin Formation and Sedimentation. Society of Economics Palaeontologists and Mineralogists Special Publication, 37, pp. 319–338. https://doi.org/10.2110/pec.85.37.0319

Royden, L.H., 1988. Late Cenozoic tectonics of the Pannonian basin system. In: Royden, L.H., Horvath, F. (Eds.), The Pannonian Basin – A Study in Basin Evolution. American Association of Petroleum Geologists Memoir, 45, pp. 27–48. https://doi.org/10.1306/M45474C3

Rupp, C., 1986. Paläoökologie der Foraminiferen in der Sandschalerzone Badenien, Miozän des Wiener Beckens. Beiträge zur Paläontologie von Österreich, 12, 1–180.

Rupp, C., Hohenegger, J., 2008. Paleoecology of planktonic foraminifera from the Baden-Sooss section (Middle Miocene, Badenian, Vienna Basin, Austria). Geologica Carpathica, 59(5), 425–445.

Rupprecht, B.J., Sachsenhofer, R.F., Zach, C., Bechtel, A., Gratzer, R., Kucher, F., 2019. Oil and Gas in the Vienna Basin: hydrocarbon generation and alteration in a classical hydrocarbon province. Petroleum Geoscience, 25, 3–29. https://doi.org/10.1144/petgeo2017-056

Sant, K., Palcu, D., Mandic, O., Krijgsman, W., 2017. Changing seas in the Early–Middle Miocene of Central Europe: a Mediterranean approach to Paratethyan stratigraphy. Terra Nova, 29, 273–281 https://doi.org/10.1111/ter.12273

Santos, A.M.P., Kazmin, A.S., Peliz, A., 2005. Decadal changes in the Canary upwelling system as revealed by satellite observations: Their impact on productivity. Journal of Marine Research, 63 (2), 359–379. https://doi.org/10.1357/0022240053693671

Schiebel, R., Hemleben, C., 2005. Modern planktic foraminifera. Paläontologische Zeitschrift, 79: 135–148.

Schiebel, R., Bijma, J., Hemleben, C., 1997. Population dynamics of the planktic foraminifer Globigerina bulloides from the eastern North At lan tic. Deep Sea Research Part I: Ocean o graphic Research Papers, 44 (9–10), 1701–1713.

Schönfeld, J., 1997. The impact of the Mediterranean Outflow Water (MOW) on Benthic foraminiferal assemblages and surface sediments at the southern Portuguese continental margin. Marine Micropaleontology, 29, 211–236.

Schönfeld, J., 1998. Recent benthic foraminiferal assemblages in deep high-energy environments from the Gulf of Cadiz (Spain). Newsletter on Micropaleontology, 58, 16–17.

Schönfeld, J., 2002. Recent benthic foraminiferal assemblages in deep high-energy environments from the Gulf of Cadiz (Spain). Marine Micropaleontology, 44 (3–4), 141–162. https://doi.org/10.1016/S0377-8398(01)00039-1

Schütz, K., Harzhauser, M., Rögl, F., Ćorić, S., Galović, I., 2007. Foraminifera and Phytoplankton from the Lower Sarmatian of the Southern Vienna Basin (Petronell, Lower Austria). Jahrbuch der Geologischen Bundesanstalt, 147(1–2), 449–488.

Shaltout, M., Omstedt, A., 2014. Recent sea surface temperature trends and future scenarios for the Mediterranean Sea. Oceanologia, 56, 411–443. https://doi.org/10.5697/oc.56-3.411

Semeniuk, T.A., 2000. Spatial variability in epiphytic foraminifera from micro- to regional scale. Journal Foraminiferal Research, 30, 99–109.

Sen Gupta, B., Smith, L.E., Machain-Castillo, M.L., 2009. Foraminifera of the Gulf of Mexico. In: Felder, D.L., Camp, D.K., (Eds.), Gulf of Mexico–Origins, Waters, and Biota. Biodiversity. Texas A and M Press College Station, Texas pp. 87–129.

Sgarrella, F., Moncharmont Zei, M., 1993. Benthic foraminifera of the Gulf of Naples (Italy): systematics and autoecology. Bollettino della Società Paleontologica Italiana, 32(2), 145–264.

Shaltout, M., Omstedt, A., 2014. Recent sea surface temperature trends and future scenarios for the Mediterranean Sea. Oceanologia, 56(3), 411–443. https://doi.org/10.5697/oc.56-3.411

Siedl, W., Strauss, P., Sachsenhofer, R.F., Harzhauser, M., Kuffner, T., Kranner, M., 2020. Revised Badenian (middle Miocene) depositional systems of the Austrian Vienna Basin based on a new sequence stratigraphic framework. Austrian Journal of Earth Sciences, 113, 87–110. https://doi.org/10.17738/ajes.2020.0006

Spezzaferri, S., Ćorić, S., 2001. Ecology of Karpatian (Early Miocene) foraminifers and calcareous nannoplankton from Laa an der Thaya, Lower Austria: a statistical approach. Geologica Carpathica, 52(6), 361–374.

Spezzaferri, S., Tamburini, F., 2007. Paleodepth variations on the Eratosthenes Seamount Eastern Mediterranean: sea level changes or subsidence? eEarth Discuss, 2, 115–132. https://doi.org/10.1029/2004PA001071

Spezzaferri, S., Ćorić, S., Hohenegger, J., Rögl, F., 2002. Basin-scale paleobiogeography and paleoecology: an example from Karpatian (Latest Burdigalian) benthic and planktonic foraminifera and calcareous nannofossils from the Central Paratethys. Geobios, 35, 241–256.

Storz, D., Schulz, H., Waniek, J.J., Schulz-Bull, D.E., Kučera, M., 2009. Seasonal and interannual variability of the planktic foraminiferal flux in the vicinity of the Azores Current. Deep Sea Research Part I: Oceanographic Research Papers, 56, 107–124.

Székely, S.F., Bindiu-Haitonic, R., Filipescu, S., Bercea, R., 2017. Biostratigraphy and paleoenvironmental reconstruction of the marine lower Miocene Chechiș Formation in the Transylvanian Basin based on foraminiferal assemblages. Carnets de géologie, 17, 11–37. https://doi.org/10.4267/2042/62041

Tim, N., Zorita, E., Hünicke, B., 2015. Decadal variability and trends of the Benguela upwelling system as simulated in a high-resolution ocean simulation. Ocean Science, 11(3), 483–502. https://doi.org/10.5194/os-11-483-2015

Wessely, G., 1983. Zur Geologie und Hydrodynamik im südlichen Wiener Becken und seiner Randzone: Mitteilungen der Österreichischen Geologischen Gesellschaft, 76, 27–68.

Wessely, G., 2006. Niederösterreich. Geologie der Österreichischen Bundesländer. Geologische Bundesanstalt Wien, 416 pp.

Westerhold, T., Marwan, N., Drury, A.J., Liebrand, D., Agnini, C., Anagnostou, E., Barnet, J.S.K., Bohaty, S.M., De Vleeschouwer, D., Florindo, F., Frederichs, T., Hodell, D.A., Holbourn, A.E., Kroon, D., Lauretano, V., Littler, K., Lourens, L.J., Lyle, M., Pälike, H., Röhl, U., Tian, J., Wilkens, R.H., Wilson, P.A., Zachos, J.C., 2020. An astronomically dated record of Earth's climate and its predictability over the last 66 million years. Science, 369/6509, 1383–1387. https://doi.org/10.1126/science.aba6853

Zachos, J., Pagani, M., Sloan, L., Thomas, E., Billups, K., 2001. Trends, rhythms, and aberrations in global climate 65 Ma to present. science, 292(5517), 686–693. https://doi.org/10.1126/science.1059412

Zachos, J., Dickens, G., Zeebe, R., 2008. An early Cenozoic perspective on greenhouse warming and carbon-cycle dynamics. Nature 451, 279–283. https://doi.org/10.1038/nature06588

Zuschin, M., Harzhauser, M., Mandic, O., 2005. Influence of Size-sorting on Diversity Estimates from tempestitic Shell Beds in the Middle Miocene of Austria. Palaios, 20, 142–158. https://doi.org/10.2210/palo.2003.p03-87

Zuschin, M., Harzhauser, M., Sauermoser, K., 2006. Patchiness of local species richness and its implication for large-scale diversity patterns: an example from the middle Miocene of the Paratethys. Lethaia, 39, 65–78. https://doi.org/10.1080/00241160600578687

Zuschin, M., Harzhauser, M., Hengst, B., Mandic, O., Roetzel, R., 2014. Long-term ecosystem stability in an Early Miocene estuary. Geology, 42, 1–4. https://doi.org/10.1130/G34761.1

Supplementary

Table S5.1. Identified species and their relative abundance including biostratigraphic dating and position within lithostratigraphic units for all samples (with full well names) according to Harzhauser et al. (2017, 2020).

Table S5.2a. Identified benthic species (in alphabetical order), their extend desiderata regarding Mode of life, oxygenation, stress markers and feeding strategy and limits (min, max) regarding salinity and bottom water temperature, compiled of the literature listed in the Methods.

Table S5.2b. Identified planktonic species (in alphabetical order), their extend desiderata regarding trophic levels and limits (min, max) regarding sea surface temperature, compiled of the literature listed in the Methods.

Table S5.3a. Results of the calculations using the Formula of Hohenegger (2005) and Báldi and Hohenegger (2008) based on benthic foraminifers regarding salinity and bottom water temperature as well as the percentage-loading (used in Fig. 2, 3, 5) regarding the diversity indices, oxygenation, mode of life, feeding strategies and stress indicators.

Table S5.3b. Results of the calculations using the Formula of Hohenegger (2005) and Báldi and Hohenegger (2008) based on planktonic foraminifers regarding sea surface temperature as well as the percentage-loading (used in Fig. 9) regarding the trophic levels.

Chapter 6

The early- middle Miocene of the Vienna Basin – Concluding integrated stratigraphic and paleoenvironmental analyses

The present thesis shows the contact of pre-Neogene sediments to the Neogene infill of The Vienna Basin (Chapter 2) and comprises the results of biostratigraphy, lithostratigraphy (Chapter 3), paleobathymetry (Chapter 4) and paleoecology (Chapter 5) derived from analyses on 52 wells of the Austrian part of the northern and central Vienna Basin. The achieved integrated stratigraphic constrains allows a correlation of the local deposits to the global stratigraphic record as well as provides new insides in the paleoecological and bathymetrical evolution of the Vienna Basin.

6.1. Integrated stratigraphic constrains

The oldest analyzed deposits of the Austrian northern Vienna Basin are represented by thin sections of **Triassic** limestones (identified by colleges of the NHM, Vienna). These underground deposits are usually deep located in the wells, except of the Lax 2 (south of the city of Vienna) drilling, where all samples (up to 866 m) consists of Triassic limestones. Despite of the Neogene focus of this thesis, another **pre–Neogene** succession has been analyzed in detail. Within the Be 11 well, ~400 m thick Lutetian (Eocene) Flysch deposits were detected. These deposits represent marly shales being a continuation of the Greifenstein Nappe with lithological similarities to the "Steinberg Flysch Fm." Spatially Ottnangian deposits are than covering these pre–Neogene basement sediments.

The lowermost Neogene units found in the central Vienna Basin can be attributed to the coastal-lagoonal Bockfließ Fm., which is of **early Ottnangian** age. In the Bernhardsthal-Mühlberg-Rabensburg area in the northern Vienna Basin, the oldest deposits are represented by open marine Lužice Fm. A transitional position is represented by the Steinberg wells, where deeper marine faunas indicate the transition from the shallow lagoonal conditions of the Bockfließ Fm. towards the open marine sediments of the Lužice Fm. The geographic gap between both occurrences is most probably a result from heavy erosion during the Styrian Tectonic Phase. The micro- and macrofaunas of both formations points to fully marine conditions. No indications of a connection to the Ottnangian Rzehakia faunas (= Oncophora beds in older literature) were detected. These developed in the North Alpine Foreland Basin during the late Ottnangian. At that time the Matzen area was already dry land or the respective

deposits have been eroded. Thus, the analyzed formations can be correlated with the Transgressive Systems Tract of the global TB 2.1. and the early Bur 3 cycle.

No marine deposits of **Karpatian** age were detected in the wells of the northern Vienna Basin. Such marine sediments are confined to the Korneuburg Basin, the Matzen Halfgraben, the adjacent Alpine-Carpathian Foredeep and the Slovak part of the north-eastern Vienna Basin. In the central and southern Vienna Basin, Karpatian deposits are represented by the Aderklaa Fm. This can be separated into the basal Gänserndorf Mb., reflecting alluvial fans, and the Schönkirchen Mb., which reflects various wetland environments with floodplains, braided rivers and lakes. Despite the geographic gap between the marine and freshwater deposits, both areas formed a continues distribution area during the Karpatian. This is documented by brackish-marine gastropods in basal parts of the Schönkirchen Mb. and by the occurrence of Karpatian foraminifers in a single horizon of the Schönkirchen Mb. The position of this horizon in the wire logs suggests a coincidence with a maximum flooding surface. This in turn, allows for the first time to interpret the Aderklaa Fm. from the viewpoint of sequence stratigraphy. Thus, the Gänserndorf Mb. corresponds to a LST, which passes into the TST of the lower Schönkirchen Mb. This is also reflected by the fining upward trends in the wire logs. The full flooding of the wetlands is expressed by the maximum flooding surface and the occurrence of marine plankton. The subsequent HST is indicated by the onset of coarsening upward patterns in the wire logs but is frequently truncated by erosion.

The total thickness of this cycle attains up to 1400 m which rivals or even surpasses the thickness of the Karpatian Laa Fm. in the Mistelbach Halfgraben and Alpine-Carpathian Foreland Basin. Therefore, we tentatively assume, that the Aderklaa Fm. spans the entire Karpatian. The observed cycle would thus correspond to the global 3rd order sea level cycle TB 2.2. and Bur 4.

After a major erosive phase and considerable tilting of lower Miocene strata during the Styrian Tectonic Phase, sedimentation started with the **lower Badenian** Rothneusiedl Fm. The stratigraphic position strongly suggests that these braided river deposits can be linked to the canyon and channel systems of the Mistelbach Halfgraben and North Alpine-Carpathian Foreland Basin. The Roggendorf conglomerates in the NACFB are most probably an equivalent, representing a W-E trending feeder.

The Spannberg Ridge forms the northern limit of the Rothneusiedl Fm. Along this tectonic feature, the formation pinches out. Therefore, the Matzen High (Spannberg Ridge) developed during the Styrian Phase and was no barrier towards the central and southern Vienna Basin as suggested in nearly all stratigraphic schemes.

The lower Badenian Mannsdorf Fm. represents the open marine settings, partly indicating even upper bathyal conditions. Its patchiness and the absence of any shallow water deposits suggest, that only

erosional relics of a formerly widely distributed deposit are preserved. Flattening of the marked middle Badenian mfs clearly proof this interpretation and reveals the remnants as lower Badenian paleobasins.

The age of the early Badenian can be constrained for the first time by the tuff age from the Bernhardsthal Field (15.8 to 15.12 Ma.), the occurrence of a Ries-Impact Moldavite at Immendorf (Grund Fm.) in the NAFB (14.56 Ma.), and the absence of Orbulina (< 14.8 Ma.). In addition, the age of the Kuchyňa tuff (15.2 Ma.), at the eastern margin of the Vienna Basin supports the estimate. This is an enormous advantage, as former correlations of the early Badenian have been mainly conceptual and/or overall wrong.

In terms of sequence stratigraphy, the lower Badenian deposits reflect a LST, represented by the Rothneusiedl Fm. and the subsequent transgression reflected by the marls of the Mannsdorf Fm. A separation into TST, mfs and HST of the Mannsdorf Fm. based only on wire logs is difficult due to the insufficient data available. Overall, the early Badenian can be correlated with the global sea level cycle TB 2.3. and the Bur 5/Lan 1 cycle.

A hiatus is obvious between the early and **middle Badenian**; indicated by strong erosion and tilting of the lower Badenian Mannsdorf Fm. The middle Badenian cycle starts with the coarse siliciclastics of the Auersthal Fm., which can be dated for the first time to be younger than 14.56 Ma based on the occurrence of *Orbulina*. It is overlain by the sand of the Matzen Fm., which passes into the pelites of the Baden Fm. The depositional environment of the Baden Fm. ranged from upper bathyal to outer neritic to coastal marine but open marine conditions prevailed in the Vienna Basin. In terms of sequence stratigraphy, the Auersthal Fm. can be explained as LST, overlain by the sands of the initial TST. The rapid deepening is indicated by the long shale line interval seen in all wire-logs, culminating in a pronounced mfs, which is used as marker throughout the Vienna Basin in seismic analysis by OMV. The HST is indicated by the serrated high amplitude SP-logs. This middle Badenian corresponds to the global 3rd order sea level cycle TB 2.4.

Interestingly, the frequently used ecozones Upper Lagenidae Zone and *Spirorutilus* Zone fall both completely within the middle Badenian and are both present in the Baden Fm. These zones form an ecologically succession due to the deepening of the basin.

The **upper Badenian** is represented by the up to 1000-m-thick Rabensburg Fm. The depositional environment was generally shallower compared to the middle Badenian and middle to inner neritic settings prevailed. In wire logs and seismic surveys, it is characterized by high amplitude and high frequency patterns and prograding sigmoidal sedimentary bodies. In terms of sequence stratigraphy, the upper Badenian represents a single cycle with a short TST, moderately developed mfs and a thick

HST, which is often truncated by the subsequent Sarmatian deposits. The LST of the upper Badenian cycle is difficult to detect in wire logs, due to the weak separation from the HST logs of the middle Badenian. Regionally, the occurrence of lignite and anhydrite indicates the onset of the upper Badenian. Thus, the upper Badenian cycle corresponds to the TB 2.5 cycle.

The stage boundary between the upper Badenian and **early Sarmatian** is often hard to reconstruct, due to major erosion and redeposition of Badenian faunas into the Sarmatian. Lowermost Sarmatian deposits of the *Anomalinoides dividens* zone was detected only in two wells (Ad78 and Span 8) and also the following *Elphidium reginum* zone was detected only in two wells (Ma 127 and Rab 11). Much more frequent the *Elphidium hauerinum* zone could be identified overlain by to the **late Sarmatian** *Porosononion granosum* ecozone. The upper Sarmatian Skalica Fm. is covering the whole studied area and is overlain by the Pannonian basin fill. The further identification and differentiation of Pannonian sediments was not focused within this thesis but a correlation using wire–logs can easily be established.

6.2. Paleoenvironmental development of the Austrian northern and central Vienna Basin

For **pre-Neogene** deposits only interpretations on paleoenvironmental conditions for the Eocene deposits are provided. These deposits represent a deep-water succession, which formed in bathyal to lower bathyal water depth with reduced oxygen levels.

The proto-Vienna Basin was flooded for the first time during the **Ottnangian** at around 18.1 Ma peaking in maximum water depth down to 300 m. Bathyal, open marine conditions became established in the northern Vienna Basin. Hence, the environmental conditions during the early Miocene in the northern part of the proto-VB were identical to those of the adjacent NACFB, where upwelling conditions brought cool bottom and surface waters (Grunert et al., 2010). This strongly suggests that the northern proto-VB was only an embayment of the North Alpine-Carpathian Foreland Basin during that time, whereas southwards a grading into the shallow, nearshore environments of the Bockfließ Fm. occurred. This is in line with the slight increase in bottom water temperature (BWT) and reduction in diversity along a north-south transect.

During the **Karpatian** the northern proto-VB attained water depth exceeding 300 m (Mistelbach Halfgraben) and represented the transition between the estuarine Korneuburg Basin and the terrestrial wetlands of the central and southern proto-VB towards the open marine NACFB. The terrestrial wetlands of the central and southern proto-VB were shortly flooded during the global sea

level high around 16.5 Ma, flushing planktonic foraminifers into the central proto-VB. The simple N-S basin architecture during the early Miocene is linked to the piggy-back stage of the tectonic evolution of the VB.

Basin geometry changed dramatically at the early/middle Miocene boundary. The tectonic regime changed from piggy-back to extensional and the **early Badenian** transgression entered new and deep paleobasins with water depths down to 400 m, leading to a cooling trend in BWT and may represent upwelling conditions. This contradicts the global warming trend associated with the Miocene Climatic Optimum. Shallow water environments with seagrass meadows developed in the north-western VB with moderate to high diversity, similar to those of the adjacent Mistelbach-Halfgraben.

Considerable oscillations in bathymetry, SST, nutrient flux, oxygenation and diversity occurred during the **middle Badenian**. The middle Badenian transgression corresponds to the wide-spread middle Langhian flooding. Initially, the relative sea level in the VB attained 350 m but soon shifted to around 250 m due to cessation of accommodation by high sedimentation rates. Phases of high productivity sparked high abundances of four-chambered globigerinids, whereas phases with warm bottom water currents and a stratified water column are reflected by blooms of *Orbulina suturalis*. This repetitive ecologic succession may be explained by periodic intensification of upwelling followed by sluggish conditions and stratification on a decadal to millennial scale.

The **late Badenian** represents mostly shallow, nearshore environments. The shallowing coincided with increasing BWT, locally counterbalancing the influence of the global cooling during the MMCT. In many parts of the basin, the foraminiferal assemblages lived in or close to the OMZ, suggesting widespread dysoxic, stressed conditions in deeper parts of the VB.

The stage boundary from the late Badenian to the **early Sarmatian** is close to the Mi4 event, which caused a global sea level fall of about 30 m (Miller et al., 2020), explaining the observed erosion and the scarcity of lowermost Sarmatian samples. The subsequent rise of the global sea level of up to 50 m explains the re-establishment of inner neritic water depths of about 20 to 50 m in most parts of the VB, leading to fully marine conditions with widespread seagrass meadows. A continuous rising of BWT is observed during the early Sarmatian continuing into the **late Sarmatian**. A slight deepening occurred at the beginning of the late Sarmatian resulting in loss of seagrass meadows indicated by *Porosononion granosum*-dominated assemblages replacing the elphidiid fauna. Further, the high abundance of miliolids, as well as the calculated PSU values suggests a distinct increase in salinity from the early to the late Sarmatian, which fits to the widespread formation of oolites at that time.